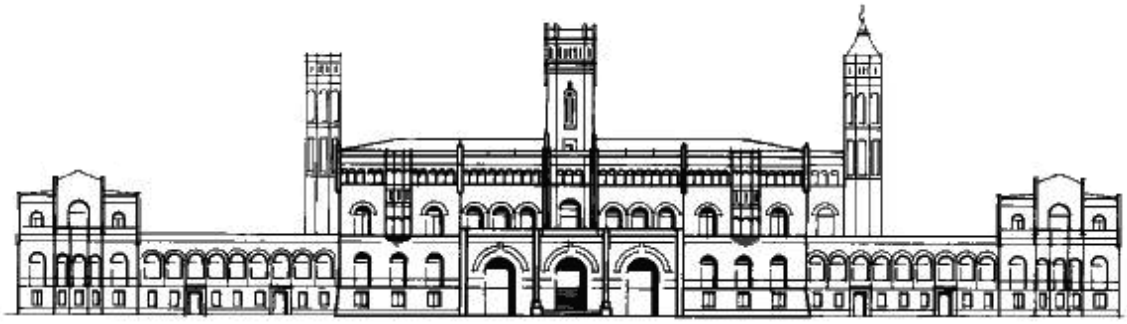

A HYBRID SS-TOA WIRELESS GEOLOCATION BASED ON PATH ATTENUATION: ROBUSTNESS INVESTIGATION UNDER IMPERFECT PATH LOSS EXPONENT

By

María Isabel Valera Martínez

PERFORMED AT
INSTITUT FÜR KOMMUNIKATIONSTECHNIK
FAKULTÄT FÜR ELEKTROTECHNIK UND INFORMATIK
LEIBNIZ UNIVERSITÄT HANNOVER
HANNOVER, GERMANY

SUBMITTED IN PARTIAL FULFILLMENT OF THE REQUIREMENTS FOR THE DEGREE OF TELECOMMUNICATIONS ENGINEER
AT
DEPARTAMENTO DE TECNOLOGÍAS DE LA INFORMACIÓN Y LAS COMUNICACIONES (DEPARTMENT OF INFORMATION TECHNOLOGIES AND COMMUNICATIONS)
ESCUELA TÉCNICA SUPERIOR DE INGENIERÍA DE TELECOMUNICACIÓN (SCHOOL OF TELECOMMUNICATIONS ENGINEERING)
UNIVERSIDAD POLITÉCNICA DE CARTAGENA (TECHNICAL UNIVERSITY OF CARTAGENA)
CARTAGENA, SPAIN

AUGUST 2009

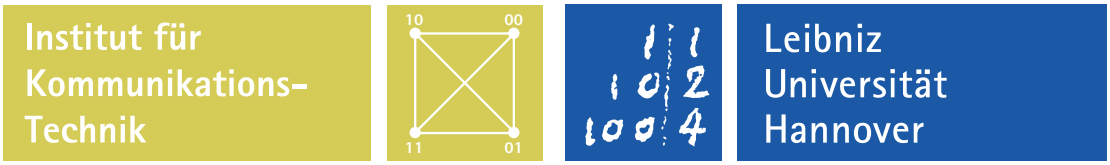

INSTITUT FÜR KOMMUNIKATIONSTECHNIK

LEIBNIZ UNIVERSITÄT HANNOVER

The undersigned hereby certify that they have read and recommend to Escuela Técnica Superior de Ingeniería de Telecomunicación (School of Telecommunications Engineering), Departamento de Tecnologías de la Información y las Comunicaciones (Department of Information Technologies and Communications), Universidad Politécnica de Cartagena (Technical University of Cartagena), Cartagena, Spain, for acceptance of a thesis entitled "**A Hybrid SS-ToA Wireless Geolocation Based on Path Attenuation: Robustness Investigation under Imperfect Path Loss Exponent**" by **María Isabel Valera Martínez** as the Final Degree Project in partial fulfillment of the requirements for the degree of **Telecommunications Engineer**.

Dated: August 2009

Supervisor: _____

Prof. Dr.-Ing. Thomas Kaiser

Readers: _____

M.Eng. Bamrung Tau Sieskul

_____

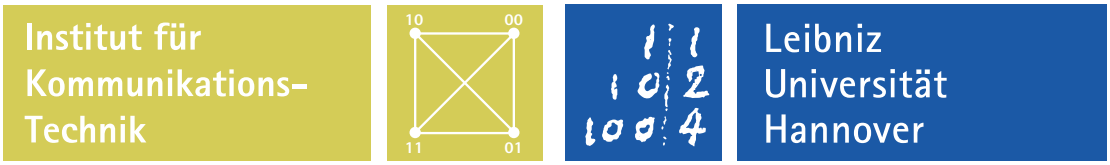

INSTITUT FÜR KOMMUNIKATIONSTECHNIK
LEIBNIZ UNIVERSITÄT HANNOVER

Date: **August 2009**

Author:	**María Isabel Valera Martínez**
Title:	**A Hybrid SS-ToA Wireless Geolocation Based on Path Attenuation: Robustness Investigation under Imperfect Path Loss Exponent**
Department:	**Departamento de Tecnologías de la Información y las Comunicaciones (Department of Information Technologies and Communications)**
Faculty:	**Escuela Técnica Superior de Ingeniería de Telecomunicación (School of Telecommunications Engineering)**
University:	**Universidad Politécnica de Cartagena (Technical University of Cartagena)**
Location:	**Cartagena, Spain**
Degree:	**T.E.**
Convocation:	**August**
Year:	**2009**


Leibniz
Universität
Hannover


UNIVERSIDAD POLITECNICA DE CARTAGENA
Fechos Allend Mar
anno mcmxcviii

Permission is herewith granted to Leibniz Universität Hannover and Universidad Politécnica de Cartagena (Technical University of Cartagena) to circulate and to have copied for non-commercial purposes, at its discretion, the above title upon the request of individuals or institutions.

Signature of Author

To my family.

Table of Contents

List of Tables

List of Figures

Abstract

Kurzfassung

Eine der Anwendungen von drahtlosen Kommunikationssystemen stellt die Ortung mobiler Nutzer dar. Die Herausforderung besteht darin, die Nutzerposition mit einer ungenauen Kenntnis des Pfadverlustexponenten (PLE), hervorgerufen durch die zum Einsatz kommenden Schätzverfahren, zu bestimmen.

In dieser Arbeit werden Lokalisierungsverfahren basierend auf der Ankunftszeit (ToA) der Signale und deren Signalstärke (SS) mit Hilfe einer hybriden SS-ToA-Methode untersucht. Das Ziel besteht darin, das Verfahren um verschiedene Signalformen wie die zweite Ableitung des gaußförmigen Monocycle-Impulses oder ein Minimum-Shift-Keying-Signal zu erweitern und die Performance des Maximum-Likelihood-Schätzers (ML) unter der imperfekten Annahme des Pfadverlustexponenten zu untersuchen. Es wurde die ToA-Schätzungsleistung des ML-Schätzers (ML) auf Basis der SS-ToA-Methode unter dem imperfekten PLE mit den asymptotischen Auswertungsmethoden evaluiert. Es zeigte sich, dass die Taylor-Entwicklung basierend auf der Berechnung der Erwartungswerte der partiellen Ableitung die besten Ergebnisse für die analytische Erfassung der asymptotischen Leistung des ML-Schätzers lieferte.

In der Schwellenregion lieferte der ML-Schätzer gegenüber dem Maximum-Korrelation-Schätzer (MC) für einen kleinen Wert des PLE-Fehlers, z.B. $\delta_\gamma = 0{,}5$, in den Indoor-Anwendungen und einen mittleren PLE-Fehler, z.B. $\delta_\gamma = 1$, in den Outdoor-Anwendungen bessere Performance. In der asymptotischen Region übertreffen

der MC- und der ML-Schätzer mit perfektem PLE den ML-Schätzer mit imperfektem PLE.

Stichwörter: Ankunftszeit-Schätzung, Maximum-Likelihood-Schätzung, Pfadverlustexponent.

Resumen

Uno de los principales requerimientos en las comunicaciones móviles consiste en la localización del terminal móvil. A pesar del incompleto conocimiento de la radio-propagación causada, por ejemplo, por la estimación del exponente de pérdidas (PLE), y las posibles fluctuaciones de dicho exponente, los sistemas inalámbricos de localización deben determinar la posición del móvil con la mayor precisión posible.

En este proyecto, se ha estudiado la localización inalámbrica a través del tiempo de llegada (ToA) desde la estación móvil hasta la estación base. El objetivo de este estudio es extender la aplicación del método híbrido del ancho de señal y el tiempo de llegada (SS-ToA) a señales con diferentes formas de onda, por ejemplo, la segunda derivada del pulso Gaussiano y una señal MSK ("minimum-shift keying"), y la investigación del estimador de máxima verosimilitud (ML) en la estimación del ToA en presencia del conocimiento imperfecto del PLE. Se ha evaluado la estimación del ToA basada en el método SS-ToA bajo el conocimiento imperfecto del PLE utilizando técnicas asintóticas de análisis. Entre los cuatro métodos teóricos de estimación obtenidos, la expansión de la serie de Taylor con el cálculo del valor esperado de la derivada cruzada proporciona los resultados más precisos para el análisis teórico del estimador ML.

Además, se obtiene que en la región de umbral, el estimador ML supera al estimador MC para valores pequeños del PLE, como $\delta_\gamma = 0.5$, en el caso de interiores, y para valores moderado, por ejemplo $\delta_\gamma = 1$, en el caso de exteriores. Sin

embargo, en la región asintótica, los estimadores MC y ML bajo el conocimiento perfecto del PLE proporcionan mayor precisión que el estimador ML teniendo en cuenta el error en el PLE.

Índice de términos: Estimación del tiempo de llegada, Estimación por máxmima verosimilitud, Exponente de pérdidas.

Abstract

One of the requirements in wireless communications is the knowledge of the mobile location. Despite the uncertain knowledge of the radio propagation caused by, e.g., the estimation of the path loss exponent (PLE), and the possible fluctuation of the PLE, wireless localization systems have to determine the mobile position as accurately as possible.

In this thesis, we consider the wireless geolocation or localization using the radio signals based on their time of arrival (ToA). The objective of this work is to extend the application of the hybrid mix of the signal strength and the time of arrival (SS-ToA) to several signal waveforms, e.g., a second-derivative Gaussian monocycle pulse and a minimum-shift keying signal, and to investigate the performance of the maximum likelihood (ML) estimator in the ToA estimation under the imperfect PLE. We evaluate the ToA estimation performance of the ML estimator based on the SS-ToA method under the imperfect PLE by using asymptotic analysis techniques. It appears that among four derivations, the Taylor expansion with the expectation of the cross-derivative provides the most accurate results for analytically capturing the asymptotic performance of the ML estimator.

In the threshold region, the ML estimator outperforms the maximum correlation (MC) estimator for the small PLE error, e.g., $\delta_\gamma = 0.5$ in the indoor case, and the moderate PLE error, e.g., $\delta_\gamma = 1$ in the outdoor case. However, in the asymptotic region the MC and ML estimators under the perfect PLE outperform the ML

estimator with the imperfect PLE.

Index Terms: Time-of-arrival estimation, Maximum likelihood estimation, Path loss exponent.

Acknowledgements

I would like to express profound gratitude to my advisor, M.Sc. Bamrung Tau Sieskul, for his invaluable support, supervision and useful suggestions throughout this research work. His moral support and continuous guidance enabled me to complete my work successfully. I am also highly thankful to Prof. Dr.-Ing. Thomas Kaiser for allowing me to work in the Institut für Kommunikationstechnik.

I am grateful to the Technical University of Cartagena for the opportunity to come to Germany to realize my final project degree. I would like to thank the School of Telecommunications Engineering and, specially, to the personnel of the Department of Information Technologies and Communications for the knowledge and the interest in the Telecommunications Engineering, which they have transmitted to me.

I am as ever, especially indebted to my parents, Mr. Valera and Mrs. Martínez, for their love and support throughout my life. I also wish to thank my brothers and sisters for their support and understanding during my study. Moreover, my sincere thanks go to my lifelong friends, who shared their love and experiences with me. I wish to express my appreciation to my colleges and friends of Cartagena, who have shared their personal and professional experiences over all the degree. Finally, i would like to thank Rosa M. Menchón, who was my most important college and support during all the degree.

M. Isabel Valera Martínez
August 2009, Hannover

Nomenclature

The nomenclature in this thesis can be arranged in the following tables.

Abbreviations	Meanings
NLoS	Non-line-of-sight
ToA	Time-of-arrival
MS	Mobile station
BS	Base station
ML	Maximum likelihood
MC	Maximum correlation
SNR	Signal-to-noise ratio
PSD	power spectral density
CRB	Cramér-Rao bound
PDF	Probability density function
MSK	Minimum-shift keying
GMSK	Gaussian minimum-shift keying
GSM	Global System for Mobile communications
FM	Frequency modulation
MSE	Mean square error
RMSE	Root mean square error
ACRB	Asymptotic Cramér-Rao bound
MCRB	Modified Cramér-Rao bound
SS	Signal strength
RSS	Received signal strength
PLE	Path loss exponent
FFT	Fast Fourier transform
TE	Taylor expansion
AB	Average bias
LUBB	Lower/upper bound of bias
DoA	Direction-of-arrival
CDF	Cumulative distribution function

Notations	Meanings
τ	Time delay
$r_b(t)$	Received signal at the b-th base station at the time t
b	Index of the base station
B	Number of the base stations
(x_b, y_b)	Coordinate of the b-th base station
(x, y)	Coordinate of the mobile station
d_b	Distance between the mobile station and the b-th base station
c	Speed of the light
τ_b	Time delay from the mobile station to the b-th base station
a_b	Loss gain from the mobile station to the b-th base station
$s(t)$	Transmitted signal at the time t
$n_b(t)$	Additive noise at the b-th base station at the time t
κ	Unitless constant depending on antenna characteristics and average channel attenuation
f_0	Center frequency of the wireless system
d_0	Close-in distance in the far field region
γ_b	Path loss exponent at the b-th BS
E_b	Energy of the received signal at the b-th
E_{s}	Energy of the transmitted signal
σ_{n}^2	Variance of the noise
T_{o}	Observation time
$p(t)$	Second-derivative Gaussian pulse at the time t
τ_{p}	Pulse-shaping factor of the second-derivative Gaussian pulse
T_{p}	Pulse width of the second-derivative Gaussian pulse
E_{r}	Energy of the received signal
SNR	Transmitted signal-to-noise ratio
$\mathrm{SNR}_{\mathrm{Rx}}$	Received signal-to-noise ratio
$S(\omega)$	Fourier transforms in angular frequency of the transmitted signal
$G(\omega)$	Fourier transforms in angular frequency of the function $g(t)$
ω	Angular frequency
$S(f)$	Fourier transforms in ordinary frequency of the transmitted signal
$\bar{\beta}$	Effective bandwidth of the transmitted signal
j	Imaginary unit
W	Square of the bandwidth of the transmitted signal
$\dot{s}(t)$	Derivative of the transmitted signal with respect to the time t at the time t
m	Modulation index
$x(t)$	Modulating signal
$\triangle f$	Deviation of frequency
T	Period of bit
R_{B}	Information bit rate
N	Number of the bits in transmitted frame

Notations	Meanings
(v_i, q_i)	Pair of successive information bits
θ	Phase in MSK signal
$\triangle\omega$	Deviation of angular frequency
$\mathbb{R}$	Set of all real numbers
ω_0	Center angular frequency of the wireless system
N_{R}	Number of the independent runs
n_{R}	Index of the independent run
$R(\omega)$	Fourier transforms in angular frequency of the received signal
$\tau_{b,0}$	True value of the ToA
$\mathrm{MSE}_{\mathrm{SS-ToA}}$	Mean square error for the ML estimator
$\mathrm{RMSE}_{\mathrm{SS-ToA}}$	Root mean square error for the ML estimator
$\hat{\tau}_{b,\mathrm{ML}}$	Estimated value of the ToA for the ML estimator
$\mathrm{MSE}_{\mathrm{ToA}}$	Mean square error for the MC estimator
$\mathrm{RMSE}_{\mathrm{ToA}}$	Root mean square error for the MC estimator
$\hat{\tau}_{b,\mathrm{MC}}$	Estimated value of the ToA for the MC estimator
$\mathrm{ACRB}_{\mathrm{SS-ToA}}$	Asymptotic Cramér-Rao bound for the ML estimator
$\mathrm{MCRB}_{\mathrm{SS-ToA}}$	Modified Cramér-Rao bound for the ML estimator
$\mathrm{ACRB}_{\mathrm{ToA}}$	Asymptotic Cramér-Rao bound for the MC estimator
$\mathrm{MCRB}_{\mathrm{ToA}}$	Modified Cramér-Rao bound for the MC estimator
$\rho(\tau_b)$	Correlation between the transmitted and the received signal
γ	Imperfect PLE
γ_0	True value of the PLE
δ_γ	Additional error of the PLE model
f_{ML}	Objective function of the ML estimator
$\rho_{\mathrm{ns},b}$	Correlation between the transmitted signal and the noise
$\rho_{\mathrm{ss},b}$	Correlation between the transmitted signal and the conjugated transmitted signal
$a_{b,0}$	True value of the gain loss
$\rho_{\mathrm{ns},0}$	Correlation between the transmitted and the noise for the true value of the ToA
$\dot{\rho}_{\mathrm{ns},b}$	First derivative of $\rho_{\mathrm{ns},b}$ with respect to τ_b
$\ddot{\rho}_{\mathrm{ns},b}$	Second derivative of $\rho_{\mathrm{ns},b}$ with respect to τ_b
$\tilde{a}_{b,0}$	Value of the gain loss for the true value of the ToA and the imperfect value of the PLE
$\bar{\gamma}_t$	Mean of the doubly truncated Gaussian distribution of the PLE
$\sigma^2_{\gamma_t}$	Variance of the doubly truncated Gaussian distribution of the PLE

Notations	Meanings
$\log(\cdot)$	Logarithm function
$\sim$	Is distributed as
$\mathcal{N}(\mu, \sigma^2)$	Normal distribution with mean μ and variance σ^2 for the real Gaussian random variable
$\mathcal{N}_{\mathcal{C}}(\mu, \sigma^2)$	Normal distribution with mean μ and variance σ^2 for the complex Gaussian random variable
$l(\cdot)$	Likelihood function
$\ln(\cdot)$	The Napierian logarithm function
$\cong$	Is approximately
$\arg\max_{\tau_b}(\cdot)$	The argument τ_b, which maximizes the function $(\cdot)$
$\arg\min_{\tau_b}(\cdot)$	The argument τ_b, which minimizes the function $(\cdot)$
$\mathcal{F}\{\cdot\}$	Fourier transform
$\mathcal{F}^{-1}\{\cdot\}$	Inverse Fourier transform
$\lvert\cdot\rvert$	Absolute value
$\Re(\cdot)$	Real part
$\Im(\cdot)$	Imaginary part
$\Gamma(\cdot)$	Gamma function
$(\cdot)!$	Factorial
$\delta(\cdot)$	Dirac delta function
$(\cdot)^{\mathrm{T}}$	Transpose
$p_v(\cdot)$	Probability density function of the variable v
$p_{v,q}(\cdot,\cdot)$	Joint probability density function of the variables v and q
$*$	Convolution
$(\cdot)^*$	Conjugate
$\mathrm{E}_x\{\cdot\}$	Expectation with respect to the random variable x
$\mathrm{erf}(\cdot)$	Error function
$\lim$	Limit
$\Phi(\cdot)$	Cumulative distribution function
$\frac{\partial}{\partial \tau_b}(\cdot)$	Partial differentiation with respect to variable τ_b

Introduction

Backgrounds

Literature Reviews

The wireless geolocation commercially emerges from the incentives of locating vehicles, people and parcels (see, e.g., [2–8]) . In addition to data communication in wireless networks, user geolocation is deemed viable due to the emergency requirement by the Federal Communications Commission and the European Commission [9].

The time-of-arrival (ToA) estimation is a favorable technique for those applications, since its accuracy depends on the signal bandwidth, which allows the designer to adjust the signal according to desired precision. Despite multipath propagation, oxygen and water vapor can cause the significant path attenuation at a high frequency.

Relation

The estimation of certain waveform parameters in the system consisted of the signal perturbed by an additive noise has attracted much attention for several decades (see, e.g., [10–12]). In [13], the use of the path loss information in the ToA estimation can improve the estimation performance in term of smaller error variance.

For direction-of-arrival (DoA) estimation, the behavior of the maximum-likelihood (ML) estimator has been investigated under a model mismatch in, e.g., [14–17]. The path loss exponent (PLE) has been considered unknown and estimated in, e.g., [18,19].

Gap

The ToA estimation problem is different from the DoA estimation, since it involves the continuous-time process rather than the discrete-time process as in the DoA estimation. The different nature makes the analysis of the ToA estimation performance rather different. The ToA estimation using the path attenuation has been shown to provide the promising performance improvement. In fact, the estimation of the PLE by any estimator cannot always achieve the true value of the PLE. Moreover, the rapid changes in the environments, because of, e.g., the movement of the mobile station (MS) or the changes in the weather, provide that the knowledge of the PLE does not coincide with the PLE in the previous observation. Since it is difficult to obtain the true PLE, the research gap emerges therefore as a vacant study on how the ML estimator behaves in the ToA estimation, when the PLE is deterministic and subject to an error.

Objectives

The objective of this work is to investigate the performance of the ML estimator in the ToA estimation under the imperfect PLE. Strictly speaking, when the perfect knowledge of the PLE is unavailable, does the ML estimator based on a hybrid mix

of the signal strength and the time of arrival (SS-ToA) still outperform the maximum correlation (MC) estimator based on the traditional ToA approach? Another objective is to extend the application of the hybrid SS-ToA concept to other signal waveforms than the orthogonal frequency division multiplexing in [13].

Scope

In this work, we mainly study the effects of the PLE in the SS-ToA approach on the wireless geolocation. The topic covered in this study is the wireless geolocation or localization using the radio signals based on their ToAs. We assume that i) the single path is considered for the sake of minimal achievable accuracy investigation, since the Cramér-Rao bound (CRB) of the multipath is lower bounded by the CRB of the single path (see, e.g., [20]), ii) the unknown ToA is constant over an observation period $(0, T_{\mathrm{o}}]$, and iii) the large-scale fading can be considered as a spatial average over the small-scale fluctuations of the signals [21, p. 847]. The estimated ToAs can be further employed to estimate the mobile position even in the presence of non-line-of-sight (NLoS) propagation by using several algorithms (see, e.g., [22]).

Problem Statement

Problem

In this work, the problem is the evaluation of the ToA estimation performance using the ML estimator based on the SS-ToA method under the imperfect PLE.

Significance

The above problem is important, because the investigation result will allow a system designer to choose the most appropriate ToA estimator in the presence of the PLE error.

Novelties, Contributions, and Merits

Novelties

Some new results are exemplified, such as the closed-form expressions of the bias and the error variance of the ToA estimation using the ML estimator under the imperfect PLE, the closed-form expression of the effective bandwidth of a transmitted minimum-shift keying (MSK) signal, and the closed-form expressions of the asymptotic CRB (ACRB) and the modified CRB (MCRB).

Contributions

Some results can be delivered to the research community in the aspects of the extension of the ML estimator based on the SS-ToA idea to a Gaussian monocycle and the MSK signal, and the analysis of the error performance of the ToA estimation using the ML estimator under the imperfect PLE, in which we point out that the previous analysis method in [14] provides the inaccurate prediction ability and we present an accurate analysis method based on a Taylor series expansion.

In addition, although our theoretical performance prediction is accurate in the asymptotic region, it is still useful since the outlier technique or the method of interval for the analysis in a threshold region (see, e.g., [23] and [16]) requires the asymptotic performance as a fundamental term.

Merits

The investigation of the error behavior of the mis-modeled estimation will help the system designer to make a decision on choosing whether the ML estimator (hybrid method) or the MC estimator (classical method) in the PLE mismatch case. The error analysis based on the presented Taylor expansion can be further applied to other mismatch problems.

Organization

In Chapter 1, the wireless systems, which is considered as the main application, is introduced.

In Chapter 2, we consider the estimation of the ToA using the ML method. The ToA estimate can be further used to determine the distance between the base station (BS) and the MS based on the system geometry. In order to obtain the estimated value of the ToA, wireless propagation and mathematical statistics are regarded as the fundamental knowledge to examining the wireless system. As the ToA estimator is designed in conjunction with the path loss, it appears as a hybrid method between the ToA and the SS (see [13]).

The transmitted signals are studied in Chapter 3, where digital frequency modulation is considered to be a basic knowledge. The transmitted signals are assumed to be the second-derivative Gaussian pulse for the indoor environments, and a digital signal with the MSK modulation for the outdoor environments. In this chapter, we also evaluate the effective bandwidths for both the transmitted signals by using the Fourier transform. As the MSK signal involves the bit information in the transmission, an assumption of the data bits is required for this pilot interval.

Without loss of generality, the bit information is assumed therein to be random with an equal probability for both bit zero and bit one. Due to the randomness of the data bits, the effective bandwidth of the transmitted signal in this scenario appears as a random quantity, which gives rise to the fluctuated performance of the ToA estimation. With the aim at involving all possible random cases, the theoretical performance in term of root mean square error (RMSE) of the ToA estimation is examined by means of the ACRB and the MCRB.

In Chapter 4, we implement the ML and the MC estimators of the ToA. The fast Fourier transform (FFT) and the convolution are considered as the background tools in this chapter. Then, the effects of different parameters, such as the PLE, the signal-to-noise ratio (SNR), and the distance between the transmitter and the receiver, on the wireless geolocation are investigated.

Chapter 5 studies the ToA estimation with the aim at investigating the effects of the PLE error. The theoretical bias and the RMSE of the ToA estimation are derived as a function of the PLE error. We also consider the Friedlander analysis method of the ToA estimation. The biases and the RMSEs of the ToA estimation of both methods are compared to the numerical bias and RMSE of the estimated ToAs obtained in the simulations. The theoretical performance is obtained by using the theory of asymptotic analysis, which is fundamentally based on a Taylor expansion.

Chapter 1

Wireless Geolocation

One of the requirements in wireless communications is the knowledge of the mobile location (see, e.g., [24,25]). Despite the NLoS propagation, wireless localization systems have to determine the mobile position as accurately as possible. In this work, we investigate the robustness of a method to find the mobile's location using only one parameter, the ToA of the received signal.

We consider the MS transmitting a signal to all BSs, which exists in the wireless network. Each BS receives the transmitted signal with a loss gain and additive noise in one ToA. The ToA is different for each BS and depends on the distance between the MS and the BS.

We show a method to estimate the coordinate of the MS using only the time delay, denoted by τ, of the signal from the MS to each BS. With the aim at obtaining the better performance of wireless geolocation, a path attenuation model is incorporated into the time delay model.

An example of a wireless network with 7 cells is shown in Fig. 1.1, where the MS sends the transmitted signal to every BS, and each of them receives a signal $r_b(t)$, where b is the index of the BS ($b = 1, 2, ..., B$; in this example $B = 7$). The

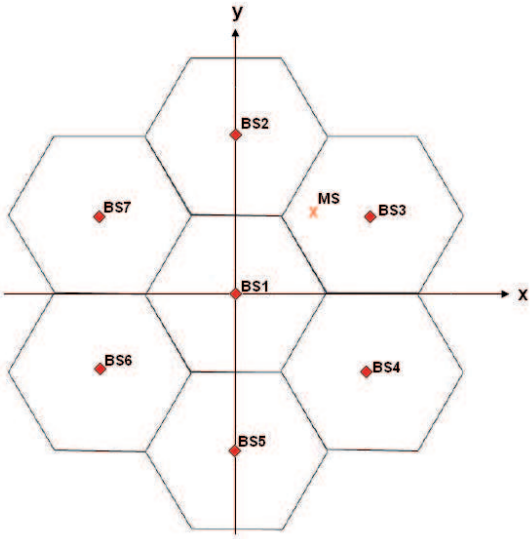

Figure 1.1: Example of a cellular network with 7 cells.

received signal expression will be analyzed in the next chapter.

Chapter 2

ToA Estimation using Maximum Likelihood

Detection and estimation of unknown parameters in the system consisted of a signal perturbed by an additive noise is widely considered (see, e.g., [10,11,26–33]). This chapter introduces the relationship between the location of the MS and the time delay of the received signal in each BS. Finally, an estimator of the ToA at any BS is formulated.

The configuration of the wireless localization can be described as follows. The MS transmits a radio signal through a wireless channel to B BSs, where B is the number of the BSs considered in the system. Thereby we assume that the b-th BS has a known location, whose coordinate can be written as (x_b, y_b). The received signal at the b-th BS is $r_b(t)$, which includes the additive noise and the transmitted signal from the MS, whose coordinate is unknown and can be expressed as (x, y).

Fig. 2.1 shows the MS and the b-th BS with their coordinates. The distance between both stations, denoted by d_b, can be noted in this figure. The distance between the MS and the b-th BS is written as

$$d_b = \sqrt{(x - x_b)^2 + (y - y_b)^2}. \tag{2.0.1}$$

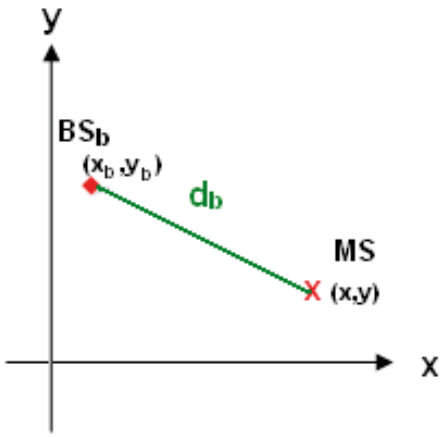

Figure 2.1: Locations of the MS and b-th BS

The signal from the MS to the b-th BS propagates through the wireless channel at the speed of the light, $c = 3 \times 10^8$ (m/s), during certain time, which is denoted by τ_b. The relationship among these parameters can be expressed as

$$d_b = c\tau_b. \tag{2.0.2}$$

Consequently, if the estimated value of τ_b is available, it is possible to obtain the coordinate of the MS using the relationship among d_b, τ_b and the mobile location. However, for the first step, the problem is the determination of τ_b. Then, let us start with the expression of the received signal (see, e.g., [25])

$$r_b(t) = a_b s(t - \tau_b) + n_b(t), \tag{2.0.3}$$

where $r_b(t)$ is the received signal in the b-th BS, a_b and τ_b are the loss gain and the time delay of the propagation to the b-th BS, and $n_b(t)$ is the additive noise at the b-th BS, assumed $n_b(t) = \Re(n_b(t)) + \mathrm{j}\Im(n_b(t))$, where $\Re(n_b(t)) \sim \mathcal{N}(0, \frac{1}{2}\sigma_{\mathrm{n}}^2)$ and $\Im(n_b(t)) \sim \mathcal{N}(0, \frac{1}{2}\sigma_{\mathrm{n}}^2)$ are the real and imaginary parts of the b-th BS noise each assumed to be a Gaussian random process with the variance $\frac{1}{2}\sigma_{\mathrm{n}}^2$ as a unilateral

power spectral density (PSD). Then, the noise is distributed as $n_b(t) \sim \mathcal{N}_{\mathcal{C}}(0, \sigma_{\mathrm{n}}^2)$, i.e., a complex-valued zero-mean white Gaussian process with the double-sided PSD σ_{n}^2 (Joule).

The multipath can be appended to (2.0.3). All the NLoS paths excluding the first LoS path can be treated as an interference term, which can be handled by an interference cancellation or joint estimation. The single path is considered herein for the purpose of minimal achievable accuracy investigation, since the CRB of the multipath is lower bounded by the CRB of the single path (see, e.g., [20]).

In (2.0.3), τ_b is the parameter to be determined. In literature, the path gain a_b is modeled as a deterministic parameter (see, e.g., [10,11,27–33]). However, it can be elaborated in a more precise way to include the propagation effect. The value of a_b can be determined from the expression of the energy of the received signal at the b-th BS as (see, e.g., [34])

$$E_b = \kappa \left(\frac{d_0}{d_b} \right)^{\gamma_b} E_{\mathrm{s}}, \tag{2.0.4}$$

where d_0 is the close-in distance in the far field region, d_b is the distance between the MS and the b-th BS, γ_b is the exponent of the path loss propagation or PLE at the b-th BS, E_{s} is the energy of the transmitted signal $s(t)$ over the period $(0, T_{\mathrm{o}}]$ given by

$$E_{\mathrm{s}} = \int_0^{T_{\mathrm{o}}} |s(t)|^2 \, \mathrm{d}t, \tag{2.0.5}$$

and κ is the unitless constant depending on antenna characteristics and average channel attenuation given by

$$\kappa = \frac{c^2}{16\pi^2 {d_0}^2 {f_0}^2}, \tag{2.0.6}$$

with the center frequency of the wireless system f_0. The channel is assumed static in such a way that the unknown parameter τ_b is invariant over the observation

period $(0, T_{\mathrm{o}}]$. In addition, we assume that the large-scale fading can be considered as a spatial average over the small-scale fluctuations of the signals [21, p. 847].

The energy of the received signal at the b-th BS can also be calculated by using its definition given by

$$\begin{aligned} E_b &= \int_0^{T_{\mathrm{o}}} |a_b s(t-\tau_b)|^2 \,\mathrm{d}t \\ &= a_b^2 \int_0^{T_{\mathrm{o}}} |s(t-\tau_b)|^2 \,\mathrm{d}t \\ &= a_b^2 E_{\mathrm{s}}. \end{aligned} \tag{2.0.7}$$

The last equality in (2.0.7) holds from the condition in which the observation time T_{o} is much larger than the ToA τ_b. Comparing (2.0.4) to (2.0.7) and taking into account (2.0.2), the expression of a_b can be written as

$$a_b = \sqrt{\kappa} \left(\frac{d_0}{c\tau_b} \right)^{\frac{1}{2}\gamma_b}. \tag{2.0.8}$$

In (2.0.8), it is possible to observe that a_b depends on τ_b. Therefore, this has to be taken into account for calculating τ_b. To estimate τ_b, which is the time delay propagation from the MS to the b-th BS, we consider the ML estimation method. This is because the ML can provide the error variance comparable to a theoretical performance bound, e.g., CRB (see, e.g., [27,29,30]). First, we need to know the distribution of the received signal given by (2.0.3), where the term $a_b s(t-\tau_b)$ is deterministic and the term $n_b(t)$ is a complex-valued zero-mean white Gaussian process with the double-sided power spectral density σ_{n}^2 (Joule). Then, the probability density function (PDF) of the received signal can be written as (see, e.g., [35–38])

$$p_{r_b(t)}(r_b(t)|\tau_b)) = \frac{1}{\pi\sigma_{\mathrm{n}}^2} \mathrm{e}^{-\frac{1}{\sigma_{\mathrm{n}}^2}|r_b(t)-a_b s(t-\tau_b)|^2}. \tag{2.0.9}$$

The likelihood function[1] can be defined as

$$l(\tau_b|r_b(t);t\in(0,T_\mathrm{o}])=\int_0^{T_\mathrm{o}}\ln\left(p_{r_b(t)}(r_b(t);t\in(0,T_\mathrm{o}]|\tau_b)\right)\mathrm{d}t. \tag{2.0.10}$$

Thereby, $l(\tau_b|r_b(t);t\in(0,T_\mathrm{o}])$ allows us to predict what values τ_b would be, given the observation data $r_b(t);t\in(0,T_\mathrm{o}]$. Afterwards, the ML method is cast into finding the most likely value of τ_b, i.e.,

$$\hat{\tau}_b=\arg\max_{\tau} l(\tau_b|r_b(t);t\in(0,T_\mathrm{o}]). \tag{2.0.11}$$

Substituting (2.0.9) into (2.0.10), the expression of $l(\tau_b|r_b(t);t\in(0,T_\mathrm{o}])$ can be derived from

$$\begin{aligned} l(\tau_b|r_b(t);t\in(0,T_\mathrm{o}]) &= \int_0^{T_\mathrm{o}}\ln\left(\frac{1}{\pi\sigma_\mathrm{n}^2}\mathrm{e}^{-\frac{1}{\sigma_\mathrm{n}^2}|r_b(t)-a_b s(t-\tau_b)|^2}\right)\mathrm{d}t \\ &= \int_0^{T_\mathrm{o}}\ln\left(\frac{1}{\pi\sigma_\mathrm{n}^2}\right)-\frac{1}{\sigma_\mathrm{n}^2}|r_b(t)-a_b s(t-\tau_b)|^2\mathrm{d}t. \end{aligned} \tag{2.0.12}$$

If (2.0.12) is inserted into (2.0.11), the expression of τ_b can be obtained as follows

$$\hat{\tau}_b=\arg\max_{\tau_b}\int_0^{T_\mathrm{o}}\ln\left(\frac{1}{\pi\sigma_\mathrm{n}^2}\right)-\frac{1}{\sigma_\mathrm{n}^2}|r_b(t)-a_b s(t-\tau_b)|^2\mathrm{d}t. \tag{2.0.13}$$

In (2.0.13), the first term can be removed, because it does not depend on τ_b. Furthermore, $\arg\max_{\tau_b}$ can be written as $\arg\min_{\tau_b}$, because the maximum of a negative quantity is the minimum of this quantity changing the sign, thus yielding

$$\hat{\tau}_b=\arg\min_{\tau_b}\frac{1}{\sigma_\mathrm{n}^2}\int_0^{T_\mathrm{o}}\left|r_b(t)-a_b s(t-\tau_b)\right|^2\mathrm{d}t. \tag{2.0.14}$$

The square in the integral can be expanded into

$$\hat{\tau}_b=\arg\min_{\tau_b}E_b-\int_0^{T_\mathrm{o}}\Re(2a_b s^*(t-\tau_b)r_b(t))\,\mathrm{d}t+a_b^2E_\mathrm{s}. \tag{2.0.15}$$

[1]This log-likelihood function is derived here in an intuitive manner (see, e.g., [39]). More details of the derivation based on the Karhunen-Loève expansion can be found in, e.g., [28, p. 279], [29, p. 37], and [31, p. 298], or based on the sampling approach in [40, p. 54].

Finally, the energy of the received signal, E_b, can be removed, because it does not depend on τ_b, hence yielding

$$\hat{\tau}_b = \arg\min_{\tau_b} a_b^2 E_\mathrm{s} - 2a_b \int_0^{T_\mathrm{o}} \Re(s^*(t-\tau_b) r_b(t))\,\mathrm{d}t. \tag{2.0.16}$$

In this way, we can determine the estimated value of τ_b, which depends on the loss gain a_b, the energy of the transmitted signal, and the correlation between the transmitted and received signals. The implementation of the ToA estimator in MATLAB® is provided in Chapter 4.

Chapter 3

Transmitted Signals

The estimation of the propagation time in the previous chapter can be applied to any transmitted signal, whose waveform must be known. In this chapter, let us consider the transmitted signal. We choose a transmitted signal which will enable a more realistic analysis of the wireless communication systems. For this purpose, we use two transmitted signals: the second-derivative Gaussian pulse and the MSK signal for indoor and outdoor environments, respectively.

The second-derivative Gaussian pulse is employed for the indoor environments, because it allows the characterization of antenna effects, which will be discussed later. Moreover, this signal cannot be used in outdoor surroundings, because its extremely wide bandwidth will interfere with other systems. In an alternative way, we shall consider the transmission of a digital signal with the MSK modulation for these environments, because this kind of the modulation is related to the existing systems, for example, GSM.

3.1 Transmitted Signal for Indoor Environments

To analyze a more realistic communication system, let us use the transmitted signal, which includes also the antenna effects. In classical impulse radio ultrawideband (IR-UWB), the subnanosecond technology is introduced in time domain (see, e.g., [41,42]). An example of time-domain signature is a Gaussian regularization of an impulse. To include the realistic transceiver, the antenna effects can be modeled as a differentiation operation. Since the pulse can be distorted as its first derivative in the channel and its second derivative at the receiver, the second-derivative Gaussian pulse is employed in this section. The second-derivative Gaussian pulse can be expressed as (see, e.g., [43])

$$\begin{aligned} p(t) &= \left(1 - 4\pi\left(\frac{t}{\tau_{\mathrm{p}}}\right)^2\right) \mathrm{e}^{-2\pi\left(\frac{t}{\tau_{\mathrm{p}}}\right)^2}; t > 0 \\ &= (1 - 2\alpha(t))\mathrm{e}^{-\alpha(t)}; t > 0. \end{aligned} \tag{3.1.1}$$

where τ_{p} is the pulse-shaping factor, $\alpha(t) = 2\pi\left(\frac{t}{\tau_{\mathrm{p}}}\right)^2$ is an even function of t, and τ_{p} is the pulse-shaping factor, which can, for example, be chosen as $\tau_{\mathrm{p}} = 0.2877$ ns to yield the pulse width T_{p} of 0.7 ns.

This pulse is shown using MATLAB® in Fig. 3.1. In this figure only the positive time part of the pulse can be observed. Therefore, it is necessary to define the transmitted signal as a delayed version of the second-derivative Gaussian pulse, which possesses a complete cycle in the positive time axis. As illustrated in Fig. 3.2, the desired transmitted signal can be written as

$$s(t) = p\left(t - \frac{1}{2}T_{\mathrm{p}}\right); t > 0. \tag{3.1.2}$$

The next step is the determination of the received signal. The transmitted signal,

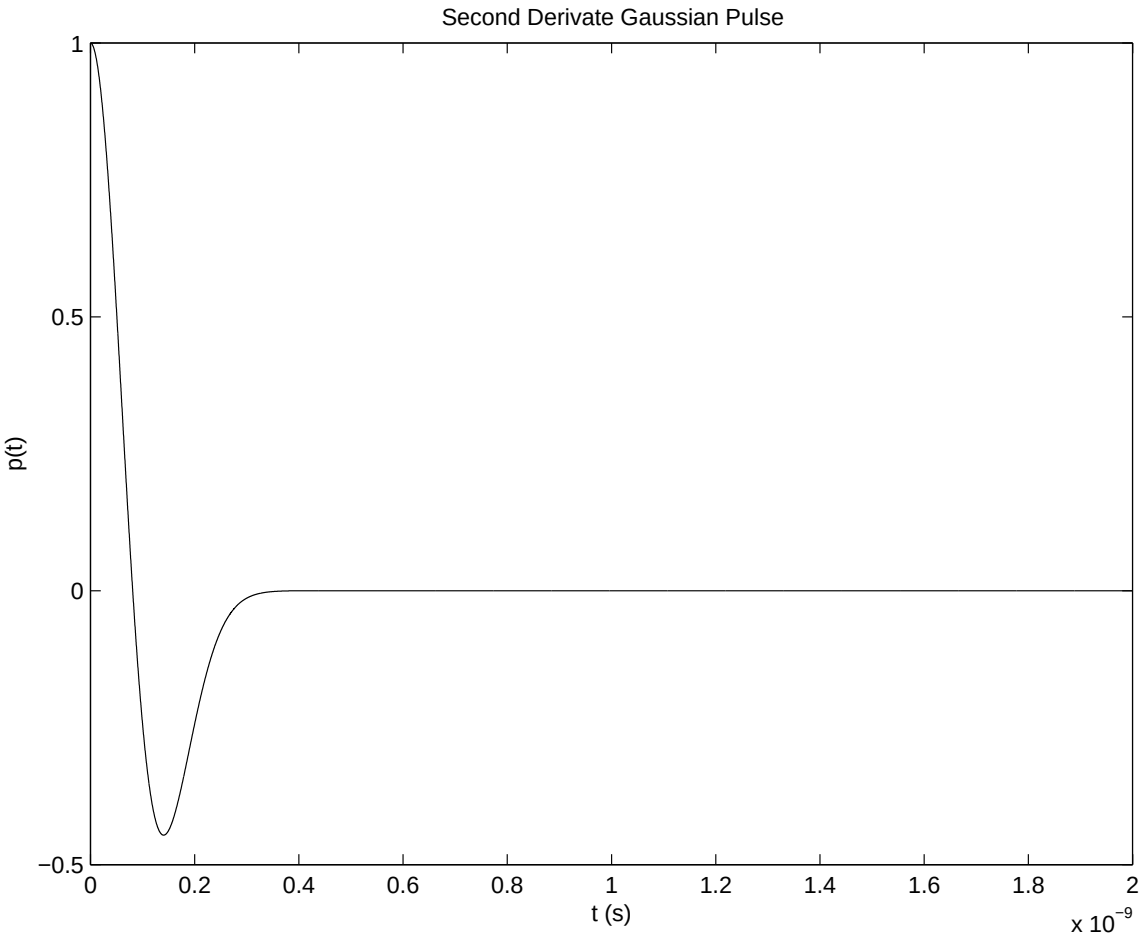

Figure 3.1: Second-derivative Gaussian pulse.

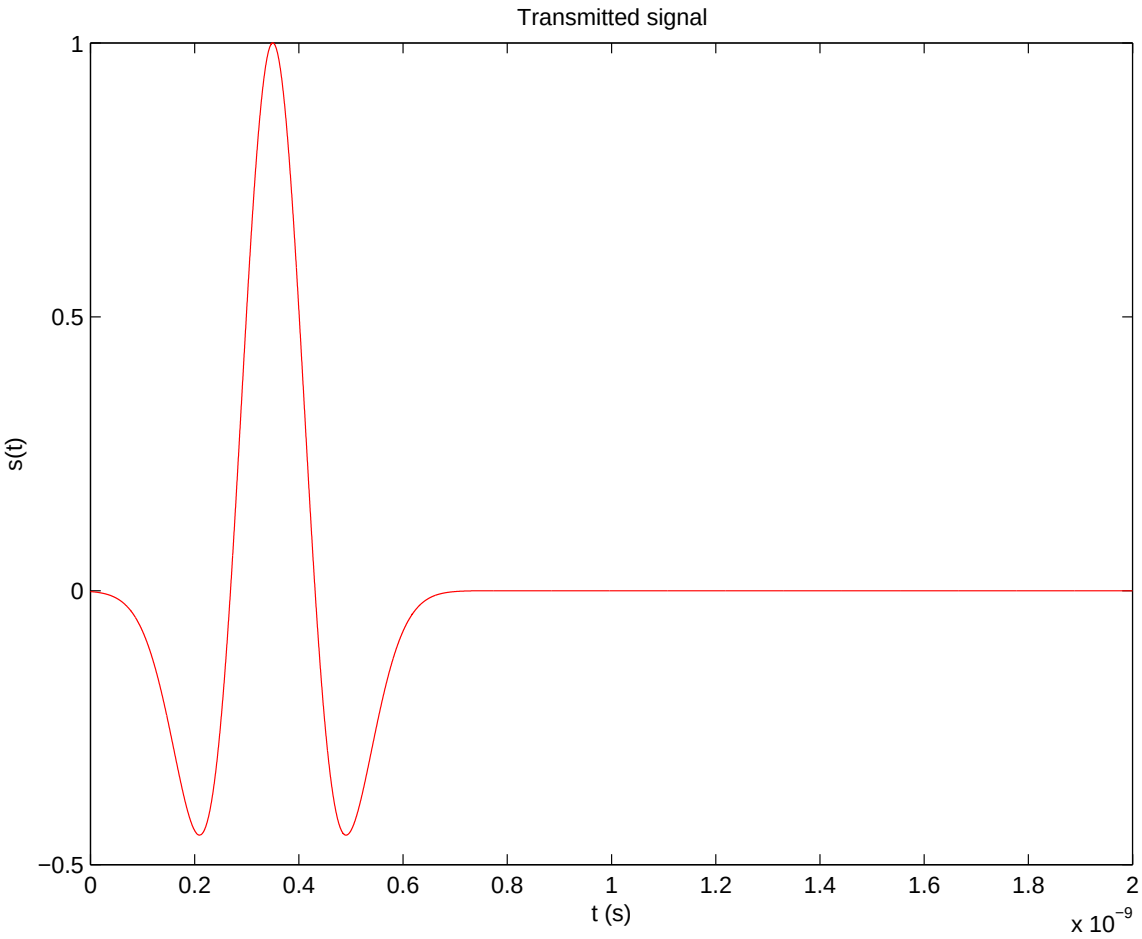

Figure 3.2: Transmitted signal.

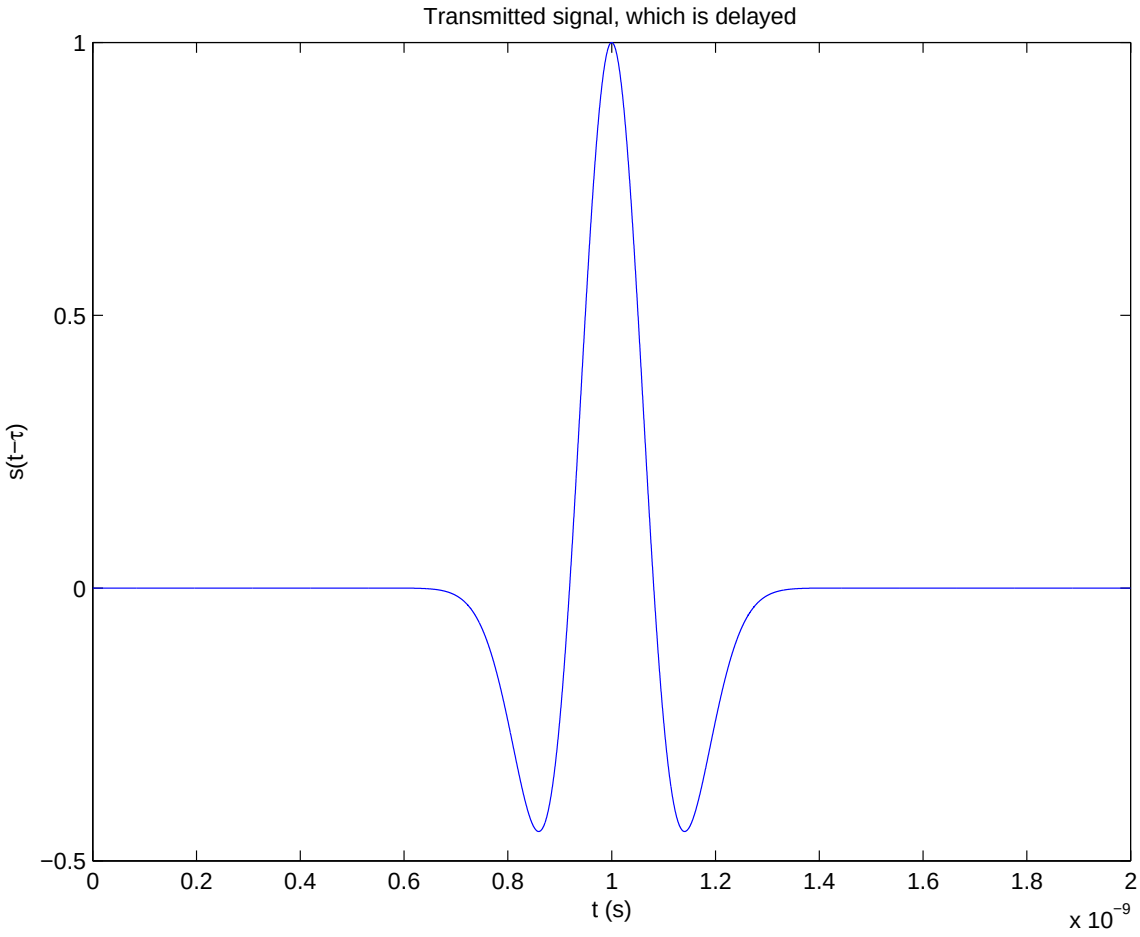

Figure 3.3: Transmitted signal, which is delayed.

which propagates through the medium between the MS and the BS, suffers a time delay. In this section, the time delay is assumed to be $\tau = 0.65$ ns. Fig. 3.3 shows the transmitted signal $s(t)$, which is delayed for τ, i.e., $s(t - \tau)$.

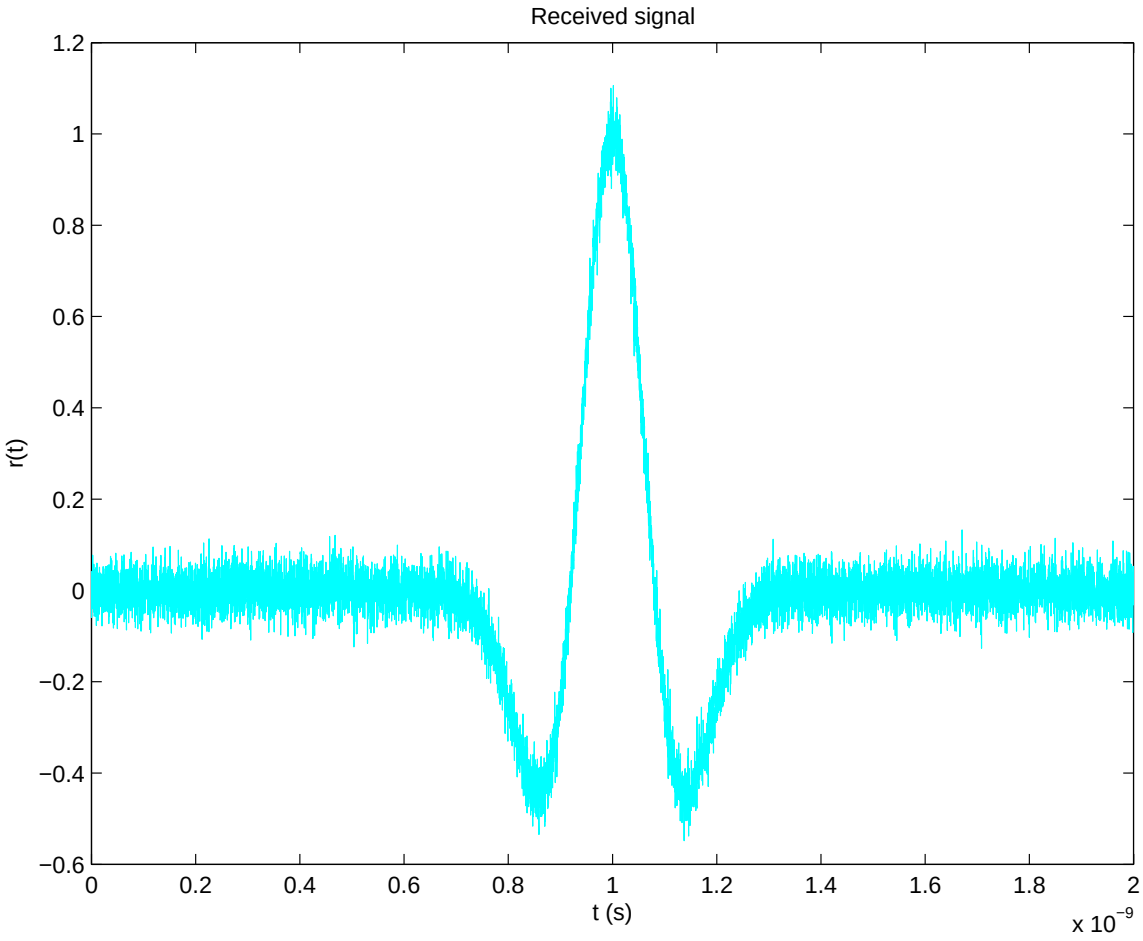

Figure 3.4: Received signal.

However, $s(t-\tau)$ is not the received signal, because the antennas at the receiver are not perfect and are subject to an additive noise. The received signal can be expressed as $r_b(t) = a_b s(t - \tau_b) + n_b(t)$, where a_b and τ_b are the loss gain and the time delay of the propagation to the b-th BS, and the additive noise at the b-th BS $n_b(t)$.

The received signal is shown in Fig. 3.4, where $\tau = 0.65$ ns, $a_b = 1$ and $\sigma_{\mathrm{n}}^2 = 0.0025$ (Joule). In order to compare among them, all the signals are plotted in the

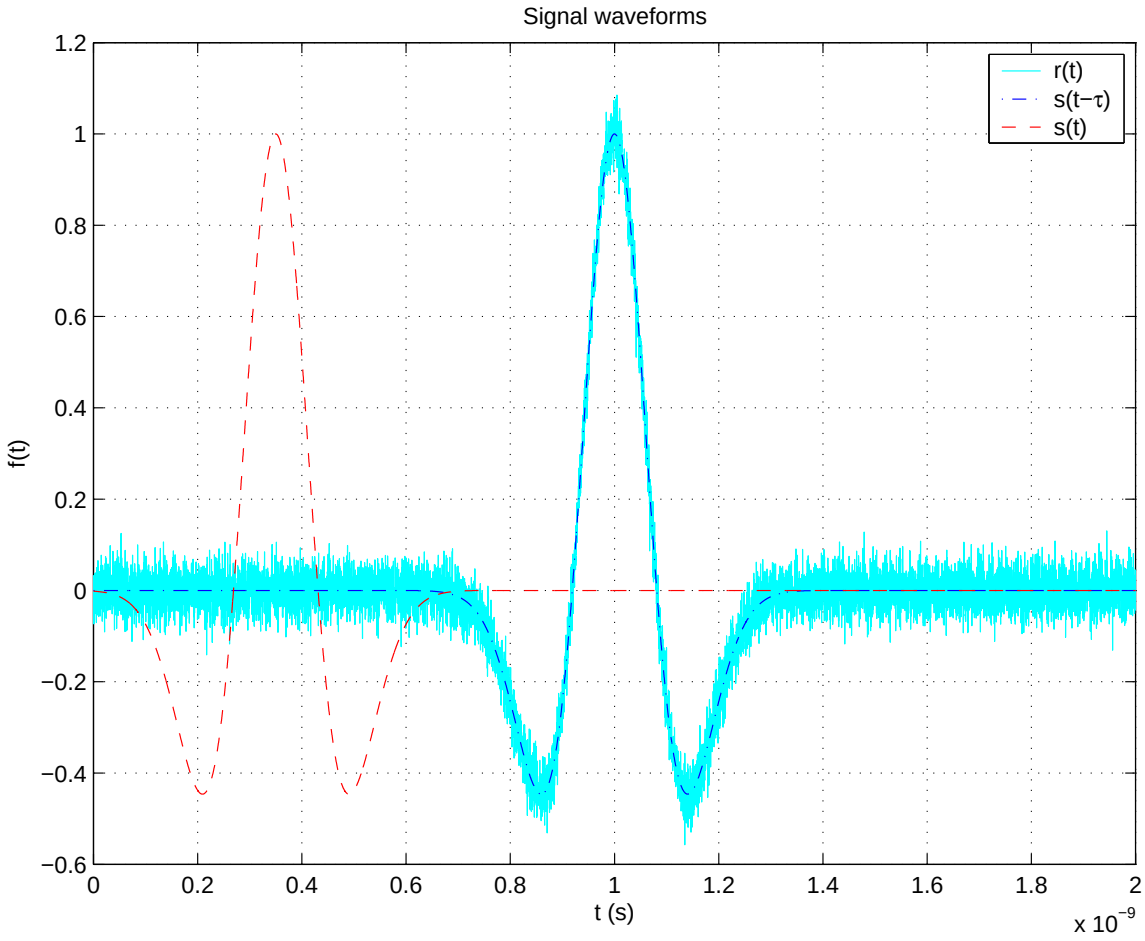

Figure 3.5: Signal waveforms.

same figure, being possible to see the time delay between the transmitted and received signals, and the noise effect in the received signal.

In Fig. 3.5, a_b is assumed to be one for simplicity. However, a_b usually depends on the distance between the b-th BS and the MS and is less than one. Now, the distance between both stations will be fixed as 6 m and the value of a_b can be obtained by using (2.0.8) and (2.0.6). For $f_0 = 1.9$ GHz, $d_0 = 100$ m and $\gamma_b = 2.5$, the value of a_b is 0.0042 which is much smaller than 1. Finally, the double-sided

power spectral density of the noise can be derived from

$$\mathrm{SNR}_{\mathrm{Rx}} = \frac{a_b^2 E_{\mathrm{s}}}{\sigma_{\mathrm{n}}^2}, \tag{3.1.3}$$

where $\mathrm{SNR}_{\mathrm{Rx}}$ is the received signal-to-noise ratio and σ_{n}^2 is the noise variance given by

$$\sigma_{\mathrm{n}}^2 = \frac{a_b^2 E_{\mathrm{s}}}{\mathrm{SNR}_{\mathrm{Rx}}}. \tag{3.1.4}$$

The received SNR has been fixed as 40 dB. Thus, by introducing this value in (3.1.4), the double-sided power spectral density of the noise is $\sigma_{\mathrm{n}}^2 = 7.7255 \times 10^{-8}$ Joule.

Fig. 3.6 and Fig. 3.7 show the transmitted and the received signals, respectively. The received signal includes the noise, the time delay and a smaller amplitude than the transmitted signal, because of the attenuation caused by the propagation through the distance of 6 m between the transmitter and the receiver.

3.2 Effective Bandwidth of Second-Derivative Gaussian Monocycle

The Fourier transforms in this work are performed without normalization, i.e., without the factor $\frac{1}{\sqrt{2\pi}}$. For notation simplicity, the Fourier transforms in angular frequency, denoted by $S(\omega)$, is equivalent to the Fourier transform in ordinary frequency, denoted by $S(f)$. Strictly speaking, we have $S(\omega) = S(2\pi f) \equiv S(f)$. The

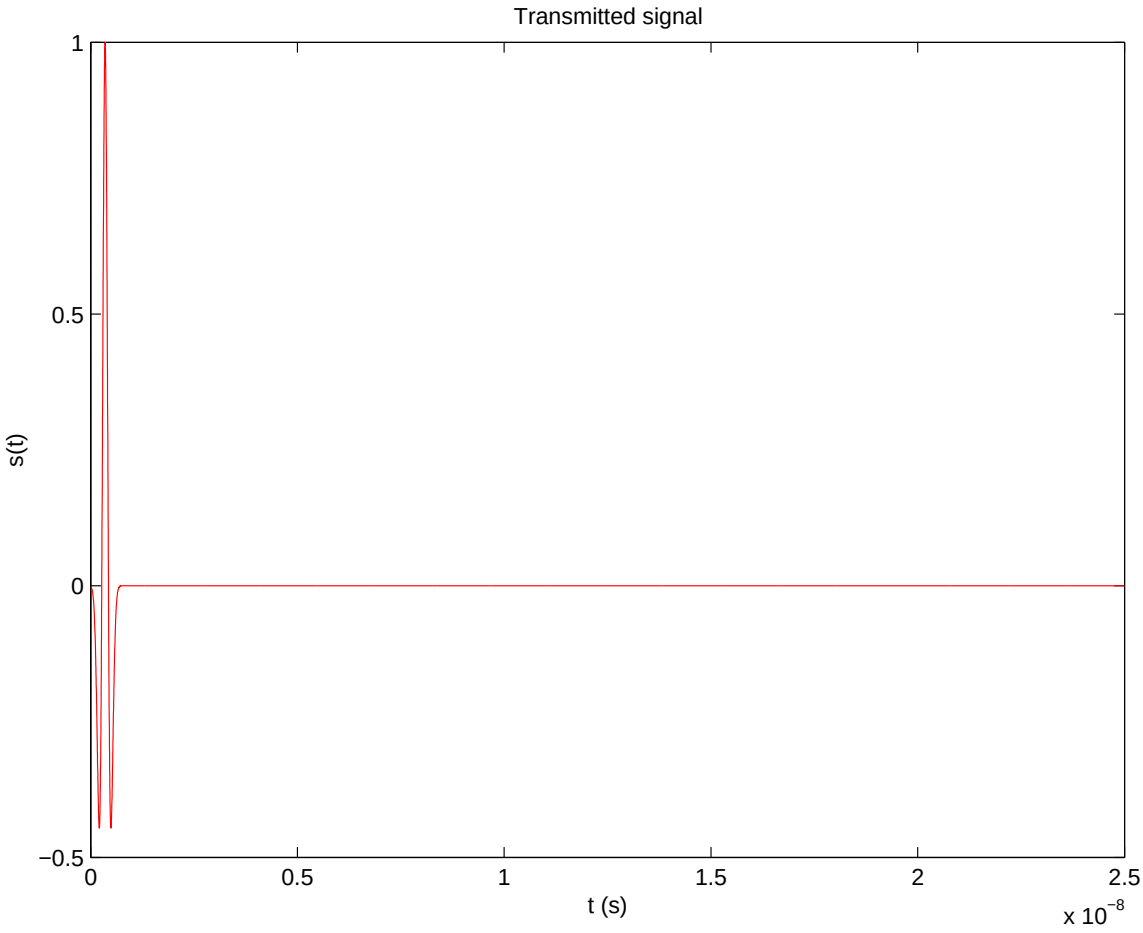

Figure 3.6: Transmitted signal for $d_b = 6$ m.

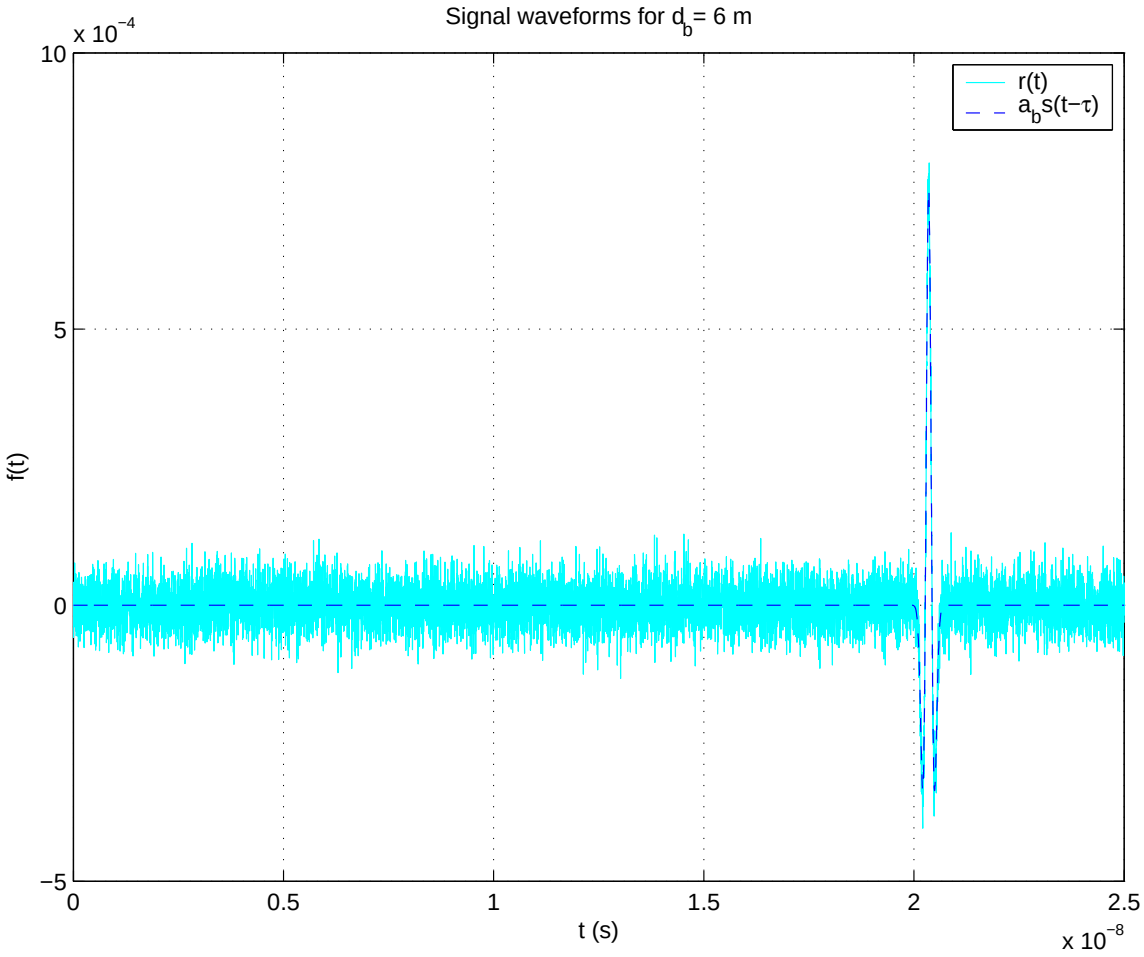

Figure 3.7: Signal waveforms for $d_b = 6$ m.

effective bandwidth can be derived from (see, e.g., [29] and [44, p.43])

$$\begin{aligned}\bar{\beta} &= \sqrt{\frac{\int_{-\infty}^{\infty} f^2 |S(f)|^2 \mathrm{d}f}{\int_{-\infty}^{\infty} |S(f)|^2 \mathrm{d}f}} \\ &= \sqrt{\frac{\int_{-\infty}^{\infty} \frac{1}{(2\pi)^2} (2\pi f)^2 |S(f)|^2 \mathrm{d}f}{\int_{-\infty}^{\infty} |S(f)|^2 \mathrm{d}f}} \\ &= \frac{1}{2\pi} \sqrt{\frac{\int_{-\infty}^{\infty} \omega^2 |S(\omega)|^2 \mathrm{d}\omega}{\int_{-\infty}^{\infty} |S(\omega)|^2 \mathrm{d}\omega}},\end{aligned} \tag{3.2.1}$$

where $S(\omega)$ is the Fourier transform of the transmitted signal $s(t)$.

Proposition 3.2.1. *The effective bandwidth calculated from the integrals assuming an infinite duration pulse is given by*

$$\bar{\beta} = \frac{1}{\tau_{\mathrm{p}}}\sqrt{\frac{5}{2\pi}}. \tag{3.2.2}$$

Proof. See Appendix A.1. □

Note that the above effective bandwidth in angular frequency, i.e., without the factor $\frac{1}{2\pi}$, coincides with the result derived for any n-th derivative Gaussian pulse in, e.g., [45, eq. (8)]. Moreover, the value of $\bar{\beta}$ in time domain is given by

$$\bar{\beta} = \frac{1}{2\pi}\sqrt{\frac{\int_{-\infty}^{\infty}\dot{s}^2(t)\mathrm{d}t}{\int_{-\infty}^{\infty}s^2(t)\mathrm{d}t}}, \tag{3.2.3}$$

where $\dot{s}(t) = \frac{\partial}{\partial t}s(t)$ is the derivative of the signal. The theoretical effective bandwidth obtained in the frequency domain is shown in Fig. 3.8, where the numerical results for the effective bandwidth in the time domain are also shown. This figure shows that the numerical results coincide with the theoretical computation.

3.3 Effective Absolute Central Frequency

In this case, we work with the carrierless system, and therefore we have to consider the effective central frequency, which is given by (see, e.g., [46, eq. (7.18)])

$$\bar{f} = \frac{1}{2\pi}\frac{\int_{-\infty}^{\infty}\omega|S(\omega)|^2\mathrm{d}\omega}{\int_{-\infty}^{\infty}|S(\omega)|^2\mathrm{d}\omega}. \tag{3.3.1}$$

The integral $\int_{-\infty}^{\infty}|S(\omega)|^2\mathrm{d}\omega$ is given by (A.1.16), and the integral $\int_{-\infty}^{\infty}\omega|S(\omega)|^2\mathrm{d}\omega$ can be written by using (A.1.10) as

$$\begin{aligned}\int_{-\infty}^{\infty}\omega|S(\omega)|^2\mathrm{d}\omega &= \int_{-\infty}^{+\infty}\frac{\tau_{\mathrm{p}}^6}{32\pi^2}\omega^5\mathrm{e}^{-\frac{\tau_{\mathrm{p}}^2}{4\pi}\omega^2}\mathrm{d}\omega \\ &= \int_{-\infty}^{0}\frac{\tau_{\mathrm{p}}^6}{32\pi^2}\omega^5\mathrm{e}^{-\frac{\tau_{\mathrm{p}}^2}{4\pi}\omega^2}\mathrm{d}\omega + \int_{0}^{+\infty}\frac{\tau_{\mathrm{p}}^6}{32\pi^2}\omega^5\mathrm{e}^{-\frac{\tau_{\mathrm{p}}^2}{4\pi}\omega^2}\mathrm{d}\omega \\ &= \frac{\tau_{\mathrm{p}}^6}{32\pi^2}\left(\int_{-\infty}^{0}\omega^5\mathrm{e}^{-\frac{\tau_{\mathrm{p}}^2}{4\pi}\omega^2}\mathrm{d}\omega + \int_{0}^{+\infty}\omega^5\mathrm{e}^{-\frac{\tau_{\mathrm{p}}^2}{4\pi}\omega^2}\mathrm{d}\omega\right).\end{aligned} \tag{3.3.2}$$

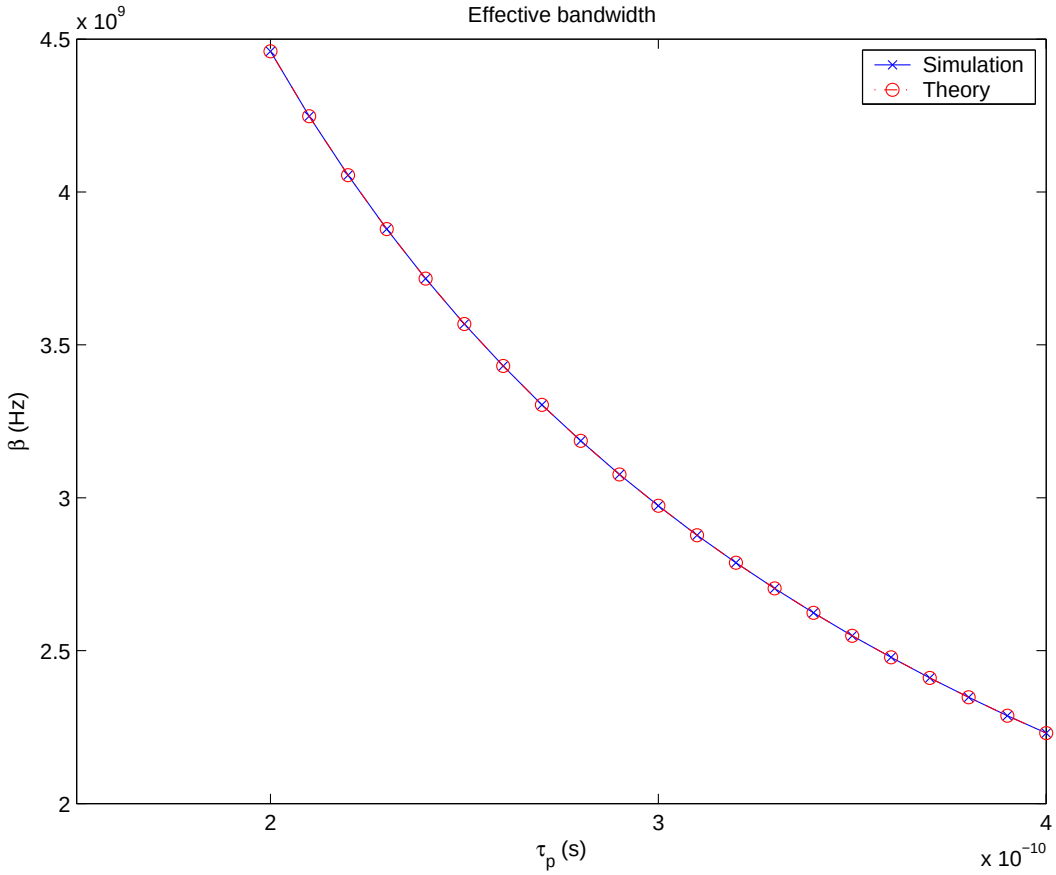

Figure 3.8: The effective bandwidth of the second-derivative Gaussian pulse.

Let $u(\omega) = -\omega$ be a dummy variable. It can be shown that

$$\begin{aligned}
\int_{-\infty}^{\infty} \omega |S(\omega)|^2 \mathrm{d}\omega &= \int_{-\infty}^{+\infty} \frac{\tau_{\mathrm{p}}^6}{32\pi^2} \omega^5 \mathrm{e}^{-\frac{\tau_{\mathrm{p}}^2}{4\pi}\omega^2} \mathrm{d}\omega \\
&= \frac{\tau_{\mathrm{p}}^6}{32\pi^2} \left(\int_{u(-\infty)}^{0} (-1)(-1) u^5 \mathrm{e}^{-\frac{\tau_{\mathrm{p}}^2}{4\pi}u^2} \mathrm{d}u + \int_{0}^{+\infty} \omega^5 \mathrm{e}^{-\frac{\tau_{\mathrm{p}}^2}{4\pi}\omega^2} \mathrm{d}\omega \right) \\
&= \frac{\tau_{\mathrm{p}}^6}{32\pi^2} \left(\int_{\infty}^{0} u^5 \mathrm{e}^{-\frac{\tau_{\mathrm{p}}^2}{4\pi}u^2} \mathrm{d}u + \int_{0}^{+\infty} \omega^5 \mathrm{e}^{-\frac{\tau_{\mathrm{p}}^2}{4\pi}\omega^2} \mathrm{d}\omega \right) \\
&= \frac{\tau_{\mathrm{p}}^6}{32\pi^2} \left(-\int_{0}^{\infty} u^5 \mathrm{e}^{-\frac{\tau_{\mathrm{p}}^2}{4\pi}u^2} \mathrm{d}u + \int_{0}^{+\infty} \omega^5 \mathrm{e}^{-\frac{\tau_{\mathrm{p}}^2}{4\pi}\omega^2} \mathrm{d}\omega \right) \\
&= 0.
\end{aligned} \tag{3.3.3}$$

Since the effective central frequency remains zero, we have to consider the effective value of the absolute central frequency. The effective absolute central frequency is defined by

$$\bar{f}_{\mathrm{abs}} = \frac{1}{2\pi} \frac{\int_{-\infty}^{\infty} |\omega| |S(\omega)|^2 \mathrm{d}\omega}{\int_{-\infty}^{\infty} |S(\omega)|^2 \mathrm{d}\omega}. \tag{3.3.4}$$

Proposition 3.3.1. *The effective absolute central frequency is given by*

$$\bar{f}_{\mathrm{abs}} = \frac{1}{\tau_{\mathrm{p}}} \frac{16}{3\pi}. \tag{3.3.5}$$

Proof. See Appendix A.2. □

In [44, p. 44], another quantity of the signal is introduced as a mean frequency. The mean frequency can be expressed in spatial frequency as [44, eq. (3.19)]

$$\bar{f}_0 = \frac{1}{2\pi} \frac{\int_0^{\infty} \omega |S(\omega)|^2 \mathrm{d}\omega}{\int_0^{\infty} |S(\omega)|^2 \mathrm{d}\omega}. \tag{3.3.6}$$

Note that the integrations are performed over the positive portion of the frequency, i.e., $\omega \in [0, \infty)$. Without difficulty, it can be shown that the mean frequency is the same as the effective absolute center frequency, i.e., $\bar{f}_0 = \bar{f}_{\mathrm{abs}}$. Moreover, by choosing $\tau_{\mathrm{p}} = 0.2877$ ns, which has been used in the second-derivative Gaussian monocycle, the effective absolute central frequency is $\bar{f}_{\mathrm{abs}} = 5.9008$ GHz.

3.4 Transmitted Signal for Outdoor Environments

With the purpose of obtaining a more realistic analysis, we use the digital transmission modulated with the MSK, because this modulation scheme is really used in the wireless system, for example, in GSM systems which use the Gaussian MSK (GMSK) modulation. The GMSK involves filtering the digital signal with a Gaussian filter and the filtered signal is modulated with the MSK. This modulation is a scheme developed to reduce the maximum phase shift, and hence keep the amplitude quasi-constant during the transmission over the band-limited wireless channel.

The MSK is a digital FM modulation with the modulation index $m = 0.5$. The mathematical expression for an MSK modulated signal with $x(t)$ as a modulating signal is given by (see, e.g., [47])

$$s(t) = A\cos\left(2\pi f_0 t + 2\pi \triangle f \int_{-\infty}^{t} x(t')\,\mathrm{d}t'\right), \tag{3.4.1}$$

where A is the amplitude of the signal, $\triangle f$ is the deviation of frequency and f_0 is the carrier frequency of the modulation. The modulating signal $x(t)$ is a digital signal, which can present two values $+1$ or -1. Then, (3.4.1) can be written by

$$s(t) = A\cos\left(\omega_0 t \pm 2\pi \triangle f t + \theta\right), \tag{3.4.2}$$

where θ is the phase, which depends on the values of the modulating signal, as we will see below. If bit rate is R_{B} and the period of bit is $T = \frac{1}{R_{\mathrm{B}}}$, it is necessary to choose $\triangle f$ in such a way that

$$2\pi \triangle f T = \frac{\pi}{2}, \tag{3.4.3}$$

which results in

$$\triangle f = \frac{1}{4T}. \tag{3.4.4}$$

The modulation index can be defined as the quotient between maximum frequency deviation and the period of the bit, i.e., (see, e.g., [47])

$$\begin{aligned} m &= \frac{2\triangle f}{T} \\ &= \frac{\frac{1}{2}T}{\frac{1}{T}} \\ &= 0.5. \end{aligned} \tag{3.4.5}$$

Although the MSK is a frequency modulation, it can be expressed in term of phase and quadrature components, i.e., (see, e.g., [47] and [48, pp. 118-128])

$$s(t) = v_i \cos\left(\pm\frac{\pi t}{2T}\right)\cos\left(2\pi f_0 t\right) + q_i \sin\left(\pm\frac{\pi t}{2T}\right)\sin\left(2\pi f_0 t\right), \tag{3.4.6}$$

where the pair (v_i, q_i) again represents the mapping of two successive information bits into one of four possible pairs, a case of which appeared in the following table.

Successive binary pairs	v_i	q_i
00	-1	-1
01	-1	+1
10	+1	-1
11	+1	+1

Table 3.1: The example of mapping the binary input sequence into the MSK pairs (v_i, q_i).

The MSK signal is thus similar to the quadrature phase shift keying (QPSK) signal, except that the shaping function $\sin\left(\pm\frac{\pi t}{2T}\right)$ multiplying the quadrature carrier term is in quadrature to the shaping function $\cos\left(\pm\frac{\pi t}{2T}\right)$ used to multiply the inphase carrier term. The term $\sin\left(\pm\frac{\pi t}{2T}\right)$ arises simply, because of the delay T after the low pass filter (LPF) shaping in the quadrature section of the modulator shown in

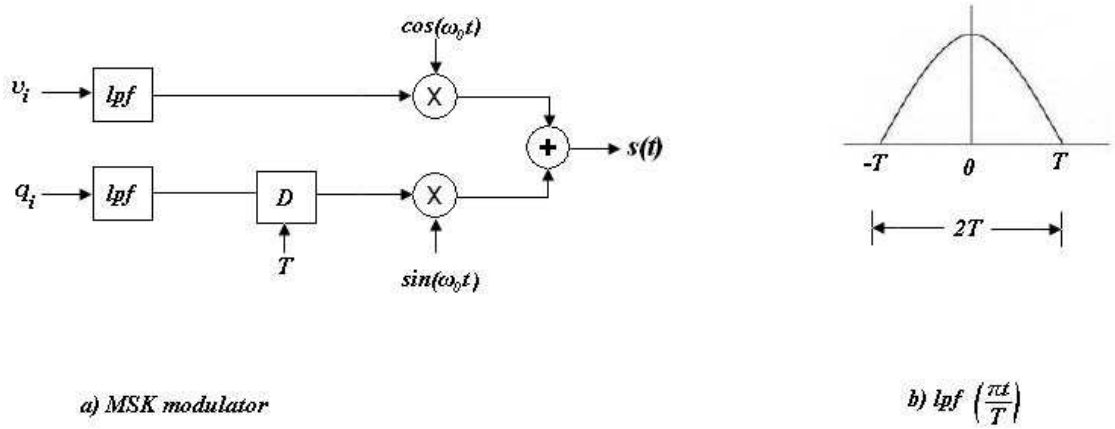

Figure 3.9: MSK modulator.

Fig. 3.9. Note that the coefficients v_i and q_i change every T s (see, e.g., [48, pp. 118-128]). By using a trigonometry identity, (3.4.6) may be rewritten in the following equivalent form [48, pp. 118-128]

$$s(t) = A\cos\left(\omega_0 t - \frac{v_i q_i \pi t}{2T} + \theta\right); \theta = \begin{cases} 0 & ; v_i = 1, \\ \pi & ; v_i = -1. \end{cases} \tag{3.4.7}$$

Note from this form of the MSK signal $s(t)$ that the signal has the desired constant amplitude. Because of the delay T separating the influence of v_i and q_i, only one of these coefficients can change at a time. The possible change of the maximum phase is thus $\frac{\pi}{2}$ rad.

In order to explain the MSK designation, we have to rewrite the expression for the MSK signal in yet another form

$$s(t) = A\cos\left(\omega_0 t \pm \triangle\omega t + \theta\right); \triangle\omega = 2\pi\triangle f, \tag{3.4.8}$$

which corresponds to (3.4.2). This form is a representative of frequency-shift keying (FSK) with the frequency deviation $\triangle f$ in Hz. As seen, the coefficients v_i and

q_i change every T s, and the maximum phase change is $\pm\frac{\pi}{2}$, i.e., $\triangle\omega T = \frac{\pi}{2}$. The previous equality is true only if the relationship between $\triangle f$ and T is $\triangle f = \frac{1}{4T}$. Consequently, we define $\triangle f = \frac{1}{4T}$ as the MSK condition, i.e., the relationship that we had supposed previously to obtain the modulation index. Therefore, the maximum phase change and the maximum frequency deviation possible in the MSK signal are $\pm\frac{\pi}{2}$ and $2\triangle f$, respectively.

This modulation presents high spectral efficiency, because it allows to transmit two symbols with only one frequency. The transmitted bits can be distinguished by the phase. The MSK presents also low ISI. However, the instantaneous changes in phase may produce little changes in the amplitude, so more difficult is the demodulation. To solve this problem, we can introduce a Gaussian filter before the MSK modulation and we obtain the GMSK modulation used, for example, in the GSM. After analyzing the mathematical expression of the MSK modulation, a MATLAB® program has been implemented to be able to modulate the series of the bits for the transmission. The function, which modulates a frame with a number of the bits in the MSK, is called `MSK mod` and the MATLAB® code of this function is shown in Appendix B.8. This function presents the following input and output parameters:

Function:

`msk=(frame,BR,f0,tau,t,tsample)`

Output parameters:

`msk` is a vector with the samples of the modulated MSK signals.

Input parameters:

`frame` is a vector with the series of the bits to be transmitted.

`BR` is the bit rate.

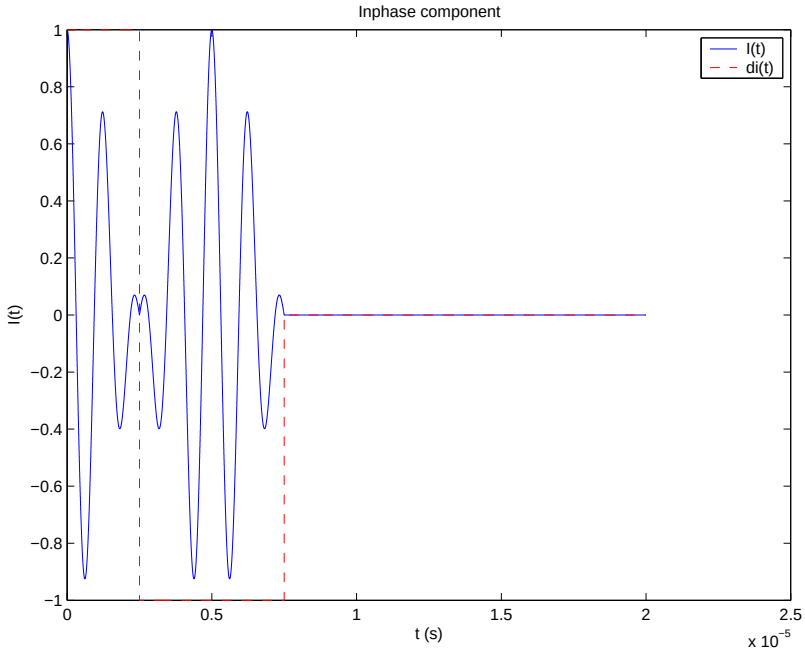

Figure 3.10: Inphase component.

`f0` is the carrier frequency for the MSK modulation.

`tau` is the time delay of the MSK signal.

`t` is a vector with the values of the time axis.

`tsample` is the sampling time.

The process to obtain the MSK signal from series of the bits, called frame, can be explained as follows. We want to transmit, for example, the `frame` $= [1100]$ and let us use $R_{\mathrm{B}} = 400$ kbps, $f_0 = 2R_{\mathrm{B}}$ Hz, sampling time = 100 ns and $\tau = 0$ s for modeling the transmitted signal. The inphase and quadrature signals are exhibited in Fig. 3.10 and Fig. 3.12. In Fig. 3.14, we have the MSK signal as the transmitted signal.

The expression of the received signal is $r_b(t) = a_b s(t-\tau_b)+n_b(t)$, where $s(t-\tau_b)$ is a delayed copy of the transmitted signal, a_b is the loss gain, and $n_b(t)$ is the additive

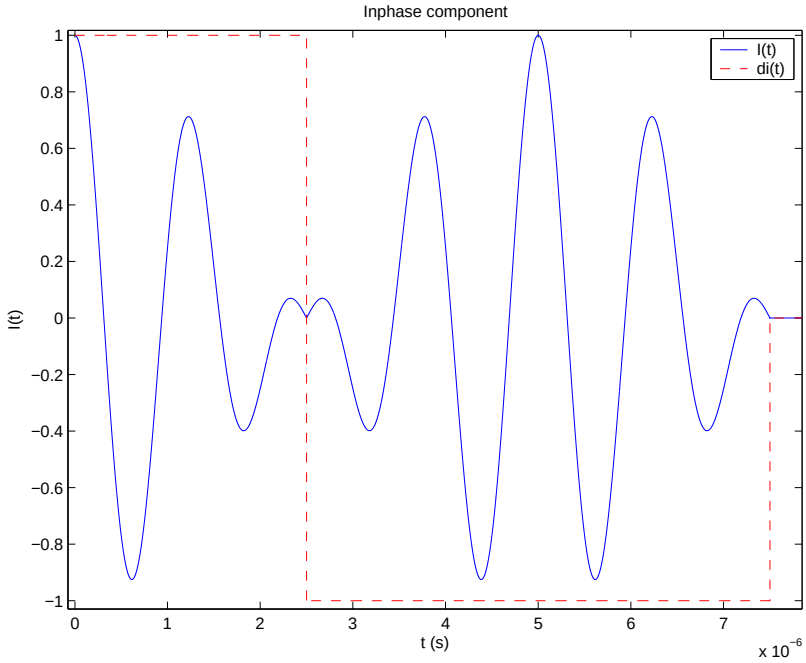

Figure 3.11: Zoomed inphase component.

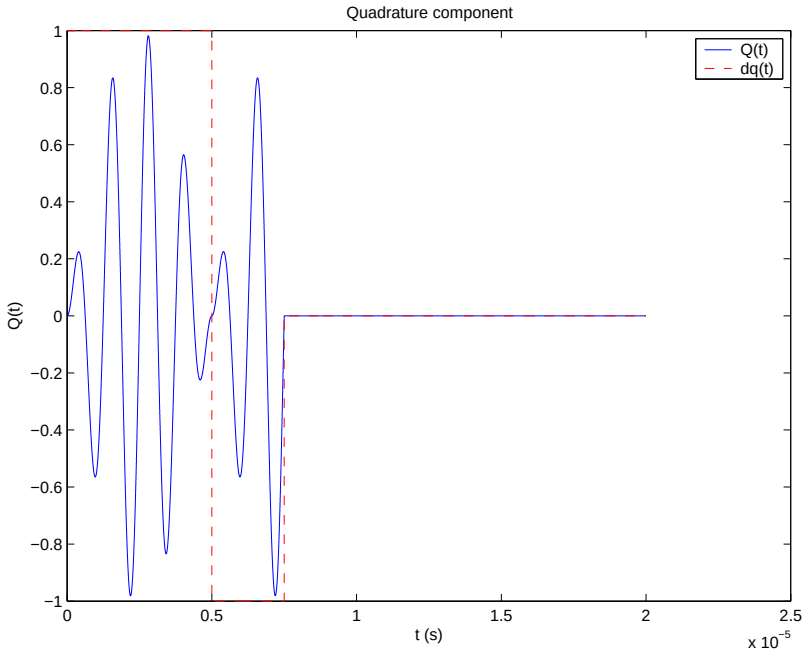

Figure 3.12: Quadrature component.

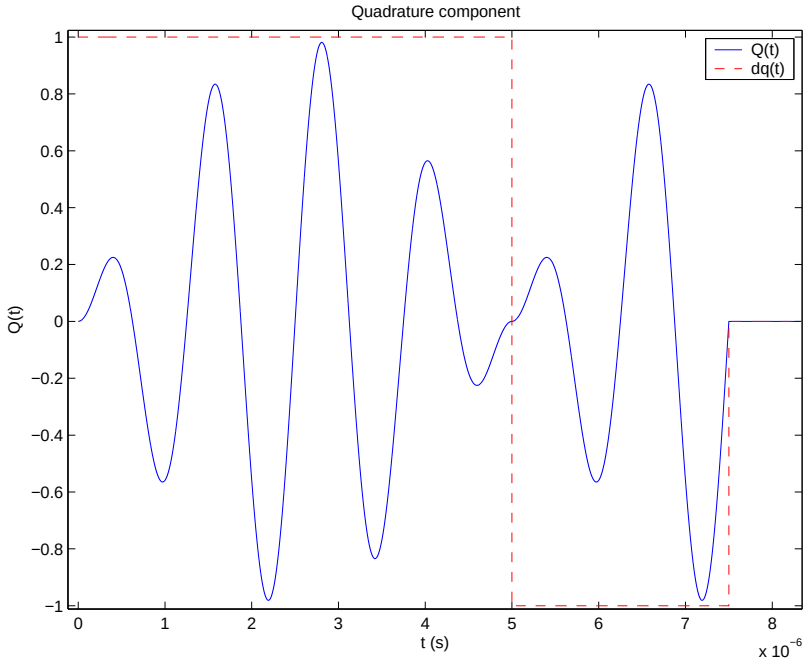

Figure 3.13: Zoomed quadrature component.

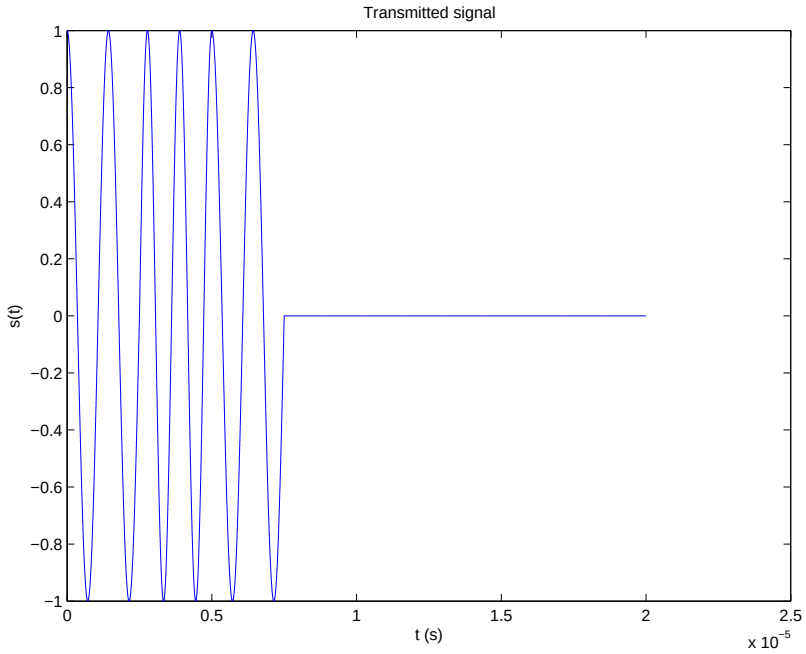

Figure 3.14: The transmitted signal.

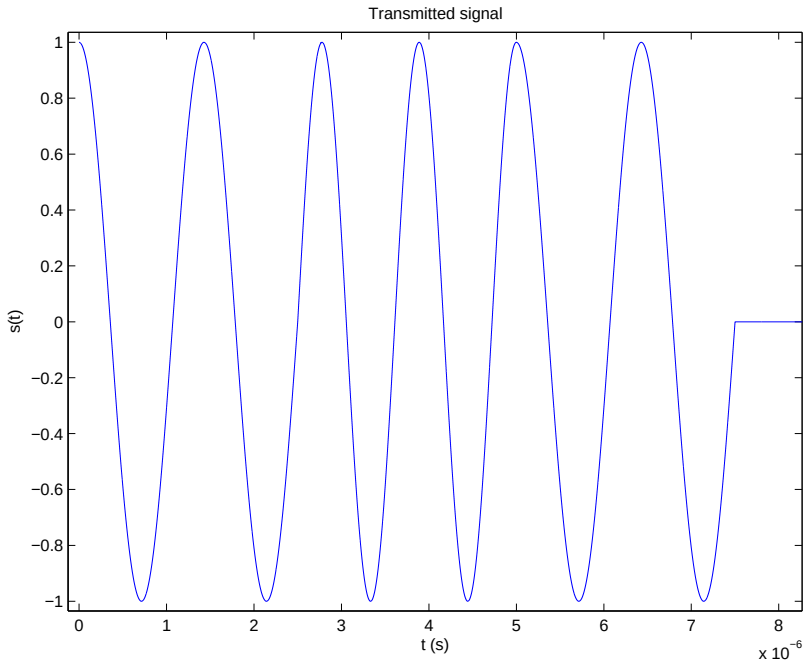

Figure 3.15: The zoomed transmitted signal.

noise at the b-th BS. To model the received signal, it is necessary to introduce a time delay into the transmitted signal, because of the transmission from the MS to the b-th BS. We have chosen $d_b = 3$ km for the distance between both stations. Then, the time delay will be $\tau_b = d_b/c$. In Fig. 3.16, the transmitted signal $s(t)$ can be compared to the delayed transmitted signal $s(t - \tau_b)$. However, $s(t - \tau_b)$ is not the received signal, the loss gain and the additive noise have to be added to $s(t - \tau_b)$ to obtain the received signal. The received signal is shown in Fig. 3.17, where the parameter $\mathrm{SNR}_{\mathrm{Rx}}$ is 60 dB, $\sigma_{\mathrm{n}}^2 = 1.2010 \times 10^{-13}$ (Joule) and $a_b = 1.7896 \times 10^{-6}$.

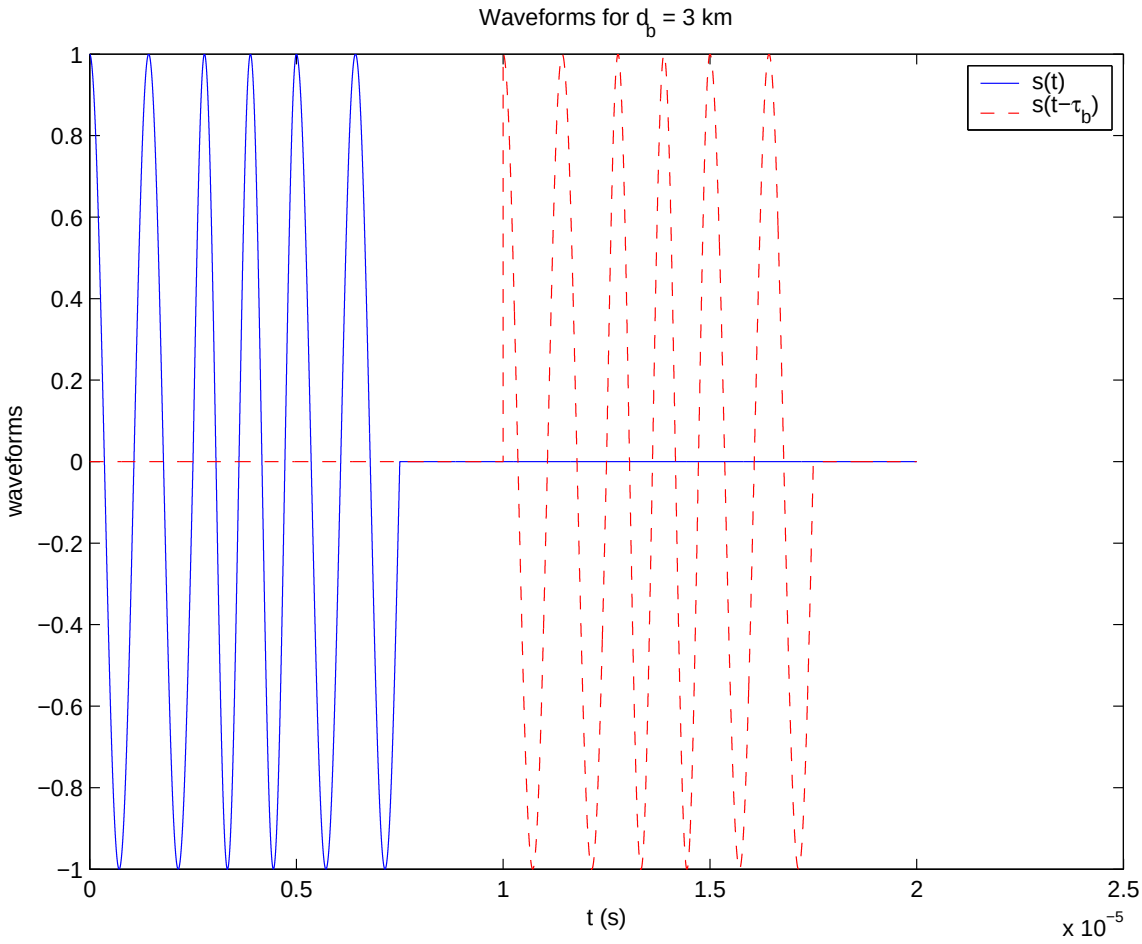

Figure 3.16: The transmitted signal, which is delayed.

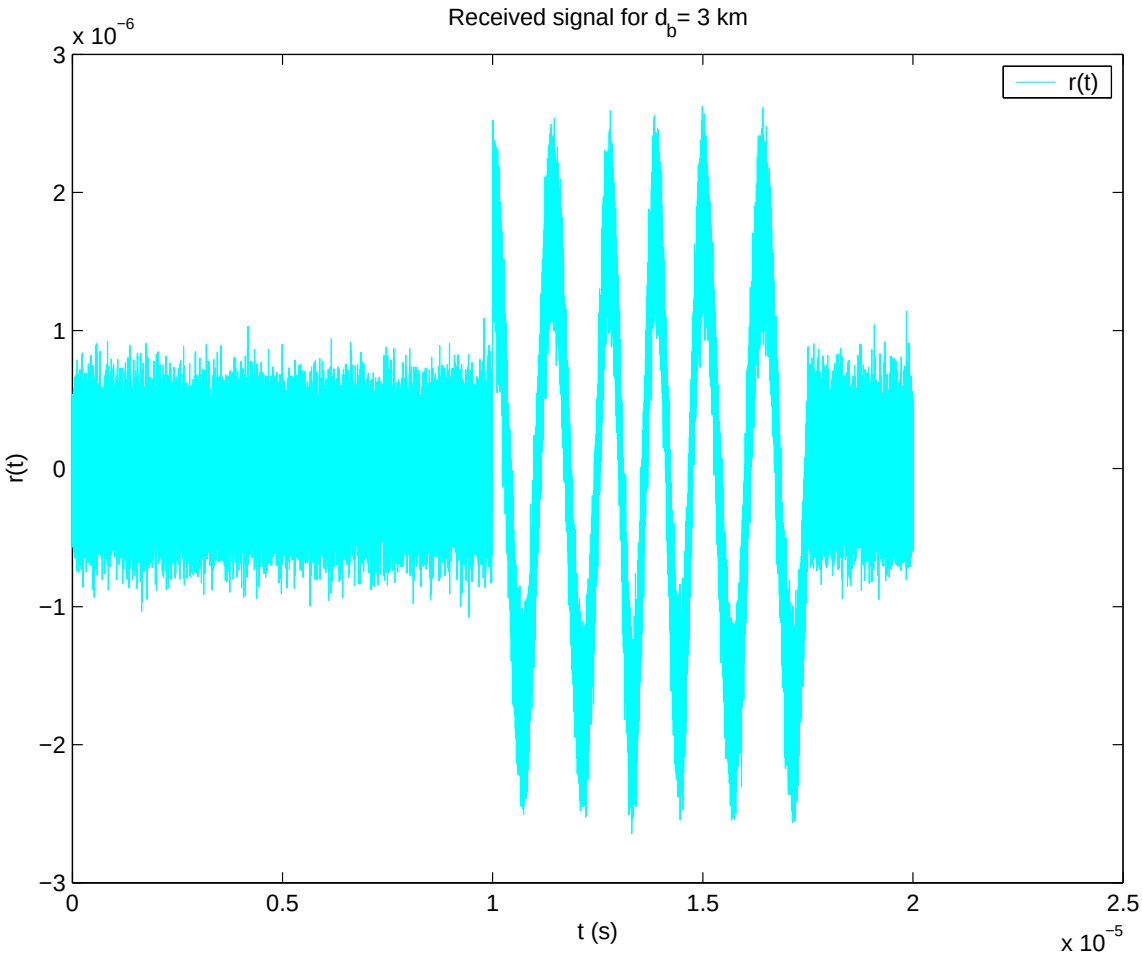

Figure 3.17: The received signal for $d_b = 3$ km, and $\mathrm{SNR}_{\mathrm{Rx}} = 60$ dB.

3.5 Effective Bandwidth of MSK Signals

This section presents the effective bandwidth, which is defined by (3.2.1), for the transmitted signal in the outdoor environments. In this case, the transmitted signal is the MSK signal defined by (3.4.7). Therefore, we need to obtain the Fourier transform of the MSK modulation. The transmitted signal expression can be written as

$$s(t) = \sum_{n=1}^{N-1} v_n \cos\left(\left(\omega_0 - \frac{v_n q_n \pi}{2T}\right) t\right), \tag{3.5.1}$$

where (v_n, q_n) is the n-th pair of the transmitted bits and N is the number of the bits in the transmitted frame. Only one of these bits changes each $\frac{T}{2}$ s, and q_n is delayed T s with respect to v_n. The pair of $(\mathbf{v}, \mathbf{q})$ includes the bit information vectors, where $\mathbf{v}$ and $\mathbf{q}$ are defined by

$$\mathbf{v} = \begin{bmatrix} v_1 & v_2 & \cdots & v_N \end{bmatrix}^{\mathrm{T}}, \tag{3.5.2}$$

and

$$\mathbf{q} = \begin{bmatrix} q_1 & q_2 & \cdots & q_N \end{bmatrix}^{\mathrm{T}}. \tag{3.5.3}$$

The variables v_n and q_n are assumed as independent variables, whose joint probability distribution can be written as

$$p_{v,q}(v_n, q_n) = p_v(v_n) p_q(q_n) = \frac{1}{4}. \tag{3.5.4}$$

It is worth noting that the signal expressed in (3.5.1) lies in the general form of digital communications signal (see, e.g., [49, eq. (1-4-1)]). Hence, this work can be modified to other modulation schemes without difficulty.

Proposition 3.5.1. *The mean of the square of the effective bandwidth of the MSK signal is given by*

$$\mathrm{E}_{\mathbf{v},\mathbf{q}}\{\bar{\beta}^2\} = f_0^2 + \frac{1}{16T^2}. \tag{3.5.5}$$

Proof. See Appendix A.3. □

The expression of the effective bandwidth in the time domain is given in (3.2.3). Therefore, to be capable of comparing the theoretical to the numerical results, it is necessary to obtain $\dot{s}(t)$ for the MKS signal. Starting with the expression of the transmitted signal given by (3.4.6), it is possible to derive the expression of $\dot{s}(t)$ from

$$\begin{aligned}\dot{s}(t) &= \frac{\partial}{\partial t}s(t) \\ &= v_i\left(-\frac{\pi}{2T}\sin\left(\pm\frac{\pi t}{2T}\right)\cos\left(2\pi f_0 t\right) - 2\pi f_0\cos\left(\pm\frac{\pi t}{2T}\right)\sin\left(2\pi f_0 t\right)\right) \\ &\quad + q_i\left(\frac{\pi}{2T}\cos\left(\pm\frac{\pi t}{2T}\right)\sin\left(2\pi f_0 t\right) + 2\pi f_0\sin\left(\pm\frac{\pi t}{2T}\right)\cos\left(2\pi f_0 t\right)\right).\end{aligned} \tag{3.5.6}$$

The changes in the bandwidth of the MSK signal with the bit time is shown in Fig. 3.18, where the theoretical value for the effective bandwidth of the MSK signal in the frequency domain can be compared to the numerical effective bandwidth defined in the time domain. We can see that the simulation presents some fluctuations, because we cannot have infinite independent runs to obtain the exact value of the expectation of $\bar{\beta}$ neither decrease more the sampling time.

3.6 Theoretical Estimation Error Performance

In this section, we study the theoretical performance of the ToA estimators. With the aim at quantifying and comparing the ML estimator to the MC estimator, the theoretical value of the RMSE for the ML and MC estimators are shown in this

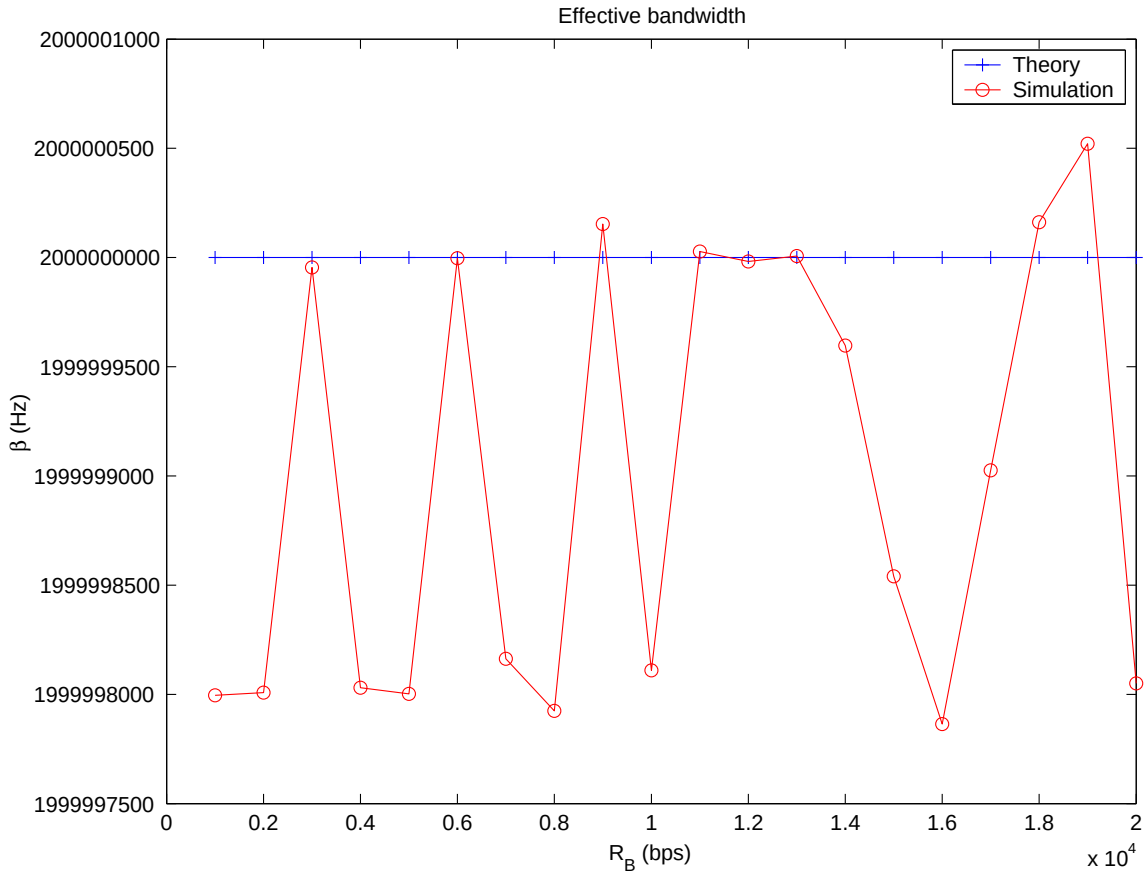

Figure 3.18: The square root of the expectation of the effective bandwidth square for an MSK signal as a function of the information bit rate R_{B} for $N = 2$ bits, $R_{\mathrm{B}} = [1, 20]$ kbps, $f_0 = 2$ GHz, $T = \frac{1}{R_{\mathrm{B}}}$ s, sampling time $= [1, 0.05]$ ns, and $N_{\mathrm{R}} = 1{,}000$ independent runs.

section. The theoretical RMSE for the ML estimator is given by [13]

$$\begin{aligned}\mathrm{RMSE}_{\text{SS-ToA}} &= \sqrt{\mathrm{MSE}_{\text{SS-ToA}}(\hat{\tau}_{b,\mathrm{ML}})} \\ &= \sqrt{\mathrm{E}_{\hat{\tau}_{b,\mathrm{ML}}}\{(\hat{\tau}_{b,\mathrm{ML}} - \tau_{b,0})^2\}} \\ &= \frac{1}{\sqrt{\mathrm{SNR}a_b^2\left(8\pi^2\bar{\beta}^2 + \frac{\gamma_b^2}{2\tau_{b,0}^2}\right)}},\end{aligned} \tag{3.6.1}$$

where SNR is the transmitted signal-to-noise ratio, which is given by

$$\mathrm{SNR} = \frac{E_{\mathrm{s}}}{\sigma_{\mathrm{n}}^2}. \tag{3.6.2}$$

Then, we have the relation between the transmitted and the received SNRs from

$$\mathrm{SNR}_{\mathrm{Rx}} = a_b^2\mathrm{SNR}. \tag{3.6.3}$$

The RMSE for the MC estimator is (see, e.g., [13])

$$\begin{aligned}\mathrm{RMSE}_{\text{ToA}} &= \sqrt{\mathrm{MSE}_{\text{ToA}}(\hat{\tau}_{b,\mathrm{MC}})} \\ &= \sqrt{\mathrm{E}_{\hat{\tau}_{b,\mathrm{MC}}}\{(\hat{\tau}_{b,\mathrm{MC}} - \tau_{b,0})^2\}} \\ &= \frac{1}{\sqrt{8\pi^2\mathrm{SNR}a_b^2\bar{\beta}^2}},\end{aligned} \tag{3.6.4}$$

where $\bar{\beta}$ is the effective bandwidth calculated previously. The error performances shown above in the square root, i.e., the expressions of the $\mathrm{MSE}_{\text{SS-ToA}}(\hat{\tau}_{b,\mathrm{ML}})$ and $\mathrm{MSE}_{\text{ToA}}(\hat{\tau}_{b,\mathrm{MC}})$, are equivalent to the CRB for the time delay estimation (see, e.g., [27–33]). Then, it is possible to see that the RMSE depends on the value of $\bar{\beta}$, which is given by (A.1.26) and (A.3.21) for the indoor and the outdoor environments, respectively. The value of $\bar{\beta}$ for the indoor environment, wich is given by (A.1.26), is a deterministic value and therefore can be substituted directly into (3.6.1) and (3.6.4). However, for the outdoor environment, the value of $\bar{\beta}$ is random, because

it depends on the values of the transmitted series of the bits. Then, it cannot be included directly into the RMSE expression.

For the outdoor surrounding, the presence of the random parameter $\bar{\beta}$ makes the calculation of the RMSE more difficult, because we have to calculate the CRB in the presence of a nuisance parameter, which is incurred by the MSK information bits in this case. Then, it is necessary to consider the CRB.

The CRB is a fundamental lower bound on the variance of any unbiased estimator. Therefore, the CRB serves as a benchmark for the performance of actual estimators. Unfortunately, the evaluation of the CRB is mathematically quite difficult when the observed signal contains, besides the parameter to be estimated, also some nuisance parameters that are unknown but whose value we are not interested in. Moreover, in the case of the estimation in the presence of nuisance parameters, the variance of any unbiased estimator is also bounded by MCRB, which is much simpler to evaluate than the true CRB. The true CRB is never below the MCRB, in other words, the MCRB is in general looser than the true CRB (see, e.g., [50]).

In this section, we derive the expression of an average of the true CRB, i.e., the expression of the ACRB, and the MCRB for the ML and MC estimators. Thereby, if the RMSE of the ML and MC estimators fall into the lower bound given by the square root of the CRB, they are regarded as efficient estimators.

3.6.1 Asymptotic Cramér-Rao Bound

In this section, we derive the ACRB for the ML and MC estimators for the outdoor environment, which coincides with the MSE. Thereby, the RMSE of the ML and MC estimators can be obtained from the square root of the ACRB of the ML and

MC estimators.

Proposition 3.6.1. *The expression of the ACRB of the MC estimator is given by*

$$\mathrm{ACRB}_{\textit{ToA}} = \frac{16f_0^2 + \frac{1}{T^2}}{8\pi^2 \mathrm{SNR} a_b^2 \left(16f_0^4 + \frac{1}{16T^4} - \frac{1}{T^2}2f_0^2\right)}. \tag{3.6.5}$$

Proof. See Appendix A.4. □

Proposition 3.6.2. *The expression of the ACRB of the ML estimator is given by*

$$\mathrm{ACRB}_{\textit{SS-ToA}} = \frac{1}{2\mathrm{SNR}a_b^2}\left(\frac{1}{2\left(\omega_0 - \frac{\pi}{2T}\right)^2 + \frac{\gamma_b^2}{2\tau_{b,0}^2}} + \frac{1}{2\left(\omega_0 + \frac{\pi}{2T}\right)^2 + \frac{\gamma_b^2}{2\tau_{b,0}^2}}\right). \tag{3.6.6}$$

Proof. See Appendix A.5. □

3.6.2 Modified Cramér-Rao Bound

In this section, we calculate the MCRB for the ML and MC estimators for the outdoor environment. In order to obtain the MCRB for the ML and MC estimators we only have to introduce the expectation of the value of $\bar{\beta}$, which is given by (3.5.5), into the expressions of the MSE for each estimator. Then, the MCRB is much simpler to evaluate than the ACRB. Therefore, by including the value of $\mathrm{E}_{\mathbf{v},\mathbf{q}}\{\bar{\beta}^2\}$, which is given by (3.5.5), into (3.6.1), we obtain the value of the RMSE of the ML estimator from the MCRB for the ML, i.e.,

$$\begin{aligned}
\mathrm{MCRB}_{\text{SS-ToA}} &= \frac{1}{\mathrm{SNR}a_b^2\left(8\pi^2\mathrm{E}_{\mathbf{v},\mathbf{q}}\{\bar{\beta}^2\} + \frac{\gamma_b^2}{2\tau_{b,0}^2}\right)} \\
&= \frac{1}{\mathrm{SNR}a_b^2\left(8\pi^2\left(f_0^2 + \frac{1}{16T^2}\right) + \frac{\gamma_b^2}{2\tau_{b,0}^2}\right)} \\
&= \frac{1}{\mathrm{SNR}a_b^2\left(8\pi^2 f_0^2 + \frac{\pi^2}{2T^2} + \frac{\gamma_b^2}{2\tau_{b,0}^2}\right)}.
\end{aligned} \tag{3.6.7}$$

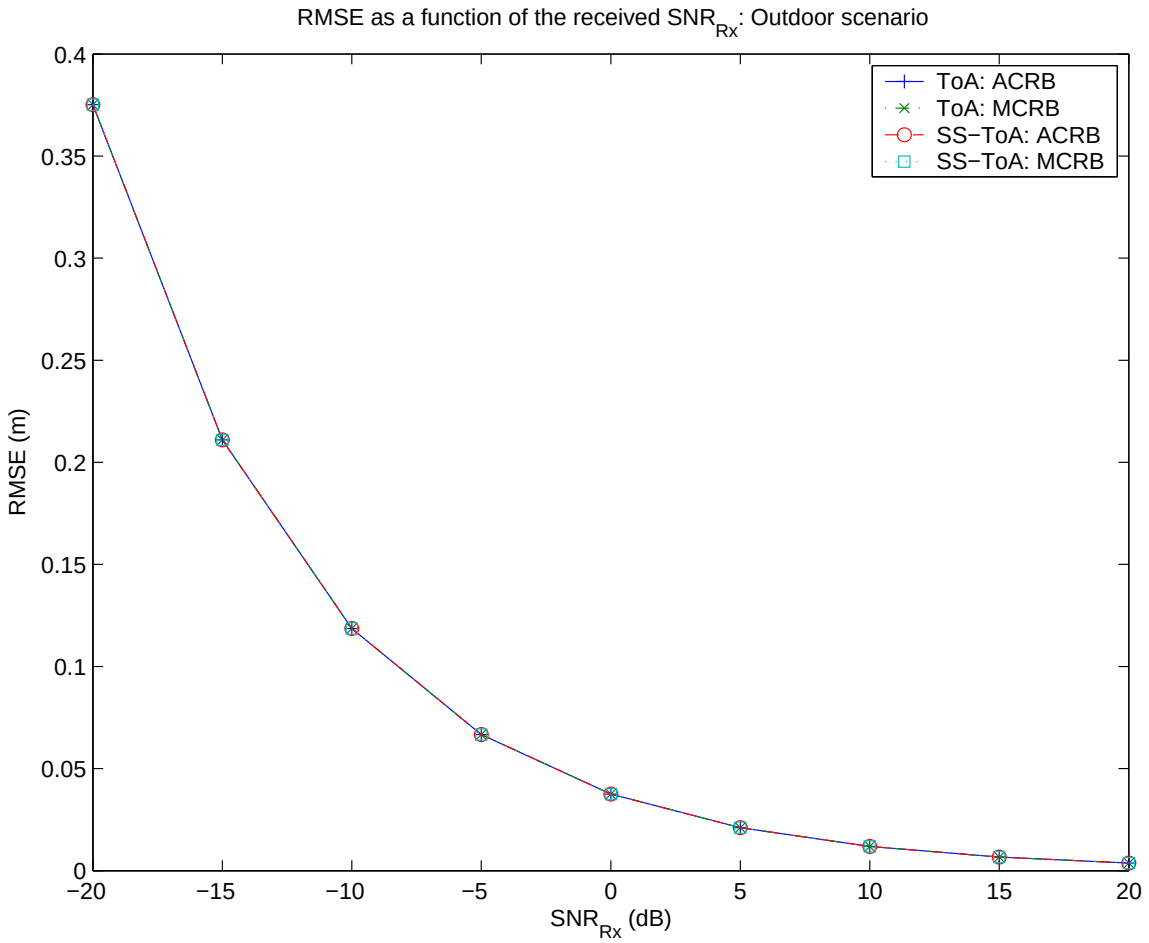

Figure 3.19: Theoretical RMSE as a function of $\mathrm{SNR}_{\mathrm{Rx}}$ for $R_{\mathrm{B}} = 12.2$ kbps, $f_0 = 900$ MHz, $T = \frac{1}{R_{\mathrm{B}}}$ s, $\gamma_b = 3$, $d_b = 1$ km, and $\bar{\beta} = 0.9$ GHz.

Similarly, by substituting the value of $\mathrm{E}_{\mathbf{v},\mathbf{q}}\{\bar{\beta}^2\}$ into (3.6.4), the RMSE of the ML estimator from the MCRB is given by

$$\begin{aligned} \mathrm{MCRB}_{\mathrm{ToA}} &= \frac{1}{\mathrm{SNR} a_b^2 8\pi^2 \mathrm{E}_{\mathbf{v},\mathbf{q}}\{\bar{\beta}^2\}} \\ &= \frac{1}{\mathrm{SNR} a_b^2 8\pi^2 \left(f_0^2 + \frac{1}{16T^2}\right)}. \end{aligned} \tag{3.6.8}$$

Fig. 3.19 shows the MCRB and the ACRB as a function of $\mathrm{SNR}_{\mathrm{Rx}}$ for the ML and MC estimators. However, in this figure we cannot appreciate the difference

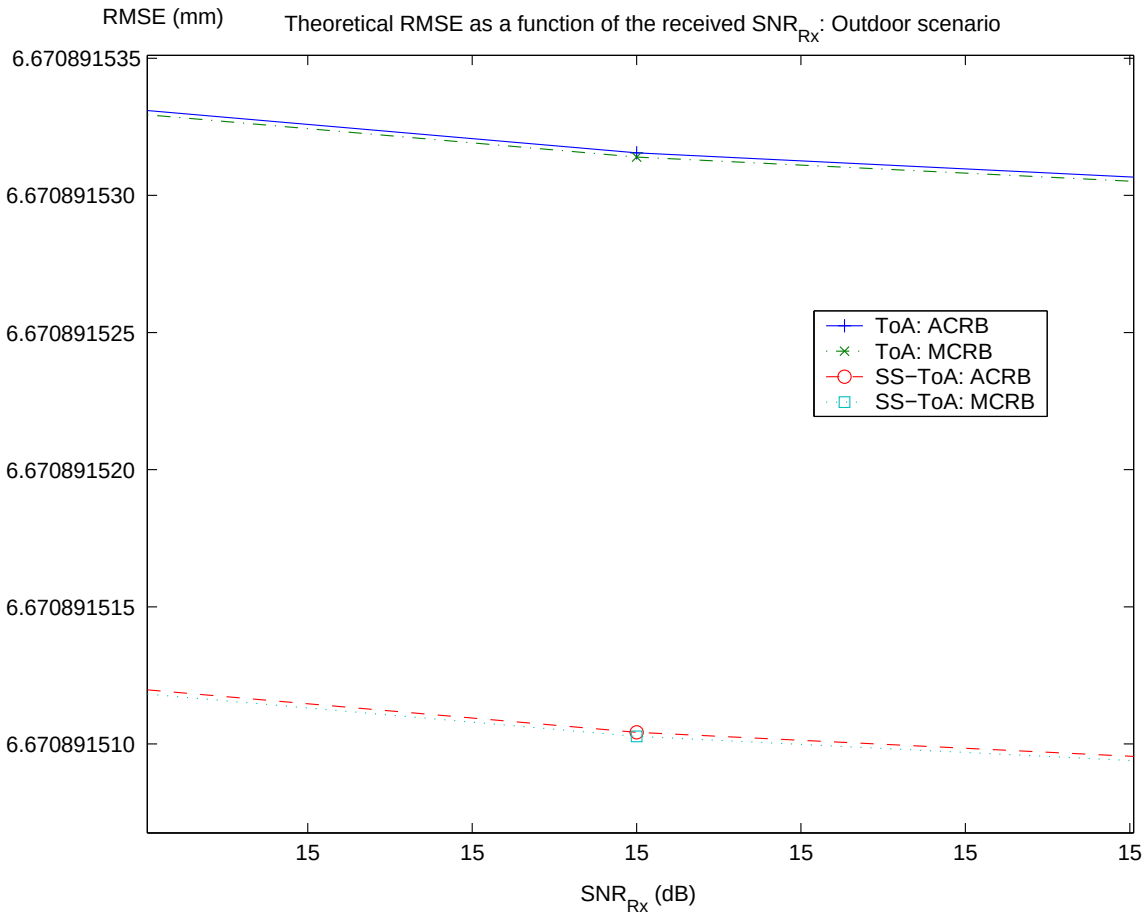

Figure 3.20: Zoomed theoretical RMSE as a function of $\mathrm{SNR_{Rx}}$ for $R_{\mathrm{B}} = 12.2$ kbps, $f_0 = 900$ MHz, $T = \frac{1}{R_{\mathrm{B}}}$ s, $\gamma_b = 3$, $d_b = 1$ km, and $\bar{\beta} = 0.9$ GHz.

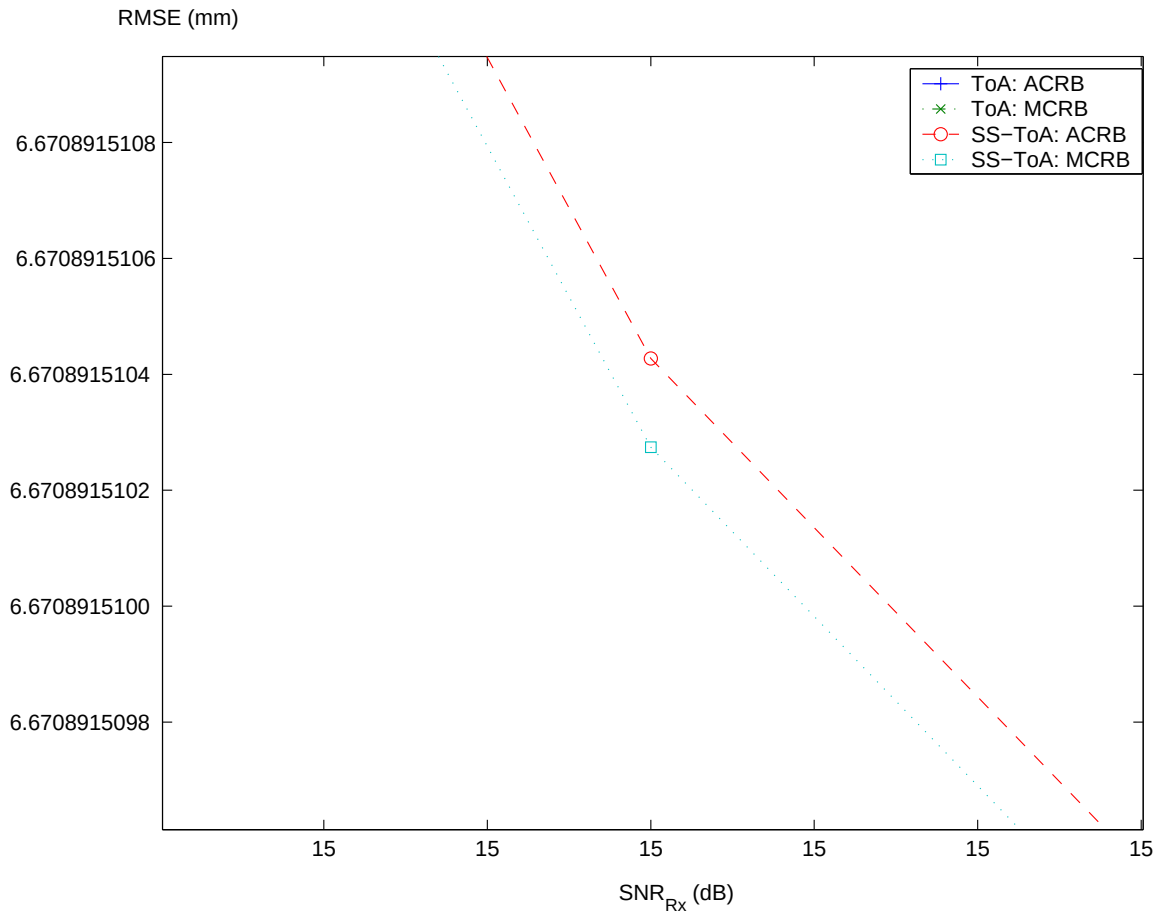

Figure 3.21: Zoomed $\mathrm{MCRB}_{\text{SS-ToA}}$ and $\mathrm{ACRB}_{\text{SS-ToA}}$ for $R_{\mathrm{B}} = 12.2$ kbps, $f_0 = 900$ MHz, $T = \frac{1}{R_{\mathrm{B}}}$ s, $\gamma_b = 3$, $d_b = 1$ km, and $\bar{\beta} = 0.9$ GHz.

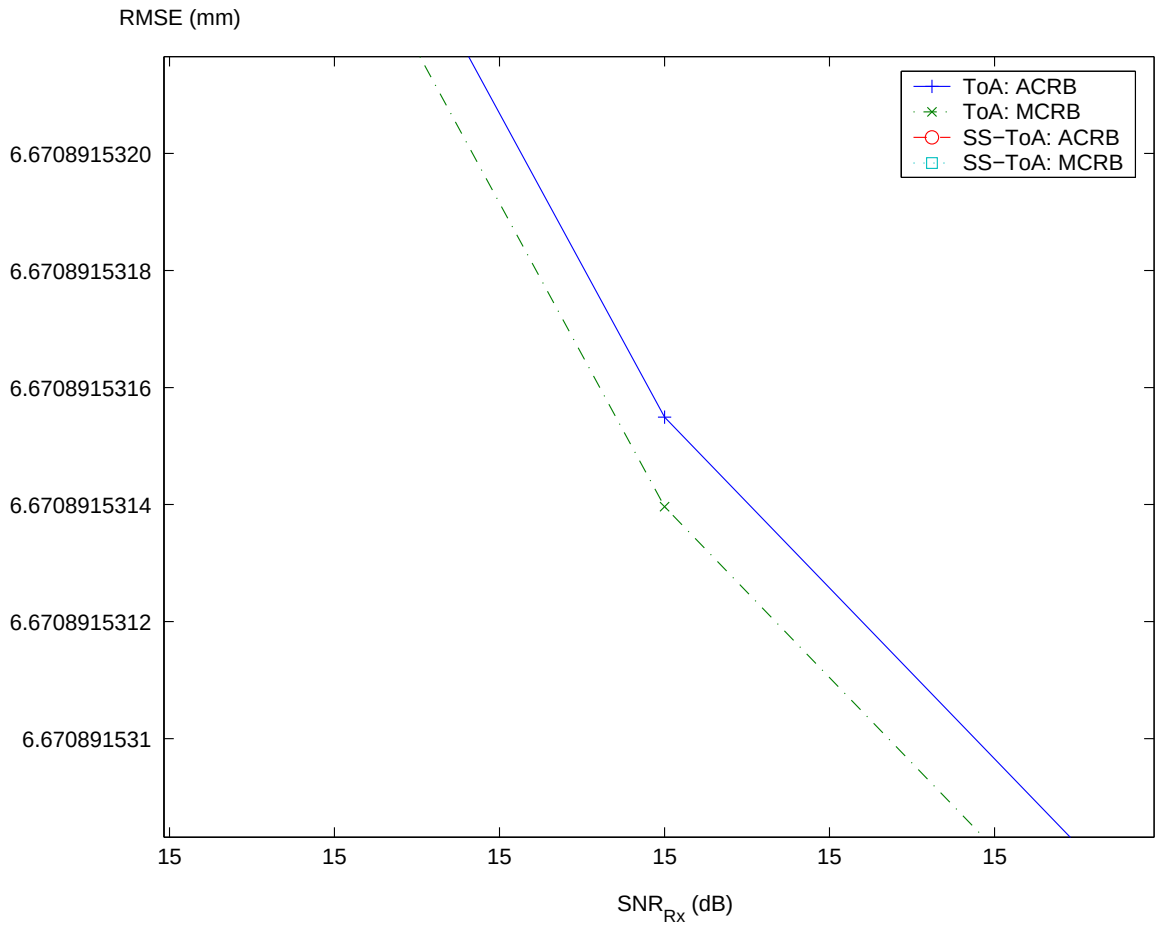

Figure 3.22: Zoomed $\mathrm{MCRB}_{\mathrm{ToA}}$ and $\mathrm{ACRB}_{\mathrm{ToA}}$ for $R_{\mathrm{B}} = 12.2$ kbps, $f_0 = 900$ MHz, $T = \frac{1}{R_{\mathrm{B}}}$ s, $\gamma_b = 3$, $d_b = 1$ km, and $\bar{\beta} = 0.9$ GHz.

between the ML and the MC estimators. Therefore, Fig. 3.20 shows a zoom of the difference between them. It is possible to observe that the ML estimator has a smaller error than the MC estimator. The ML estimator has a better accuracy, because it incorporates the path attenuation model into the time delay model in the calculation of the ToA.

In Fig. 3.21 and Fig. 3.22, it is possible to see the difference between the MCRB and the ACRB for the ML and MC estimators, respectively. As expected, the MCRB is always below the ACRB for both estimators, because the MCRB is looser than the ACRB.

Fig. 3.23 shows the RMSE as a function of the central frequency f_0 for the ML and MC estimators. In this figure, it is possible to observe that the RMSE decreases when the central frequency increases. However, for the values of f_0 between 100 MHz and 2 GHz, the difference between the MCRB and the ACRB cannot be appreciated as in the previous figure. However, if we zoom in this figure, we can also see that the MCRB is always below the ACRB.

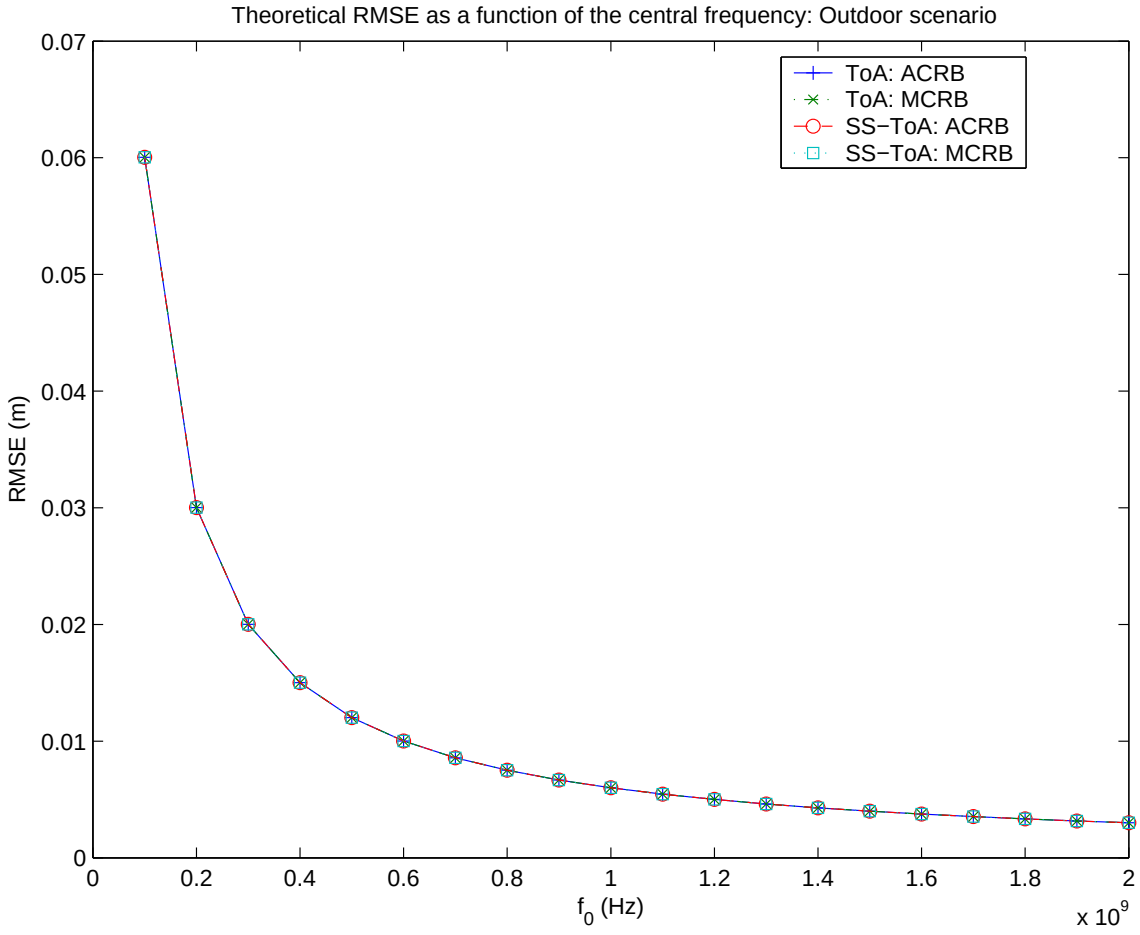

Figure 3.23: Theoretical RMSE as a function of the central frequency f_0 for $R_{\mathrm{B}} = 12.2$ kbps, $\mathrm{SNR}_{\mathrm{Rx}} = 15$ dB, $T = \frac{1}{R_{\mathrm{B}}}$ s, $\gamma_b = 4$, and $d_b = 1$ km.

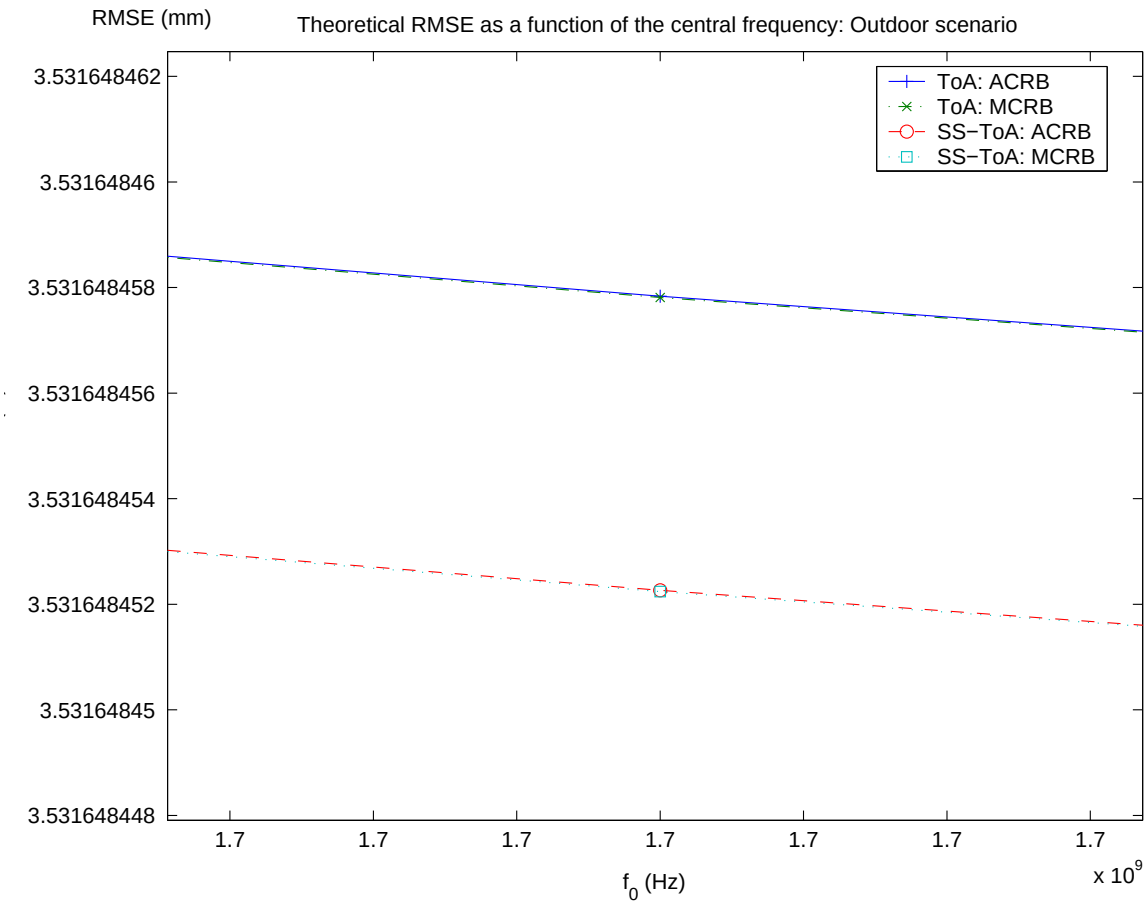

Figure 3.24: Zoomed theoretical RMSE as a function of the central frequency f_0 for $R_{\mathrm{B}} = 12.2$ kbps, $\mathrm{SNR}_{\mathrm{Rx}} = 15$ dB, $T = \frac{1}{R_{\mathrm{B}}}$ s, $\gamma_b = 4$, and $d_b = 1$ km.

Chapter 4

Basic Implementation of the ToA Estimators

In this chapter, we discuss about the programming details, which will be implemented to obtain the value of the ToA of the received signal for the indoor and outdoor surroundings. The ML estimator will be implemented according to the expression shown in (2.0.16). This estimator is compared to the MC estimator, whose definition is addressed later. A lot of simulations will be run to illustrate how the SNR, the path loss exponent γ_b, and the real value of the ToA affect the estimation of the time delay from the transmitter to the receiver stations.

With the aim at reducing the computational load, the frequency domain has been applied to resolve the expression obtained in (2.0.16). In this expression, we want to resolve the correlation between the transmitted and received signals defined by

$$\rho(\tau_b) = \int_0^{T_o} \Re(s^*(t-\tau_b) r_b(t)) \mathrm{d}t. \tag{4.0.1}$$

The convolution is defined by $(f * g)(x) = \int_{\mathbb{R}} f(y) g(x-y) \mathrm{d}y$. Then, we can rewrite

(4.0.1) as

$$\begin{aligned}\rho(\tau_b) &= \int_0^{T_\mathrm{o}} \Re(r_b(t)s^*(-(\tau_b - t)))\mathrm{d}t \\ &= \Re((r * s^*)(-\tau_b)).\end{aligned} \tag{4.0.2}$$

The convolution theorem states that (see, e.g., [51])

$$\mathcal{F}\{g_1 * g_2\} = \mathcal{F}\{g_1\} \cdot \mathcal{F}\{g_2\}. \tag{4.0.3}$$

By using the previous property, (4.0.2) can be resolved as (see, e.g., [32, p. 49])

$$\begin{aligned}\rho(\tau_b) &= \Re\left(\mathcal{F}^{-1}\left\{\mathcal{F}\{r(t)\} \cdot \mathcal{F}\{s^*(-(\tau_b - t)\}\right\}\right) \\ &= \Re\left(\mathcal{F}^{-1}\left\{R(f) \cdot S^*(f)\right\}\right),\end{aligned} \tag{4.0.4}$$

where $R(f)$ and $S^*(f)$ are the Fourier transforms of the received and transmitted signals, respectively. Therefore, the correlation is implemented in the frequency domain, where the convolution becomes a multiplication, which can reduce the computational load.

In this section, the ML and MC estimators are compared to each other. The expression of the ML estimator is shown in (2.0.16) and the MC estimator is defined by

$$\begin{aligned}\hat{\tau}_{b,\mathrm{MC}} &= \arg\max_{\tau_b} \int_0^{T_\mathrm{o}} \Re(s^*(t - \tau_b)r_b(t))\mathrm{d}t \\ &= \arg\max_{\tau_b} \rho(\tau_b),\end{aligned} \tag{4.0.5}$$

where $\rho(\tau_b)$ is the correlation computed from (4.0.4).

The RMSEs of the ML and MC estimators are calculated as a function of the SNR, which is the signal-to-noise ratio at the transmitter, the path loss exponent and the real value of the ToA. The expression of the RMSE is defined by

$$\mathrm{RMSE}(\hat{\tau}_b) = \sqrt{\mathrm{E}_{\hat{\tau}_b}\{(\hat{\tau}_b - \tau_{b,0})^2\}}, \tag{4.0.6}$$

where $\hat{\tau}_b$ is the estimated time delay by the ML or MC estimators and $\tau_{b,0}$ is the real value of the ToA. The expectation is performed with respect to $\hat{\tau}_b$. However, we cannot achieve the exact value of the expectation, because we can calculate it from only a finite number of the estimations of $\hat{\tau}_b$, i.e.,

$$\begin{aligned} \mathrm{E}_{\hat{\tau}_b}\{(\hat{\tau}_b - \tau_{b,0})^2\} &= \lim_{N_\mathrm{R}\to\infty} \frac{1}{N_\mathrm{R}} \sum_{n_\mathrm{R}=1}^{N_\mathrm{R}} (\hat{\tau}_b[n_\mathrm{R}] - \tau_{b,0})^2 \\ &\cong \frac{1}{N_\mathrm{R}} \sum_{n_\mathrm{R}=1}^{N_\mathrm{R}} (\hat{\tau}_b[n_\mathrm{R}] - \tau_{b,0})^2, \end{aligned} \tag{4.0.7}$$

where N_R is a large number of independent runs, and $\hat{\tau}_b[n_\mathrm{R}]$ is the estimated value of the ToA in the n_R-th run.

In this chapter, the ML and MC estimators are implemented in the MATLAB® in order to compare them to their theoretical results, whose expressions have been obtained in the previous chapter. Moreover, different MATLAB® files are implemented for the indoor and outdoor environments, because the transmitted signals are different and they cannot be implemented by using the same MATLAB® code. Then, each environment is studied in the next sections.

4.1 ToA Estimator Implementation for Indoor Environments

This section exhibits the investigation of the estimate of the time delay in the indoor environment with the distance between the transmitter and the receiver from 5 cm to 6 m, and the second-derivative Gaussian pulse for the transmitted signal. Moreover, the parameter d_0 is chosen to be 5 cm, which coincides with the minimum distance to estimate for this environment.

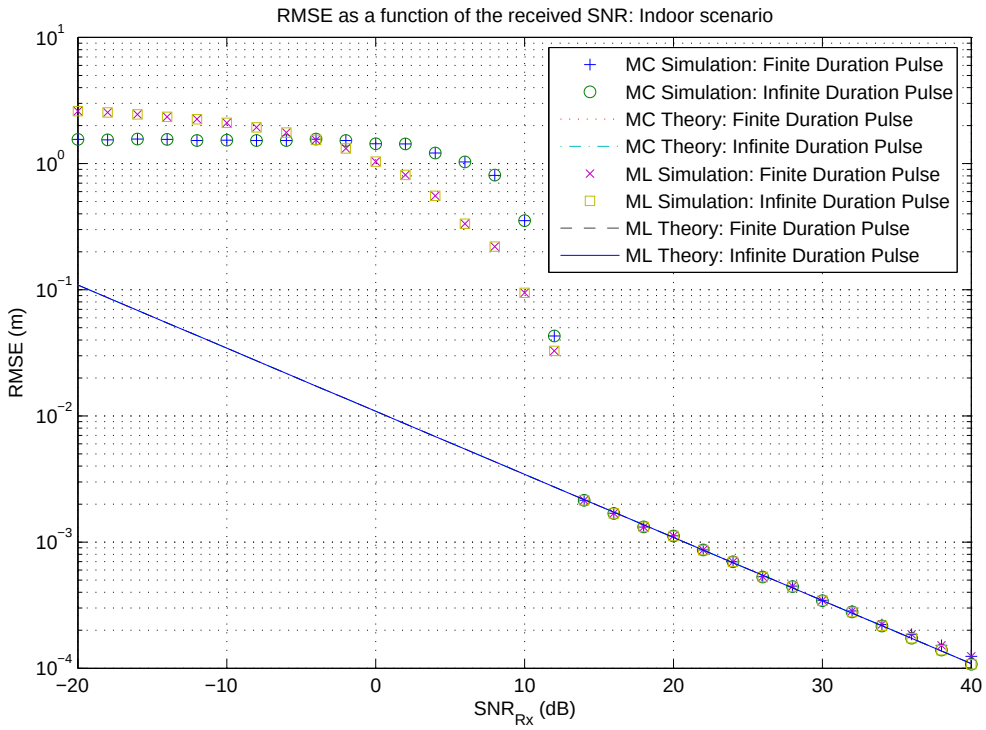

Figure 4.1: RMSE of the position estimate as a function of the $\mathrm{SNR}_{\mathrm{Rx}}$ (dB) for $\gamma_b = 2$, $d_b = 3$ m, $\bar{\beta} = 3.1007 \times 10^9$ Hz, sampling time $= 0.2$ ps, and $N_{\mathrm{R}} = 1{,}000$ independent runs.

Let us start studying the RMSE as a function of the SNR. In this case, the path loss exponent is 2, because this value can model the indoor environments, e.g., the office buildings (same or multiple floor) or the factories.

In Fig. 4.1, the RMSE of the estimate of the distance between the transmitter and the receiver stations for the ML and MC estimators is shown as a function of the received SNR. In this figure, the transmitted signal is considered as a signal with the infinite duration, i.e.,

$$s(t) = p\left(t - \frac{1}{2}T_{\mathrm{p}}\right); t > 0, \tag{4.1.1}$$

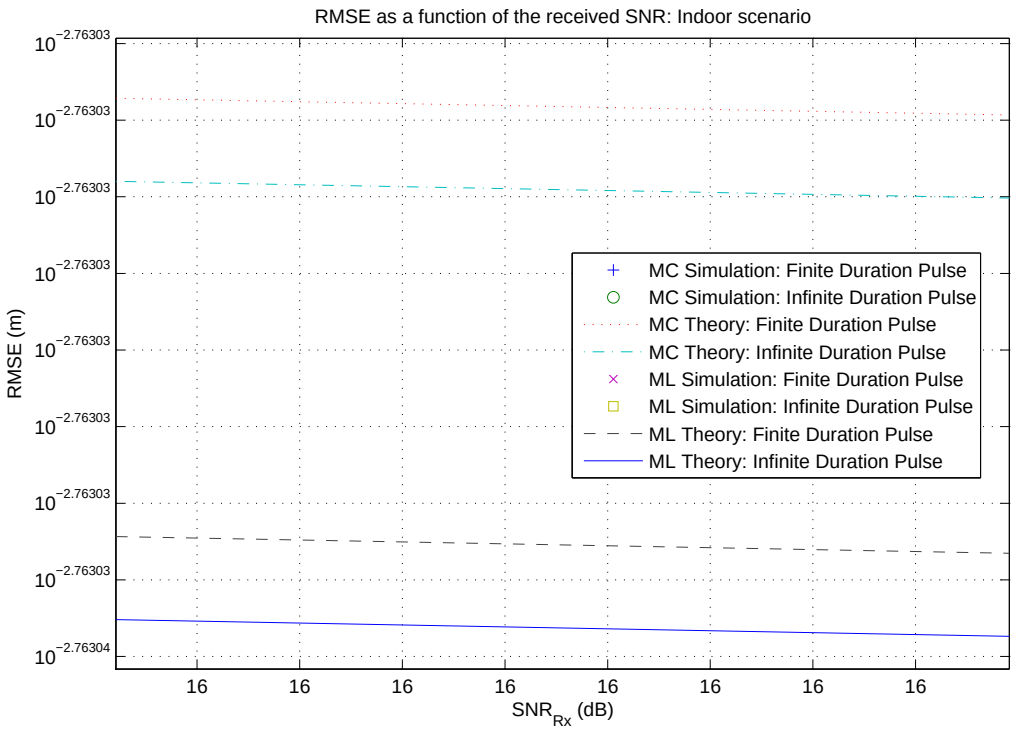

Figure 4.2: Zoomed RMSE of the position estimate as a function of the $\mathrm{SNR}_{\mathrm{Rx}}$ (dB) for $\gamma_b = 2$, $d_b = 3$ m, $\bar{\beta} = 3.1007 \times 10^9$ Hz, sampling time $= 0.2$ ps, and $N_{\mathrm{R}} = 1{,}000$ independent runs.

and with the finite duration, i.e.,

$$s(t) = \begin{cases} p(t - \frac{1}{2}T_{\mathrm{p}}) & ; 0 < t \leq T_{\mathrm{s}}, \\ 0 & ; t \in (-\infty, 0] \cup (T_{\mathrm{s}}, \infty), \end{cases} \tag{4.1.2}$$

where $p(t)$ is given in (3.1.1), T_{s} is the pulse time, and T_{p} is the the pulse width. The exact value of the effective bandwidth of (4.1.2) is given from (see [52])

$$\bar{\beta}(T_{\mathrm{s}}) = \frac{1}{\tau_{\mathrm{p}}\sqrt{2\pi}} \sqrt{\frac{15\mathrm{erf}\left(\frac{T_{\mathrm{s}}}{\tau_{\mathrm{p}}}\sqrt{\pi}\right) + \left(-30\left(\frac{T_{\mathrm{s}}}{\tau_{\mathrm{p}}}\right) + 28\left(\frac{T_{\mathrm{s}}}{\tau_{\mathrm{p}}}\right)^3 - 8\pi^2\left(\frac{T_{\mathrm{s}}}{\tau_{\mathrm{p}}}\right)^5\right) \mathrm{e}^{-\pi\left(\frac{T_{\mathrm{s}}}{\tau_{\mathrm{p}}}\right)^2}}{3\mathrm{erf}\left(\frac{T_{\mathrm{s}}}{\tau_{\mathrm{p}}}\sqrt{\pi}\right) + \left(2\left(\frac{T_{\mathrm{s}}}{\tau_{\mathrm{p}}}\right) + 4\pi\left(\frac{T_{\mathrm{s}}}{\tau_{\mathrm{p}}}\right)^3\right) \mathrm{e}^{-\pi\left(\frac{T_{\mathrm{s}}}{\tau_{\mathrm{p}}}\right)^2}}}, \tag{4.1.3}$$

where $\mathrm{erf}(\cdot)$ is the error function defined by (see, e.g., [53, p. 278])

$$\mathrm{erf}(x) = \frac{2}{\sqrt{\pi}} \int_0^x e^{-x'^2} dx'. \tag{4.1.4}$$

If we take the limit of $\bar{\beta}$ in (4.1.3) in which T_{s} tends to the infinity, we have the same result as that for the infinite duration, i.e.,

$$\begin{aligned} &\lim_{T_{\mathrm{s}} \to +\infty} \bar{\beta}(T_{\mathrm{s}}) = \frac{1}{\tau_{\mathrm{p}}\sqrt{2\pi}} \\ &\quad \lim_{T_{\mathrm{s}} \to +\infty} \sqrt{\frac{15\mathrm{erf}\left(\frac{T_{\mathrm{s}}}{\tau_{\mathrm{p}}}\sqrt{\pi}\right) + \left(-30\left(\frac{T_{\mathrm{s}}}{\tau_{\mathrm{p}}}\right) + 28\left(\frac{T_{\mathrm{s}}}{\tau_{\mathrm{p}}}\right)^3 - 8\pi^2\left(\frac{T_{\mathrm{s}}}{\tau_{\mathrm{p}}}\right)^5\right) \mathrm{e}^{-\pi\left(\frac{T_{\mathrm{s}}}{\tau_{\mathrm{p}}}\right)^2}}{3\mathrm{erf}\left(\frac{T_{\mathrm{s}}}{\tau_{\mathrm{p}}}\sqrt{\pi}\right) + \left(2\left(\frac{T_{\mathrm{s}}}{\tau_{\mathrm{p}}}\right) + 4\pi\left(\frac{T_{\mathrm{s}}}{\tau_{\mathrm{p}}}\right)^3\right) \mathrm{e}^{-\pi\left(\frac{T_{\mathrm{s}}}{\tau_{\mathrm{p}}}\right)^2}}} \\ &= \frac{1}{\tau_{\mathrm{p}}\sqrt{2\pi}} \lim_{T_{\mathrm{s}} \to +\infty} \sqrt{\frac{15\mathrm{erf}\left(\frac{T_{\mathrm{s}}}{\tau_{\mathrm{p}}}\sqrt{\pi}\right)}{3\mathrm{erf}\left(\frac{T_{\mathrm{s}}}{\tau_{\mathrm{p}}}\sqrt{\pi}\right)}} \\ &= \frac{1}{\tau_{\mathrm{p}}\sqrt{2\pi}} \sqrt{\frac{15}{3}} \\ &= \frac{1}{\tau_{\mathrm{p}}} \sqrt{\frac{5}{2\pi}}. \end{aligned} \tag{4.1.5}$$

Thus, the result obtained in (4.1.5) coincides with the value of $\bar{\beta}$ for the infinite duration pulse, which is given by (A.1.26).

In Fig. 4.1, we consider for the finite duration pulse with $T_{\mathrm{s}} = T_{\mathrm{p}}$. In this figure, it can be seen that the received SNR at which the ML and the MC estimates fall into their asymptotic error, is approximately 14 dB. The use of the ToA estimation can gain the accuracy of more than 2 mm for a positioning system. In the non-asymptotic region, the MC estimator has a smaller error than the ML estimator for the received SNR lower than -4 dB. Then, the ML estimator outperforms the MC estimator for the values of the SNR larger than -4 dB. Fig. 4.2 shows the zoomed area of the theoretical results for the ML and MC estimators, where the transmitted signal is assumed to have the finite and the infinite durations. In this figure, it can be observed that the ML estimator has a lower error variance than the MC estimator, because in the calculation of the ToA the MC estimator uses only the time delay model while the ML estimator uses both the path attenuation knowledge and the time delay model. Moreover, by comparing the results for the infinite duration pulse as the transmitted signal to the finite duration pulse as the transmitted signal, it can be seen that the estimation for the infinite duration pulse presents a lower error variance than the estimation for the finite duration pulse, because the effective bandwidth of the transmitted signals with the infinite duration pulse is larger than that of the transmitted signals with the finite duration pulse. Therefore, if the value of $\bar{\beta}$ increases, the RMSE decreases.

In Tab. 4.1, the path loss exponent γ_b is shown for different environments.

The RMSE is represented in Fig. 4.3 as a function of γ_b, whose value has been selected from the range [1.6,3.5] according to the considered indoor surrounding.

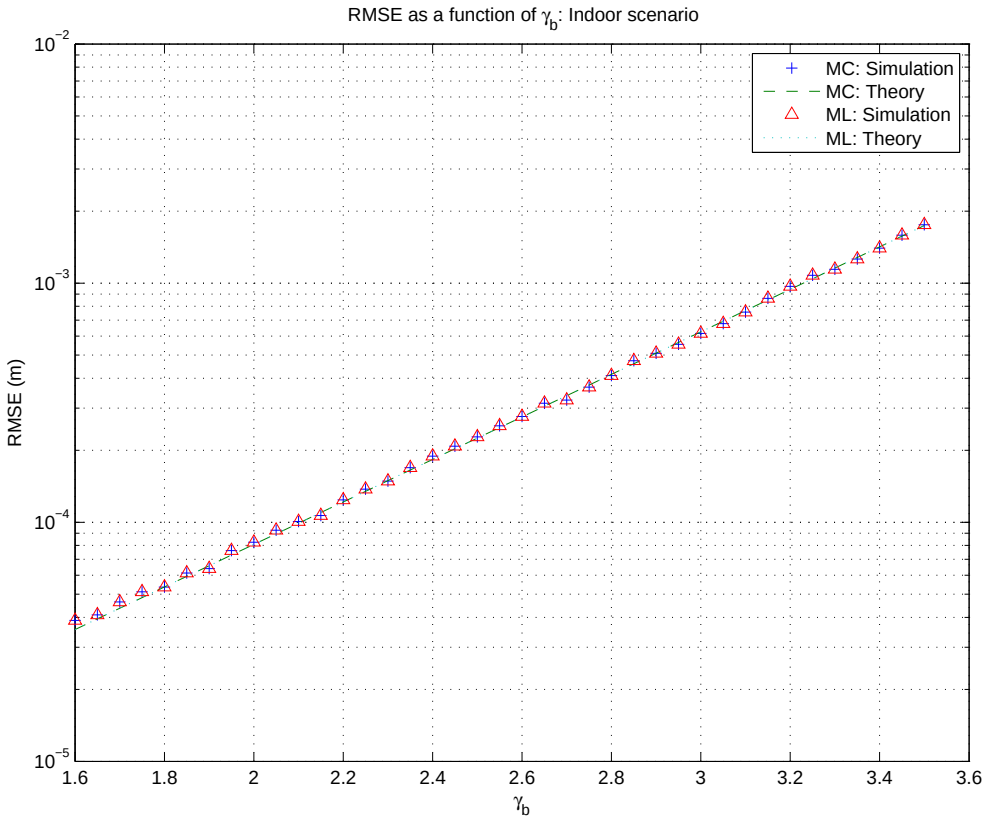

Figure 4.3: RMSE of the position estimate as a function of γ_b for the finite duration pulse as the transmitted signal, transmitted $\mathrm{SNR} = 100$ dB, $d_b = 3$ m, $\bar{\beta} = 3.1007 \times 10^9$ Hz, sampling time $= 0.2$ ps, and $N_{\mathrm{R}} = 1{,}000$ independent runs.

Environment	γ_b
Urban macrocells	3.7-6.5
Urban microcells	2.7-3.5
Office building (same floor)	1.6-3.5
Office building (multiple floor)	2.0-6.0
Store	1.8-2.2
Factory	1.6-3.3
Home	3.0

Table 4.1: The values of γ_b for different environments (see, e.g., [1, p. 47]).

In this figure, the transmitted signal is considered as a signal with the finite duration pulse in order to investigate the effect of finite integration in the calculation of the effective bandwidth.

The Fig. 4.4 shows the RMSE as a function of the distance between the transmitter and receiver stations, where the transmitted signal is a finite duration pulse. We can observe in this figure that the RMSE grows up linearly with the real value of the distance d_b. However, the accuracy is high for the indoor environment.

4.2 ToA Estimator Implementation for Outdoor Environments

As same as the indoor case, in this section let us study how the SNR affects the ML estimation of the time delay from the transmitter to the receiver station. In Fig. 4.5, it is possible to see that the sampling time is not sufficient for these parameters, because the error of the simulations is the same for the SNR larger than 46 dB. However, MATLAB® cannot compute the finer estimated ToA by using a smaller sampling time, because the hardware memory is limited. Therefore we cannot

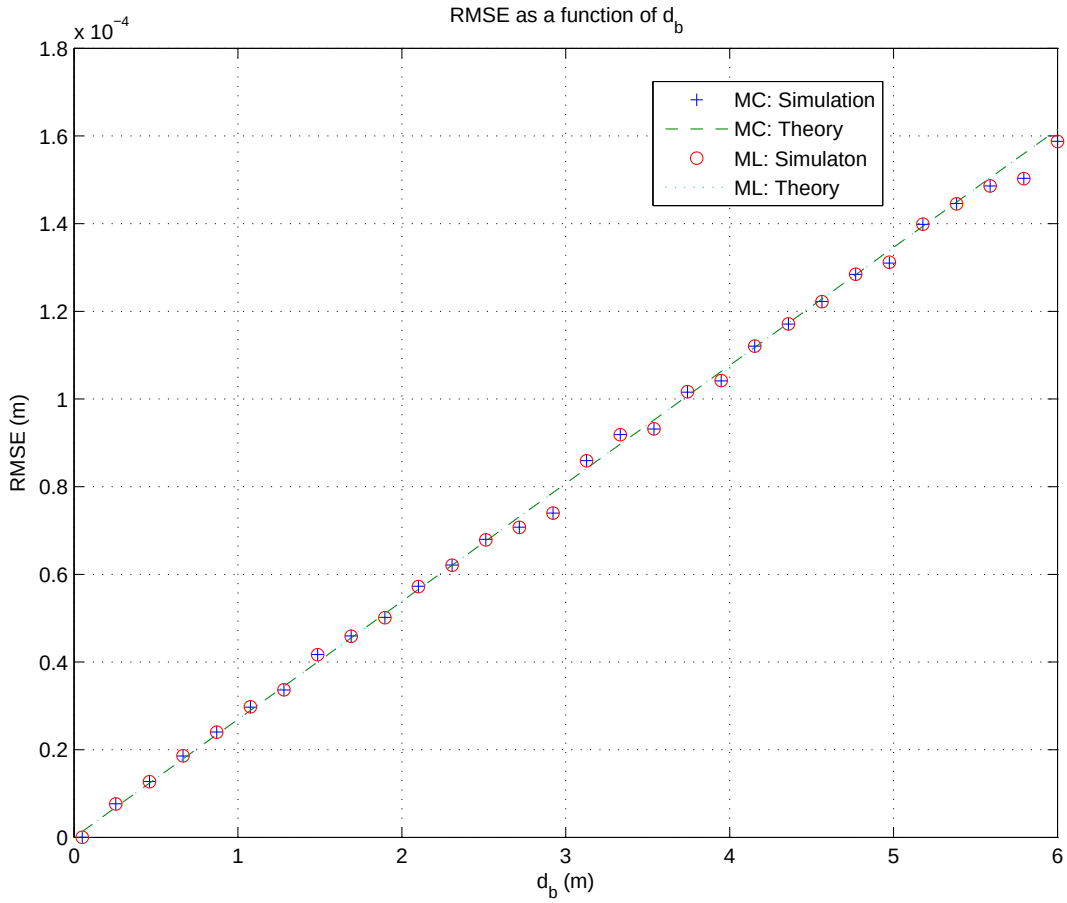

Figure 4.4: RMSE of the position estimate as a function of the distance between the transmitter and the receiver for the finite pulse duration as the transmitted signal, transmitted $\mathrm{SNR} = 100$ dB, $\gamma_b = 2$, $\bar{\beta} = 3.1007 \times 10^9$ Hz, sampling time $= 0.0333$ ps, and $N_{\mathrm{R}} = 1{,}000$ independent runs.

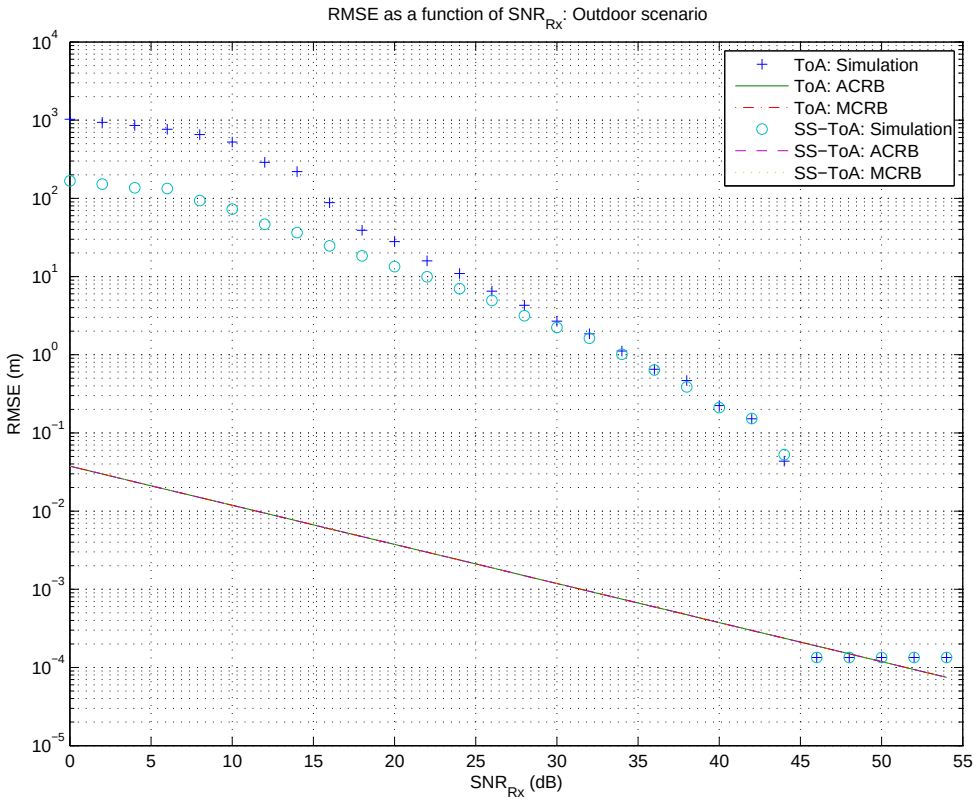

Figure 4.5: RMSE as a function of $\mathrm{SNR}_{\mathrm{Rx}}$ for $d_b = 500$ m, $\gamma_b = 4$, $f_0 = 0.9$ GHz, $R_{\mathrm{B}} = 140$ kbps, sampling time $= 8.8536$ ps, 20 independent runs for the frame realization, and 50 independent runs for the noise realization.

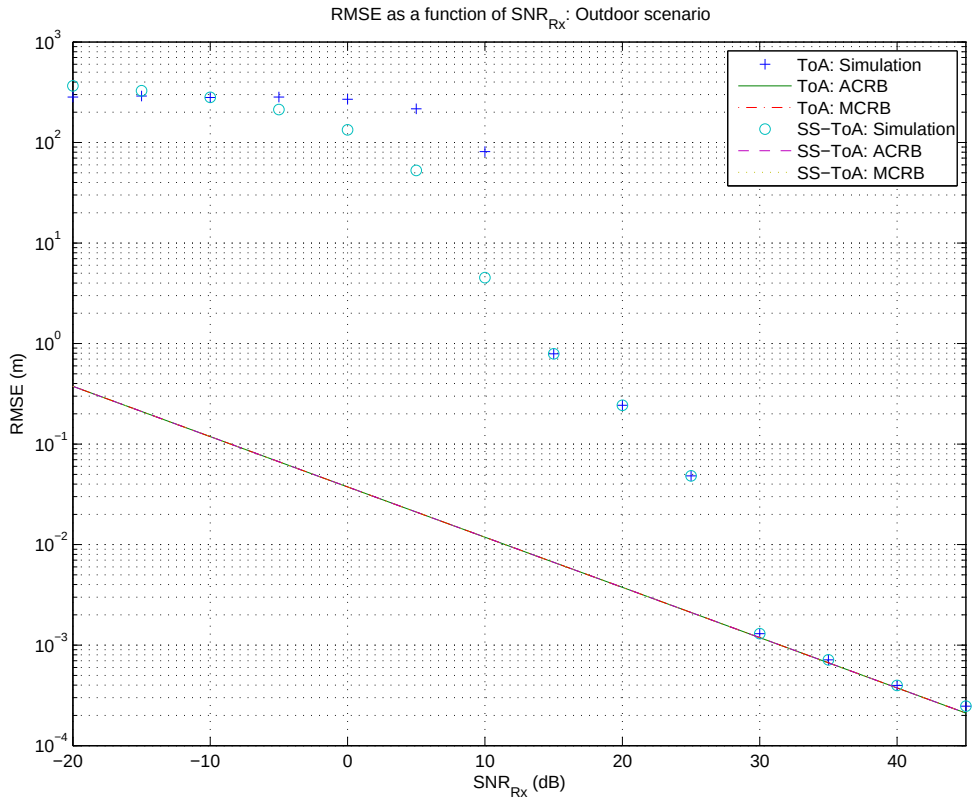

Figure 4.6: RMSE as a function of $\mathrm{SNR}_{\mathrm{Rx}}$ for $d_b = 500$ m, $\gamma_b = 4$, $f_0 = 0.9$ GHz, $R_{\mathrm{B}} = 15$ Mbps, sampling time $= 1.7420$ ps, 20 independent runs for the frame realization, and 50 independent runs for the noise realization.

simulate a real wireless GSM system.

In order to prove that the theoretical RMSEs are precise, we do the simulation for an unrealistic high bit rate. Fig. 4.6 shows the RMSEs as a function of the SNR. In this figure, it is possible to observe that the RMSEs of the ML and MC estimators falls into their asymptotic theoretical RSMEs for values of the SNR larger than 30 dB. In Fig. 4.6, it is also possible to observe that for the received SNR smaller than -10 dB, the MC estimator outperforms the ML estimator. However, for the $\mathrm{SNR}_{\mathrm{Rx}}$ larger than -10 dB, the ML estimator outperforms the MC estimator. It means that the ML estimator outperforms the MC estimator in the threshold region and in the asymptotic region.

Chapter 5

Imperfect Path Loss Exponent: Mis-modeled Estimation and Error Performance Analysis

The PLE is a key parameter in the localization algorithms based on the distance estimation, where the distance is estimated from the received signal strength (RSS). However, the analysis in many wireless networking problems assumes that the value of the path PLE is known *a priori*. This assumption is often too ideal for the real environment, and an accurate estimate is crucial for the study and design of the wireless systems.

It is possible to find some related works where the problem of the unknown PLE is taken into account in the wireless location. In [54] and [55], the PLEs are assumed to be unknown. In [54], the PLEs are assumed different and random with uniform and normal distributions, where based on the RSS, the consideration of the different PLEs for each link increases the localization accuracy compared to the identical PLE assumption. However, in [55], the wireless NLoS geolocation is based on the path attenuation in which the PLEs are deterministic. This study also

proposes the estimation of the different PLEs prior to the mobile position estimation. In [56], the PLE is calibrated from the measurements and in [18] and [19], several algorithm for the PLE estimation are studied. In [19], the algorithms for the estimation of the path loss between any sensor and any arbitrary point inside the network are designed using the path loss measurements between sensors. Moreover, [57] shows a handover algorithm, which is based on the least squares estimate of path loss parameters for each MS-BS link.

In this chapter, we assume that the PLE is known, but its value is however not exactly the same as the true value. It means in this manner that the knowledge of the PLE is imperfect and we can term it the imperfect PLE. We then consider the imperfect PLE in the ToA estimation with the aim at investigating the effects of the PLE error.

5.1 Introduction

Let us consider the imperfect PLE, because the real value of the PLE is often incompletely available. The rapid changes in the environments, because of, e.g., the movement of the MS or the changes in the weather, provide that the knowledge of the PLE does not coincide with the PLE in a previous observation. The problem to be studied in the sequel can be formulated as follows. We assume that the PLE is subject to an additive error, i.e.,

$$\gamma = \gamma_0 + \delta_\gamma, \tag{5.1.1}$$

where γ_0 is the real value of the PLE and δ_γ is the additive error. Then, the theoretical error performance of the ToA estimation will be explored.

In Chapter 2, we have obtained the theoretical performance of the ToA estimation using the ML estimator, which is given by (2.0.16), with the perfect knowledge of the PLE. Only the ML function is considered herein, since the ML estimator requires the knowledge of the PLE, whereas the MC estimator does not need the knowledge of the PLE. Let us reconsider the objective function of the ML estimator

$$\begin{aligned} f_{\mathrm{ML}}(\tau_b) &= a_b^2(\tau_b|\gamma)E_{\mathrm{s}} - 2a_b(\tau_b|\gamma)\int_0^{T_{\mathrm{o}}} \Re(s^*(t-\tau_b)r_b(t))\,\mathrm{d}t \\ &= a_b^2(\tau_b|\gamma)E_{\mathrm{s}} - 2a_b(\tau_b)\rho(\tau_b). \end{aligned} \tag{5.1.2}$$

The expression (5.1.2) lies in an ideal situation, where the PLE is assumed to be perfectly known. However, in this chapter, we consider the imperfect PLE and therefore the ML objective function should take into account the imperfect PLE value, i.e.,

$$f_{\mathrm{ML}}(\tau_b|\tilde{\gamma}) = a_b^2(\tau_b|\tilde{\gamma})E_{\mathrm{s}} - 2a_b(\tau_b|\tilde{\gamma})\rho(\tau_b), \tag{5.1.3}$$

where $\tilde{\gamma}$ is any value of the PLE to be inserted into the ML function. In the former works, the sensitivity analysis of the ML estimator under model error is investigated for the application of direction-of-arrival estimation (see, e.g., [14,16,17]). This idea can be applied to investigate the mis-modeled estimation[1] in (5.1.3).

Using the imperfect value γ for the PLE, the ML estimate is given by

$$\hat{\tau}_{b,\mathrm{ML}}(\gamma) = \arg\min_{\tau_b} a_b^2(\tau_b|\gamma)E_{\mathrm{s}} - 2a_b(\tau_b|\gamma)\rho(\tau_b). \tag{5.1.4}$$

Note that $\hat{\tau}_{b,\mathrm{ML}}(\gamma)$ is introduced, since we want to mention that the mis-modeled ML estimate in this chapter is different from, actually a generalized version of, (2.0.16).

[1]The mis-modeled estimation is referred herein to as the estimation of τ_b under the use of the mis-specified value of γ_0, i.e., γ.

5.2 Friedlander Analysis Method

In [14] the theoretical expression of the error between the estimated and the real ToAs is given by (see [14, eq. 20])

$$\hat{\tau}_{b,\mathrm{ML}}(\gamma) - \tau_{b,0} = -\frac{(\gamma-\gamma_0)\left.\frac{\partial^2}{\partial\gamma\partial\tau_b} f_{\mathrm{ML}}(\tau_b|\gamma)\right|_{\tau_b=\tau_{b,0}}}{\mathrm{E}_{n_b(t)}\left\{\left.\frac{\partial^2}{\partial\tau_b\partial\tau_b} f_{\mathrm{ML}}(\tau_b|\gamma)\right|_{\tau_b=\tau_{b,0}}\right\}}. \tag{5.2.1}$$

A close idea to the above expansion is also considered in [16]. The previous expression shows the error between the estimated and the real values of the ToA. In order to find the explicit form of (5.2.1), it is necessary to develop each term from this expression. Basic results for the first and second derivatives of the ML function under the imperfect PLE are provided in Appendix A.6.

Proposition 5.2.1. *Using the Friedlander analysis method in* (5.2.1)*, the error between the estimated and the true values of the ToA is given by*

$$\begin{aligned}\hat{\tau}_{b,\mathrm{ML}}(\gamma) - \tau_{b,0} = &-\frac{1}{\frac{1}{\tau_{b,0}^2}\gamma(1+\gamma)E_{\mathrm{s}}\tilde{a}_{b,0} - \frac{1}{\tau_{b,0}^2}\gamma\left(1+\frac{1}{2}\gamma\right)E_{\mathrm{s}}a_{b,0} + 8\pi^2\bar{\beta}^2E_{\mathrm{s}}a_{b,0}} \\ &(\gamma-\gamma_0)\left(\frac{1}{\tau_{b,0}}(E_{\mathrm{s}}a_{b,0}+\rho_{\mathrm{ns},0}-E_{\mathrm{s}}\tilde{a}_{b,0})\right. \\ &\left.-\frac{1}{\tau_{b,0}}\gamma\ln\left(\frac{d_0}{c\tau_{b,0}}\right)\left(E_{\mathrm{s}}\tilde{a}_{b,0}-\frac{1}{2}E_{\mathrm{s}}a_{b,0}-\frac{1}{2}\rho_{\mathrm{ns},0}\right)-\ln\left(\frac{d_0}{c\tau_{b,0}}\right)\dot{\rho}_{\mathrm{ns},0}\right),\end{aligned} \tag{5.2.2}$$

where $\tilde{a}_{b,0}$ is the loss gain for the true value of the ToA and the imperfect PLE, $\rho_{\mathrm{ns},0}$ is the correlation between the noise and the transmitted signal at the true value of the ToA, and $\dot{\rho}_{\mathrm{ns},0}$ is the first derivative of the correlation between the noise and the transmitted signal

at the true value of the ToA, which are given by

$$\tilde{a}_{b,0} = a_b(\tau_{b,0}|\gamma), \tag{5.2.3a}$$

$$\rho_{\mathrm{ns},0} = \rho_{\mathrm{ns},b}|_{\tau_b=\tau_{b,0}}\,, \tag{5.2.3b}$$

$$\dot{\rho}_{\mathrm{ns},0} = \frac{\partial}{\partial\tau_b}\rho_{\mathrm{ns},b}\bigg|_{\tau_b=\tau_{b,0}}, \tag{5.2.3c}$$

with $\rho_{\mathrm{ns},b} = \int_0^{T_\mathrm{o}} \Re(n(t)s^*(t-\tau_b))\mathrm{d}t$ *being the correlation between the delayed transmitted signal and the noise.*

Proof. Substituting (A.6.17) and (A.6.20) into (5.2.1), we obtain

$$\begin{aligned}\hat{\tau}_{b,\mathrm{ML}}(\gamma) - \tau_{b,0} = -&\frac{1}{\frac{1}{\tau_{b,0}^2}\gamma(1+\gamma)E_\mathrm{s}\tilde{a}_{b,0}^2 - \frac{1}{\tau_{b,0}^2}\gamma\left(1+\frac{1}{2}\gamma\right)E_\mathrm{s}\tilde{a}_{b,0}a_{b,0} + 8\pi^2\bar{\beta}^2E_\mathrm{s}\tilde{a}_{b,0}a_{b,0}} \\ &(\gamma-\gamma_0)\left(\frac{1}{\tau_{b,0}}\tilde{a}_{b,0}(E_\mathrm{s}a_{b,0}+\rho_{\mathrm{ns},0}-E_\mathrm{s}\tilde{a}_{b,0})\right. \\ &\left.-\frac{1}{\tau_{b,0}}\gamma\ln\left(\frac{d_0}{c\tau_{b,0}}\right)\tilde{a}_{b,0}\left(E_\mathrm{s}\tilde{a}_{b,0}-\frac{1}{2}E_\mathrm{s}a_{b,0}-\frac{1}{2}\rho_{\mathrm{ns},0}\right) - \ln\left(\frac{d_0}{c\tau_{b,0}}\right)\tilde{a}_{b,0}\dot{\rho}_{\mathrm{ns},0}\right).\end{aligned} \tag{5.2.4}$$

Some algebraic manipulation yields the final expression (5.2.2). □

5.2.1 Bias of the Friedlander Analysis Method

Proposition 5.2.2. *Using the Friedlander analysis method, the bias of the ML estimation under the imperfect PLE is given by*

$$\mathrm{E}_{n_b(t)}\left\{\hat{\tau}_{b,\mathrm{ML}}(\gamma) - \tau_{b,0}\right\} = -\frac{(\gamma-\gamma_0)(a_{b,0}-\tilde{a}_{b,0}) - \gamma(\gamma-\gamma_0)\ln\left(\frac{d_0}{c\tau_{b,0}}\right)\left(\tilde{a}_{b,0}-\frac{1}{2}a_{b,0}\right)}{8\pi^2\bar{\beta}^2\tau_{b,0}^2a_{b,0} - \left(\gamma(a_{b,0}-\tilde{a}_{b,0}) + \gamma^2\left(\frac{1}{2}a_{b,0}-\tilde{a}_{b,0}\right)\right)}\tau_{b,0}. \tag{5.2.5}$$

Proof. See Appendix A.7. □

It is possible to observe that in (5.2.5) the bias depends on neither the energy of the transmitted signal nor the noise variance.

Perfect PLE

Remark 5.2.1. When the PLE is perfect, the bias reduces to

$$\mathrm{E}_{n_b(t)}\left\{\hat{\tau}_{b,\mathrm{ML}}(\gamma)-\tau_{b,0}\right\}\big|_{\gamma=\gamma_0}=0. \tag{5.2.6}$$

Large Effective Bandwidth

Remark 5.2.2. For a large effective bandwidth, the bias tends to

$$\lim_{\bar{\beta}\to\infty}\mathrm{E}_{n_b(t)}\left\{\hat{\tau}_{b,\mathrm{ML}}(\gamma)-\tau_{b,0}\right\}=0. \tag{5.2.7}$$

The Bias as a Function of PLE Error

Remark 5.2.3. We can investigate the bias as a function of $\delta_\gamma=\gamma-\gamma_0$ from

$$\begin{aligned}&\mathrm{E}_{n_b(t)}\left\{\hat{\tau}_{b,\mathrm{ML}}(\gamma)-\tau_{b,0}\right\}\\&=-\frac{\delta_\gamma\left(1-\left(\frac{d_0}{c\tau_{b,0}}\right)^{\frac{1}{2}\delta_\gamma}+(\gamma_0+\delta_\gamma)\ln\left(\frac{d_0}{c\tau_{b,0}}\right)\left(\frac{1}{2}-\left(\frac{d_0}{c\tau_{b,0}}\right)^{\frac{1}{2}\delta_\gamma}\right)\right)}{8\pi^2\bar{\beta}^2\tau_{b,0}^2-(\gamma_0+\delta_\gamma)\left(1-\left(\frac{d_0}{c\tau_{b,0}}\right)^{\frac{1}{2}\delta_\gamma}+(\gamma_0+\delta_\gamma)\left(\frac{1}{2}-\left(\frac{d_0}{c\tau_{b,0}}\right)^{\frac{1}{2}\delta_\gamma}\right)\right)}\tau_{b,0}.\end{aligned} \tag{5.2.8}$$

5.2.2 The Error Variance of the ML Estimator Using the Friedlander Analysis Method without the Expectation of the Cross-derivative

Proposition 5.2.3. *Using the Friedlander analysis method without the expectation of the cross-derivative, the error variance of the ML estimation under the imperfect PLE is given*

by

$$\mathrm{E}_{n_b(t)}\left\{(\hat{\tau}_{b,\mathrm{ML}}(\gamma)-\tau_{b,0})^2\right\} = \frac{\tau_{b,0}^2(\gamma-\gamma_0)^2}{\left(\frac{\tilde{a}_{b,0}}{a_{b,0}}\gamma(1+\gamma)-\gamma\left(1+\frac{1}{2}\gamma\right)+8\pi^2\bar{\beta}^2\tau_{b,0}^2\right)^2} \left(\left(1-\frac{\tilde{a}_{b,0}}{a_{b,0}}+\gamma\ln\left(\frac{d_0}{c\tau_{b,0}}\right)\left(\frac{1}{2}-\frac{\tilde{a}_{b,0}}{a_{b,0}}\right)\right)^2 +\frac{1}{2}\frac{1}{a_{b,0}^2}\frac{\sigma_{\mathrm{n}}^2}{E_{\mathrm{s}}}\left(1+\frac{1}{2}\gamma\ln\left(\frac{d_0}{c\tau_{b,0}}\right)\right)^2+\frac{1}{a_{b,0}^2}\frac{\sigma_{\mathrm{n}}^2}{E_{\mathrm{s}}}2\pi^2\bar{\beta}^2\tau_{b,0}^2\ln^2\left(\frac{d_0}{c\tau_{b,0}}\right)\right). \tag{5.2.9}$$

Proof. See Appendix A.8. □

Perfect PLE

Remark 5.2.4. When the PLE is perfect, the error variance reduces to

$$\mathrm{E}_{n_b(t)}\left\{(\hat{\tau}_{b,\mathrm{ML}}(\gamma)-\tau_{b,0})^2\right\}\big|_{\gamma=\gamma_0} = 0. \tag{5.2.10}$$

Large Effective Bandwidth

Remark 5.2.5. For a large effective bandwidth, the error variance tends to

$$\lim_{\bar{\beta}\to\infty}\mathrm{E}_{n_b(t)}\left\{(\hat{\tau}_{b,\mathrm{ML}}(\gamma)-\tau_{b,0})^2\right\} = 0. \tag{5.2.11}$$

The Variance as a Function of PLE Error

Remark 5.2.6. We can investigate the error variance as a function of $\delta_\gamma = \gamma - \gamma_0$ from

$$
\begin{aligned}
&\mathrm{E}_{n_b(t)}\left\{(\hat{\tau}_{b,\mathrm{ML}}(\gamma)-\tau_{b,0})^2\right\} \\
&= \frac{\tau_{b,0}^2\delta_\gamma^2}{\left((\gamma_0+\delta_\gamma)(1+\gamma_0+\delta_\gamma)\left(\frac{d_0}{c\tau_{b,0}}\right)^{\frac{1}{2}\delta_\gamma}-(\gamma_0+\delta_\gamma)\left(1+\frac{1}{2}\gamma_0+\frac{1}{2}\delta_\gamma\right)+8\pi^2\bar{\beta}^2\tau_{b,0}^2\right)^2} \\
&\left(\left(1-\left(\frac{d_0}{c\tau_{b,0}}\right)^{\frac{1}{2}\delta_\gamma}+(\gamma_0+\delta_\gamma)\ln\left(\frac{d_0}{c\tau_{b,0}}\right)\left(\frac{1}{2}-\left(\frac{d_0}{c\tau_{b,0}}\right)^{\frac{1}{2}\delta_\gamma}\right)\right)^2\right. \\
&\left.+\frac{1}{2}\frac{1}{a_{b,0}^2}\frac{\sigma_\mathrm{n}^2}{E_\mathrm{s}}\left(1+\frac{1}{2}(\gamma_0+\delta_\gamma)\ln\left(\frac{d_0}{c\tau_{b,0}}\right)\right)^2+\frac{1}{a_{b,0}^2}\frac{\sigma_\mathrm{n}^2}{E_\mathrm{s}}2\pi^2\bar{\beta}^2\tau_{b,0}^2\ln^2\left(\frac{d_0}{c\tau_{b,0}}\right)\right) \\
&= \frac{\tau_{b,0}^2\delta_\gamma^2}{\left(\left(\frac{d_0}{c\tau_{b,0}}\right)^{\frac{1}{2}\delta_\gamma}(\gamma_0+\delta_\gamma)(1+\gamma_0+\delta_\gamma)-(\gamma_0+\delta_\gamma)\left(1+\frac{1}{2}\gamma_0+\frac{1}{2}\delta_\gamma\right)+8\pi^2\bar{\beta}^2\tau_{b,0}^2\right)^2} \\
&\left(\left(1-\left(\frac{d_0}{c\tau_{b,0}}\right)^{\frac{1}{2}\delta_\gamma}+(\gamma_0+\delta_\gamma)\ln\left(\frac{d_0}{c\tau_{b,0}}\right)\left(\frac{1}{2}-\left(\frac{d_0}{c\tau_{b,0}}\right)^{\frac{1}{2}\delta_\gamma}\right)\right)^2\right. \\
&\left.+\frac{1}{2}\frac{1}{a_{b,0}^2\mathrm{SNR}}\left(1+\frac{1}{2}(\gamma_0+\delta_\gamma)\ln\left(\frac{d_0}{c\tau_{b,0}}\right)\right)^2+\frac{1}{a_{b,0}^2\mathrm{SNR}}2\pi^2\bar{\beta}^2\tau_{b,0}^2\ln^2\left(\frac{d_0}{c\tau_{b,0}}\right)\right).
\end{aligned}
\tag{5.2.12}
$$

5.2.3 The Error Variance of the ML Estimator Using the Friedlander Analysis Method with the Expectation of the Cross-derivative

In this section, we can formulate the error between the real and the estimated ToAs by

$$
\hat{\tau}_{b,\mathrm{ML}}(\gamma)-\tau_{b,0} = -\frac{(\gamma-\gamma_0)\mathrm{E}_{n_b(t)}\left\{\frac{\partial^2}{\partial\gamma\partial\tau_b}f_{\mathrm{ML}}(\tau_b|\gamma)\Big|_{\tau_b=\tau_{b,0}}\right\}}{\mathrm{E}_{n_b(t)}\left\{\frac{\partial^2}{\partial\tau_b\partial\tau_b}f_{\mathrm{ML}}(\tau_b|\gamma)\Big|_{\tau_b=\tau_{b,0}}\right\}}. \tag{5.2.13}
$$

Proposition 5.2.4. *Using the Friedlander analysis method with the expectation of the cross-derivative, the error variance of the ML estimation under the imperfect PLE is given by*

$$\begin{aligned}
&\mathrm{E}_{n_b(t)}\left\{(\hat{\tau}_{b,\mathrm{ML}}(\gamma)-\tau_{b,0})^2\right\} \\
&= \frac{(\gamma-\gamma_0)^2\left(\frac{1}{\tau_{b,0}}E_{\mathrm{s}}\tilde{a}_{b,0}(a_{b,0}-\tilde{a}_{b,0})-\frac{1}{\tau_{b,0}}\gamma\ln\left(\frac{d_0}{c\tau_{b,0}}\right)E_{\mathrm{s}}\tilde{a}_{b,0}\left(\tilde{a}_{b,0}-\frac{1}{2}a_{b,0}\right)\right)^2}{\left(\frac{1}{\tau_{b,0}^2}\gamma(1+\gamma)E_{\mathrm{s}}\tilde{a}_{b,0}^2-\frac{1}{\tau_{b,0}^2}\gamma\left(1+\frac{1}{2}\gamma\right)E_{\mathrm{s}}\tilde{a}_{b,0}a_{b,0}+8\pi^2\bar{\beta}^2E_{\mathrm{s}}\tilde{a}_{b,0}a_{b,0}\right)^2} \\
&= \frac{\tau_{b,0}^2(\gamma-\gamma_0)^2\left(1-\frac{\tilde{a}_{b,0}}{a_{b,0}}+\gamma\ln\left(\frac{d_0}{c\tau_{b,0}}\right)\left(\frac{1}{2}-\frac{\tilde{a}_{b,0}}{a_{b,0}}\right)\right)^2}{\left(\frac{\tilde{a}_{b,0}}{a_{b,0}}\gamma(1+\gamma)-\gamma\left(1+\frac{1}{2}\gamma\right)+8\pi^2\bar{\beta}^2\tau_{b,0}^2\right)^2}.
\end{aligned} \tag{5.2.14}$$

Remark 5.2.7. If we take the limit of $\frac{E_{\mathrm{s}}}{\sigma_{\mathrm{n}}^2}$ to the infinity in (5.2.9), the expression in (5.2.9) is equal to (5.2.14). It can be implied that the result in (5.2.14) is the large SNR approximation of that in (5.2.9), see Fig. 5.4 and Fig. 5.5.

Perfect PLE

Remark 5.2.8. When the PLE is perfect, the error variance reduces to

$$\mathrm{E}_{n_b(t)}\left\{(\hat{\tau}_{b,\mathrm{ML}}(\gamma)-\tau_{b,0})^2\right\}\big|_{\gamma=\gamma_0}=0. \tag{5.2.15}$$

Large Effective Bandwidth

Remark 5.2.9. For a large effective bandwidth, the error variance tends to

$$\lim_{\bar{\beta}\to\infty}\mathrm{E}_{n_b(t)}\left\{(\hat{\tau}_{b,\mathrm{ML}}(\gamma)-\tau_{b,0})^2\right\}=0. \tag{5.2.16}$$

The Variance as a Function of PLE Error

Remark 5.2.10. We can investigate the error variance as a function of $\delta_\gamma = \gamma - \gamma_0$ from

$$\begin{aligned}
&\mathrm{E}_{n_b(t)}\left\{\left(\hat{\tau}_{b,\mathrm{ML}}(\gamma) - \tau_{b,0}\right)^2\right\} \\
&= \frac{\tau_{b,0}^2\delta_\gamma^2\left(1 - \left(\frac{d_0}{c\tau_{b,0}}\right)^{\frac{1}{2}\delta_\gamma} + (\gamma_0+\delta_\gamma)\ln\left(\frac{d_0}{c\tau_{b,0}}\right)\left(\frac{1}{2} - \left(\frac{d_0}{c\tau_{b,0}}\right)^{\frac{1}{2}\delta_\gamma}\right)\right)^2}{\left(\left(\frac{d_0}{c\tau_{b,0}}\right)^{\frac{1}{2}\delta_\gamma}(\gamma_0+\delta_\gamma)(1+\gamma_0+\delta_\gamma) - (\gamma_0+\delta_\gamma)\left(1+\frac{1}{2}\gamma_0+\frac{1}{2}\delta_\gamma\right) + 8\pi^2\bar{\beta}^2\tau_{b,0}^2\right)^2}.
\end{aligned} \tag{5.2.17}$$

In (5.2.17), we can see that the error variance depends on neither the energy of the transmitted signal nor the noise variance for this method.

5.2.4 Comments on the Friedlander Analysis Method

However, when $\gamma = \gamma_0$, i.e., for the perfect PLE, we can see in (5.2.10) and in (5.2.15) that the error variances of the ML estimation computed from the Friedlander method without the expectation of the cross-derivative and with the expectation of the cross-derivative become zero. This result is inconsistent with the intuition, since the error variance should reduce to the square of (3.6.1). Therefore, the error variance of the ML estimator calculated by the Friedlander method without or with the expectation of the cross-derivative cannot well predict the error performance.

The major reason of the inaccurate prediction ability by the Friedlander methods is that the Taylor expansion in [14, eq. (19)] has missed the derivative term at the true values of γ_0 and $\tau_{b,0}$. Next we correct the expansion based on the Taylor series.

5.3 Theoretical Error Performance Based on the First-Order Taylor Series

The first-order Taylor series of the $\frac{\partial}{\partial\tau_b}f_{\mathrm{ML}}(\tau_b|\tilde{\gamma})$ in two variables around the true values $\tau_{b,0}$ and γ_0 can be written as (see, e.g., [58–60])

$$\begin{aligned}\frac{\partial}{\partial\tau_b}f_{\mathrm{ML}}(\tau_b|\tilde{\gamma}) = \frac{\partial}{\partial\tau_b}f_{\mathrm{ML}}(\tau_b|\tilde{\gamma})\Big|_{\substack{\tau_b=\tau_{b,0}\\\tilde{\gamma}=\gamma_0}} + \frac{\partial^2}{\partial\tau_b\partial\tau_b}f_{\mathrm{ML}}(\tau_b|\tilde{\gamma})\Big|_{\substack{\tau_b=\tau_{b,0}\\\tilde{\gamma}=\gamma_0}}(\tau_b-\tau_{b,0})\\ + \frac{\partial^2}{\partial\tilde{\gamma}\partial\tau_b}f_{\mathrm{ML}}(\tau_b|\tilde{\gamma})\Big|_{\substack{\tau_b=\tau_{b,0}\\\tilde{\gamma}=\gamma_0}}(\tilde{\gamma}-\gamma_0) + o((\tau_b-\tau_{b,0})^2+(\tilde{\gamma}-\gamma_0)^2).\end{aligned} \tag{5.3.1}$$

The estimated value $\tau_b = \hat{\tau}_{b,\mathrm{ML}}(\gamma)$ minimizes $f_{\mathrm{ML}}(\tau_b|\tilde{\gamma})$ using a mis-modeled PLE. Then, $\frac{\partial}{\partial\tau_b}f_{\mathrm{ML}}(\tau_b|\tilde{\gamma})\Big|_{\substack{\tau_b=\hat{\tau}_{b,\mathrm{ML}}(\gamma)\\\tilde{\gamma}=\gamma}} = 0$, which results in

$$\begin{aligned}0 = \frac{\partial}{\partial\tau_b}f_{\mathrm{ML}}(\tau_b|\tilde{\gamma})\Big|_{\substack{\tau_b=\tau_{b,0}\\\tilde{\gamma}=\gamma}} + \frac{\partial^2}{\partial\tau_b\partial\tau_b}f_{\mathrm{ML}}(\tau_b|\tilde{\gamma})\Big|_{\substack{\tau_b=\tau_{b,0}\\\tilde{\gamma}=\gamma}}(\hat{\tau}_{b,\mathrm{ML}}(\gamma)-\tau_{b,0})\\ + \frac{\partial^2}{\partial\tilde{\gamma}\partial\tau_b}f_{\mathrm{ML}}(\tau_b|\tilde{\gamma})\Big|_{\substack{\tau_b=\tau_{b,0}\\\tilde{\gamma}=\gamma}}(\gamma-\gamma_0) + o((\tau_b-\tau_{b,0})^2+(\gamma-\gamma_0)^2).\end{aligned} \tag{5.3.2}$$

We assume that there is a point $\breve{\tau}$ in the line segment between $\tau_{b,0}$ and $\hat{\tau}_{b,\mathrm{ML}}(\gamma)$ such that the term $o((\hat{\tau}_{b,\mathrm{ML}}(\gamma)-\tau_{b,0})^2+(\tilde{\gamma}-\gamma_0)|_{\tau_b=\hat{\tau}_{b,0}} = 0$ vanishes, i.e., (see, e.g., [60])

$$\begin{aligned}0 = \frac{\partial}{\partial\tau_b}f_{\mathrm{ML}}(\tau_b|\gamma)\Big|_{\tau_b=\tau_{b,0}} + \frac{\partial^2}{\partial\tau_b\partial\tau_b}f_{\mathrm{ML}}(\tau_b|\gamma)\Big|_{\tau_b=\breve{\tau}}(\hat{\tau}_{b,\mathrm{ML}}(\gamma)-\tau_{b,0})\\ + \frac{\partial^2}{\partial\gamma\partial\tau_b}f_{\mathrm{ML}}(\tau_b|\gamma)\Big|_{\tau_b=\breve{\tau}}(\gamma-\gamma_0).\end{aligned} \tag{5.3.3}$$

For a continuous derivative $\frac{\partial^2}{\partial\tau_b\partial\tau_b}f_{\mathrm{ML}}(\tau_b|\gamma)$, the quantity $\frac{\partial^2}{\partial\tau_b\partial\tau_b}f_{\mathrm{ML}}(\tau_b|\gamma)\Big|_{\tau_b=\breve{\tau}}$ converges to $\mathrm{E}_{n_b(t)}\left\{\frac{\partial^2}{\partial\tau_b\partial\tau_b}f_{\mathrm{ML}}(\tau_b|\gamma)\Big|_{\tau_b=\tau_{b,0}}\right\}$ with probability one. Moreover, for a continuous derivative $\frac{\partial^2}{\partial\gamma\partial\tau_b}f_{\mathrm{ML}}(\tau_b|\gamma)$, the quantity $\frac{\partial^2}{\partial\gamma\partial\tau_b}f_{\mathrm{ML}}(\tau_b|\gamma)\Big|_{\tau_b=\breve{\tau}}$ also converges to

$\mathrm{E}_{n_b(t)}\left\{\frac{\partial^2}{\partial\gamma\partial\tau_b}f_{\mathrm{ML}}(\tau_b|\gamma)\Big|_{\tau_b=\tau_{b,0}}\right\}$ with probability one. Then, including these results into (5.3.3), we can obtain (see, e.g., [61])

$$\hat{\tau}_{b,\mathrm{ML}}(\gamma)-\tau_{b,0}=-\frac{\frac{\partial}{\partial\tau_b}f_{\mathrm{ML}}(\tau_b|\gamma)\Big|_{\tau_b=\tau_{b,0}}+(\gamma-\gamma_0)\mathrm{E}_{n_b(t)}\left\{\frac{\partial^2}{\partial\gamma\partial\tau_b}f_{\mathrm{ML}}(\tau_b|\gamma)\Big|_{\tau_b=\tau_{b,0}}\right\}}{\mathrm{E}_{n_b(t)}\left\{\frac{\partial^2}{\partial\tau_b\partial\tau_b}f_{\mathrm{ML}}(\tau_b|\gamma)\Big|_{\tau_b=\tau_{b,0}}\right\}}. \tag{5.3.4}$$

Proposition 5.3.1. *Using the anlysis method derived from the Taylor expansion with the expectation of the cross-derivative, the error between the estimated and the true values of the ToA can be given by*

$$\begin{aligned}
&\hat{\tau}_{b,\mathrm{ML}}(\gamma)-\tau_{b,0}\\
&=-\left(\frac{1}{\frac{1}{\tau_{b,0}^2}\gamma(1+\gamma)E_{\mathrm{s}}\tilde{a}_{b,0}-\frac{1}{\tau_{b,0}^2}\gamma\left(1+\frac{1}{2}\gamma\right)E_{\mathrm{s}}a_{b,0}+8\pi^2\bar{\beta}^2E_{\mathrm{s}}a_{b,0}}\right)\\
&\quad\left(-\frac{1}{\tau_{b,0}}\gamma\left(E_{\mathrm{s}}\tilde{a}_{b,0}-E_{\mathrm{s}}a_{b,0}-\rho_{\mathrm{ns},0}\right)-2\dot{\rho}_{\mathrm{ns},0}\right.\\
&\quad\left.+\frac{1}{\tau_{b,0}}(\gamma-\gamma_0)E_{\mathrm{s}}(a_{b,0}-\tilde{a}_{b,0})-\frac{1}{\tau_{b,0}}\gamma(\gamma-\gamma_0)\ln\left(\frac{d_0}{c\tau_{b,0}}\right)E_{\mathrm{s}}\left(\tilde{a}_{b,0}-\frac{1}{2}a_{b,0}\right)\right).
\end{aligned} \tag{5.3.5}$$

Proof. See Appendix A.9. □

5.3.1 The Bias of the ML Estimator under the Imperfect PLE

Proposition 5.3.2. *Using the analysis method derived from the Taylor expansion, the bias of the ML estimation under the imperfect PLE is given by*

$$\mathrm{E}_{n_b(t)}\left\{\hat{\tau}_{b,\mathrm{ML}}(\gamma)-\tau_{b,0}\right\}=-\frac{(2\gamma-\gamma_0)\left(a_{b,0}-\tilde{a}_{b,0}\right)+\gamma(\gamma-\gamma_0)\ln\left(\frac{d_0}{c\tau_{b,0}}\right)\left(\frac{1}{2}a_{b,0}-\tilde{a}_{b,0}\right)}{8\pi^2\bar{\beta}^2\tau_{b,0}^2a_{b,0}-\left(\gamma(a_{b,0}-\tilde{a}_{b,0})+\gamma^2\left(\frac{1}{2}a_{b,0}-\tilde{a}_{b,0}\right)\right)}\tau_{b,0}. \tag{5.3.6}$$

Proof. See Appendix A.10. □

It can be seen that the bias depends on neither the energy of the transmitted signal nor the noise variance. This result corresponds to the fact that when the channel parameter, i.e., the PLE, is not well identified, even though the transmitted SNR is high we cannot obtain the consistent estimate of the ToA.

Perfect PLE

Remark 5.3.1. When the PLE is perfect, the bias reduces to

$$\mathrm{E}_{n_b(t)}\left\{\hat{\tau}_{b,\mathrm{ML}}(\gamma)-\tau_{b,0}\right\}\big|_{\gamma=\gamma_0}=0. \tag{5.3.7}$$

Large Effective Bandwidth

Remark 5.3.2. For a large effective bandwidth, the bias tends to

$$\lim_{\bar{\beta}\to\infty}\mathrm{E}_{n_b(t)}\left\{\hat{\tau}_{b,\mathrm{ML}}(\gamma)-\tau_{b,0}\right\}=0. \tag{5.3.8}$$

The Bias as a Function of δ_γ

Remark 5.3.3. We can investigate the bias as function of $\delta_\gamma=\gamma-\gamma_0$ from

$$\begin{aligned}
&\mathrm{E}_{n_b(t)}\left\{\hat{\tau}_{b,\mathrm{ML}}(\gamma)-\tau_{b,0}\right\}\\
&=-\frac{(2\gamma-\gamma_0)\left(1-\frac{\tilde{a}_{b,0}}{a_{b,0}}\right)+(\gamma-\gamma_0)\gamma\ln\left(\frac{d_0}{c\tau_{b,0}}\right)\left(\frac{1}{2}-\frac{\tilde{a}_{b,0}}{a_{b,0}}\right)}{8\pi^2\bar{\beta}^2\tau_{b,0}^2-\gamma\left(\left(1-\frac{\tilde{a}_{b,0}}{a_{b,0}}\right)+\gamma\left(\frac{1}{2}-\frac{\tilde{a}_{b,0}}{a_{b,0}}\right)\right)}\tau_{b,0}\\
&=-\frac{(\gamma_0+2\delta_\gamma)\left(1-\left(\frac{d_0}{c\tau_{b,0}}\right)^{\frac{1}{2}\delta_\gamma}\right)+\delta_\gamma(\gamma_0+\delta_\gamma)\ln\left(\frac{d_0}{c\tau_{b,0}}\right)\left(\frac{1}{2}-\left(\frac{d_0}{c\tau_{b,0}}\right)^{\frac{1}{2}\delta_\gamma}\right)}{8\pi^2\bar{\beta}^2\tau_{b,0}^2-(\gamma_0+\delta_\gamma)\left(1-\left(\frac{d_0}{c\tau_{b,0}}\right)^{\frac{1}{2}\delta_\gamma}+(\gamma_0+\delta_\gamma)\left(\frac{1}{2}-\left(\frac{d_0}{c\tau_{b,0}}\right)^{\frac{1}{2}\delta_\gamma}\right)\right)}\tau_{b,0}.
\end{aligned} \tag{5.3.9}$$

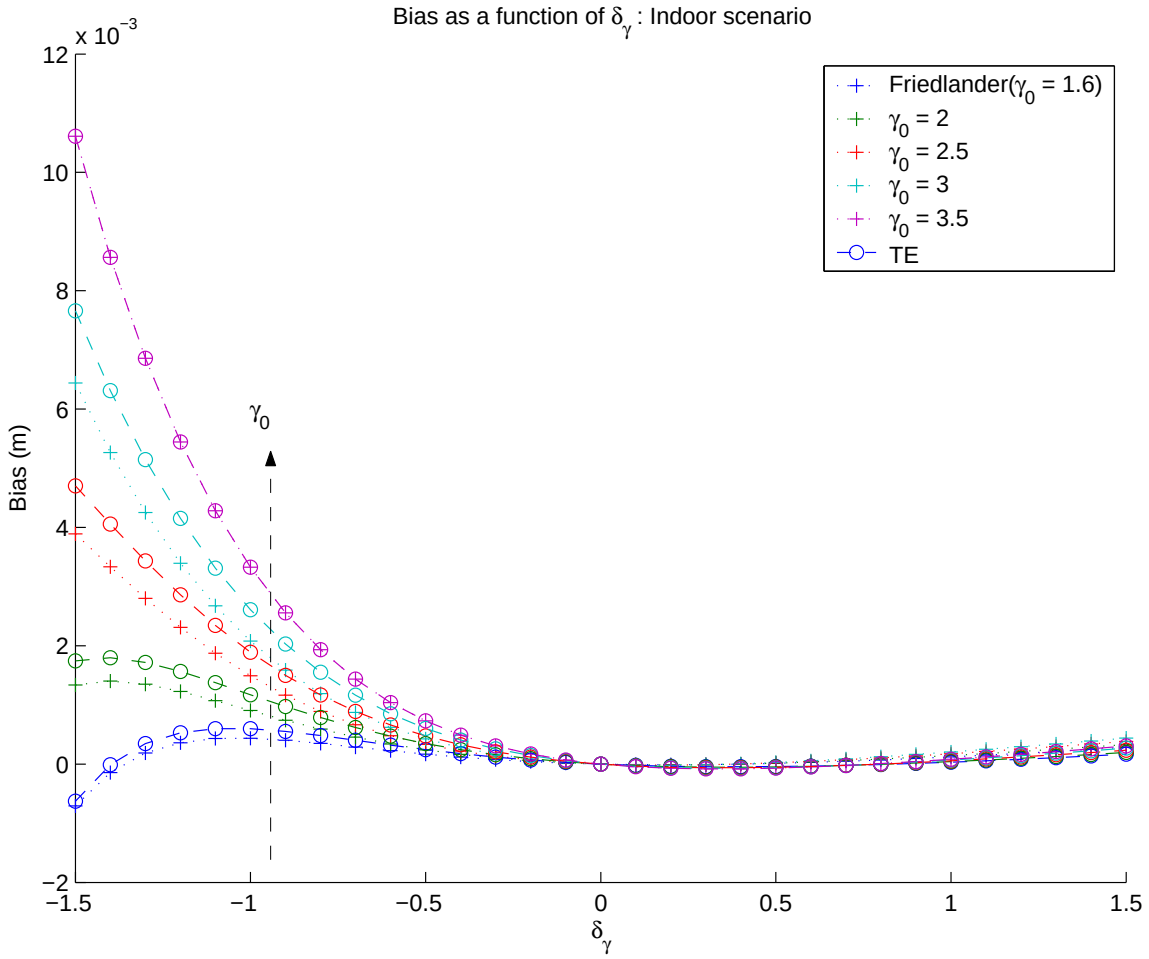

Figure 5.1: Comparison of the theoretical bias of the position estimate as a function of δ_γ for the Friedlander and the Taylor expansion methods for the imperfect PLE, several values of γ_0, $d_b = 3$ m, and $\bar{\beta} = 3.1007 \times 10^9$ Hz.

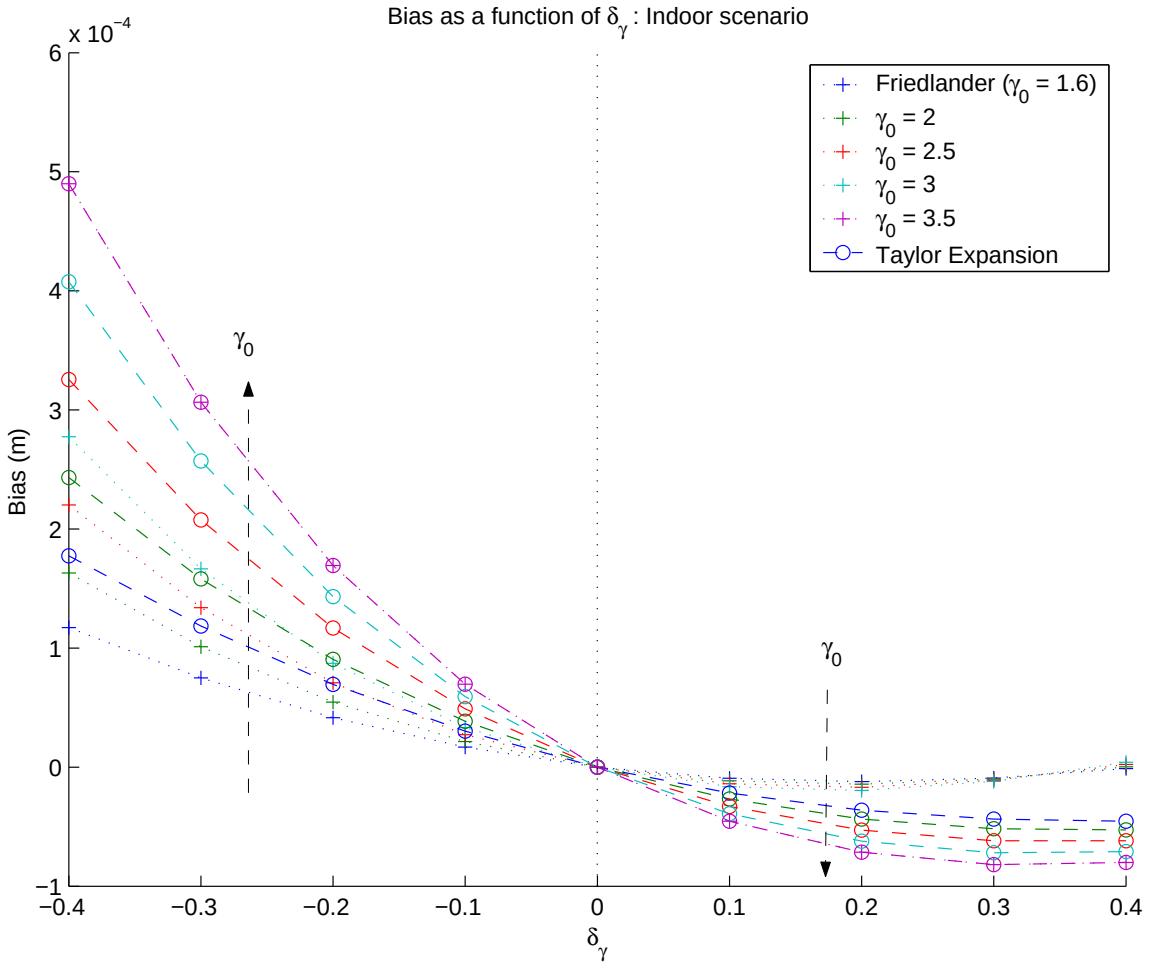

Figure 5.2: Zoomed comparison of the theoretical bias of the position estimate as a function of δ_γ for the Friedlander and the Taylor expansion methods for several values of γ_0, $d_b = 3$ m, and $\bar{\beta} = 3.1007 \times 10^9$ Hz.

5.3.2 The Error Variance of the ML Estimator for the Imperfect PLE without the Expectation of the Cross-derivative

In this section, let us consider the error between the estimated and the real ToAs defined by

$$\hat{\tau}_{b,\mathrm{ML}}(\gamma) - \tau_{b,0} = -\frac{\frac{\partial}{\partial \tau_b} f_{\mathrm{ML}}(\tau_b|\gamma)\Big|_{\tau_b=\tau_{b,0}} + (\gamma-\gamma_0)\ \frac{\partial^2}{\partial\gamma\partial\tau_b} f_{\mathrm{ML}}(\tau_b|\gamma)\Big|_{\tau_b=\tau_{b,0}}}{\mathrm{E}_{n_b(t)}\left\{\frac{\partial^2}{\partial\tau_b\partial\tau_b} f_{\mathrm{ML}}(\tau_b|\gamma)\Big|_{\tau_b=\tau_{b,0}}\right\}}. \tag{5.3.10}$$

It can be observed that the bias obtained from (A.9.2) is the same as that from (5.3.10). However, the error variance obtained from (A.9.2) is not the same as the expression (5.3.10).

Proposition 5.3.3. *Using the analysis method derived from the Taylor expansion without the expectation of the cross-derivative, the error variance of the ML estimation under the imperfect PLE is given by*

$$\begin{aligned}
&\mathrm{E}_{n_b(t)}\left\{(\hat{\tau}_{b,\mathrm{ML}}(\gamma)-\tau_{b,0})^2\right\} \\
&= \left(\left((2\gamma-\gamma_0)\left(1-\frac{\tilde{a}_{b,0}}{a_{b,0}}\right)+\gamma(\gamma-\gamma_0)\ln\left(\frac{d_0}{c\tau_{b,0}}\right)\left(\frac{1}{2}-\frac{\tilde{a}_{b,0}}{a_{b,0}}\right)\right)^2\right. \\
&\quad +\frac{1}{2}\frac{1}{a_{b,0}^2}\frac{\sigma_{\mathrm{n}}^2}{E_{\mathrm{s}}}\left(\gamma+(\gamma-\gamma_0)\left(1+\frac{1}{2}\gamma\ln\left(\frac{d_0}{c\tau_{b,0}}\right)\right)\right)^2 \\
&\quad \left.+\frac{1}{a_{b,0}^2}\frac{\sigma_{\mathrm{n}}^2}{E_{\mathrm{s}}}2\pi^2\bar{\beta}^2\tau_{b,0}^2\left(2+(\gamma-\gamma_0)\ln\left(\frac{d_0}{c\tau_{b,0}}\right)\right)^2\right) \\
&\quad \tau_{b,0}^2\left(\frac{\tilde{a}_{b,0}}{a_{b,0}}\gamma(1+\gamma)-\gamma\left(1+\frac{1}{2}\gamma\right)+8\pi^2\bar{\beta}^2\tau_{b,0}^2\right)^{-2}.
\end{aligned} \tag{5.3.11}$$

Proof. See Appendix A.11. □

Perfect PLE

Remark 5.3.4. For the perfect PLE the error variance reduces to

$$\mathrm{E}_{n_b(t)}\left\{(\hat{\tau}_{b,\mathrm{ML}}(\gamma)-\tau_{b,0})^2\right\}\big|_{\gamma=\gamma_0}=\frac{1}{a_{b,0}^2\mathrm{SNR}\left(8\pi^2\bar{\beta}^2+\frac{\gamma_0^2}{2\tau_{b,0}^2}\right)}. \tag{5.3.12}$$

Proof. See Appendix A.12. □

Therefore, if we take the square root onto the last expression, we obtain the RMSE, which is identical to the expression given by (3.6.1).

Large Effective Bandwidth

Remark 5.3.5. For the large effective bandwidth, the error variance remains zero, i.e.,

$$\lim_{\bar{\beta}\to\infty}\mathrm{E}_{n_b(t)}\left\{(\hat{\tau}_{b,\mathrm{ML}}(\gamma)-\tau_{b,0})^2\right\}=0. \tag{5.3.13}$$

The Error Variance as a Function of PLE Error

Remark 5.3.6. We can investigate the error variance as a function of $\delta_\gamma=\gamma-\gamma_0$ from

$$\begin{aligned}
&\mathrm{E}_{n_b(t)}\left\{(\hat{\tau}_{b,\mathrm{ML}}(\gamma)-\tau_{b,0})^2\right\}\\
&=\Bigg(\left((\gamma_0+2\delta_\gamma)\left(1-\left(\frac{d_0}{c\tau_{b,0}}\right)^{\frac{1}{2}\delta_\gamma}\right)+\delta_\gamma(\gamma_0+\delta_\gamma)\ln\left(\frac{d_0}{c\tau_{b,0}}\right)\left(\frac{1}{2}-\left(\frac{d_0}{c\tau_{b,0}}\right)^{\frac{1}{2}\delta_\gamma}\right)\right)^2\\
&\quad+\frac{1}{2}\frac{1}{a_{b,0}^2\mathrm{SNR}}\left((\gamma_0+\delta_\gamma)+\delta_\gamma\left(1+\frac{1}{2}(\gamma_0+\delta_\gamma)\ln\left(\frac{d_0}{c\tau_{b,0}}\right)\right)\right)^2\\
&\quad+\frac{1}{a_{b,0}^2\mathrm{SNR}}2\pi^2\bar{\beta}^2\tau_{b,0}^2\left(2+\delta_\gamma\ln\left(\frac{d_0}{c\tau_{b,0}}\right)\right)^2\Bigg)\\
&\quad\tau_{b,0}^2\left(\left(\frac{d_0}{c\tau_{b,0}}\right)^{\frac{1}{2}\delta_\gamma}(\gamma_0+\delta_\gamma)(1+\gamma_0+\delta_\gamma)-(\gamma_0+\delta_\gamma)\left(1+\frac{1}{2}(\gamma_0+\delta_\gamma)\right)+8\pi^2\bar{\beta}^2\tau_{b,0}^2\right)^{-2}.
\end{aligned} \tag{5.3.14}$$

The Error Variance for Infinite SNR

Remark 5.3.7. Then, for infinite SNR we have

$$\lim_{\mathrm{SNR}\to\infty} \mathrm{E}_{n_b(t)}\left\{(\hat{\tau}_{b,\mathrm{ML}}(\gamma)-\tau_{b,0})^2\right\} = \frac{\left((\gamma_0+2\delta_\gamma)\left(1-\left(\frac{d_0}{c\tau_{b,0}}\right)^{\frac{1}{2}\delta_\gamma}\right)+\delta_\gamma(\gamma_0+\delta_\gamma)\ln\left(\frac{d_0}{c\tau_{b,0}}\right)\left(\frac{1}{2}-\left(\frac{d_0}{c\tau_{b,0}}\right)^{\frac{1}{2}\delta_\gamma}\right)\right)^2}{\left(\left(\frac{d_0}{c\tau_{b,0}}\right)^{\frac{1}{2}\delta_\gamma}(\gamma_0+\delta_\gamma)(1+\gamma_0+\delta_\gamma)-(\gamma_0+\delta_\gamma)\left(1+\frac{1}{2}(\gamma_0+\delta_\gamma)\right)+8\pi^2\bar{\beta}^2\tau_{b,0}^2\right)^2}\tau_{b,0}^2. \tag{5.3.15}$$

5.3.3 The Error Variance of the ML Estimator under the Imperfect PLE with the Expectation of the Cross-derivative

Proposition 5.3.4. *Using the analysis method derived from the Taylor expansion with the expectation of the cross-derivative, the error variance of the ML estimation under the imperfect PLE is given by*

$$\mathrm{E}_{n_b(t)}\left\{(\hat{\tau}_{b,\mathrm{ML}}(\gamma)-\tau_{b,0})^2\right\} = \frac{\left((2\gamma-\gamma_0)\left(1-\frac{\tilde{a}_{b,0}}{a_{b,0}}\right)+\gamma(\gamma-\gamma_0)\ln\left(\frac{d_0}{c\tau_{b,0}}\right)\left(\frac{1}{2}-\frac{\tilde{a}_{b,0}}{a_{b,0}}\right)\right)^2+\frac{1}{a_{b,0}^2}\frac{\sigma_{\mathrm{n}}^2}{E_{\mathrm{s}}}\left(\frac{1}{2}\gamma^2+8\pi^2\bar{\beta}^2\tau_{b,0}^2\right)}{\left(\frac{\tilde{a}_{b,0}}{a_{b,0}}\gamma(1+\gamma)-\gamma\left(1+\frac{1}{2}\gamma\right)+8\pi^2\bar{\beta}^2\tau_{b,0}^2\right)^2}\tau_{b,0}^2. \tag{5.3.16}$$

Proof. See Appendix A.13. □

Perfect PLE

Remark 5.3.8. For the perfect PLE the error variance reduces to

$$\mathrm{E}_{n_b(t)}\left\{(\hat{\tau}_{b,\mathrm{ML}}(\gamma)-\tau_{b,0})^2\right\}\Big|_{\gamma=\gamma_0} = \frac{1}{\mathrm{SNR}a_{b,0}^2\left(8\pi^2\bar{\beta}^2+\frac{\gamma_0^2}{2\tau_{b,0}^2}\right)}. \tag{5.3.17}$$

Proof. See Appendix A.14. □

Therefore, if we take the square root onto (5.3.17), we obtain the RMSE, which is identical to the expression given by (3.6.1).

Large Effective Bandwidth

Remark 5.3.9. For the large effective bandwidth, the error variance remains zero, i.e.,

$$\lim_{\bar{\beta}\to\infty} \mathrm{E}_{n_b(t)} \left\{ (\hat{\tau}_{b,\mathrm{ML}}(\gamma) - \tau_{b,0})^2 \right\} = 0. \tag{5.3.18}$$

The Error Variance as a Function of PLE Error

Remark 5.3.10. We can investigate the error variance as a function of $\delta_\gamma = \gamma - \gamma_0$ from

$$\begin{aligned}
&\mathrm{E}_{n_b(t)} \left\{ (\hat{\tau}_{b,\mathrm{ML}}(\gamma) - \tau_{b,0})^2 \right\} \\
&= \Bigg(\Bigg((\gamma_0 + 2\delta_\gamma) \left(1 - \left(\frac{d_0}{c\tau_{b,0}} \right)^{\frac{1}{2}\delta_\gamma} \right) + \delta_\gamma(\gamma_0 + \delta_\gamma) \ln \left(\frac{d_0}{c\tau_{b,0}} \right) \left(\frac{1}{2} - \left(\frac{d_0}{c\tau_{b,0}} \right)^{\frac{1}{2}\delta_\gamma} \right) \Bigg)^2 \\
&\quad + \frac{1}{a_{b,0}^2 \mathrm{SNR}} \left(\frac{1}{2}(\gamma_0 + \delta_\gamma)^2 + 8\pi^2 \bar{\beta}^2 \tau_{b,0}^2 \right) \Bigg) \\
&\quad \tau_{b,0}^2 \left(\left(\frac{d_0}{c\tau_{b,0}} \right)^{\frac{1}{2}\delta_\gamma} (\gamma_0 + \delta_\gamma)(1 + \gamma_0 + \delta_\gamma) - (\gamma_0 + \delta_\gamma) \left(1 + \frac{1}{2}\gamma_0 + \frac{1}{2}\delta_\gamma \right) + 8\pi^2 \bar{\beta}^2 \tau_{b,0}^2 \right)^{-2}.
\end{aligned} \tag{5.3.19}$$

The Error Variance for Infinite SNR

Remark 5.3.11. Then, for infinite SNR we have

$$\lim_{\mathrm{SNR}\to\infty} \mathrm{E}_{n_b(t)}\left\{(\hat{\tau}_{b,\mathrm{ML}}(\gamma)-\tau_{b,0})^2\right\} = \frac{\left((\gamma_0+2\delta_\gamma)\left(1-\left(\frac{d_0}{c\tau_{b,0}}\right)^{\frac{1}{2}\delta_\gamma}\right)+\delta_\gamma(\gamma_0+\delta_\gamma)\ln\left(\frac{d_0}{c\tau_{b,0}}\right)\left(\frac{1}{2}-\left(\frac{d_0}{c\tau_{b,0}}\right)^{\frac{1}{2}\delta_\gamma}\right)\right)^2}{\left(\left(\frac{d_0}{c\tau_{b,0}}\right)^{\frac{1}{2}\delta_\gamma}(\gamma_0+\delta_\gamma)(1+\gamma_0+\delta_\gamma)-(\gamma_0+\delta_\gamma)\left(1+\frac{1}{2}\gamma_0+\frac{1}{2}\delta_\gamma\right)+8\pi^2\bar{\beta}^2\tau_{b,0}^2\right)^2}\tau_{b,0}^2. \tag{5.3.20}$$

According to (5.3.15), it is possible to observe in Fig. 5.3 that for a large SNR the Taylor expansion methods with and without the expectation of the cross-derivative for calculating the error variance give the same result. As in Remark 5.2.7, the Friedlander analysis methods with and without the expectation of the cross-derivative provide the same result in Fig. 5.3. For a large SNR, we can also observe that the Friedlander method without the expectation of the cross-derivative does not coincide with the Taylor expansion methods for a large SNR.

Fig. 5.4 and Fig. 5.5 show the theoretical error variances for the Friedlander and the Taylor expansion methods with and without the expectation of the cross-derivative for different values of the true PLE and the $\mathrm{SNR}_{\mathrm{Rx}}$.

Fig. 5.6 and Fig. 5.7 show the Taylor expansion method with the expectation of the cross-derivative for the RMSE of the position estimate as a function of δ_γ for several values of γ_0 and the $\mathrm{SNR}_{\mathrm{Rx}}$. Note that in Fig. 5.6 the error variance increases fast for the negatives values of the PLE error, and in Fig. 5.7 the RMSE increases when the $\mathrm{SNR}_{\mathrm{Rx}}$ decreases. Moreover, in Fig.5.8 and Fig. 5.9 we can observe the Taylor expansion method with the expectation of the cross-derivative for the RMSE of the position estimate as a function of δ_γ for the infinite $\mathrm{SNR}_{\mathrm{Rx}}$,

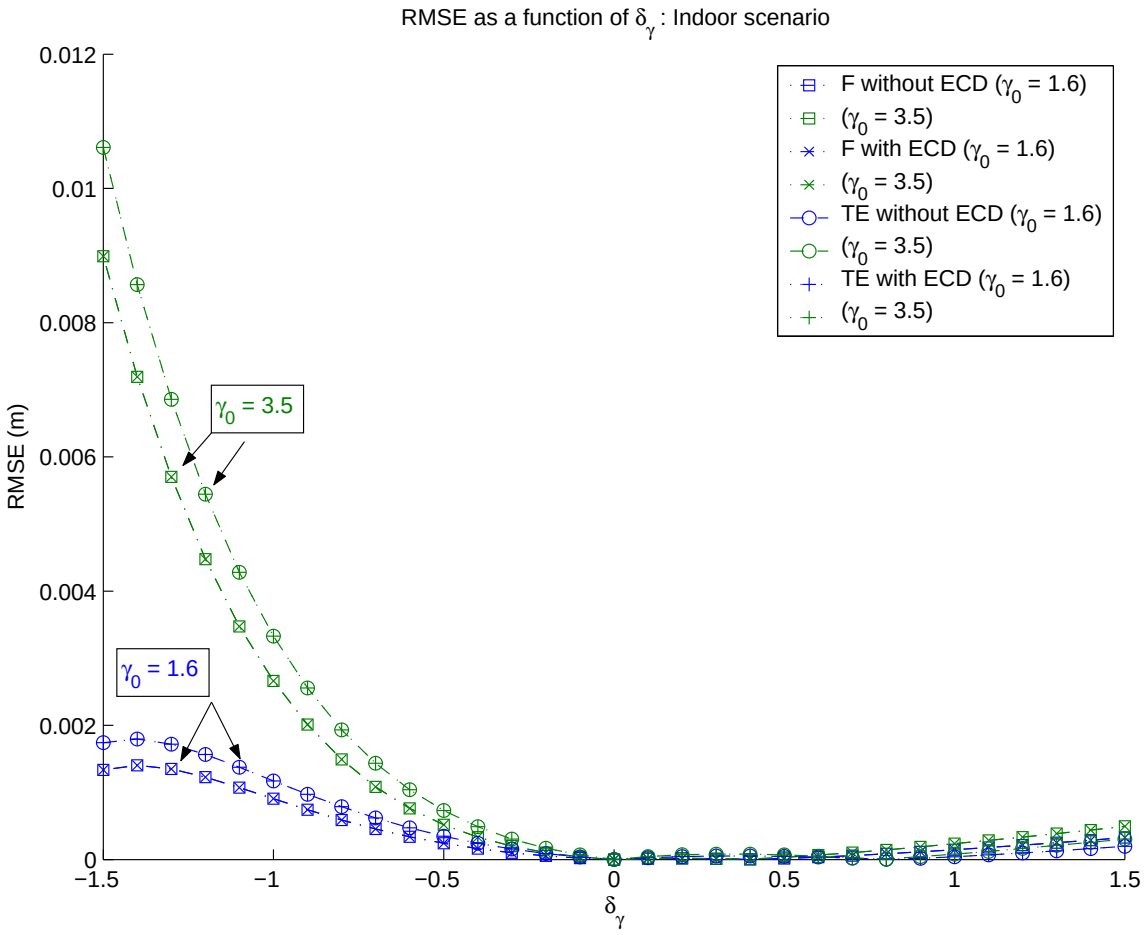

Figure 5.3: Comparison of the theoretical RMSE of the position estimate as a function of δ_γ for the Friedlander with or without the expectation of the cross-derivative and the Taylor expansion methods with or without the expectation of the cross-derivative for the imperfect PLE, several values of γ_0, $d_b = 3$ m, transmitted $\mathrm{SNR} = 200$ dB, and $\bar{\beta} = 3.1007 \times 10^9$ Hz.

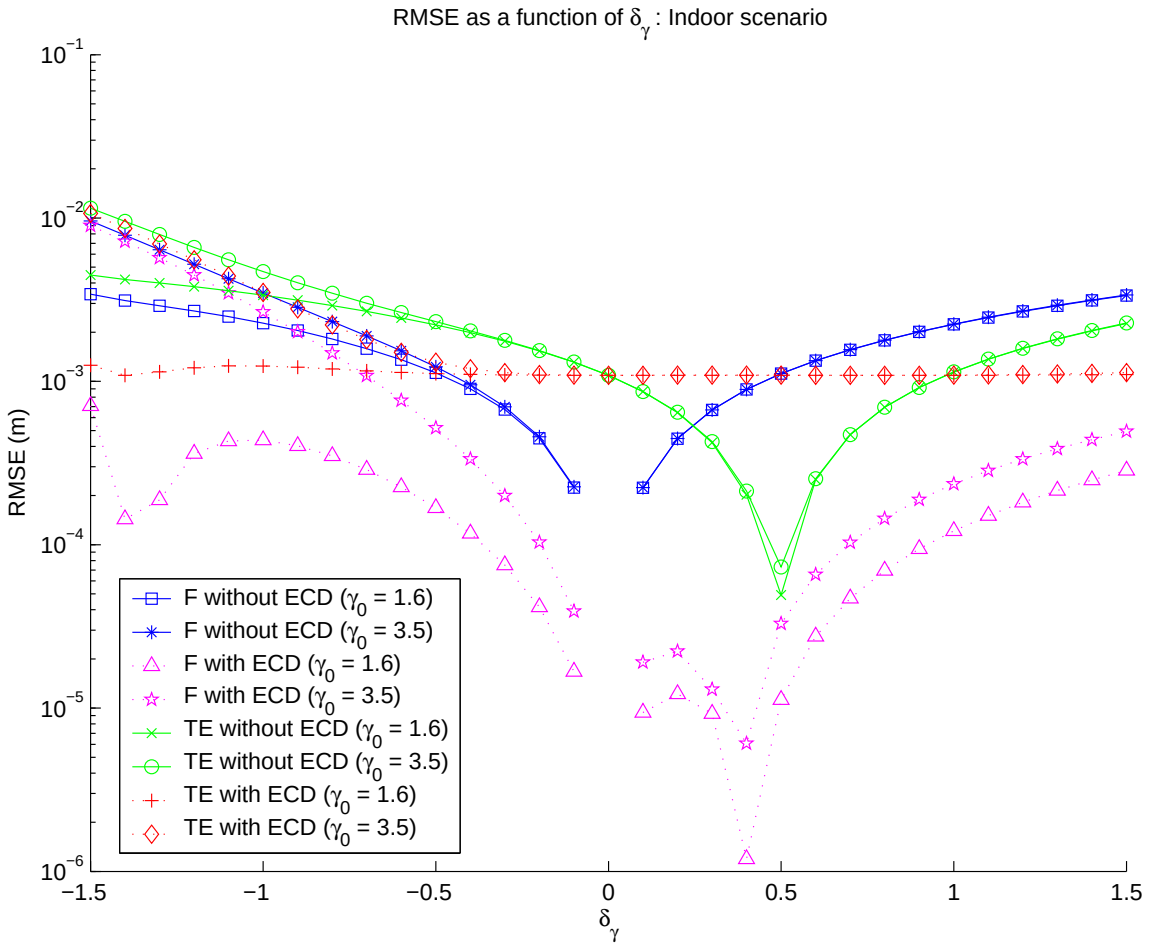

Figure 5.4: Comparison of the theoretical RMSE of the position estimate as a function of δ_γ for the Friedlander and the Taylor expansion methods with or without the expectation of the cross-derivative for the imperfect PLE, several values of γ_0, $d_b = 3$ m, $\mathrm{SNR}_{\mathrm{Rx}} = 20$ dB, and $\bar{\beta} = 3.1007 \times 10^9$ Hz.

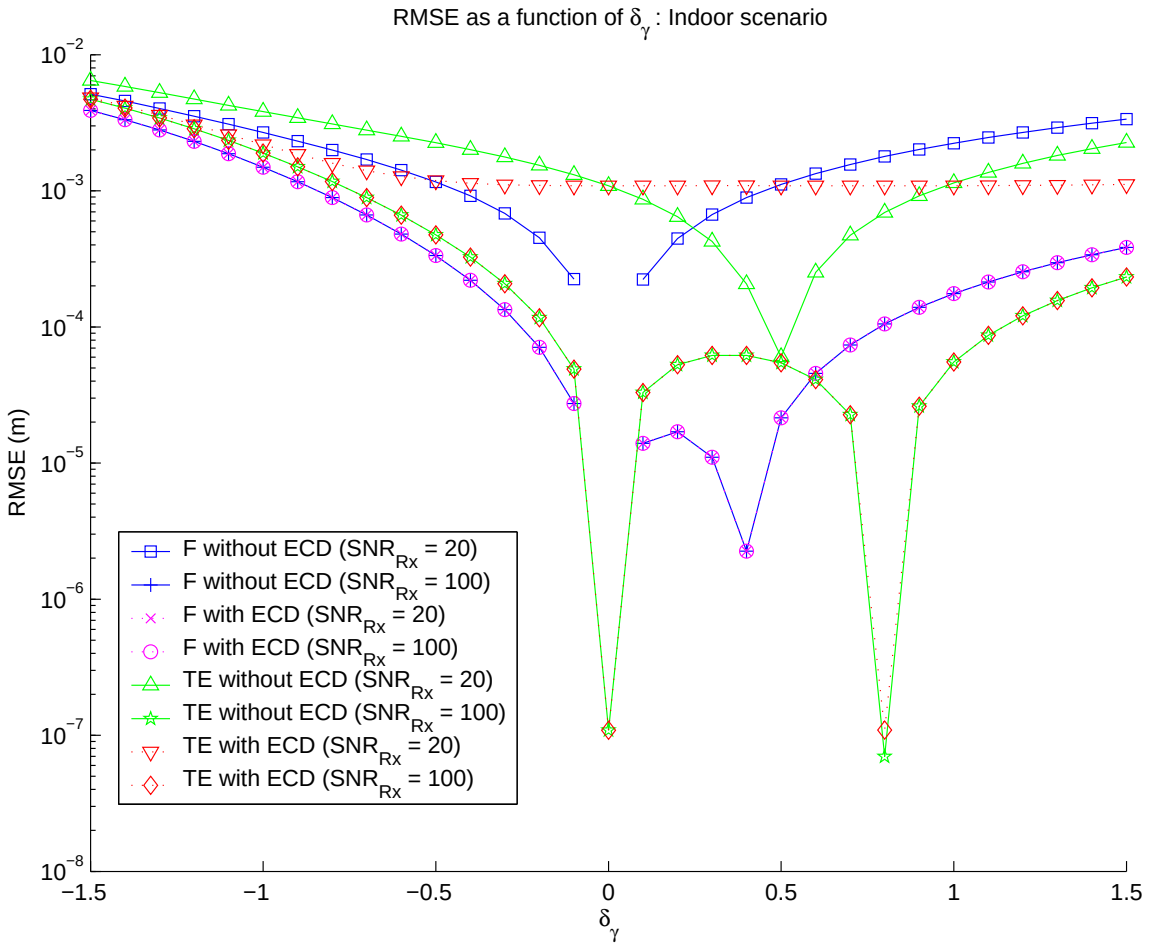

Figure 5.5: Comparison of the theoretical RMSE of the position estimate as a function of δ_γ for the Friedlander and the Taylor expansion methods with or without the expectation of the cross-derivative for the imperfect PLE, several values of $\mathrm{SNR_{Rx}}$, $d_b = 3$ m,$\gamma_0 = 2.5$, and $\bar{\beta} = 3.1007 \times 10^9$ Hz.

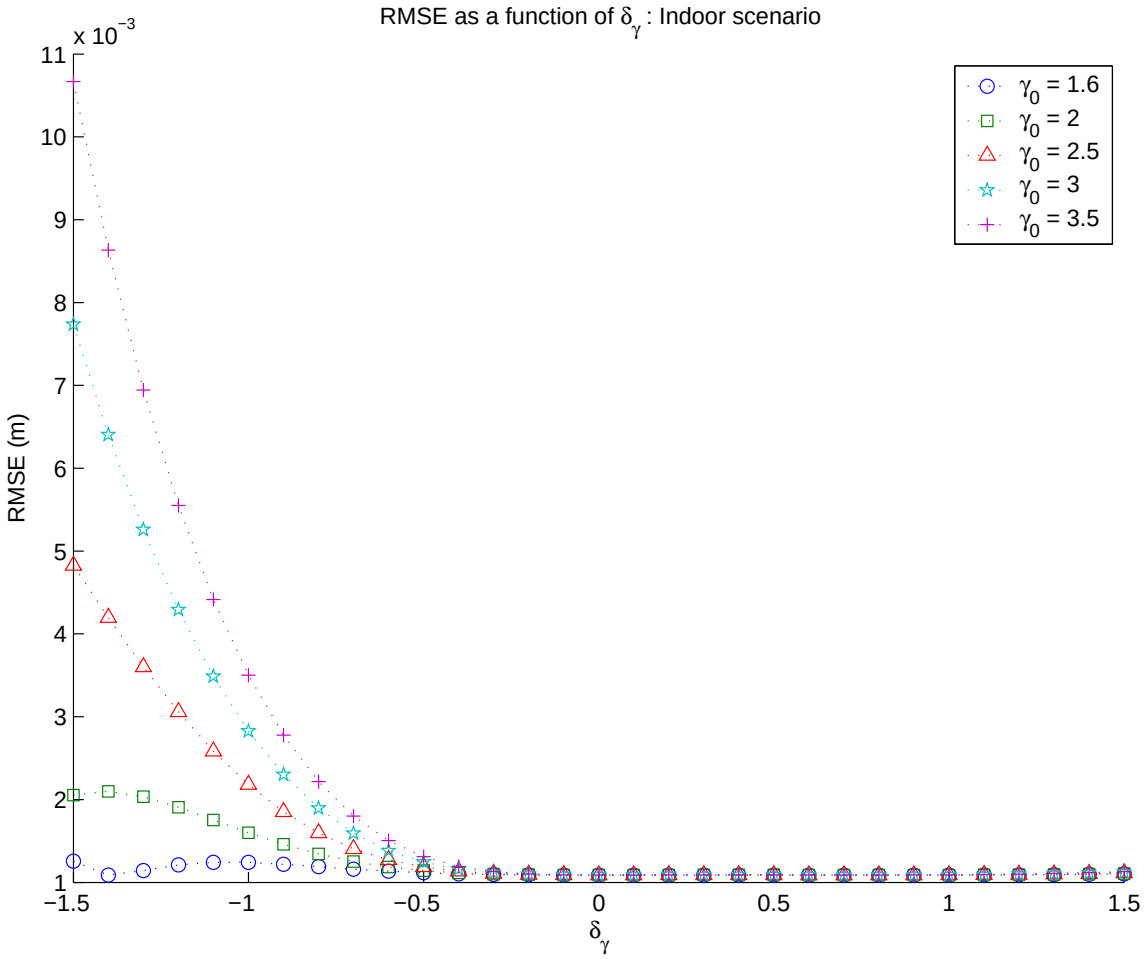

Figure 5.6: Taylor expansion method with the expectation of the cross-derivative for the RMSE of the position estimate as a function of δ_γ for the indoor scenario, several values of γ_0, $\mathrm{SNR}_{\mathrm{Rx}} = 20$ dB, $d_b = 3$ m, and $\bar{\beta} = 3.1007 \times 10^9$ Hz.

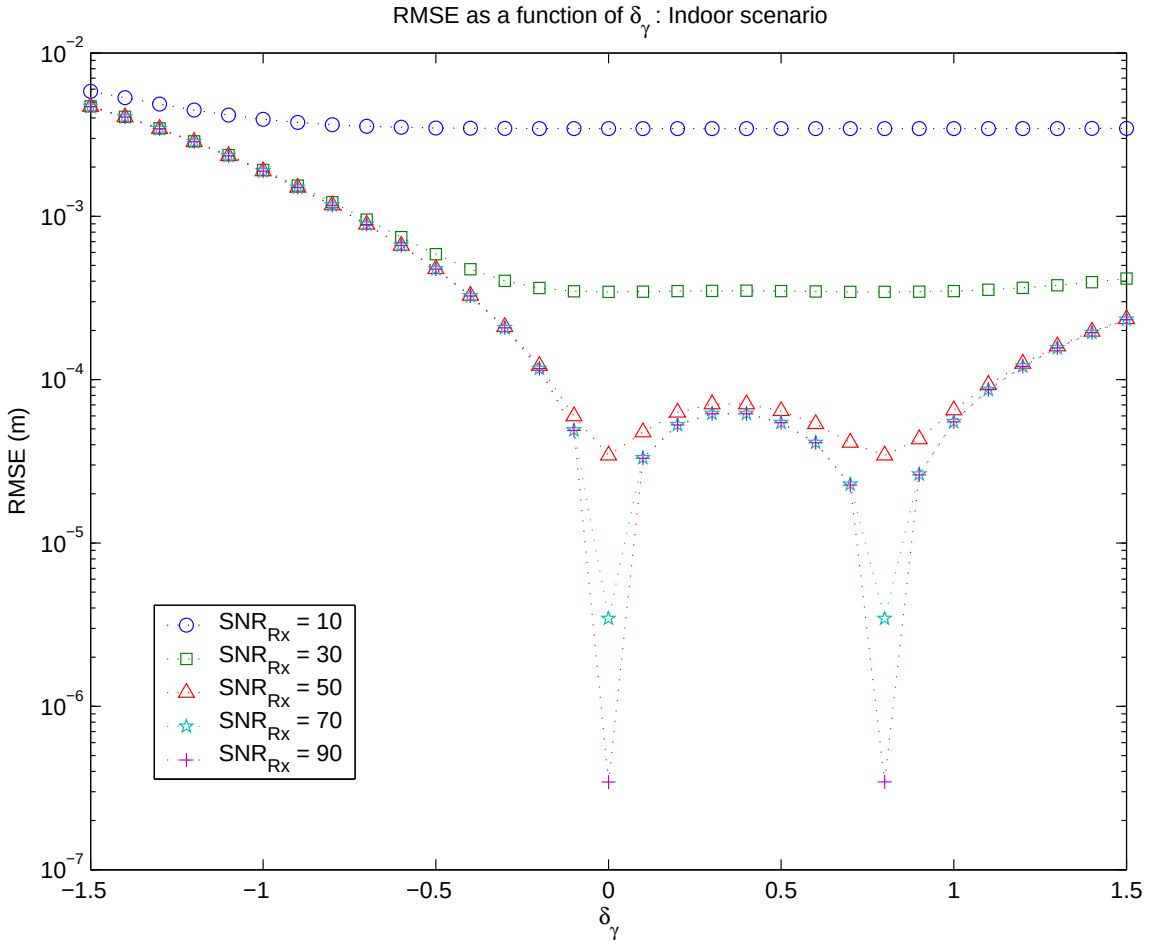

Figure 5.7: Taylor expansion method with the expectation of the cross-derivative for the RMSE of the position estimate as a function of δ_γ for the indoor scenario, several values of $\mathrm{SNR}_{\mathrm{Rx}}$, $\gamma = 2.5$, $d_b = 3$ m, and $\bar{\beta} = 3.1007 \times 10^9$ Hz.

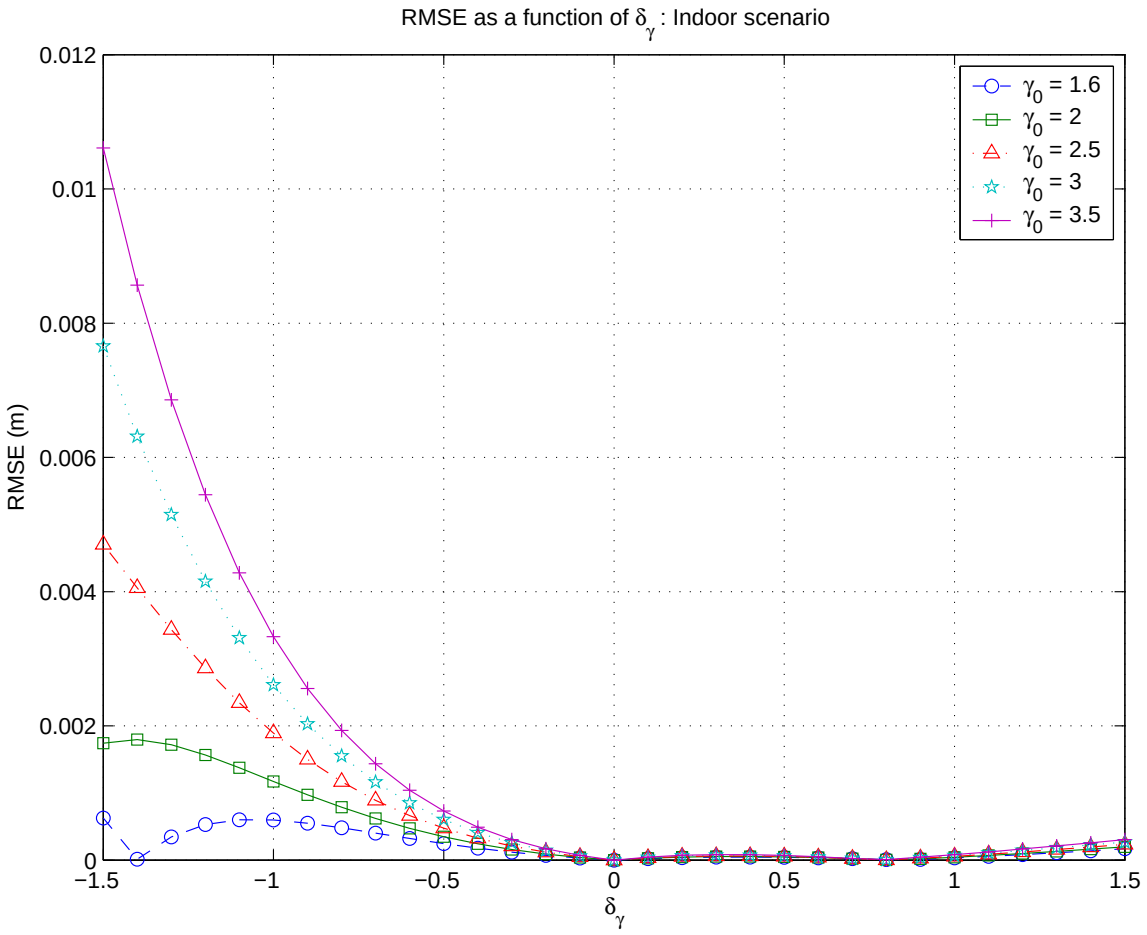

Figure 5.8: Taylor expansion method with the expectation of the cross-derivative for the RMSE of the position estimate as a function of δ_γ for the indoor scenario for infinite SNR, $d_b = 3$ m, and $\bar{\beta} = 3.1007 \times 10^9$ Hz.

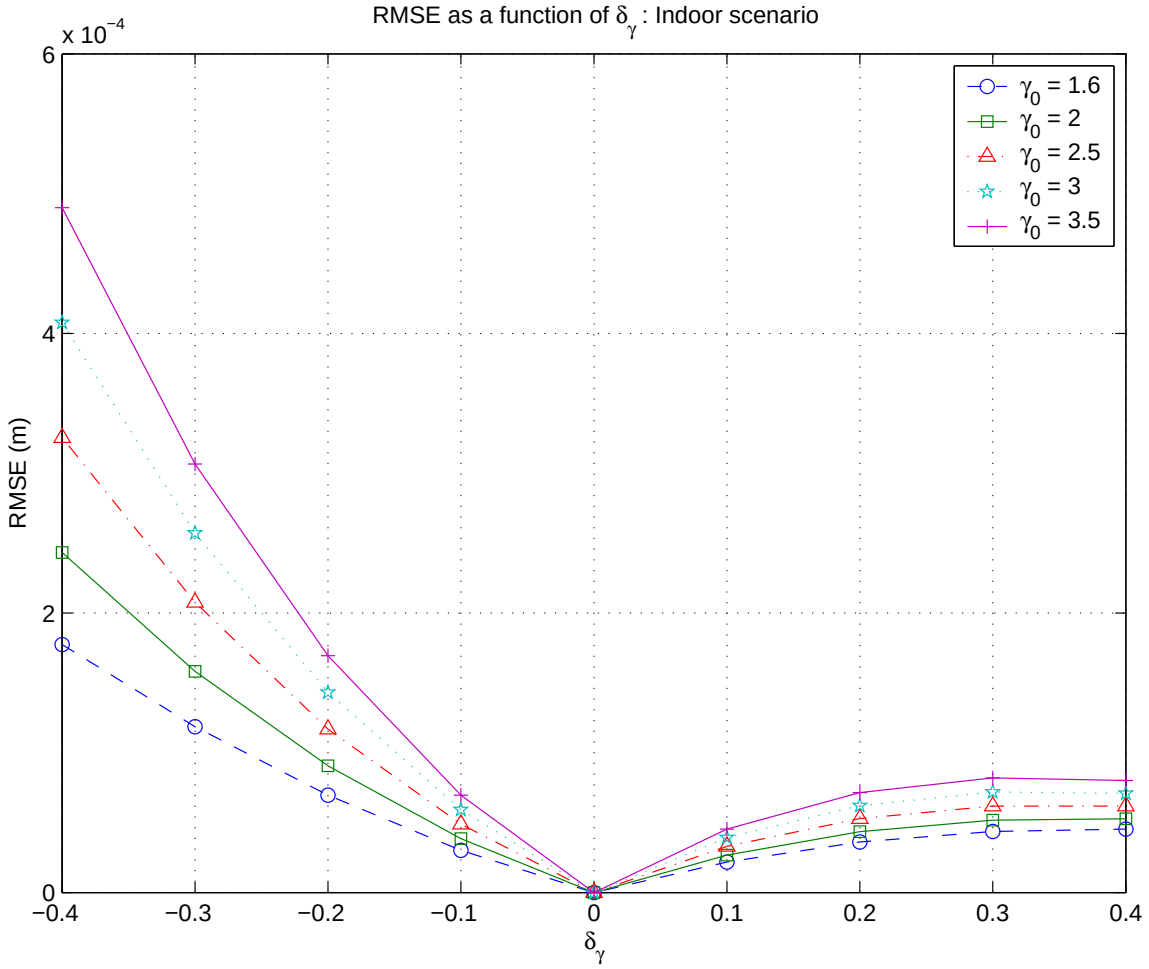

Figure 5.9: Taylor expansion method with the expectation of the cross-derivative for the zoomed RMSE of the position estimate as a function of δ_γ for the indoor scenario for infinite SNR, $d_b = 3$ m, and $\bar{\beta} = 3.1007 \times 10^9$ Hz.

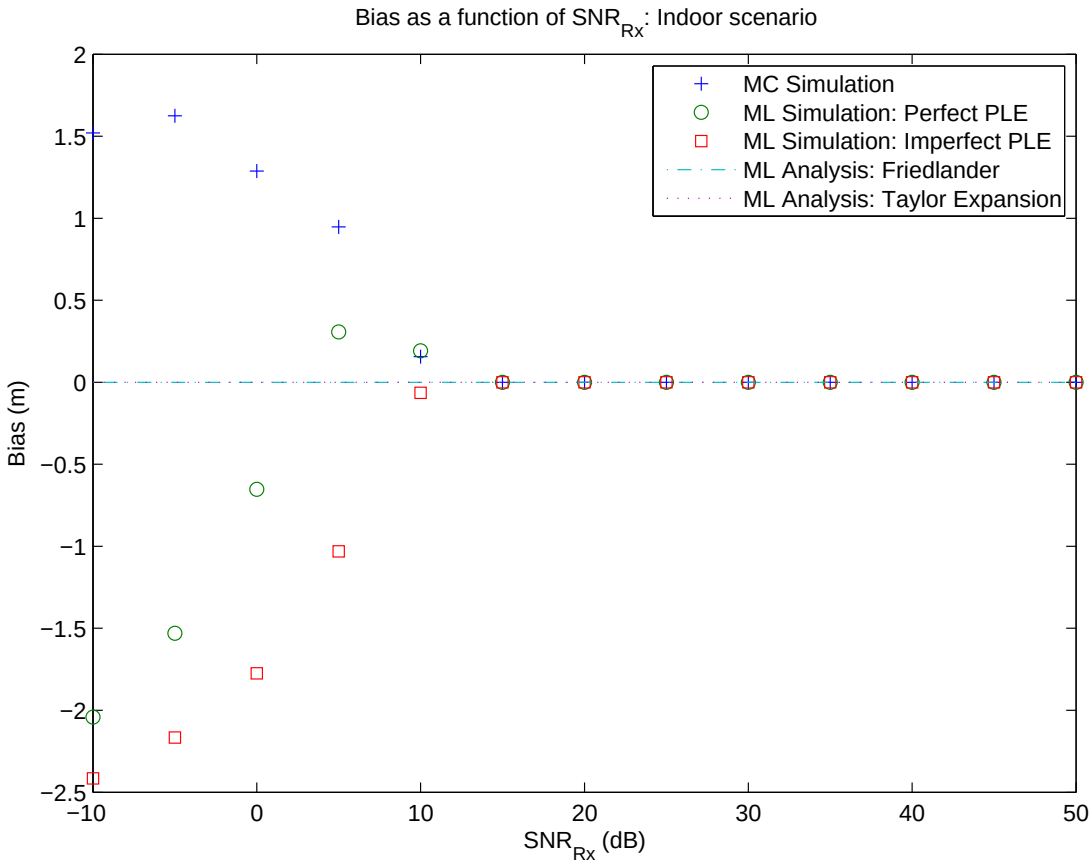

Figure 5.10: Bias of the position estimate as a function of $\mathrm{SNR}_{\mathrm{Rx}}$ for the imperfect PLE, $\gamma_0 = 2$, $\delta_\gamma = 0.5$, $d_b = 3$ m, $\bar{\beta} = 3.1007 \times 10^9$ Hz, sampling time $= 0.01$ ps, and $N_{\mathrm{R}} = 1{,}000$ independent runs.

where we can see that the error variance is also higher for the negative values of the PLE error than for the positives values of the PLE error.

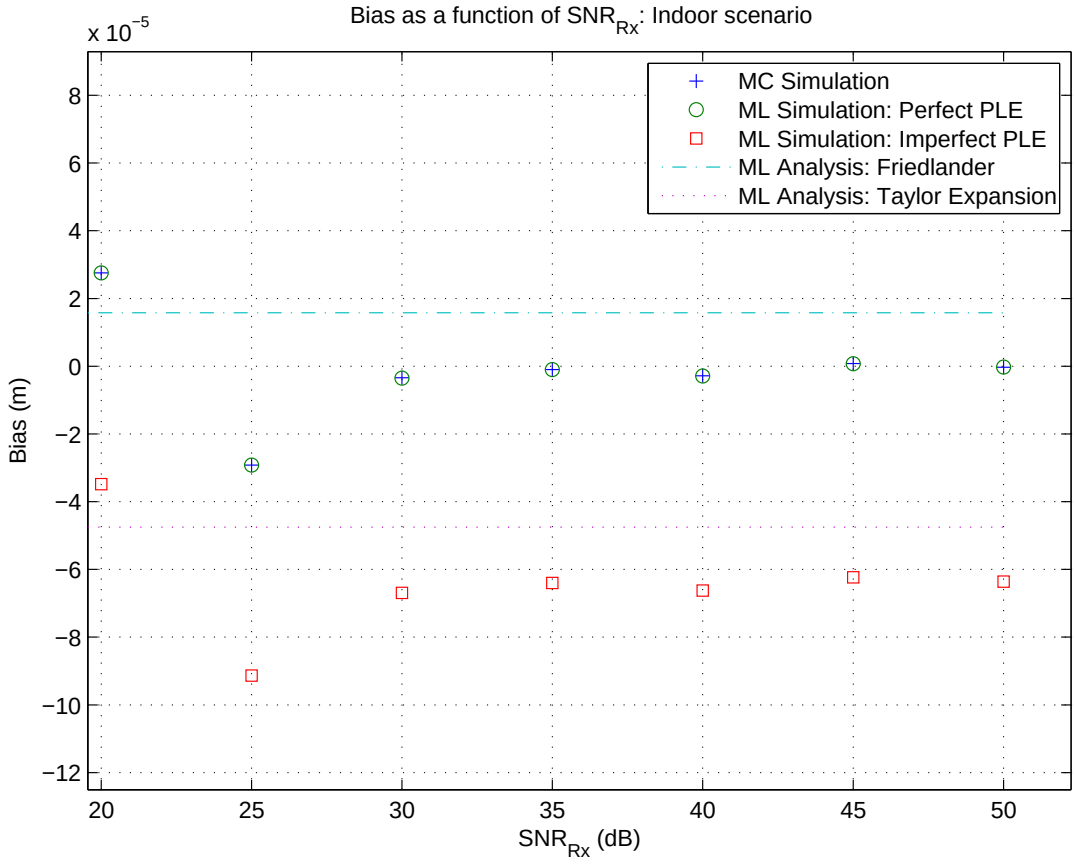

Figure 5.11: Zoomed bias of the position estimate as a function of $\mathrm{SNR}_{\mathrm{Rx}}$ for the imperfect PLE, $\gamma_0 = 2$, $\delta_\gamma = 0.5$, $d_b = 3$ m, $\bar{\beta} = 3.1007 \times 10^9$ Hz, sampling time $= 0.01$ ps, and $N_{\mathrm{R}} = 1{,}000$ independent runs.

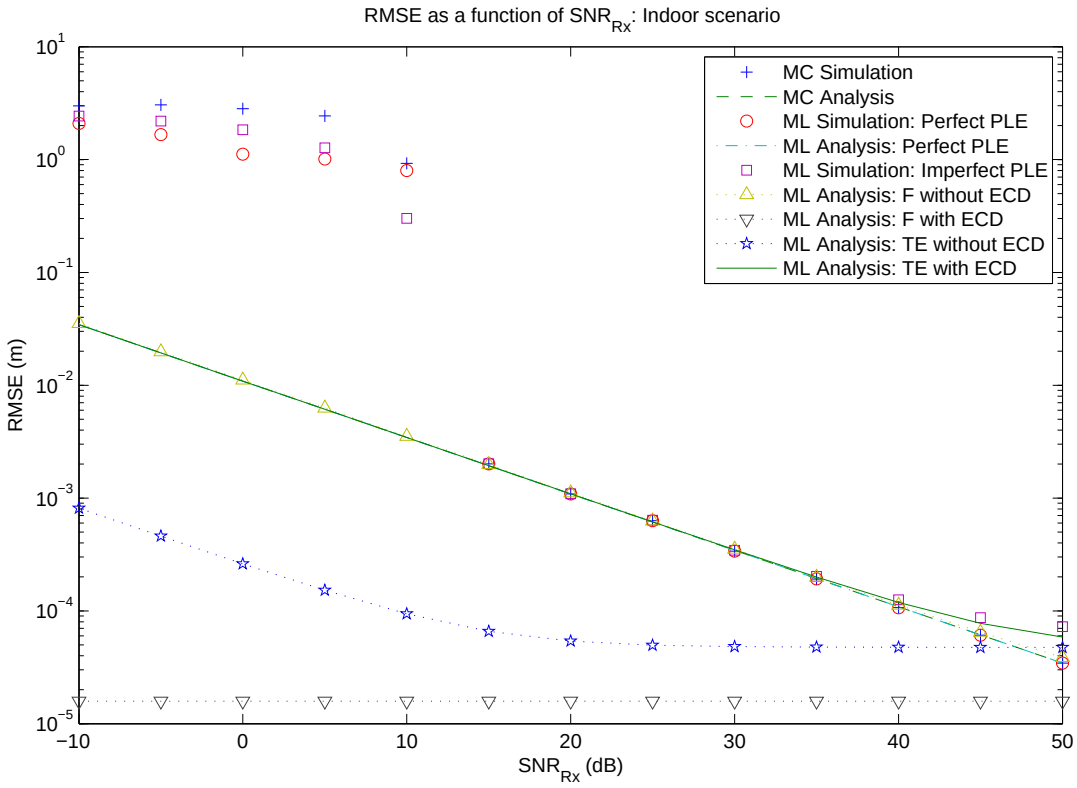

Figure 5.12: RMSE of the position estimate as a function of $\mathrm{SNR}_{\mathrm{Rx}}$ for the imperfect PLE, $\gamma_0 = 2$, $\delta_\gamma = 0.5$, $d_b = 3$ m, $\bar{\beta} = 3.1007 \times 10^9$ Hz, sampling time $= 0.01$ ps, and $N_{\mathrm{R}} = 1{,}000$ independent runs.

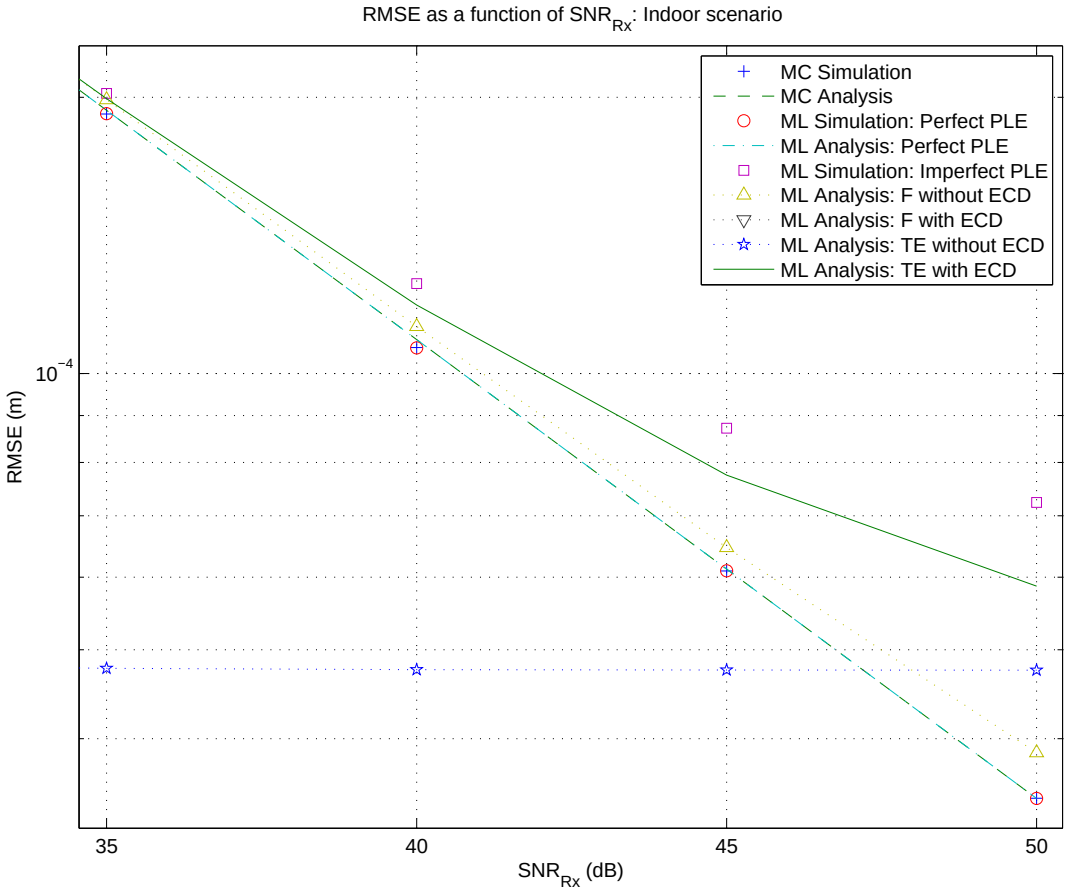

Figure 5.13: Zoomed RMSE of the position estimate as a function of $\mathrm{SNR}_{\mathrm{Rx}}$ for the imperfect PLE, $\gamma_0 = 2$, $\delta_\gamma = 0.5$, $d_b = 3$ m, $\bar{\beta} = 3.1007 \times 10^9$ Hz, sampling time $= 0.01$ ps, and $N_{\mathrm{R}} = 1{,}000$ independent runs.

5.4 Numerical Discussions about the Simulations and the Theoretical Analysis for Indoor Environments

Fig. 5.10 and Fig. 5.12 show the bias and the RMSE of the position estimate as a function of $\mathrm{SNR}_{\mathrm{Rx}}$ for the imperfect PLE and the indoor environment. In these figures, it is possible to observe that the ML and MC estimates fall into their asymptotic errors. In addition, Fig. 5.11 shows the zoomed asymptotic region of the bias, where it is possible to observe that the empirical bias of the ML estimate with the imperfect PLE presents higher error than the MC and ML estimates with the perfect PLE. Moreover, it can be seen that the Taylor expansion performance presents higher accuracy than the Friendlander analysis method for the imperfect PLE.

The RMSEs of the position estimate as a function of $\mathrm{SNR}_{\mathrm{Rx}}$ for the perfect and the imperfect PLEs, and the indoor environments are shown in Fig. 5.12. Note that in the threshold region, the ML estimators with the perfect and the imperfect PLEs present smaller error than the MC estimator. Then, for a small PLE error, e.g., $\delta_\gamma = 0.5$, we can conclude that in the threshold region, the ML estimator presents higher accuracy than the MC estimator even in the presence of the imperfect PLE. In addition, Fig. 5.13 shows a zoomed portion of the asymptotic region of the RMSE, where we can see that the MC and ML estimators with the perfect PLE fall into their asymptotic theoretical RMSEs and they also present the smaller error variance than the ML estimator with the imperfect PLE. Furthermore, it can be observed that the Taylor expansion with the expectation of the cross-derivative is the most accurate prediction of the RMSE for the imperfect PLE.

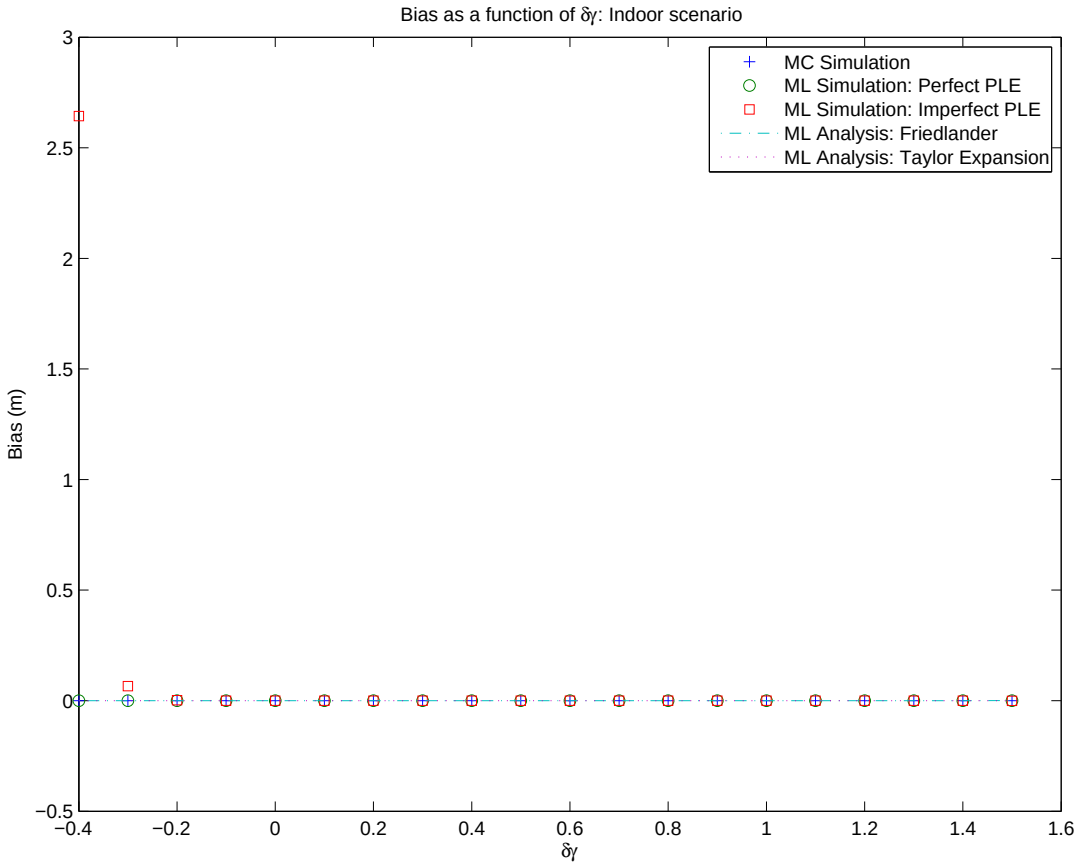

Figure 5.14: Bias of the position estimate as a function of δ_γ for the imperfect PLE, $\gamma_0 = 2$, $\mathrm{SNR}_{\mathrm{Rx}} = 20$ dB, $d_b = 3$ m, $\bar{\beta} = 3.1007 \times 10^9$ Hz, sampling time $= 0.01$ ps, and $N_{\mathrm{R}} = 5{,}000$ independent runs.

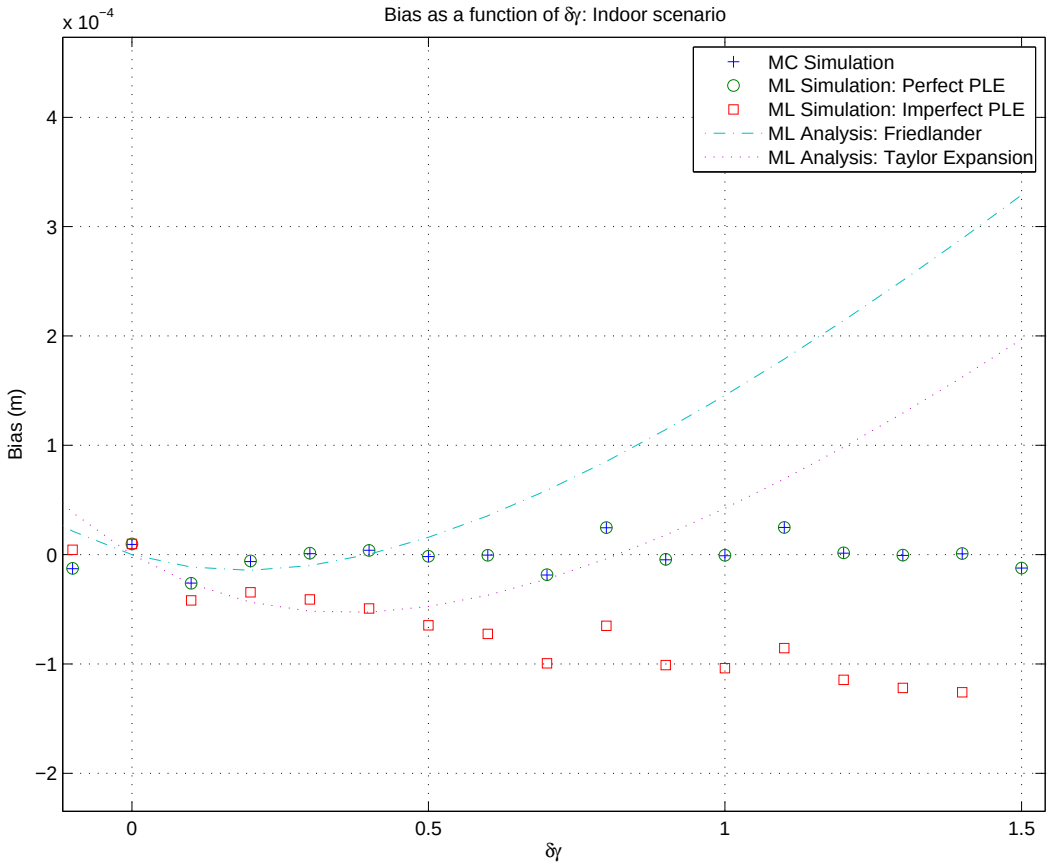

Figure 5.15: Zoomed bias of the position estimate as a function of δ_γ for the imperfect PLE, $\gamma_0 = 2$, $\mathrm{SNR}_{\mathrm{Rx}} = 20$ dB, $d_b = 3$ m, $\bar{\beta} = 3.1007 \times 10^9$ Hz, sampling time $= 0.01$ ps, and $N_{\mathrm{R}} = 5{,}000$ independent runs.

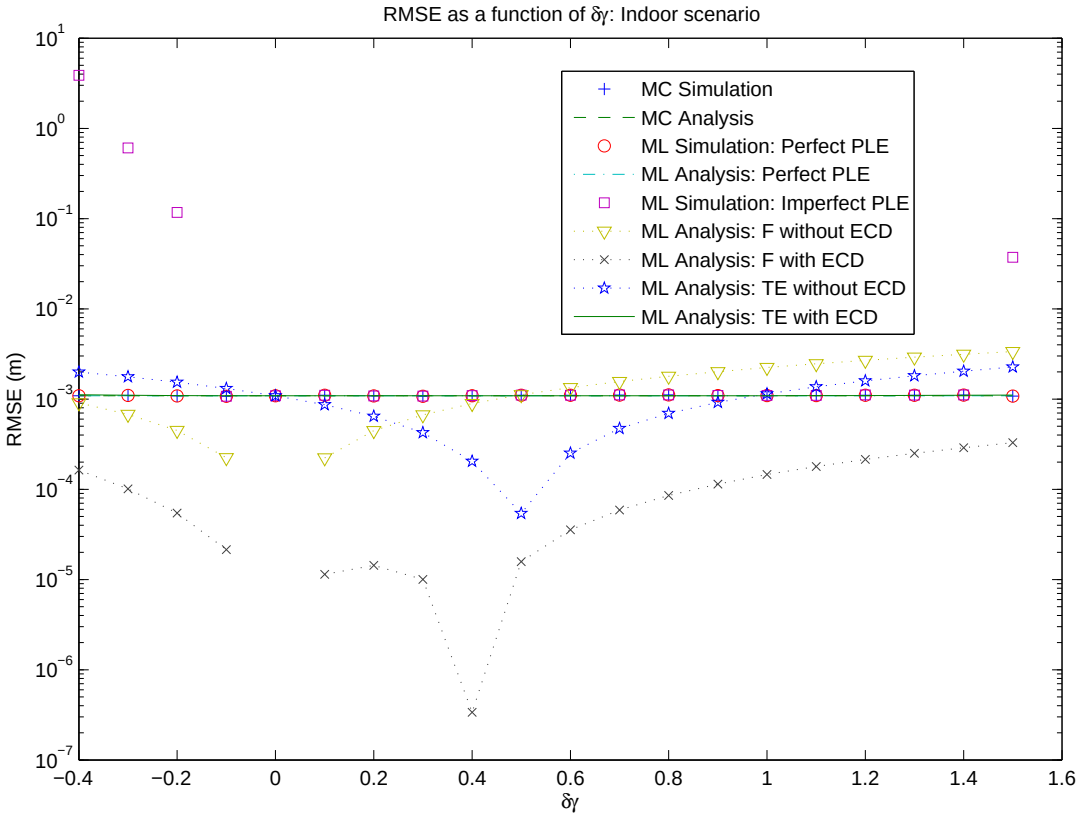

Figure 5.16: RMSE of the position estimate as a function of δ_γ for the imperfect PLE, $\gamma_0 = 2$, $\mathrm{SNR}_{\mathrm{Rx}} = 20$ dB, $d_b = 3$ m, $\bar{\beta} = 3.1007 \times 10^9$ Hz, sampling time $= 0.01$ ps, and $N_{\mathrm{R}} = 5{,}000$ independent runs.

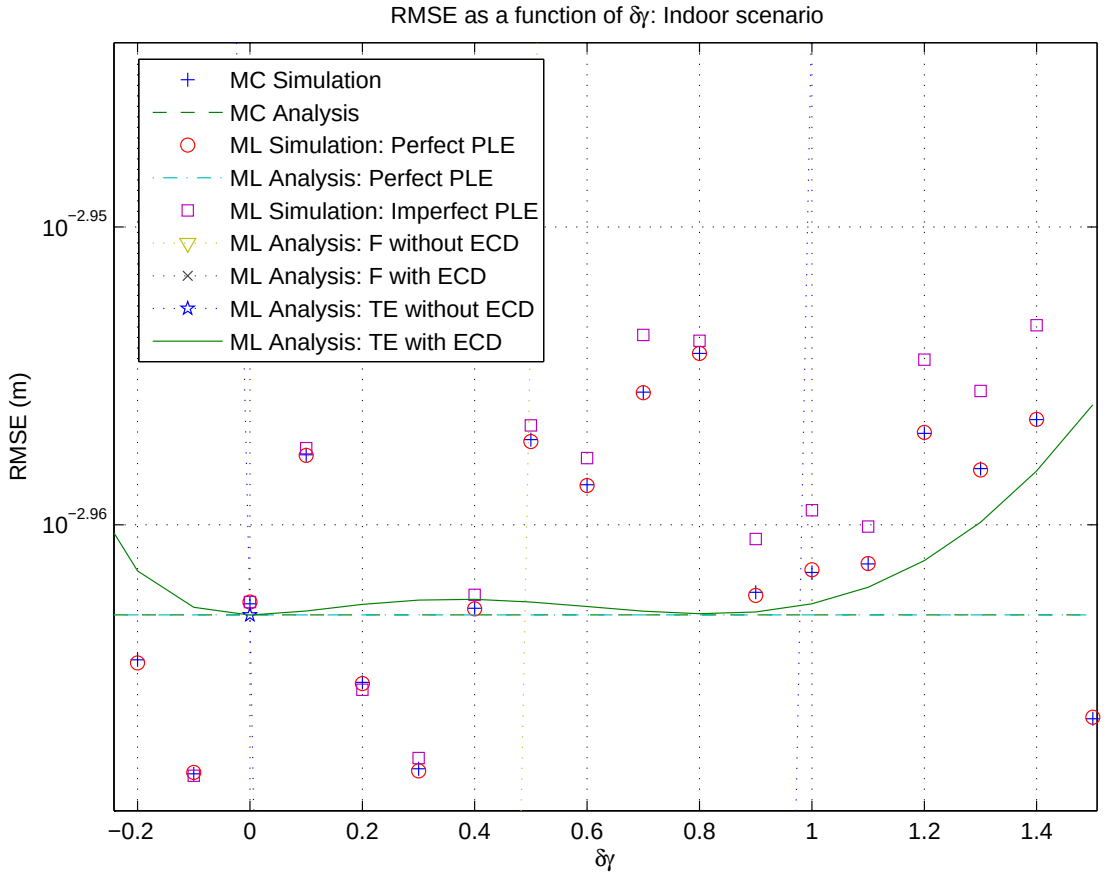

Figure 5.17: Zoomed RMSE of the position estimate as a function of δ_γ for the imperfect PLE, $\gamma_0 = 2$, $\mathrm{SNR}_{\mathrm{Rx}} = 20$ dB, $d_b = 3$ m, $\bar{\beta} = 3.1007 \times 10^9$ Hz, sampling time $= 0.01$ ps, and $N_{\mathrm{R}} = 5{,}000$ independent runs.

The bias and the RMSE of the position estimate as a function of δ_γ for the imperfect PLE and the indoor environments are shown in figures 5.14 and 5.16. Observe that the MC and the ML estimates with the perfect PLE coincide with their asymptotic theoretical performance and they do not depend on the value of δ_γ. However, the ML estimate with the imperfect PLE depend on the PLE error and therefore we can see that the ML estimate falls into the Taylor expansion performance for small values of δ_γ. Moreover, we can observe that the most accurate prediction of the RMSE for the ML estimator with the imperfect PLE error is the Taylor expansion with the expectation of the cross-derivative, as seen in Fig. 5.13. The zoomed asymptotic regions of the bias and the RMSE are exhibited in Fig. 5.15 and Fig. 5.17, respectively, where we can seen that the errors from the real estimation present some fluctuation because of the inadequate sampling time and the finite number of independent runs, which are limited by the hardware simulation. Furthermore, Fig. 5.15 verifies that the MC and the ML estimators with the perfect PLE are asymptotically unbiased. Unfortunately, the ML estimator under the imperfect PLE is asymptotically biased.

5.5 Theoretical Error Performance for Outdoor Environments

In the last two sections, we mentioned that the Taylor expansion method gives the highest theoretical performance accuracy of the error between the estimated and true values of the ToA. For this reason, in this section we consider only the expression of the bias by using the Taylor expansion method for the outdoor case,

i.e., for the digital signal with the MSK modulation.

The bias of the Taylor expansion method is given by (5.3.6), which depends on the effective bandwidth. As seen in Chapter 3, the effective bandwidth of the MSK signal is random, because it depends on the transmitted bit information vectors, which are random. Similarly as done in Chapter 3, we shall derive the expression of the averaged bias (AB), and the lower/upper bound of bias (LUBB).

5.5.1 Averaged Bias

In order to obtain the AB by using the Taylor expansion method for the outdoor case, we should take the expectation of the bias, which is given by (5.3.6), with respect to the random variables $\mathbf{v}$ and $\mathbf{q}$.

Proposition 5.5.1. *Using the analysis method derived from the Taylor expansion, the averaged bias of the ML estimation under the imperfect PLE in the outdoor is given by*

$$\begin{aligned}
&\mathrm{E}_{n_b(t),\mathbf{v},\mathbf{q}}\{\hat{\tau}_{b,\mathrm{ML}}(\gamma)-\tau_{b,0}\} \\
&= -\frac{1}{2}\tau_{b,0}\left((2\gamma-\gamma_0)\left(a_{b,0}-\tilde{a}_{b,0}\right)+\gamma(\gamma-\gamma_0)\ln\left(\frac{d_0}{c\tau_{b,0}}\right)\left(\frac{1}{2}a_{b,0}-\tilde{a}_{b,0}\right)\right) \\
&\quad\left(\frac{1}{2\tau_{b,0}^2 a_{b,0}\left(\omega_0-\frac{\pi}{2T}\right)^2-\left(\gamma(a_{b,0}-\tilde{a}_{b,0})+\gamma^2\left(\frac{1}{2}a_{b,0}-\tilde{a}_{b,0}\right)\right)}\right. \\
&\quad\left.+\frac{1}{2\tau_{b,0}^2 a_{b,0}\left(\omega_0+\frac{\pi}{2T}\right)^2-\left(\gamma(a_{b,0}-\tilde{a}_{b,0})+\gamma^2\left(\frac{1}{2}a_{b,0}-\tilde{a}_{b,0}\right)\right)}\right).
\end{aligned} \tag{5.5.1}$$

Proof. See Appendix A.15. □

5.5.2 Lower/Upper Bound of Bias

In this section, we calculate the LUBB of the bias by using the Taylor expansion method for the outdoor environment. In order to obtain the LUBB we only have to evaluate the expectation of the value of $\bar{\beta}$.

Proposition 5.5.2. *By including the value of* $\mathrm{E}_{\mathbf{v},\mathbf{q}}\{\bar{\beta}^2\}$*, which is given by* (3.5.5)*, into* (5.3.6)*, we obtain the LUBB of the bias of the ML estimator with the imperfect PLE for the outdoor case from*

$$\mathrm{E}_{n_b(t),\mathbf{v},\mathbf{q}}\{\hat{\tau}_{b,\mathrm{ML}}(\gamma)-\tau_{b,0}\} \geq -\frac{(2\gamma-\gamma_0)\left(a_{b,0}-\tilde{a}_{b,0}\right)+\gamma(\gamma-\gamma_0)\ln\left(\frac{d_0}{c\tau_{b,0}}\right)\left(\frac{1}{2}a_{b,0}-\tilde{a}_{b,0}\right)}{8\pi^2\tau_{b,0}^2 a_{b,0}\left(f_0^2+\frac{1}{16T^2}\right)-\left(\gamma(a_{b,0}-\tilde{a}_{b,0})+\gamma^2\left(\frac{1}{2}a_{b,0}-\tilde{a}_{b,0}\right)\right)}\tau_{b,0}, \tag{5.5.2}$$

when the right-hand side in (5.5.2) *is positive. The upper bound can be expressed as*

$$\mathrm{E}_{n_b(t),\mathbf{v},\mathbf{q}}\{\hat{\tau}_{b,\mathrm{ML}}(\gamma)-\tau_{b,0}\} \leq -\frac{(2\gamma-\gamma_0)\left(a_{b,0}-\tilde{a}_{b,0}\right)+\gamma(\gamma-\gamma_0)\ln\left(\frac{d_0}{c\tau_{b,0}}\right)\left(\frac{1}{2}a_{b,0}-\tilde{a}_{b,0}\right)}{8\pi^2\tau_{b,0}^2 a_{b,0}\left(f_0^2+\frac{1}{16T^2}\right)-\left(\gamma(a_{b,0}-\tilde{a}_{b,0})+\gamma^2\left(\frac{1}{2}a_{b,0}-\tilde{a}_{b,0}\right)\right)}\tau_{b,0}, \tag{5.5.3}$$

when the right-hand side in (5.5.3) *is negative.*

5.5.3 Numerical Discussions about the Simulations and the Theoretical Analysis for Outdoor Environments

The figures 5.18 and 5.20 exhibit the bias and the RMSE of the position estimate as a function of $\mathrm{SNR}_{\mathrm{Rx}}$, where it can be observed that when the $\mathrm{SNR}_{\mathrm{Rx}}$ increases, the MC and ML estimates with and without the PLE error fall into their asymptotic errors. Fig. 5.19 shows a zoomed region, which contains the AB and the LUBB for the outdoor case. Note that the LUBB becomes the upper bound of the bias,

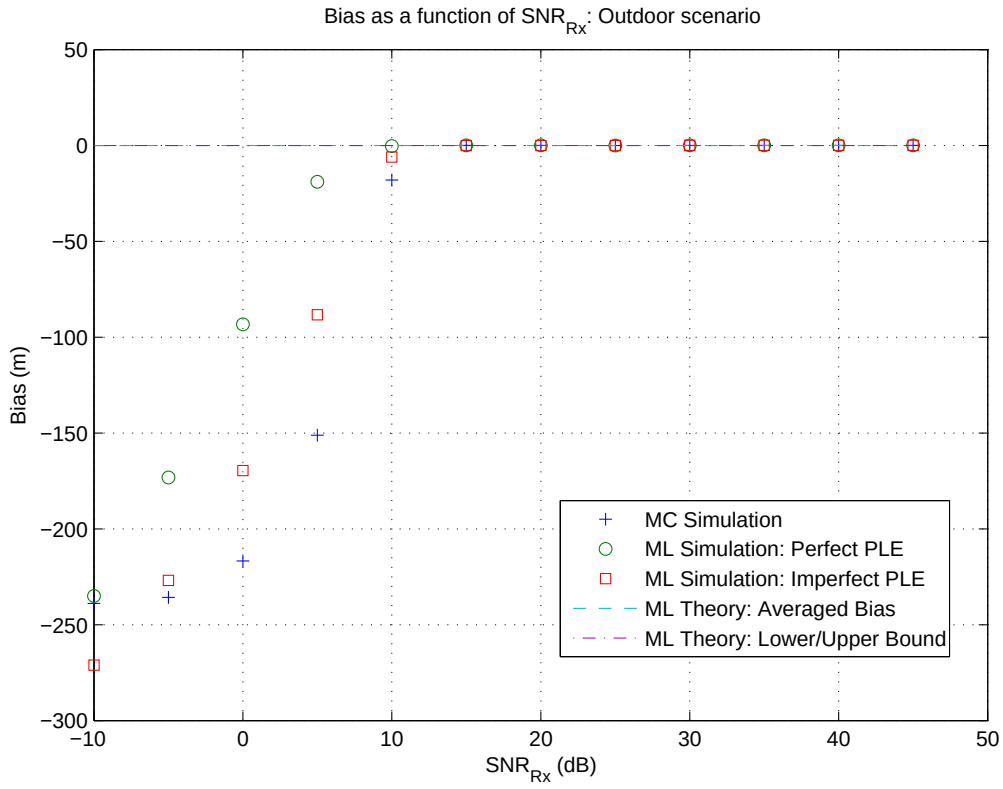

Figure 5.18: Bias of the position estimate as a function of $\mathrm{SNR}_{\mathrm{Rx}}$ for the imperfect PLE, $\gamma_0 = 5$, $\delta_\gamma = 1$, $d_b = 500$ m, $R_{\mathrm{B}} = 15$ Mbps, $f_0 = 900$ MHz, sampling time $= 1.7420$ ps, 20 independent runs for the frame realization, and 50 independent runs for the noise realization.

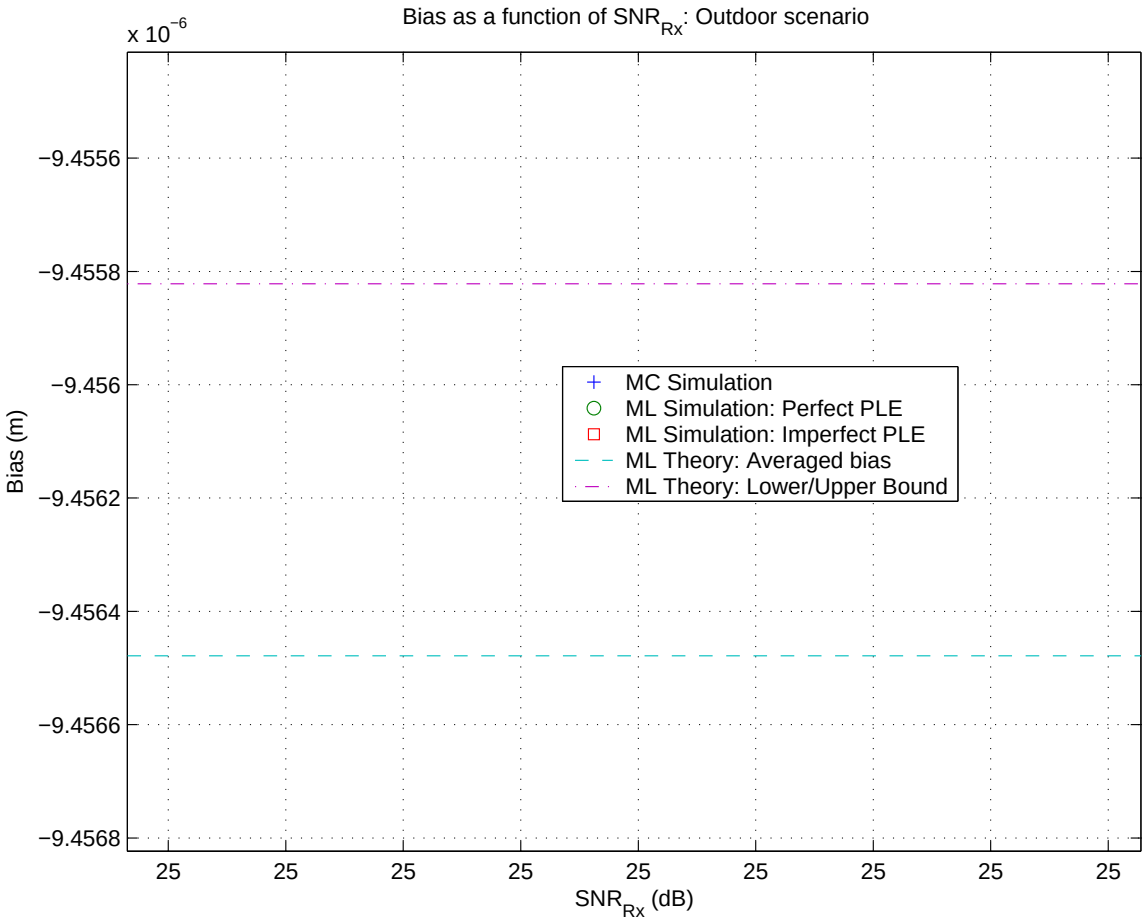

Figure 5.19: Zoomed portion of the AB and the LUBB of the position estimate as a function of $\mathrm{SNR_{Rx}}$ for the imperfect PLE, $\gamma_0 = 5$, $\delta_\gamma = 1$, $d_b = 500$ m, $R_{\mathrm{B}} = 15$ Mbps, $f_0 = 900$ MHz, sampling time $= 1.7420$ ps, 20 independent runs for the frame realization, and 50 independent runs for the noise realization.

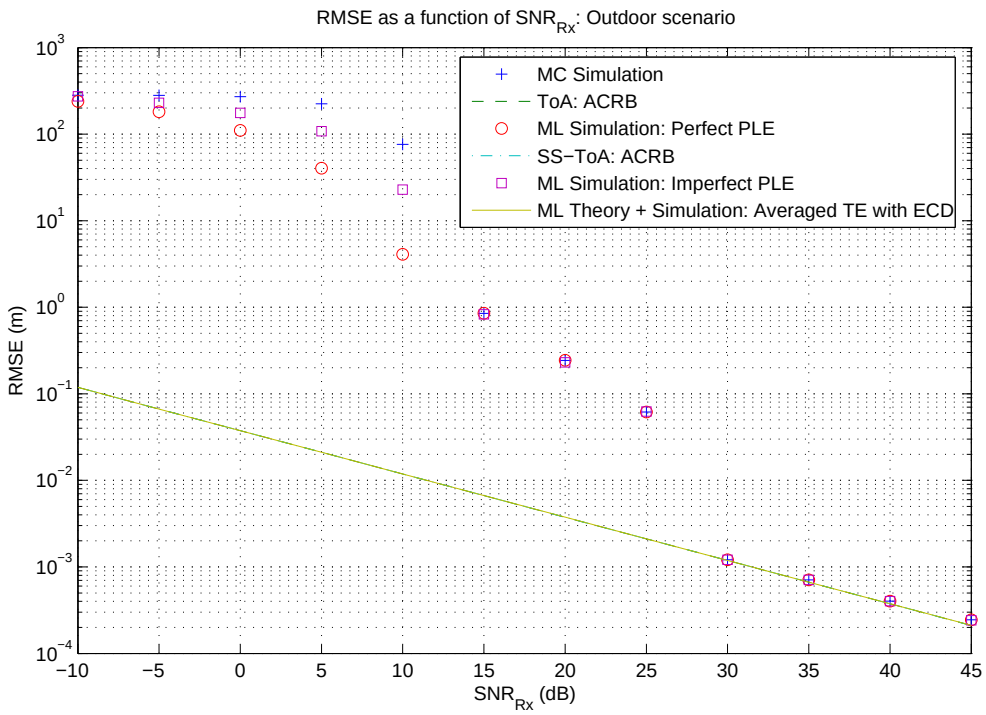

Figure 5.20: RMSE of the position estimate as a function of $\mathrm{SNR}_{\mathrm{Rx}}$ for the imperfect PLE, $\gamma_0 = 5$, $\delta_\gamma = 1$, $d_b = 500$ m, $R_{\mathrm{B}} = 15$ Mbps, $f_0 = 900$ MHz, sampling time $= 1.7420$ ps, 20 independent runs for the frame realization, and 50 independent runs for the noise realization.

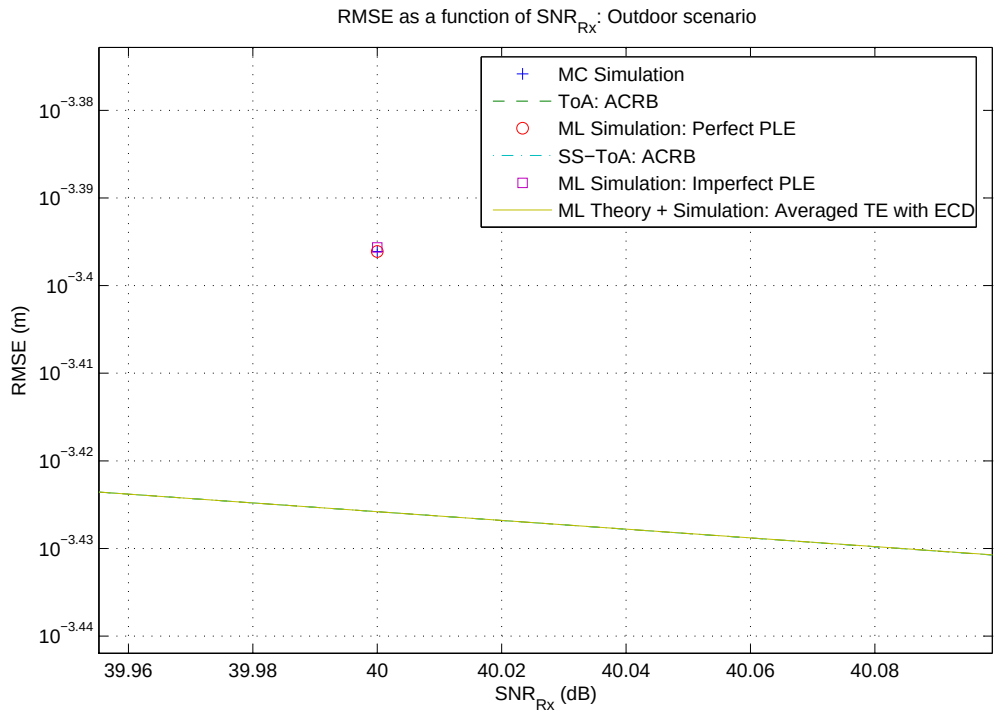

Figure 5.21: Zoomed RMSE of the position estimate as a function of $\mathrm{SNR_{Rx}}$ for the imperfect PLE, $\gamma_0 = 5$, $\delta_\gamma = 1$, $d_b = 500$ m, $R_{\mathrm{B}} = 15$ Mbps, $f_0 = 900$ MHz, sampling time $= 1.7420$ ps, 20 independent runs for the frame realization, and 50 independent runs for the noise realization.

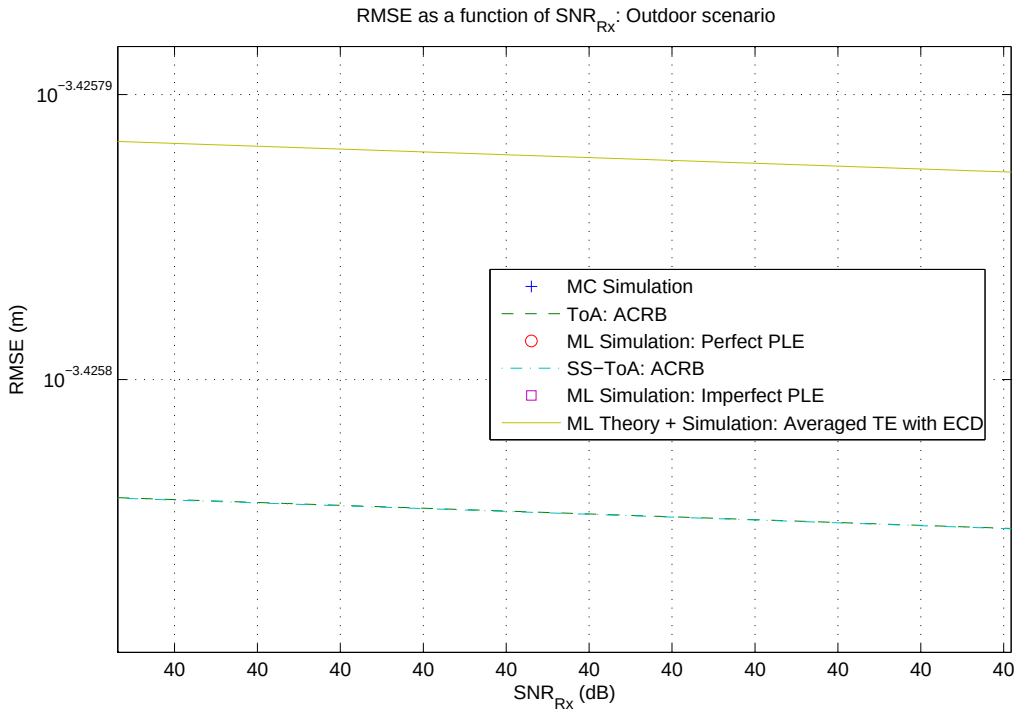

Figure 5.22: Zoomed RMSE for the imperfect PLE, $\gamma_0 = 5$, $\delta_\gamma = 1$, $d_b = 500$ m, $R_{\mathrm{B}} = 15$ Mbps, $f_0 = 900$ MHz, sampling time $= 1.7420$ ps, 20 independent runs for the frame realization, and 50 independent runs for the noise realization.

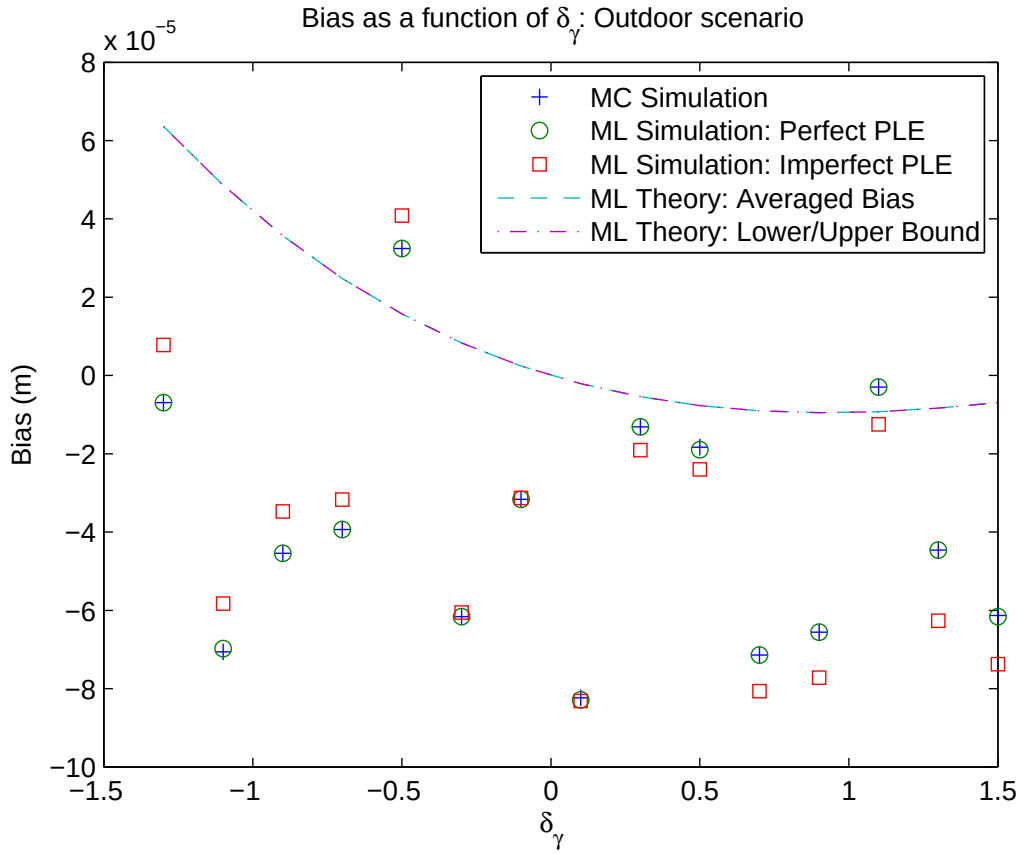

Figure 5.23: Bias of the position estimate as a function of δ_γ for the imperfect PLE, $\gamma_0 = 5$, $\mathrm{SNR}_{\mathrm{Rx}} = 32$ dB, $d_b = 500$ m, $R_{\mathrm{B}} = 15$ Mbps, $f_0 = 900$ MHz, sampling time $= 0.3484$ ps, 20 independent runs for the frame realization, and 50 independent runs for the noise realization.

which is above the AB, as the bias is negative. Moreover, in Fig. 5.21 and Fig. 5.22, a zoomed portion of the asymptotic region of the RMSE is shown. In the zoomed zone of the RMSE in Fig. 5.21, we can observe that the MC estimate and the ML estimate with the perfect PLE are identical, and they also present a lower error than the ML estimate with the imperfect PLE. However, the MC estimate provides worse accuracy than the ML estimates with or without the PLE error in the threshold region, as seen in Fig. 5.12 in the indoor.

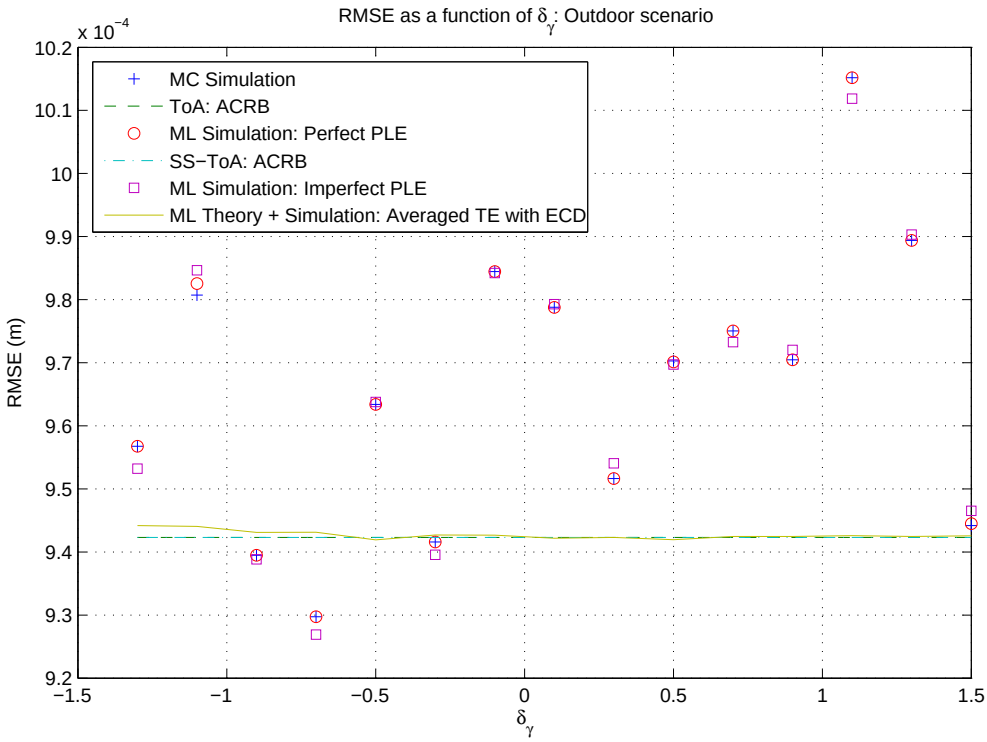

Figure 5.24: RMSE of the position estimate as a function of δ_γ for the imperfect PLE, $\gamma_0 = 5$, $\mathrm{SNR}_{\mathrm{Rx}} = 32$ dB, $d_b = 500$ m, $R_{\mathrm{B}} = 15$ Mbps, $f_0 = 900$ MHz, sampling time $= 0.3484$ ps, 20 independent runs for the frame realization, and 50 independent runs for the noise realization.

In Fig. 5.23 and Fig. 5.24, we can observe the bias and the RMSE of the position estimate as a function of δ_γ for the imperfect PLE and for the outdoor environments. Note that the numerical errors present some fluctuations because of the insufficient sampling time and the finite number of the independent runs. Unfortunately, the sampling time cannot be decreased neither the number of the independent runs can be increased, because they are limited by the hardware simulation. Moreover, we can see in Fig. 5.23 and Fig. 5.24 that the bias and the RMSE present very small values because of the high received SNR. However, a lower SNR does not guarantee the simulation results to be in the asymptotic region.

Chapter 6

Conclusions and Prospective Directions

6.1 Conclusions

In this thesis, we have extended the application of the hybrid SS-ToA concept to the second-derivative Gaussian pulse and the MSK signal waveforms.

Moreover, the PLE is a key parameter in the localization algorithms based on the distance estimation. However, the true value of the PLE is unknown and therefore we should take into account the mis-modeled PLE into the ToA estimation. In order at including the PLE error into the ToA estimation, we have analyzed the ML estimation under the imperfect PLE by using the Friedlander and the Taylor expansion analysis methods. As observed in the previous chapter, we have found that the analysis method using the Taylor expansion with the cross-derivative expectation provides the highest theoretical performance accuracy of the error between the estimated and true values of the ToA. In addition, in the Taylor expansion analysis method, the theoretical performance of the error variance with the highest accuracy is given by the Taylor expansion analysis method with the expectation of the cross-derivative.

As seen in the numerical discussions about the simulations and the theoretical analysis for the indoor and outdoor environments, the ML estimators with the perfect and the imperfect PLEs present the smaller error than the MC estimator in the threshold region. Then, in the threshold region and for a small PLE error, the ML estimator presents higher accuracy than the MC estimator even in the presence of the imperfect PLE. However, in the asymptotic region the MC and ML with perfect PLE estimators outperform the ML estimator with imperfect PLE.

Then, in the presence of the PLE error, we could finally summarize that in the threshold region, the ML estimator outperforms the the MC estimator for the small PLE error, e.g., $\delta_\gamma = 0.5$ in the indoor case, and the moderate PLE error, e.g., $\delta_\gamma = 1$ in the outdoor case. However, in the asymptotic region the MC and ML estimators under the perfect PLE outperform the ML estimator with the imperfect PLE.

6.2 Prospective Directions

Three promising studies can be cast into the future works, such as partitioned convolution, non-asymptotic analysis and random path loss exponent error. Since the wireless communication systems often work with a very high central frequency, which leads to a large effective bandwidth, the time resolution for computing the convolution should be very fine and therefore a very long memory is required. To support this demand, the partitioned convolution might be a solution. The motivation to observe the non-asymptotic region analytically is that Fig. 5.12 and Fig. 5.20 illustrate that in a low SNR, even though the PLE is subject to the error, the ML estimator can still outperform the MC estimator. Alternatively, the consideration of the random PLE will be more solid, since it will cover the conducted results and

treat this thesis as a special case.

6.2.1 Partitioned Convolution

In this thesis, we have used the convolution to compute the ML and MC estimates. However, we have found some computational problems in the simulation of the real wireless systems, because of the hardware limitations. In [62, p. 313], a partitioned convolution is discussed by convoluting the partitioned input signal by the filter and then summing all output segments. In [63] and [64], the algorithm of the real-time partitioned convolution is studied and implemented on a digital signal processor platform. In this manner, an efficient convolution is attained with the advantage of low input/output delay. Then, the convolution required by the MC and ML estimators can be handled in a personal computer by means of the partitioned convolution and therefore it allows to simulate the real wireless systems.

6.2.2 Non-asymptotic Analysis

In this thesis, we have studied the bias and the RMSEs of the MC and ML estimators of the ToA and the effects of the imperfect PLE in the mis-modeled estimation of the ToA by using the ML estimator. However, we only analyze the asymptotic region of the estimation and therefore the next step in the research could be the analysis of the non-asymptotic region, i.e., threshold region and non-informative region.

Some related works provide the analysis of the threshold region, see, e.g., [16] and [23]. In [23], the threshold effects are studied in the estimation of the parameters of single-frequency tones from a finite number of noisy discrete-time observations. The study in [23] concentrated on the presence of the threshold in the RMSE

of a non-linear estimation caused by a low $\mathrm{SNR}_{\mathrm{Rx}}$, and in the frequency estimation because of the occurrence of the outliers. The study [16] extends the analysis of the asymptotic and threshold region of the MSE performance of the ML estimator for the DoA estimation. The performance of the MSE prediction in the presence of signal model mismatch is provided in [16].

6.2.3 Random Path Loss Exponent Error

In this thesis, the effect of the imperfect PLE are studied by assuming a deterministic PLE error. Therefore, the analysis of the random imperfect PLE is another possible future line of the research. In this section, we postulate a PLE error model, where the PLE is assumed to have a doubly truncated Gaussian distribution.

We assume δ_γ as a variable with Gaussian distribution with mean 0 and variance σ_γ^2, i.e., $\delta_\gamma \sim \mathcal{N}(0, \sigma_\gamma^2)$. Thereby, the PLE has also a Gaussian distribution with mean γ_0 and variance σ_γ^2, i.e., $\gamma \sim \mathcal{N}(\gamma_0, \sigma_\gamma^2)$. However, the PLE cannot be less than zero and be infinite. Therefore, the PLE has to present a doubly truncated Gaussian distribution given by (see, e.g., [65,66])

$$p_\gamma(\gamma) = \frac{1}{\frac{1}{\sqrt{2\pi}\sigma_\gamma}\int_{\gamma_{\min}-\gamma_0}^{\gamma_{\max}-\gamma_0} \mathrm{e}^{-\frac{1}{2\sigma_\gamma^2}\delta_\gamma^2}\mathrm{d}\delta_\gamma} \frac{1}{\sqrt{2\pi}\sigma_\gamma}\mathrm{e}^{-\frac{1}{2\sigma_\gamma^2}(\gamma-\gamma_0)^2}. \tag{6.2.1}$$

For a convenient form, we have

$$p_\gamma(\gamma) = \frac{1}{\Phi(\frac{1}{\sigma_\gamma}(\gamma_{\max}-\gamma_0)) - \Phi(\frac{1}{\sigma_\gamma}(\gamma_{\min}-\gamma_0))} \frac{1}{\sqrt{2\pi}\sigma_\gamma}\mathrm{e}^{-\frac{1}{2\sigma_\gamma^2}(\gamma-\gamma_0)^2}, \tag{6.2.2}$$

where $\Phi(u) = P(U \leq u)$ is the cumulative distribution function (CDF) of the standard random variable written by (see, e.g., [66])

$$\Phi(u) = \frac{1}{\sqrt{2\pi}}\int_{-\infty}^{u} \mathrm{e}^{-\frac{1}{2}u'^2}\mathrm{d}u'. \tag{6.2.3}$$

It can also be written as $\Phi(u) = \frac{1}{2}\left(1 + \mathrm{erf}\left(\frac{1}{\sqrt{2}u}\right)\right)$, where $\mathrm{erf}(\cdot)$ is the error function. Then, (6.2.2) can be written as (see, e.g., [65])

$$\begin{aligned} p_\gamma(\gamma) &= \frac{2}{\mathrm{erf}\left(\frac{1}{\sqrt{2}\sigma_\gamma}(\gamma_{\max}-\gamma_0)\right) - \mathrm{erf}\left(\frac{1}{\sqrt{2}\sigma_\gamma}(\gamma_{\min}-\gamma_0)\right)} \frac{1}{\sqrt{2\pi}\sigma_\gamma} \mathrm{e}^{-\frac{1}{2\sigma_\gamma^2}(\gamma-\gamma_0)^2} \\ &= \frac{2}{\mathrm{erf}\left(\frac{1}{\sqrt{2}\sigma_\gamma}(\gamma_{\max}-\gamma_0)\right) - \mathrm{erf}\left(\frac{1}{\sqrt{2}\sigma_\gamma}(\gamma_{\min}-\gamma_0)\right)} \frac{1}{\sqrt{2\pi}\sigma_\gamma} \mathrm{e}^{-\frac{1}{2\sigma_\gamma^2}\delta_\gamma^2}. \end{aligned} \tag{6.2.4}$$

The mean and the variance $\bar{\gamma}_t$ and $\sigma_{\gamma_t}^2$ of the doubly truncated Gaussian distribution are given by (see, e.g., [66, p.33])

$$\begin{aligned} \bar{\gamma}_t &= \gamma_0 + \frac{\frac{1}{\sqrt{2\pi}}\mathrm{e}^{-\frac{1}{2\sigma_\gamma^2}(\gamma_{\min}-\gamma_0)^2} - \frac{1}{\sqrt{2\pi}}\mathrm{e}^{-\frac{1}{2\sigma_\gamma^2}(\gamma_{\max}-\gamma_0)^2}}{\Phi\left(\frac{1}{\sigma_\gamma}(\gamma_{\max}-\gamma_0)\right) - \Phi\left(\frac{1}{\sigma_\gamma}(\gamma_{\min}-\gamma_0)\right)}\sigma_\gamma \\ &= \gamma_0 + 2\frac{\frac{1}{\sqrt{2\pi}}\mathrm{e}^{-\frac{1}{2\sigma_\gamma^2}(\gamma_{\min}-\gamma_0)^2} - \frac{1}{\sqrt{2\pi}}\mathrm{e}^{-\frac{1}{2\sigma_\gamma^2}(\gamma_{\max}-\gamma_0)^2}}{\mathrm{erf}\left(\frac{1}{\sqrt{2}\sigma_\gamma}(\gamma_{\max}-\gamma_0)\right) - \mathrm{erf}\left(\frac{1}{\sqrt{2}\sigma_\gamma}(\gamma_{\min}-\gamma_0)\right)}\sigma_\gamma, \end{aligned} \tag{6.2.5}$$

$$\begin{aligned} \sigma_{\gamma_t}^2 &= \sigma_\gamma^2\left(1 + \frac{\frac{\gamma_{\min}-\gamma_0}{\sqrt{2\pi}\sigma_\gamma}\mathrm{e}^{-\frac{1}{2\sigma_\gamma^2}(\gamma_{\min}-\gamma_0)^2} - \frac{\gamma_{\max}-\gamma_0}{\sqrt{2\pi}\sigma_\gamma}\mathrm{e}^{-\frac{1}{2\sigma_\gamma^2}(\gamma_{\max}-\gamma_0)^2}}{\Phi\left(\frac{1}{\sigma_\gamma}(\gamma_{\max}-\gamma_0)\right) - \Phi\left(\frac{\gamma_{\min}-\gamma_0}{\sigma_\gamma}\right)}\right) - (\bar{\gamma}_t-\gamma_0)^2 \\ &= \sigma_\gamma^2\left(1 + 2\frac{\frac{\gamma_{\min}-\gamma_0}{\sqrt{2\pi}\sigma_\gamma}\mathrm{e}^{-\frac{1}{2\sigma_\gamma^2}(\gamma_{\min}-\gamma_0)^2} - \frac{\gamma_{\max}-\gamma_0}{\sqrt{2\pi}\sigma_\gamma}\mathrm{e}^{-\frac{1}{2\sigma_\gamma^2}(\gamma_{\max}-\gamma_0)^2}}{\mathrm{erf}\left(\frac{1}{\sqrt{2}\sigma_\gamma}(\gamma_{\max}-\gamma_0)\right) - \mathrm{erf}\left(\frac{1}{\sqrt{2}\sigma_\gamma}(\gamma_{\min}-\gamma_0)\right)}\right) - (\bar{\gamma}_t-\gamma_0)^2. \end{aligned} \tag{6.2.6}$$

The error expressions of the ML estimator, such as the bias in (5.3.6) and the error variance in (5.3.16), are valid for a deterministic PLE. A possible way is the investigation of the error performance for (5.3.6) and (5.3.16) in the case of the random PLE.

Appendix A

Lengthy Algebraic Derivations

A.1 Proof of Proposition 3.2.1

Consider the Fourier transform of the second-derivative monocycle with finite duration pulse from

$$\begin{aligned} S(\omega) &= \int_{-\infty}^{\infty} s(t)\mathrm{e}^{-\mathrm{j}\omega t}\mathrm{d}t \\ &= \int_{-\frac{1}{2}T_\mathrm{p}}^{\frac{1}{2}T_\mathrm{p}} \left(1 - 4\pi\left(\frac{t}{\tau_\mathrm{p}}\right)^2\right)\mathrm{e}^{-2\pi\left(\frac{t}{\tau_\mathrm{p}}\right)^2}\mathrm{e}^{-\mathrm{j}\omega t}\mathrm{d}t. \end{aligned} \tag{A.1.1}$$

It can be separated into two terms

$$\begin{aligned} S(\omega) &= \int_{-\frac{1}{2}T_\mathrm{p}}^{\frac{1}{2}T_\mathrm{p}} \mathrm{e}^{-2\pi\left(\frac{t}{\tau_\mathrm{p}}\right)^2}\mathrm{e}^{-\mathrm{j}\omega t}\mathrm{d}t - \int_{-\frac{1}{2}T_\mathrm{p}}^{\frac{1}{2}T_\mathrm{p}} 4\pi\left(\frac{t}{\tau_\mathrm{p}}\right)^2\mathrm{e}^{-2\pi\left(\frac{t}{\tau_\mathrm{p}}\right)^2}\mathrm{e}^{-\mathrm{j}\omega t}\mathrm{d}t \\ &\cong \mathcal{F}\left\{\mathrm{e}^{-2\pi\left(\frac{t}{\tau_\mathrm{p}}\right)^2}\right\} - \mathcal{F}\left\{4\pi\left(\frac{t}{\tau_\mathrm{p}}\right)^2\mathrm{e}^{-2\pi\left(\frac{t}{\tau_\mathrm{p}}\right)^2}\right\} \\ &= \mathcal{F}\left\{\mathrm{e}^{-\left(\frac{t}{\frac{\tau_\mathrm{p}}{\sqrt{2\pi}}}\right)^2}\right\} - \frac{4\pi}{2\pi}\mathcal{F}\left\{\left(\frac{t}{\frac{\tau_\mathrm{p}}{\sqrt{2\pi}}}\right)^2\mathrm{e}^{-\left(\frac{t}{\frac{\tau_\mathrm{p}}{\sqrt{2\pi}}}\right)^2}\right\} \\ &= \mathcal{F}\left\{\mathrm{e}^{-\left(\frac{t}{\frac{\tau_\mathrm{p}}{\sqrt{2\pi}}}\right)^2}\right\} - 2\mathcal{F}\left\{\left(\frac{t}{\frac{\tau_\mathrm{p}}{\sqrt{2\pi}}}\right)^2\mathrm{e}^{-\left(\frac{t}{\frac{\tau_\mathrm{p}}{\sqrt{2\pi}}}\right)^2}\right\}. \end{aligned} \tag{A.1.2}$$

The second equality in (A.1.2) is actually an approximation, since the pulse has a finite duration. However, the derivation in (A.1.2) provides a simple but accurate approximation. The effect of finite and infinite duration signals for the effective bandwidth is investigated in the next section (see (4.1.3)). Using the time-scaling property of the Fourier transform (see, e.g., [51, pp. 252-253]), i.e.,

$$\mathcal{F}\{g(\eta t)\} = \frac{1}{|\eta|} G\left(\frac{\omega}{\eta}\right), \tag{A.1.3}$$

(A.1.2) can be rewritten as

$$S(\omega) = \left|\frac{\tau_{\mathrm{p}}}{\sqrt{2\pi}}\right| \mathcal{F}\left\{\mathrm{e}^{-t^2}\right\}\Big|_{\omega=\frac{\tau_{\mathrm{p}}}{\sqrt{2\pi}}\omega} - 2\left|\frac{\tau_{\mathrm{p}}}{\sqrt{2\pi}}\right| \mathcal{F}\left\{t^2\mathrm{e}^{-t^2}\right\}\Big|_{\omega=\frac{\tau_{\mathrm{p}}}{\sqrt{2\pi}}\omega}. \tag{A.1.4}$$

The frequency derivative property of the Fourier transform is given by (see, e.g., [51, pp. 252-253])

$$\mathcal{F}\{t^n g(t)\} = \mathrm{j}^n \frac{\partial^2 G(\omega)}{\partial \omega^2}. \tag{A.1.5}$$

Using the previous property in (A.1.4), we obtain

$$S(\omega) = \left|\frac{\tau_{\mathrm{p}}}{\sqrt{2\pi}}\right| \mathcal{F}\left\{\mathrm{e}^{-t^2}\right\}\Big|_{\omega=\frac{\tau_{\mathrm{p}}}{\sqrt{2\pi}}\omega} - 2\mathrm{j}^2\left|\frac{\tau_{\mathrm{p}}}{\sqrt{2\pi}}\right| \frac{\partial^2}{\partial\omega^2}\mathcal{F}\left\{\mathrm{e}^{-t^2}\right\}\Big|_{\omega=\frac{\tau_{\mathrm{p}}}{\sqrt{2\pi}}\omega}. \tag{A.1.6}$$

The solution of this Fourier transform is $\mathcal{F}\left\{\mathrm{e}^{-\eta t^2}\right\} = \sqrt{\frac{\pi}{\eta}}\mathrm{e}^{-\frac{\omega^2}{4\eta}}$ (see, e.g., [51, pp. 252-253]), where $\Re(\eta) > 0$. For the case $\eta = 1$, we have

$$\begin{aligned}
S(\omega) &= \sqrt{\pi}\left|\frac{\tau_{\mathrm{p}}}{\sqrt{2\pi}}\right| \mathrm{e}^{-\frac{\omega^2}{4}}\Big|_{\omega=\frac{\tau_{\mathrm{p}}}{\sqrt{2\pi}}\omega} + 2\sqrt{\pi}\left|\frac{\tau_{\mathrm{p}}}{\sqrt{2\pi}}\right| \frac{\partial^2}{\partial\omega^2}\mathrm{e}^{-\frac{\omega^2}{4}}\Big|_{\omega=\frac{\tau_{\mathrm{p}}}{\sqrt{2\pi}}\omega} \\
&= \sqrt{\pi}\left|\frac{\tau_{\mathrm{p}}}{\sqrt{2\pi}}\right| \mathrm{e}^{-\frac{\omega^2}{4}}\Big|_{\omega=\frac{\tau_{\mathrm{p}}}{\sqrt{2\pi}}\omega} + 2\sqrt{\pi}\left|\frac{\tau_{\mathrm{p}}}{\sqrt{2\pi}}\right| \frac{\partial}{\partial\omega}\left(-\frac{2\omega}{4}\mathrm{e}^{-\frac{\omega^2}{4}}\right)\Big|_{\omega=\frac{\tau_{\mathrm{p}}}{\sqrt{2\pi}}\omega} \\
&= \sqrt{\pi}\left|\frac{\tau_{\mathrm{p}}}{\sqrt{2\pi}}\right| \mathrm{e}^{-\frac{\omega^2}{4}}\Big|_{\omega=\frac{\tau_{\mathrm{p}}}{\sqrt{2\pi}}\omega} - \sqrt{\pi}\left|\frac{\tau_{\mathrm{p}}}{\sqrt{2\pi}}\right| \left(\mathrm{e}^{-\frac{\omega^2}{4}} - \frac{2\omega^2}{4}\mathrm{e}^{-\frac{\omega^2}{4}}\right)\Big|_{\omega=\frac{\tau_{\mathrm{p}}}{\sqrt{2\pi}}\omega} \\
&= \sqrt{\pi}\left|\frac{\tau_{\mathrm{p}}}{\sqrt{2\pi}}\right| \frac{\omega^2}{2}\mathrm{e}^{-\frac{\omega^2}{4}}\Big|_{\omega=\frac{\tau_{\mathrm{p}}}{\sqrt{2\pi}}\omega} \\
&= \frac{\tau_{\mathrm{p}}}{2\sqrt{2}}\omega^2\mathrm{e}^{-\frac{\omega^2}{4}}\Big|_{\omega=\frac{\tau_{\mathrm{p}}}{\sqrt{2\pi}}\omega}.
\end{aligned} \tag{A.1.7}$$

Finally, substituting the value of ω into (A.1.7), the expression of the Fourier transform of the transmitted signal $s(t)$ can be rewritten as

$$S(\omega) = \frac{\tau_{\mathrm{p}}^3}{4\sqrt{2}\pi}\omega^2 \mathrm{e}^{-\frac{\tau_{\mathrm{p}}^2}{8\pi}\omega^2}. \tag{A.1.8}$$

The Fourier transform of $s(t)$ can be also expressed as a function of the frequency. By changing $\omega = 2\pi f$, $S(f)$ can be obtained from

$$S(\omega) = S(2\pi f) \equiv S(f) = \frac{\pi}{\sqrt{2}}\tau_{\mathrm{p}}^3 f^2 \mathrm{e}^{-\frac{\pi}{2}\tau_{\mathrm{p}}^2 f^2}. \tag{A.1.9}$$

In order to obtain the effective bandwidth of the transmitted signal defined by (3.2.1), the value of $|S(\omega)|^2$ can be derived as

$$|S(\omega)|^2 = \frac{\tau_{\mathrm{p}}^6}{32\pi^2}\omega^4 \mathrm{e}^{-\frac{\tau_{\mathrm{p}}^2}{4\pi}\omega^2}. \tag{A.1.10}$$

The value of $\int_{-\infty}^{\infty} |S(\omega)|^2 \mathrm{d}\omega$ can be written as

$$\begin{aligned} \int_{-\infty}^{\infty} |S(\omega)|^2 \mathrm{d}\omega &= \int_{-\infty}^{\infty} \frac{\tau_{\mathrm{p}}^6}{32\pi^2}\omega^4 \mathrm{e}^{-\frac{\tau_{\mathrm{p}}^2}{4\pi}\omega^2} \mathrm{d}\omega \\ &= \frac{\tau_{\mathrm{p}}^6}{32\pi^2} \int_{-\infty}^{\infty} \omega^4 \mathrm{e}^{-\frac{\tau_{\mathrm{p}}^2}{4\pi}\omega^2} \mathrm{d}\omega \\ &= \frac{\tau_{\mathrm{p}}^6}{16\pi^2} \int_{0}^{\infty} \omega^4 \mathrm{e}^{-\frac{\tau_{\mathrm{p}}^2}{4\pi}\omega^2} \mathrm{d}\omega. \end{aligned} \tag{A.1.11}$$

In (A.1.11), there is an integral whose form is $\int_0^{\infty} x^n \mathrm{e}^{-\eta x^2} \mathrm{d}x$. In order to obtain the solution, we ought to make the next variable change

$$y = \eta x^2 \Longrightarrow \mathrm{d}y = 2\eta x \mathrm{d}x. \tag{A.1.12}$$

Consequently, we have

$$\begin{aligned} x^2 = \frac{y}{\eta} \Longrightarrow \mathrm{d}x = \frac{1}{2\eta(\frac{y}{\eta})^{\frac{1}{2}}} \mathrm{d}y, \\ x \in [0, \infty) \Longrightarrow y \in [0, \infty). \end{aligned} \tag{A.1.13}$$

Using (A.1.12) and (A.1.13), the integral $\int_0^\infty x^n \mathrm{e}^{-\eta x^2} \mathrm{d}x$ may be rewritten as a function of y in the following equivalent form

$$\begin{aligned}\int_0^\infty x^n \mathrm{e}^{-\eta x^2} \mathrm{d}x &= \int_0^\infty (x^2)^{\frac{n}{2}} \mathrm{e}^{-\eta x^2} \mathrm{d}x \\ &= \int_0^\infty \mathrm{e}^{-y} \left(\frac{y}{\eta}\right)^{\frac{n}{2}} \frac{1}{2\eta(\frac{y}{\eta})^{\frac{1}{2}}} \mathrm{d}y \\ &= \frac{1}{2}\left(\frac{1}{\eta}\right)^{\frac{n+1}{2}} \int_0^\infty y^{\frac{n-1}{2}} \mathrm{e}^{-y} \mathrm{d}y.\end{aligned} \tag{A.1.14}$$

To resolve (A.1.14), by utilizing the Euler integral defined by $\Gamma(m) = \int_0^\infty y^{m-1} \mathrm{e}^{-y} \mathrm{d}y$ (see, e.g., [67]), where $\Gamma(m)$ is the Gamma function that provides $\Gamma(m) = (m-1)!$. In this case, we have $m - 1 = \frac{n-1}{2}$, i.e., $m = \frac{n+1}{2}$. The solution of the integral can be obtained from

$$\int_0^\infty x^n \mathrm{e}^{-\eta x^2} \mathrm{d}x = \frac{1}{2}\left(\frac{1}{\eta}\right)^{\frac{n+1}{2}} \Gamma\left(\frac{n+1}{2}\right). \tag{A.1.15}$$

Thereby, by defining $\eta = \frac{\tau_\mathrm{p}^2}{4\pi}$ and $n = 4$ and using (A.1.15), the solution of (A.1.11) is given by

$$\begin{aligned}\int_{-\infty}^\infty |S(\omega)|^2 \mathrm{d}\omega &= \frac{\tau_\mathrm{p}^6}{16\pi^2}\left(\frac{4\pi}{\tau_\mathrm{p}^2}\right)^{\frac{5}{2}} \Gamma\left(\frac{5}{2}\right) \\ &= \frac{3}{4}\pi\tau_\mathrm{p}.\end{aligned} \tag{A.1.16}$$

Then, the energy of the transmitted signal in the frequency domain is

$$\begin{aligned}E_\mathrm{s} &= \frac{1}{2\pi}\int_{-\infty}^\infty |S(\omega)|^2 \mathrm{d}\omega \\ &= \frac{\tau_\mathrm{p}^6}{16\pi^2}\left(\frac{4\pi}{\tau_\mathrm{p}^2}\right)^{\frac{5}{2}} \Gamma\left(\frac{5}{2}\right) \\ &= \frac{3}{8}\tau_\mathrm{p}.\end{aligned} \tag{A.1.17}$$

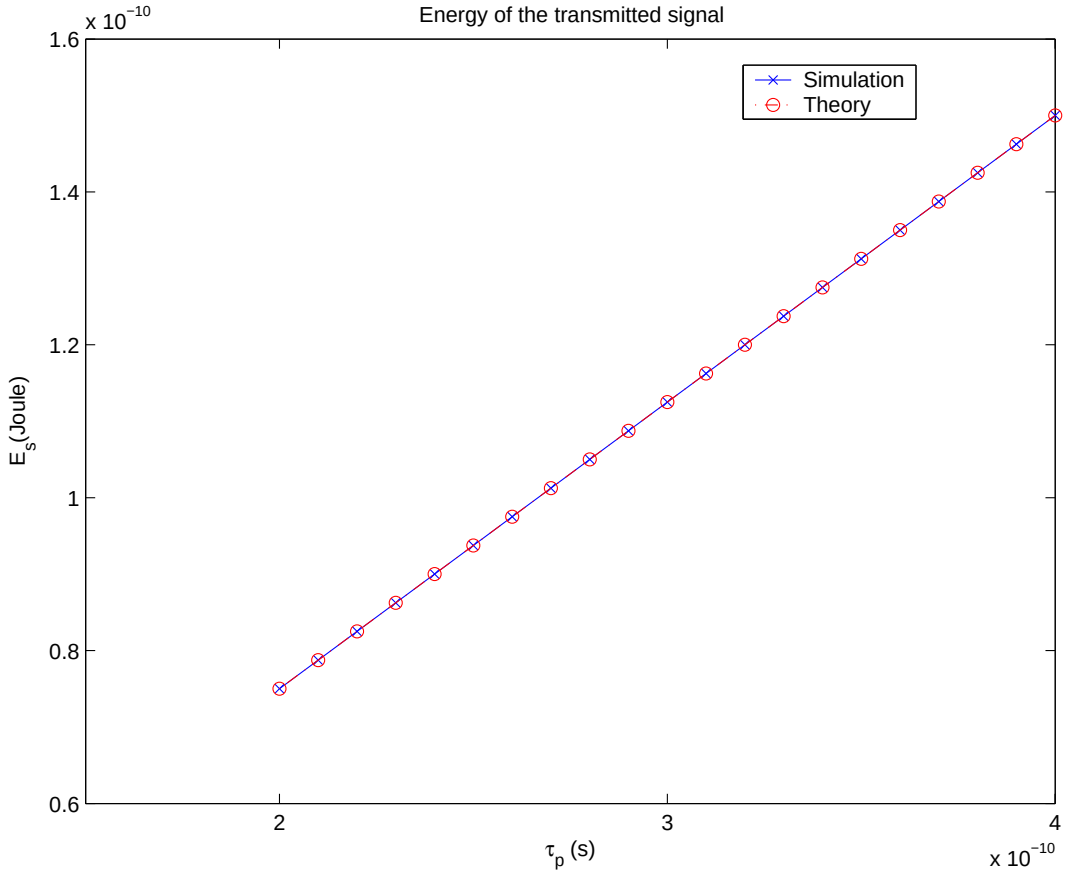

Figure A.1: Energy of the transmitted signal.

The value obtained in (A.1.17) is the energy of the transmitted signal, which can also be expressed in the time domain as

$$E_{\mathrm{s}} = \int_{-\infty}^{\infty} s^2(t)\mathrm{d}t. \tag{A.1.18}$$

The result of $\int_{-\infty}^{\infty} \omega^2 |S(\omega)|^2 \mathrm{d}\omega$ is derived as follows

$$\begin{aligned} \int_{-\infty}^{\infty} \omega^2 |S(\omega)|^2 \mathrm{d}\omega &= \int_{-\infty}^{\infty} \frac{\tau_{\mathrm{p}}^6}{32\pi^2} \omega^6 \mathrm{e}^{-\frac{\tau_{\mathrm{p}}^2}{4\pi}\omega^2} \mathrm{d}\omega \\ &= \frac{\tau_{\mathrm{p}}^6}{32\pi^2} 2 \int_{0}^{\infty} \omega^6 \mathrm{e}^{-\frac{\tau_{\mathrm{p}}^2}{4\pi}\omega^2} \mathrm{d}\omega. \end{aligned} \tag{A.1.19}$$

Applying (A.1.15) in (A.1.19) and letting $\eta = \frac{\tau_{\mathrm{p}}^2}{4\pi}$ and $n = 6$, we have

$$\int_{-\infty}^{\infty} \omega^2 |S(\omega)|^2 \mathrm{d}\omega = \frac{\tau_{\mathrm{p}}^6}{16\pi^2} \left(\frac{4\pi}{\tau_{\mathrm{p}}^2}\right)^{\frac{7}{2}} \Gamma\left(\frac{7}{2}\right). \tag{A.1.20}$$

Then, the square of the bandwidth of the transmitted signal in frequency and time domain are given, respectively, by

$$\begin{aligned} W &= \frac{1}{2\pi} \int_{-\infty}^{\infty} \omega^2 |S(\omega)|^2 \mathrm{d}\omega \\ &= \frac{15\pi}{4\tau_{\mathrm{p}}}, \end{aligned} \tag{A.1.21}$$

and

$$W = \int_{-\infty}^{\infty} \dot{s}^2(t) \mathrm{d}t. \tag{A.1.22}$$

where $\dot{s}(t) = \frac{\partial}{\partial t} s(t)$ can be solved as

$$\begin{aligned} \dot{s}(t) &= \frac{\partial}{\partial t} s(t) \\ &= (1 - 2\alpha(t)) \mathrm{e}^{-\alpha(t)} \frac{\partial}{\partial t} \alpha(t) - 2\mathrm{e}^{-\alpha(t)} \frac{\partial}{\partial t} \alpha(t) \\ &= (-3 + 2\alpha(t)) \mathrm{e}^{-\alpha(t)} \frac{\partial}{\partial t} \alpha(t). \end{aligned} \tag{A.1.23}$$

Then, we have

$$\begin{aligned} \dot{s}^2(t) &= (-3 + 2\alpha(t))^2 \mathrm{e}^{-2\alpha(t)} \left(\frac{\partial}{\partial t} \alpha(t)\right)^2 \\ &= (4\alpha^2(t) - 12\alpha(t) + 9) \mathrm{e}^{-2\alpha(t)} \left(\frac{\partial}{\partial t} \alpha(t)\right)^2. \end{aligned} \tag{A.1.24}$$

We calculate the square of the bandwidth of the transmitted signal $s(t)$, where $\alpha(t) = 2\pi \left(\frac{t - \frac{1}{2}T_{\mathrm{p}}}{\tau_{\mathrm{p}}}\right)^2$. Therefore, in (A.1.24), $\frac{\partial}{\partial t} \alpha(t)$ is

$$\frac{\partial}{\partial t} \alpha(t) = \frac{1}{\tau_{\mathrm{p}}^2} 4\pi (t - \frac{1}{2} T_{\mathrm{p}}). \tag{A.1.25}$$

Finally, the effective bandwidth expression in the frequency domain is

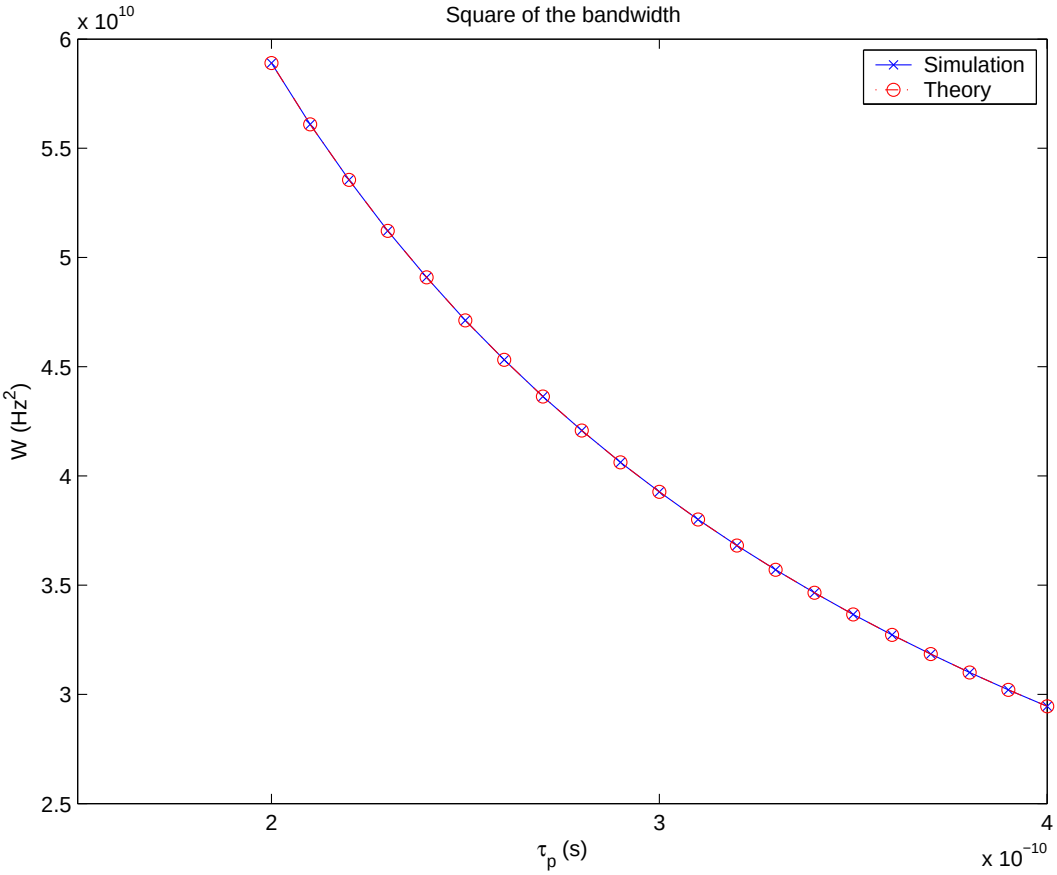

Figure A.2: The square of the bandwidth of the transmitted signal.

$$
\begin{aligned}
\bar{\beta} &= \frac{1}{2\pi}\sqrt{\frac{\int_{-\infty}^{\infty}\omega^2|S(\omega)|^2\mathrm{d}\omega}{\int_{-\infty}^{\infty}|S(\omega)|^2\mathrm{d}\omega}} \\
&= \frac{1}{2\pi}\sqrt{\frac{\frac{\tau_{\mathrm{p}}^6}{32\pi^2}\left(\frac{4\pi}{\tau_{\mathrm{p}}^2}\right)^{\frac{7}{2}}\Gamma\left(\frac{7}{2}\right)}{\frac{\tau_{\mathrm{p}}^6}{32\pi^2}\left(\frac{4\pi}{\tau_{\mathrm{p}}^2}\right)^{\frac{5}{2}}\Gamma\left(\frac{5}{2}\right)}} \\
&= \frac{1}{2\pi}\sqrt{\frac{\left(\frac{4\pi}{\tau_{\mathrm{p}}^2}\right)^{\frac{7}{2}}\Gamma\left(\frac{7}{2}\right)}{\left(\frac{4\pi}{\tau_{\mathrm{p}}^2}\right)^{\frac{5}{2}}\Gamma\left(\frac{5}{2}\right)}} \\
&= \frac{1}{2\pi}\sqrt{\left(\frac{4\pi}{\tau_{\mathrm{p}}^2}\right)\frac{\Gamma\left(\frac{5}{2}+1\right)}{\Gamma\left(\frac{5}{2}\right)}} \\
&= \frac{1}{2\pi}\sqrt{\left(\frac{4\pi}{\tau_{\mathrm{p}}^2}\right)\frac{5}{2}\frac{\Gamma\left(\frac{5}{2}\right)}{\Gamma\left(\frac{5}{2}\right)}} \\
&= \sqrt{\frac{5}{2\pi\tau_{\mathrm{p}}^2}} \\
&= \frac{1}{\tau_{\mathrm{p}}}\sqrt{\frac{5}{2\pi}}.
\end{aligned}
\tag{A.1.26}
$$

A.2 Proof of Proposition 3.3.1

Next we have to evaluate

$$
\begin{aligned}
\int_{-\infty}^{\infty}|\omega||S(\omega)|^2\mathrm{d}\omega &= \frac{\tau_{\mathrm{p}}^6}{32\pi^2}\left(\int_{-\infty}^{0}|\omega|\omega^4\mathrm{e}^{-\frac{\tau_{\mathrm{p}}^2}{4\pi}\omega^2}\mathrm{d}\omega + \int_{0}^{+\infty}|\omega|\omega^4\mathrm{e}^{-\frac{\tau_{\mathrm{p}}^2}{4\pi}\omega^2}\mathrm{d}\omega\right) \\
&= \frac{\tau_{\mathrm{p}}^6}{32\pi^2}\left(\int_{-\infty}^{0}|\omega^5|\mathrm{e}^{-\frac{\tau_{\mathrm{p}}^2}{4\pi}\omega^2}\mathrm{d}\omega + \int_{0}^{+\infty}\omega^5\mathrm{e}^{-\frac{\tau_{\mathrm{p}}^2}{4\pi}\omega^2}\mathrm{d}\omega\right).
\end{aligned}
\tag{A.2.1}
$$

Let $u(\omega) = -\omega$ be a dummy variable. It can be shown that

$$\begin{aligned}\int_{-\infty}^{\infty} |\omega||S(\omega)|^2 \mathrm{d}\omega &= \frac{\tau_\mathrm{p}^6}{32\pi^2}\left(\int_{u(-\infty)}^{0}(-1)|(-u)^5|\mathrm{e}^{-\frac{\tau_\mathrm{p}^2}{4\pi}u^2}\mathrm{d}u + \int_0^{+\infty}\omega^5\mathrm{e}^{-\frac{\tau_\mathrm{p}^2}{4\pi}\omega^2}\mathrm{d}\omega\right)\\ &= \frac{\tau_\mathrm{p}^6}{32\pi^2}\left(-\int_0^{\infty}(-1)u^5\mathrm{e}^{-\frac{\tau_\mathrm{p}^2}{4\pi}u^2}\mathrm{d}u + \int_0^{+\infty}\omega^5\mathrm{e}^{-\frac{\tau_\mathrm{p}^2}{4\pi}\omega^2}\mathrm{d}\omega\right)\\ &= \frac{\tau_\mathrm{p}^6}{32\pi^2}2\int_0^{\infty}\omega^5\mathrm{e}^{-\frac{\tau_\mathrm{p}^2}{4\pi}\omega^2}\mathrm{d}\omega.\end{aligned} \tag{A.2.2}$$

Thereby, by assigning $\eta = \frac{\tau_\mathrm{p}^2}{4\pi}$ and $n = 5$ in (A.1.15), the solution of (A.2.1) is given by

$$\begin{aligned}\int_{-\infty}^{\infty} |\omega||S(\omega)|^2 \mathrm{d}\omega &= \frac{\tau_\mathrm{p}^6}{16\pi^2}\left(\frac{4\pi}{\tau_\mathrm{p}^2}\right)^{\frac{6}{2}}\Gamma\left(\frac{6}{2}\right)\\ &= \frac{\tau_\mathrm{p}^6}{16\pi^2}\left(\frac{4\pi}{\tau_\mathrm{p}^2}\right)^{3}\Gamma\left(3\right)\\ &= 8\pi.\end{aligned} \tag{A.2.3}$$

Substituting (A.1.16) and (A.2.3) into (3.3.4), we obtain

$$\begin{aligned}\bar{f}_\mathrm{abs} &= \frac{1}{2\pi}\frac{8\pi}{\frac{3\pi}{4}\tau_\mathrm{p}}\\ &= \frac{1}{\tau_\mathrm{p}}\frac{16}{3\pi}.\end{aligned} \tag{A.2.4}$$

A.3 Proof of Proposition 3.5.1

The Fourier transform of the transmitted signal can be calculated by

$$\begin{aligned}S(\omega) &= \mathcal{F}\{s(t)\}\\ &= \mathcal{F}\left\{\sum_{n=1}^{N-1} v_n \cos\left(\left(\omega_0 - \frac{v_n q_n \pi}{2T}\right)t\right)\right\}.\end{aligned} \tag{A.3.1}$$

The linearity property of the Fourier transform states for any complex numbers ϵ and ϑ that $\mathcal{F}\{\epsilon g_1(x) + \vartheta g_2(x)\} = \epsilon\mathcal{F}\{g_1(x)\} + \vartheta\mathcal{F}\{g_2(x)\}$ (see, e.g., [51]). Therefore,

(A.3.1) can be rewritten as

$$S(\omega) = \sum_{n=1}^{N-1} v_n \mathcal{F}\left\{\cos\left(\left(\omega_0 - \frac{v_n q_n \pi}{2T}\right) t\right)\right\}. \tag{A.3.2}$$

The Fourier transform shown in (A.3.2) has the form $\mathcal{F}\{\cos(\eta x)\} = \pi(\delta(\omega - \eta) + \delta(\omega + \eta))$ (see, e.g., [51]), where $\eta = \omega_0 - \frac{v_n q_n \pi}{2T}$. Then, we have

$$S(\omega) = \sum_{n=1}^{N-1} v_n \pi \left(\delta\left(\omega - \omega_0 + \frac{v_n q_n \pi}{2T}\right) + \delta\left(\omega + \omega_0 - \frac{v_n q_n \pi}{2T}\right)\right). \tag{A.3.3}$$

The expression of $|S(\omega)|^2$ can be obtained as follows

$$\begin{aligned}
|S(\omega)|^2 &= S(\omega) \cdot S^*(\omega) \\
&= \left(\sum_{n=1}^{N-1} v_n \pi \left(\delta\left(\omega - \omega_0 + \frac{v_n q_n \pi}{2T}\right) + \delta\left(\omega + \omega_0 - \frac{v_n q_n \pi}{2T}\right)\right)\right) \\
&\quad \left(\sum_{n'=1}^{N-1} v_{n'} \pi \left(\delta\left(\omega - \omega_0 + \frac{v_{n'} q_{n'} \pi}{2T}\right) + \delta\left(\omega + \omega_0 - \frac{v_{n'} q_{n'} \pi}{2T}\right)\right)\right) \\
&= \pi^2 \sum_{n=1}^{N-1} \sum_{n'=1}^{N-1} v_n v_{n'} \left(\delta\left(\omega - \omega_0 + \frac{v_n q_n \pi}{2T}\right) + \delta\left(\omega + \omega_0 - \frac{v_n q_n \pi}{2T}\right)\right) \\
&\quad \left(\delta\left(\omega - \omega_0 + \frac{v_{n'} q_{n'} \pi}{2T}\right) + \delta\left(\omega + \omega_0 - \frac{v_{n'} q_{n'} \pi}{2T}\right)\right) \\
&= \pi^2 \sum_{n=1}^{N-1} \sum_{n'=1}^{N-1} v_n v_{n'} \left(\delta\left(\omega - \omega_0 + \frac{v_n q_n \pi}{2T}\right) \delta\left(\omega - \omega_0 + \frac{v_{n'} q_{n'} \pi}{2T}\right)\right. \\
&\quad + \delta\left(\omega + \omega_0 - \frac{v_n q_n \pi}{2T}\right) \delta\left(\omega - \omega_0 + \frac{v_{n'} q_{n'} \pi}{2T}\right) \\
&\quad + \delta\left(\omega - \omega_0 + \frac{v_n q_n \pi}{2T}\right) \delta\left(\omega + \omega_0 - \frac{v_{n'} q_{n'} \pi}{2T}\right) \\
&\quad \left. + \delta\left(\omega + \omega_0 - \frac{v_n q_n \pi}{2T}\right) \delta\left(\omega + \omega_0 - \frac{v_{n'} q_{n'} \pi}{2T}\right)\right).
\end{aligned} \tag{A.3.4}$$

The Dirac delta function (or the Dirac measure, or the Dirac distribution), denoted by $\delta(x)$ (see, e.g., [51] and [68, p. 292]), has the following properties:

1. $\delta(x) \geq 0$ for $-\infty < x < +\infty$,

2. $\delta(x) = 0$ for $x \neq 0$,

3. $f(x)\delta(x-x_0) = f(x_0)\delta(x-x_0)$ for any function $f(x)$,

4. $\int_{-\infty}^{\infty} \delta(x)\mathrm{d}x = 1$.

For any continuous function $f(x)$ defined in the interval $x \in (-\infty, +\infty)$,

$$\int_{-\infty}^{\infty} f(x)\,\delta(x)\mathrm{d}x = f(0). \tag{A.3.5}$$

Furthermore, for any real or complex value x_0 and for any continuous function $f(x)$ on $\mathbb{R}$, the Dirac delta provides

$$\int_{-\infty}^{\infty} f(x)\delta(x-x_0)\,\mathrm{d}x = f(x_0). \tag{A.3.6}$$

The expression (A.3.4) contents the terms with the form $\delta(\omega-\omega_a)\cdot\delta(\omega-\omega_b)$, which can be developed by using the 3th property of the Dirac delta. By defining $x = \omega - \omega_a$, and therefore $\delta(\omega-\omega_a)$ as $f(x)$ and $\delta(\omega-\omega_b)$ as $\delta(x-x_0)$, we can write

$$\begin{aligned}\delta(\omega-\omega_a)\cdot\delta(\omega-\omega_b) &= \delta(x)\delta(x+\omega_a-\omega_b)\\ &= \delta(\omega_b-\omega_a)\delta(x+\omega_a-\omega_b),\end{aligned} \tag{A.3.7}$$

where by using the second property of the Dirac delta, the term $\delta(\omega_b-\omega_a) = 0$ if $\omega_a \neq \omega_b$. Then, the multiplication yields

$$\delta(\omega-\omega_a)\cdot\delta(\omega-\omega_b) = \begin{cases} 0 & ;\omega_a \neq \omega_b, \\ \delta^2(\omega-\omega_a) & ;\omega_a = \omega_b. \end{cases} \tag{A.3.8}$$

We can analyze the different terms of (A.3.4) by using the previous result as

$$\delta\left(\omega-\omega_0+\frac{v_n q_n \pi}{2T}\right)\delta\left(\omega-\omega_0+\frac{v_{n'} q_{n'} \pi}{2T}\right)=\begin{cases}0 & ;v_n q_n \neq v_{n'} q_{n'},\\ \delta^2\left(\omega-\omega_0+\frac{v_n q_n \pi}{2T}\right) & ;v_n q_n = v_{n'} q_{n'},\end{cases} \tag{A.3.9a}$$

$$\delta\left(\omega+\omega_0-\frac{v_n q_n \pi}{2T}\right)\delta\left(\omega+\omega_0-\frac{v_{n'} q_{n'} \pi}{2T}\right)=\begin{cases}0 & ;v_n q_n \neq v_{n'} q_{n'},\\ \delta^2\left(\omega+\omega_0-\frac{v_n q_n \pi}{2T}\right) & ;v_n q_n = v_{n'} q_{n'},\end{cases} \tag{A.3.9b}$$

$$\delta\left(\omega+\omega_0-\frac{v_n q_n \pi}{2T}\right)\delta\left(\omega-\omega_0+\frac{v_{n'} q_{n'} \pi}{2T}\right)=\begin{cases}0 & ;2\omega_0 \neq \frac{v_n q_n \pi}{2T}+\frac{v_{n'} q_{n'} \pi}{2T},\\ \delta^2\left(\omega+\omega_0-\frac{v_n q_n \pi}{2T}\right) & ;2\omega_0 = \frac{v_n q_n \pi}{2T}+\frac{v_{n'} q_{n'} \pi}{2T},\end{cases} \tag{A.3.9c}$$

$$\delta\left(\omega-\omega_0+\frac{v_n q_n \pi}{2T}\right)\delta\left(\omega+\omega_0-\frac{v_{n'} q_{n'} \pi}{2T}\right)=\begin{cases}0 & ;2\omega_0 \neq \frac{v_n q_n \pi}{2T}+\frac{v_{n'} q_{n'} \pi}{2T},\\ \delta^2\left(\omega-\omega_0+\frac{v_n q_n \pi}{2T}\right) & ;2\omega_0 = \frac{v_n q_n \pi}{2T}+\frac{v_{n'} q_{n'} \pi}{2T}.\end{cases} \tag{A.3.9d}$$

Observe that the conditions in (A.3.9c) and (A.3.9d) are the same and require more analysis. The condition $2\omega_0 = \frac{v_n q_n \pi}{2T} + \frac{v_{n'} q_{n'} \pi}{2T}$ is true only when $v_n q_n = v_{n'} q_{n'} = 1$ and $\omega_0 = \frac{\pi}{2T}$. We can rewrite the condition $\omega_0 = \frac{\pi}{2T}$ as a function of the central frequency and the bit rate as

$$2\pi f_0 = \frac{1}{2}\pi R_{\mathrm{B}}. \tag{A.3.10}$$

Then, the previous condition yields $4f_0 = R_{\mathrm{B}}$, i.e., the bit rate should be four times much bigger that the central frequency. However, this condition is not realistic because no real wireless systems operate with a bit rate higher than the central frequency. For example, in the GSM systems, the typical values of the central frequency are 900 MHz and 2 GHz, and the GSM systems provide the bit rates of up to 140 kbps (see, e.g., [48, p. 12]).

Moreover, if the bit rate is chosen such that $\omega_0 = \frac{1}{2}\pi R_{\mathrm{B}}$ holds, then under the condition $2\omega_0 = \frac{v_n q_n \pi}{2T} + \frac{v_{n'} q_{n'} \pi}{2T}$, the expression $|S(\omega)|^2$ can be obtained from

$$|S(\omega)|^2 = 2\pi^2 \sum_{n=1}^{N-1} \left(\delta^2 \left(\omega - \omega_0 + \frac{v_n q_n \pi}{2T} \right) + \delta^2 \left(\omega + \omega_0 - \frac{v_n q_n \pi}{2T} \right) \right). \tag{A.3.11}$$

Note that in the final calculation of $\bar{\beta}$, the factors of 2 appears at the nominator, $\int_{-\infty}^{\infty} \omega^2 |S(\omega)|^2 \mathrm{d}\omega$, and at the denominator, $\int_{-\infty}^{\infty} |S(\omega)|^2 \mathrm{d}\omega$. Then, both factors of 2 will cancel each other. Therefore, our analysis can support the condition $\omega_0 = \frac{1}{2}\pi R_{\mathrm{B}}$ with the same value of the effective bandwidth. In what follows, we will assume $\omega_0 \neq \frac{1}{2}\pi R_{\mathrm{B}}$ for simplicity. Then, the final expression of $|S(\omega)|^2$ can be written as

$$|S(\omega)|^2 = \pi^2 \sum_{n=1}^{N-1} \left(\delta^2 \left(\omega - \omega_0 + \frac{v_n q_n \pi}{2T} \right) + \delta^2 \left(\omega + \omega_0 - \frac{v_n q_n \pi}{2T} \right) \right). \tag{A.3.12}$$

Evaluating $\int_{-\infty}^{\infty} |S(\omega)|^2 \mathrm{d}\omega$, we can derive

$$\begin{aligned}
\int_{-\infty}^{\infty} |S(\omega)|^2 \mathrm{d}\omega &= \int_{-\infty}^{\infty} \pi^2 \sum_{n=1}^{N-1} \left(\delta^2 \left(\omega - \omega_0 + \frac{v_n q_n \pi}{2T} \right) + \delta^2 \left(\omega + \omega_0 - \frac{v_n q_n \pi}{2T} \right) \right) \mathrm{d}\omega \\
&= \pi^2 \sum_{n=1}^{N-1} \int_{-\infty}^{\infty} \delta^2 \left(\omega - \omega_0 + \frac{v_n q_n \pi}{2T} \right) + \delta^2 \left(\omega + \omega_0 - \frac{v_n q_n \pi}{2T} \right) \mathrm{d}\omega \\
&= \pi^2 \sum_{n=1}^{N-1} \int_{-\infty}^{\infty} \delta \left(\omega - \omega_0 + \frac{v_n q_n \pi}{2T} \right) \delta \left(\omega - \omega_0 + \frac{v_n q_n \pi}{2T} \right) \mathrm{d}\omega \\
&\quad + \pi^2 \sum_{n=1}^{N-1} \int_{-\infty}^{\infty} \delta \left(\omega + \omega_0 - \frac{v_n q_n \pi}{2T} \right) \delta \left(\omega + \omega_0 - \frac{v_n q_n \pi}{2T} \right) \mathrm{d}\omega.
\end{aligned} \tag{A.3.13}$$

The last property of the Dirac delta may be used to solve (A.3.13). Then, by defining $\delta(x)$ as $\delta\left(\omega - \omega_0 + \frac{v_n q_n \pi}{2T}\right)$ and $f(x)$ as $\delta\left(\omega - \omega_0 + \frac{v_n q_n \pi}{2T}\right)$ in (A.3.5), we have

$$\pi^2 \sum_{n=1}^{N-1} \int_{-\infty}^{\infty} \delta \left(\omega - \omega_0 + \frac{v_n q_n \pi}{2T} \right) \delta \left(\omega - \omega_0 + \frac{v_n q_n \pi}{2T} \right) \mathrm{d}\omega = \pi^2 \sum_{n=1}^{N-1} \delta(0). \tag{A.3.14}$$

Similarly, by taking $\delta(x)$ as $\delta\left(\omega+\omega_0-\frac{v_n q_n \pi}{2T}\right)$ and $f(x)$ as $\delta\left(\omega+\omega_0-\frac{v_n q_n \pi}{2T}\right)$, we have

$$\pi^2 \sum_{n=1}^{N-1} \int_{-\infty}^{\infty} \delta\left(\omega+\omega_0-\frac{v_n q_n \pi}{2T}\right) \delta\left(\omega+\omega_0-\frac{v_n q_n \pi}{2T}\right) \mathrm{d}\omega = \pi^2 \sum_{n=1}^{N-1} \delta(0). \quad \text{(A.3.15)}$$

Substituting (A.3.14) and (A.3.15) into (A.3.13) we obtain

$$\begin{aligned} \int_{-\infty}^{\infty} |S(\omega)|^2 \mathrm{d}\omega &= \pi^2 \sum_{n=1}^{N-1} \delta(0) + \pi^2 \sum_{n=1}^{N-1} \delta(0) \\ &= 2\pi^2 \sum_{n=1}^{N-1} \delta(0) \\ &= 2\pi^2 (N-1)\delta(0). \end{aligned} \quad \text{(A.3.16)}$$

The next step to obtain $\bar{\beta}$ is the calculation of $\int_{-\infty}^{\infty} \omega^2 |S(\omega)|^2 \mathrm{d}\omega$, which can be solved from

$$\begin{aligned} \int_{-\infty}^{\infty} \omega^2 |S(\omega)|^2 \mathrm{d}\omega &= \int_{-\infty}^{\infty} \omega^2 \pi^2 \sum_{n=1}^{N-1} \left(\delta^2\left(\omega-\omega_0+\frac{v_n q_n \pi}{2T}\right) + \delta^2\left(\omega+\omega_0-\frac{v_n q_n \pi}{2T}\right)\right) \mathrm{d}\omega \\ &= \pi^2 \sum_{n=1}^{N-1} \int_{-\infty}^{\infty} \omega^2 \left(\delta^2\left(\omega-\omega_0+\frac{v_n q_n \pi}{2T}\right) + \delta^2\left(\omega+\omega_0-\frac{v_n q_n \pi}{2T}\right)\right) \mathrm{d}\omega \\ &= \pi^2 \sum_{n=1}^{N-1} \int_{-\infty}^{\infty} \omega^2 \delta^2\left(\omega-\omega_0 \mathrm{d}\omega+\frac{v_n q_n \pi}{2T}\right) \\ &\quad + \pi^2 \sum_{n=1}^{N-1} \int_{-\infty}^{\infty} \omega^2 \delta^2\left(\omega+\omega_0-\frac{v_n q_n \pi}{2T}\right) \mathrm{d}\omega. \end{aligned} \quad \text{(A.3.17)}$$

By letting $\delta(x)$ be $\delta\left(\omega-\omega_0+\frac{v_n q_n \pi}{2T}\right)$ and $f(x)$ be $\omega^2\delta\left(\omega-\omega_0+\frac{v_n q_n \pi}{2T}\right)$ in (A.3.6), the integral in the first term of (A.3.17) is

$$\int_{-\infty}^{\infty} \omega^2 \delta\left(\omega-\omega_0+\frac{v_n q_n \pi}{2T}\right) \delta\left(\omega-\omega_0+\frac{v_n q_n \pi}{2T}\right) \mathrm{d}\omega = \left(\omega_0-\frac{v_n q_n \pi}{2T}\right)^2 \delta(0). \quad \text{(A.3.18)}$$

By letting $\delta(x)$ be $\delta\left(\omega+\omega_0-\frac{v_n q_n \pi}{2T}\right)$ and $f(x)$ be $\omega^2\delta\left(\omega+\omega_0-\frac{v_n q_n \pi}{2T}\right)$ in (A.3.6), the integral in the second term of (A.3.17) can be resolved as

$$\int_{-\infty}^{\infty}\omega^2\delta\left(\omega+\omega_0-\frac{v_n q_n\pi}{2T}\right)\delta\left(\omega+\omega_0-\frac{v_n q_n\pi}{2T}\right)\mathrm{d}\omega=\left(-\omega_0+\frac{v_n q_n\pi}{2T}\right)^2\delta(0). \tag{A.3.19}$$

Consequently, the solution of (A.3.17) is

$$\begin{aligned}\int_{-\infty}^{\infty}\omega^2|S(\omega)|^2\mathrm{d}\omega&=\pi^2\sum_{n=1}^{N-1}\left(\omega_0-\frac{v_n q_n\pi}{2T}\right)^2\delta(0)+\pi^2\sum_{n=1}^{N-1}\left(-\omega_0+\frac{v_n q_n\pi}{2T}\right)^2\delta(0)\\&=2\pi^2\sum_{n=1}^{N-1}\left(\omega_0-\frac{v_n q_n\pi}{2T}\right)^2\delta(0)\\&=2\pi^2\delta(0)\sum_{n=1}^{N-1}\left(\omega_0-\frac{v_n q_n\pi}{2T}\right)^2.\end{aligned} \tag{A.3.20}$$

Finally, we obtain the value of $\bar{\beta}$ from

$$\begin{aligned}\bar{\beta}&=\frac{1}{2\pi}\sqrt{\frac{\int_{-\infty}^{\infty}\omega^2|S(\omega)|^2\mathrm{d}\omega}{\int_{-\infty}^{\infty}|S(\omega)|^2\mathrm{d}\omega}}\\&=\frac{1}{2\pi}\sqrt{\frac{2\pi^2\delta(0)\sum_{n=1}^{N-1}(\omega_0-\frac{v_n q_n\pi}{2T})^2}{2\pi^2\delta(0)(N-1)}}\\&=\frac{1}{2\pi}\sqrt{\frac{\sum_{n=1}^{N-1}(\omega_0-\frac{v_n q_n\pi}{2T})^2}{N-1}}.\end{aligned} \tag{A.3.21}$$

The PDF of v_n and q_m is given by the discrete value of -1 and $+1$. The PDF of v_n and q_m can be written as

$$p_v(v_n)=\frac{1}{2}(\delta(v_n+1)+\delta(v_n-1)), \tag{A.3.22a}$$

$$p_q(q_n)=\frac{1}{2}(\delta(q_n+1)+\delta(q_n-1)). \tag{A.3.22b}$$

The variables v_n and q_n are assumed as independent variables, whose joint probability distribution can be written as $p_{v,q}(v_n,q_n)=p_v(v_n)p_q(q_n)$. The transmitted

information is random. Therefore, the value of $\bar{\beta}$ is also random. Then, we need to determine the expectation of $\bar{\beta}$, i.e.,

$$\begin{aligned}
\mathrm{E}_{\mathbf{v},\mathbf{q}}\{\bar{\beta}^2\} &= \mathrm{E}_{\mathbf{v},\mathbf{q}}\left\{\left(\frac{1}{2\pi}\sqrt{\frac{\sum_{n=1}^{N-1}(\omega_0-\frac{v_n q_n \pi}{2T})^2}{N-1}}\right)^2\right\} \\
&= \frac{1}{4\pi^2}\sum_{k=1}^{4} p_{v,q}(v_n,q_n)\frac{\sum_{n=1}^{N-1}\left(\omega_0-\frac{v_n q_n \pi}{2T}\right)^2}{N-1} \\
&= \frac{1}{4\pi^2(N-1)}\sum_{n=1}^{N-1}\sum_{k=1}^{4} p_v(v_n)p_q(q_n)\left(\omega_0-\frac{v_n q_n \pi}{2T}\right)^2 \\
&= \frac{1}{4\pi^2(N-1)}\sum_{n=1}^{N-1}\frac{1}{4}\left(\left(\omega_0-\frac{(+1)(+1)\pi}{2T}\right)^2+\left(\omega_0-\frac{(+1)(-1)\pi}{2T}\right)^2\right. \\
&\quad \left.+\left(\omega_0-\frac{(-1)(+1)\pi}{2T}\right)^2+\left(\omega_0-\frac{(-1)(-1)\pi}{2T}\right)^2\right) \\
&= \frac{1}{8\pi^2(N-1)}\sum_{n=1}^{N-1}\left(\omega_0-\frac{\pi}{2T}\right)^2+\left(\omega_0+\frac{\pi}{2T}\right)^2 \\
&= \frac{1}{8\pi^2(N-1)}(N-1)\left(2{\omega_0}^2+2\left(\frac{\pi}{2T}\right)^2\right) \\
&= \frac{1}{4\pi^2}\left((2\pi f_0)^2+\left(\frac{\pi}{2T}\right)^2\right) \\
&= f_0^2+\frac{1}{16T^2}.
\end{aligned} \tag{A.3.23}$$

A.4 Proof of Proposition 3.6.1

The ACRB of the MC estimator can be developed as

$$\begin{aligned}
\mathrm{ACRB}_{\mathrm{ToA}} &= \mathrm{E}_{\mathbf{v},\mathbf{q}}\left\{\mathrm{MSE}_{\mathrm{ToA}}(\hat{\tau}_{b,\mathrm{MC}})\right\} \\
&= \mathrm{E}_{\mathbf{v},\mathbf{q}}\left\{\frac{1}{a_b^2\mathrm{SNR}8\pi^2\bar{\beta}^2}\right\} \\
&= \frac{1}{a_b^2\mathrm{SNR}8\pi^2}\mathrm{E}_{\mathbf{v},\mathbf{q}}\left\{\frac{1}{\bar{\beta}^2}\right\}.
\end{aligned} \tag{A.4.1}$$

Then, we need the value of $\mathrm{E}_{\mathbf{v},\mathbf{q}}\left\{\frac{1}{\bar{\beta}^2}\right\}$, which can been derived from

$$
\begin{aligned}
\mathrm{E}_{\mathbf{v},\mathbf{q}}\left\{\frac{1}{\bar{\beta}^2}\right\} &= \mathrm{E}_{\mathbf{v},\mathbf{q}}\left\{\left(2\pi\sqrt{\frac{N-1}{\sum_{n=1}^{N-1}(\omega_0-\frac{v_n q_n \pi}{2T})^2}}\right)^2\right\} \\
&= 4\pi^2\sum_{k=1}^{4} p_{v,q}(v_n,q_n)\frac{N-1}{\sum_{n=1}^{N-1}\left(\omega_0-\frac{v_n q_n\pi}{2T}\right)^2} \\
&= 4\pi^2(N-1)\sum_{k=1}^{4} p_v(v_n)p_q(q_n)\frac{1}{\sum_{n=1}^{N-1}\left(\omega_0-\frac{v_n q_n\pi}{2T}\right)^2} \\
&= 4\pi^2(N-1)\left(\frac{1}{4}\frac{1}{\sum_{n=1}^{N-1}\left(\omega_0-\frac{(+1)(+1)\pi}{2T}\right)^2}+\frac{1}{4}\frac{1}{\sum_{n=1}^{N-1}\left(\omega_0-\frac{(+1)(-1)\pi}{2T}\right)^2}\right. \\
&\quad \left.+\frac{1}{4}\frac{1}{\sum_{n=1}^{N-1}\left(\omega_0-\frac{(-1)(+1)\pi}{2T}\right)^2}+\frac{1}{4}\frac{1}{\sum_{n=1}^{N-1}\left(\omega_0-\frac{(-1)(-1)\pi}{2T}\right)^2}\right) \\
&= \pi^2(N-1)\left(\frac{2}{\sum_{n=1}^{N-1}\left(\omega_0-\frac{\pi}{2T}\right)^2}+\frac{2}{\sum_{n=1}^{N-1}\left(\omega_0+\frac{\pi}{2T}\right)^2}\right) \\
&= 2\pi^2(N-1)\left(\frac{1}{(N-1)\left(\omega_0-\frac{\pi}{2T}\right)^2}+\frac{1}{(N-1)\left(\omega_0+\frac{\pi}{2T}\right)^2}\right) \\
&= \frac{\left(\omega_0-\frac{\pi}{2T}\right)^2+\left(\omega_0+\frac{\pi}{2T}\right)^2}{\left(\omega_0-\frac{\pi}{2T}\right)^2\left(\omega_0+\frac{\pi}{2T}\right)^2}2\pi^2 \\
&= \frac{2\omega_0^2+2\left(\frac{\pi}{2T}\right)^2}{\left(\omega_0-\frac{\pi}{2T}\right)^2\left(\omega_0+\frac{\pi}{2T}\right)^2}2\pi^2 \\
&= \frac{\omega_0^2+\left(\frac{\pi}{2T}\right)^2}{\left(\left(\omega_0-\frac{\pi}{2T}\right)\left(\omega_0+\frac{\pi}{2T}\right)\right)^2}4\pi^2 \\
&= \frac{\omega_0^2+\left(\frac{\pi}{2T}\right)^2}{\left(\omega_0^2-\left(\frac{\pi}{2T}\right)^2\right)^2}4\pi^2 \\
&= \frac{\omega_0^2+\left(\frac{\pi}{2T}\right)^2}{\omega_0^4+\left(\frac{\pi}{2T}\right)^4-2\omega_0^2\left(\frac{\pi}{2T}\right)^2}4\pi^2 \\
&= \frac{4f_0^2+\frac{1}{4T^2}}{16f_0^4+\frac{1}{16T^4}-\frac{1}{T^2}2f_0^2}4 \\
&= \frac{16f_0^2+\frac{1}{T^2}}{16f_0^4+\frac{1}{16T^4}-\frac{1}{T^2}2f_0^2}.
\end{aligned}
\tag{A.4.2}
$$

Finally, by including the value of $\mathrm{E}_{\mathbf{v},\mathbf{q}}\left\{\frac{1}{\bar{\beta}^2}\right\}$ into (A.4.1),we obtain (3.6.5).

A.5 Proof of Proposition 3.6.2

Similarly, the ACRB of the ML estimator can be developed as

$$\begin{aligned}
\mathrm{ACRB}_{\text{SS-ToA}} &= \mathrm{E}_{\mathbf{v},\mathbf{q}}\left\{\mathrm{MSE}_{\text{SS-ToA}}(\hat{\tau}_{b,\mathrm{ML}})\right\} \\
&= \mathrm{E}_{\mathbf{v},\mathbf{q}}\left\{\frac{1}{a_b^2\mathrm{SNR}(8\pi^2\bar{\beta}^2+\frac{\gamma_b^2}{2\tau_{b,0}^2})}\right\} \\
&= \frac{1}{a_b^2\mathrm{SNR}}\mathrm{E}_{\mathbf{v},\mathbf{q}}\left\{\frac{1}{8\pi^2\bar{\beta}^2+\frac{\gamma_b^2}{2\tau_{b,0}^2}}\right\} \\
&= \frac{1}{a_b^2\mathrm{SNR}}\sum_{k=1}^{4}\frac{1}{8\pi^2\left(\frac{1}{2\pi}\sqrt{\frac{\sum_{n=1}^{N-1}(\omega_0-\frac{v_n q_n \pi}{2T})^2}{N-1}}\right)^2+\frac{\gamma_b^2}{2\tau_{b,0}^2}}p_v(v_n)p_q(q_n) \\
&= \frac{1}{a_b^2\mathrm{SNR}}\sum_{k=1}^{4}\frac{1}{8\pi^2\frac{1}{4\pi^2}\frac{\sum_{n=1}^{N-1}(\omega_0-\frac{v_n q_n \pi}{2T})^2}{N-1}+\frac{\gamma_b^2}{2\tau_{b,0}^2}}p_v(v_n)p_q(q_n).
\end{aligned} \tag{A.5.1}$$

The, the expression A.5.1 can be solved as

$$
\begin{aligned}
\mathrm{ACRB}_{\text{SS-ToA}} = \frac{1}{a_b^2 \mathrm{SNR}} \Bigg(& \frac{1}{4} \frac{1}{\frac{2}{N-1}\sum_{n=1}^{N-1}\left(\omega_0 - \frac{(+1)(+1)\pi}{2T}\right)^2 + \frac{\gamma_b^2}{2\tau_{b,0}^2}} \\
& + \frac{1}{4} \frac{1}{\frac{2}{N-1}\sum_{n=1}^{N-1}\left(\omega_0 - \frac{(+1)(-1)\pi}{2T}\right)^2 + \frac{\gamma_b^2}{2\tau_{b,0}^2}} \\
& + \frac{1}{4} \frac{1}{\frac{2}{N-1}\sum_{n=1}^{N-1}\left(\omega_0 - \frac{(-1)(+1)\pi}{2T}\right)^2 + \frac{\gamma_b^2}{2\tau_{b,0}^2}} \\
& + \frac{1}{4} \frac{1}{\frac{2}{N-1}\sum_{n=1}^{N-1}\left(\omega_0 - \frac{(-1)(-1)\pi}{2T}\right)^2 + \frac{\gamma_b^2}{2\tau_{b,0}^2}} \Bigg) \\
= \frac{1}{a_b^2 \mathrm{SNR}} \Bigg(& \frac{1}{4} \frac{2}{\frac{2}{N-1}\sum_{n=1}^{N-1}\left(\omega_0 - \frac{\pi}{2T}\right)^2 + \frac{\gamma_b^2}{2\tau_{b,0}^2}} \\
& + \frac{1}{4} \frac{2}{\frac{2}{N-1}\sum_{n=1}^{N-1}\left(\omega_0 + \frac{\pi}{2T}\right)^2 + \frac{\gamma_b^2}{2\tau_{b,0}^2}} \Bigg) \\
= \frac{1}{2a_b^2 \mathrm{SNR}} \Bigg(& \frac{1}{\frac{2}{N-1}(N-1)\left(\omega_0 - \frac{\pi}{2T}\right)^2 + \frac{\gamma_b^2}{2\tau_{b,0}^2}} \\
& + \frac{1}{\frac{2}{N-1}(N-1)\left(\omega_0 + \frac{\pi}{2T}\right)^2 + \frac{\gamma_b^2}{2\tau_{b,0}^2}} \Bigg) \\
= \frac{1}{2a_b^2 \mathrm{SNR}} \Bigg(& \frac{1}{2\left(\omega_0 - \frac{\pi}{2T}\right)^2 + \frac{\gamma_b^2}{2\tau_{b,0}^2}} + \frac{1}{2\left(\omega_0 + \frac{\pi}{2T}\right)^2 + \frac{\gamma_b^2}{2\tau_{b,0}^2}} \Bigg).
\end{aligned}
\tag{A.5.2}
$$

A.6 Basic Results for the First and Second Derivatives of the ML Function under the Imperfect PLE

Then, we need to find a form of the derivative $\frac{\partial}{\partial \tau_b} a_b(\tau_b|\gamma)$. The expression of the loss gain is given by

$$a_b(\tau_b|\gamma) = \sqrt{\kappa}\left(\frac{d_0}{c\tau_b}\right)^{\frac{1}{2}\gamma}. \tag{A.6.1}$$

Therefore, we have

$$\frac{\partial}{\partial \tau_b} a_b(\tau_b|\gamma) = -\frac{1}{2\tau_b}\gamma a_b(\tau_b|\gamma). \tag{A.6.2}$$

The first and the second derivatives of $f_{\mathrm{ML}}(\tau_b|\gamma)$ with respect to τ_b can be derived, by using the result given by (A.6.2), as

$$\begin{aligned}
\frac{\partial}{\partial \tau_b} f_{\mathrm{ML}}(\tau_b|\gamma) &= 2a_b(\tau_b|\gamma)E_{\mathrm{s}}\frac{\partial}{\partial \tau_b}a_b(\tau_b|\gamma) - 2\rho(\tau_b)\frac{\partial}{\partial \tau_b}a_b(\tau_b|\gamma) - 2a_b(\tau_b|\gamma)\frac{\partial}{\partial \tau_b}\rho(\tau_b) \\
&= -\frac{1}{\tau_b}\gamma E_{\mathrm{s}} a_b^2(\tau_b|\gamma) + \frac{1}{\tau_b}\gamma a_b(\tau_b|\gamma)\rho(\tau_b) - 2a_b(\tau_b|\gamma)\frac{\partial}{\partial \tau_b}\rho(\tau_b) \\
&= -\frac{1}{\tau_b}\gamma\left(E_{\mathrm{s}} a_b(\tau_b|\gamma) - \rho(\tau_b)\right)a_b(\tau_b|\gamma) - 2a_b(\tau_b|\gamma)\frac{\partial}{\partial \tau_b}\rho(\tau_b),
\end{aligned} \tag{A.6.3}$$

$$
\begin{aligned}
\frac{\partial^2}{\partial\tau_b^2}f_{\mathrm{ML}}(\tau_b|\gamma) &= \frac{1}{\tau_b^2}\gamma E_{\mathrm{s}}a_b^2(\tau_b|\gamma) - \frac{1}{\tau_b}2\gamma E_{\mathrm{s}}a_b(\tau_b|\gamma)\frac{\partial}{\partial\tau_b}a_b(\tau_b|\gamma) - \frac{1}{\tau_b^2}\gamma a_b(\tau_b|\gamma)\rho(\tau_b) \\
&\quad + \frac{1}{\tau_b}\gamma a_b(\tau_b|\gamma)\frac{\partial}{\partial\tau_b}\rho(\tau_b) + \frac{1}{\tau_b}\gamma\rho(\tau_b)\frac{\partial}{\partial\tau_b}a_b(\tau_b|\gamma) - 2\left(\frac{\partial}{\partial\tau_b}a_b(\tau_b|\gamma)\right)\left(\frac{\partial}{\partial\tau_b}\rho(\tau_b)\right) \\
&\quad - 2a_b(\tau_b|\gamma)\frac{\partial^2}{\partial\tau_b^2}\rho(\tau_b) \\
&= \frac{1}{\tau_b^2}\gamma E_{\mathrm{s}}a_b^2(\tau_b|\gamma) - \frac{1}{\tau_b}2\gamma E_{\mathrm{s}}a_b(\tau_b|\gamma)\left(-\frac{1}{2\tau_b}\gamma a_b(\tau_b|\gamma))\right) - \frac{1}{\tau_b^2}\gamma a_b(\tau_b|\gamma)\rho(\tau_b) \\
&\quad + \frac{1}{\tau_b}\gamma a_b(\tau_b|\gamma)\frac{\partial}{\partial\tau_b}\rho(\tau_b) + \rho(\tau_b)\frac{1}{\tau_b}\gamma\left(-\frac{1}{2\tau_b}\gamma a_b(\tau_b|\gamma)\right) \\
&\quad - \left(-\frac{1}{\tau_b}\gamma a_b(\tau_b|\gamma)\right)\frac{\partial}{\partial\tau_b}\rho(\tau_b) - 2a_b(\tau_b|\gamma)\frac{\partial^2}{\partial\tau_b^2}\rho(\tau_b) \\
&= \frac{1}{\tau_b^2}\gamma E_{\mathrm{s}}a_b^2(\tau_b|\gamma) + \frac{\gamma^2}{\tau_b^2}E_{\mathrm{s}}a_b^2(\tau_b|\gamma) - \frac{1}{\tau_b^2}\gamma a_b(\tau_b|\gamma)\rho(\tau_b) \\
&\quad + \frac{1}{\tau_b}\gamma a_b(\tau_b|\gamma)\frac{\partial}{\partial\tau_b}\rho(\tau_b) - \frac{1}{2\tau_b^2}\gamma^2 a_b(\tau_b|\gamma)\rho(\tau_b) + \frac{1}{\tau_b}\gamma a_b(\tau_b|\gamma)\frac{\partial}{\partial\tau_b}\rho(\tau_b) \\
&\quad - 2a_b(\tau_b|\gamma)\frac{\partial^2}{\partial\tau_b^2}\rho(\tau_b) \\
&= \frac{1}{\tau_b^2}\gamma(1+\gamma)E_{\mathrm{s}}a_b^2(\tau_b|\gamma) - \frac{1}{\tau_b^2}\gamma\left(1+\frac{1}{2}\gamma\right)a_b(\tau_b|\gamma)\rho(\tau_b) \\
&\quad + \frac{1}{\tau_b}2\gamma a_b(\tau_b|\gamma)\frac{\partial}{\partial\tau_b}\rho(\tau_b) - 2a_b(\tau_b|\gamma)\frac{\partial^2}{\partial\tau_b^2}\rho(\tau_b).
\end{aligned}
\tag{A.6.4}
$$

In (A.6.3) and (A.6.4), the expression of $\rho(\tau_b)$ is given by

$$
\begin{aligned}
\rho(\tau_b) &= \int_0^{T_{\mathrm{o}}} \Re(r_b(t)s^*(t-\tau_b))\mathrm{d}t \\
&= \int_0^{T_{\mathrm{o}}} \Re((a_b(\tau_{b,0}|\gamma_0)s(t-\tau_{b,0}) + n(t))s^*(t-\tau_b))\mathrm{d}t \\
&= a_b(\tau_{b,0}|\gamma_0)\rho_{\mathrm{ss},b} + \rho_{\mathrm{ns},b},
\end{aligned}
\tag{A.6.5}
$$

where we define

$$
\rho_{\mathrm{ss},b} = \int_0^{T_{\mathrm{o}}} \Re(s(t-\tau_{b,0})s^*(t-\tau_b))\mathrm{d}t, \tag{A.6.6a}
$$

$$
\rho_{\mathrm{ns},b} = \int_0^{T_{\mathrm{o}}} \Re(n(t)s^*(t-\tau_b))\mathrm{d}t. \tag{A.6.6b}
$$

For simplicity, we can rewrite

$$\rho(\tau_b) = a_{b,0}\rho_{\mathrm{ss},b} + \rho_{\mathrm{ns},b}, \tag{A.6.7}$$

where $a_{b,0} = a_b(\tau_{b,0}|\gamma_0)$ is the true value of the loss gain. Moreover, the expression of $\rho(\tau_b)$ for $\tau_b = \tau_{b,0}$ is given by

$$\rho(\tau_{b,0}) = \rho(\tau_b)|_{\tau_b=\tau_{b,0}}\,. \tag{A.6.8}$$

The first derivative of (A.6.7) with respect to τ_b for $\tau_b = \tau_{b,0}$ can be written as

$$\frac{\partial}{\partial\tau_b}\rho(\tau_b)\bigg|_{\tau_b=\tau_{b,0}} = a_{b,0}\,\frac{\partial}{\partial\tau_b}\rho_{\mathrm{ss},b}\bigg|_{\tau_b=\tau_{b,0}} + \frac{\partial}{\partial\tau_b}\rho_{\mathrm{ns},b}\bigg|_{\tau_b=\tau_{b,0}}, \tag{A.6.9}$$

where $\frac{\partial}{\partial\tau_b}\rho_{\mathrm{ss},b}\Big|_{\tau_b=\tau_{b,0}}$ can be shown as

$$\begin{aligned}
\frac{\partial}{\partial\tau_b}\rho_{\mathrm{ss},b}\bigg|_{\tau_b=\tau_{b,0}} &= \int_0^{T_\mathrm{o}} \Re\left(s(t-\tau_{b,0})\frac{\partial}{\partial\tau_b}s^*(t-\tau_b)\right)\mathrm{d}t\bigg|_{\tau_b=\tau_{b,0}} \\
&= -\int_{-\tau_b}^{T_\mathrm{o}-\tau_b} \Re\left(s(t'-(\tau_{b,0}-\tau_b))\frac{\partial}{\partial t'}s^*(t')\right)\mathrm{d}t'\bigg|_{\tau_b=\tau_{b,0}} \\
&= -\frac{1}{2}\,|s(t')|^2\Big|_{t'=-\tau_{b,0}}^{t'=T_\mathrm{o}-\tau_{b,0}} \\
&= 0.
\end{aligned} \tag{A.6.10}$$

Then, (A.6.9) can be written as

$$\frac{\partial}{\partial\tau_b}\rho(\tau_b)\bigg|_{\tau_b=\tau_{b,0}} = \frac{\partial}{\partial\tau_b}\rho_{\mathrm{ns},b}\bigg|_{\tau_b=\tau_{b,0}}. \tag{A.6.11}$$

The second derivative of (A.6.7) with respect to τ_b for $\tau_b = \tau_{b,0}$ is given by

$$\frac{\partial^2}{\partial\tau_b^2}\rho(\tau_b)\bigg|_{\tau_b=\tau_{b,0}} = a_{b,0}\,\frac{\partial^2}{\partial\tau_b^2}\rho_{\mathrm{ss},b}\bigg|_{\tau_b=\tau_{b,0}} + \frac{\partial^2}{\partial\tau_b^2}\rho_{\mathrm{ns},b}\bigg|_{\tau_b=\tau_{b,0}}, \tag{A.6.12}$$

where the first term can be obtained from

$$\begin{aligned}\frac{\partial^2}{\partial\tau_b^2}\rho_{\mathrm{ss},b}\bigg|_{\tau_b=\tau_{b,0}} &= \int_0^{T_\mathrm{o}} \Re\left(s(t-\tau_{b,0})\frac{\partial^2}{\partial\tau_b^2}s^*(t-\tau_b)\right)\mathrm{d}t\bigg|_{\tau_b=\tau_{b,0}} \\ &= -\int_{-\tau_b}^{T_\mathrm{o}-\tau_b} \Re\left(s(t'-(\tau_{b,0}-\tau_b))\frac{\partial^2}{\partial t'^2}s^*(t')\right)\mathrm{d}t'\bigg|_{\tau_b=\tau_{b,0}} \\ &= \Re\left(s(t')\frac{\partial}{\partial t'}s^*(t')\right)\bigg|_{t'=-\tau_{b,0}}^{t'=T_\mathrm{o}-\tau_{b,0}} - \int_{-\infty}^{+\infty}\left|\frac{\partial}{\partial t'}s(t')\right|^2\mathrm{d}t' \\ &= -\int_{-\infty}^{+\infty}\left|\frac{\partial}{\partial t'}s(t')\right|^2\mathrm{d}t'.\end{aligned} \tag{A.6.13}$$

By using the expression of the effective bandwidth in the time domain given by (3.2.3), we have

$$\frac{\partial^2}{\partial\tau_b^2}\rho_{\mathrm{ss},b}\bigg|_{\tau_b=\tau_{b,0}} = -4\pi^2\bar{\beta}^2E_\mathrm{s}. \tag{A.6.14}$$

Therefore, (A.6.12) can be shown as

$$\frac{\partial^2}{\partial\tau_b^2}\rho(\tau_b)\bigg|_{\tau_b=\tau_{b,0}} = -4\pi^2\bar{\beta}^2E_\mathrm{s}a_{b,0} + \ddot{\rho}_{\mathrm{ns},0}, \tag{A.6.15}$$

where $\ddot{\rho}_{\mathrm{ns},0} = \frac{\partial^2}{\partial\tau_b^2}\rho_{\mathrm{ns},b}\Big|_{\tau_b=\tau_{b,0}}$ and therefore $\mathrm{E}_{n_b(t)}\left\{\ddot{\rho}_{\mathrm{ns},0}\right\} = 0$. Substituting (A.6.11) and (A.6.15) into (A.6.4) for $\tau_b = \tau_{b,0}$, we obtain

$$\begin{aligned}\frac{\partial^2}{\partial\tau_b^2}f_{\mathrm{ML}}(\tau_b|\gamma)\bigg|_{\tau_b=\tau_{b,0}} &= \frac{1}{\tau_{b,0}^2}\gamma(1+\gamma)E_\mathrm{s}\tilde{a}_{b,0}^2 - \frac{1}{\tau_{b,0}^2}\gamma\left(1+\frac{1}{2}\gamma\right)\tilde{a}_{b,0}\rho(\tau_{b,0}) \\ &\quad + \frac{1}{\tau_{b,0}}2\gamma\tilde{a}_{b,0}\dot{\rho}_{\mathrm{ns},0} - 2\tilde{a}_{b,0}\left(-4\pi^2\bar{\beta}^2E_\mathrm{s}a_{b,0} + \ddot{\rho}_{\mathrm{ns},0}\right).\end{aligned} \tag{A.6.16}$$

Therefore, the expected value of (A.6.16) with respect to the noise for $\tau_b = \tau_{b,0}$ is given by

$$\begin{aligned}\mathrm{E}_{n_b(t)}\left\{\frac{\partial^2}{\partial\tau_b\partial\tau_b}f_{\mathrm{ML}}(\tau_b|\gamma)\bigg|_{\tau_b=\tau_{b,0}}\right\} &= \frac{1}{\tau_{b,0}^2}\gamma(1+\gamma)E_\mathrm{s}\tilde{a}_{b,0}^2 - \frac{1}{\tau_{b,0}^2}\gamma\left(1+\frac{1}{2}\gamma\right)E_\mathrm{s}\tilde{a}_{b,0}a_{b,0} \\ &\quad + 8\pi^2\bar{\beta}^2E_\mathrm{s}\tilde{a}_{b,0}a_{b,0}.\end{aligned} \tag{A.6.17}$$

The derivative of the loss gain with respect to γ is given by

$$\frac{\partial}{\partial\gamma}a_b(\tau_b|\gamma) = \frac{1}{2}\ln\left(\frac{d_0}{c\tau_b}\right)a_b(\tau_b|\gamma). \tag{A.6.18}$$

Then, we can derive

$$\begin{aligned}
\frac{\partial^2}{\partial\gamma\partial\tau_b}f_{\mathrm{ML}}(\tau_b|\gamma) &= -\frac{1}{\tau_b}E_{\mathrm{s}}a_b^2(\tau_b|\gamma) - \frac{1}{\tau_b}2\gamma E_{\mathrm{s}}a_b(\tau_b|\gamma)\frac{\partial}{\partial\gamma}a_b(\tau_b|\gamma) + \frac{1}{\tau_b}a_b(\tau_b|\gamma)\rho(\tau_b) \\
&\quad + \frac{1}{\tau_b}\gamma\rho(\tau_b)\frac{\partial}{\partial\gamma}a_b(\tau_b|\gamma) - 2\left(\frac{\partial}{\partial\gamma}a_b(\tau_b|\gamma)\right)\left(\frac{\partial}{\partial\tau_b}\rho(\tau_b)\right) \\
&= -\frac{1}{\tau_b}E_{\mathrm{s}}a_b^2(\tau_b|\gamma) - \frac{1}{\tau_b}\gamma 2E_{\mathrm{s}}a_b(\tau_b|\gamma)\left(\frac{1}{2}\ln\left(\frac{d_0}{c\tau_b}\right)a_b(\tau_b|\gamma)\right) \\
&\quad + \frac{1}{\tau_b}a_b(\tau_b|\gamma)\rho(\tau_b) + \frac{1}{\tau_b}\gamma\rho(\tau_b)\left(\frac{1}{2}\ln\left(\frac{d_0}{c\tau_b}\right)a_b(\tau_b|\gamma)\right) \\
&\quad - 2\left(\frac{1}{2}\ln\left(\frac{d_0}{c\tau_b}\right)a_b(\tau_b|\gamma)\right)\frac{\partial}{\partial\tau_b}\rho(\tau_b) \\
&= -\frac{1}{\tau_b}E_{\mathrm{s}}a_b^2(\tau_b|\gamma) - \frac{1}{\tau_b}\gamma\ln\left(\frac{d_0}{c\tau_b}\right)E_{\mathrm{s}}a_b^2(\tau_b|\gamma) \\
&\quad + \frac{1}{\tau_b}a_b(\tau_b|\gamma)\rho(\tau_b) + \frac{1}{2\tau_b}\gamma\ln\left(\frac{d_0}{c\tau_b}\right)a_b(\tau_b|\gamma)\rho(\tau_b) \\
&\quad - \ln\left(\frac{d_0}{c\tau_b}\right)a_b(\tau_b|\gamma)\frac{\partial}{\partial\tau_b}\rho(\tau_b) \\
&= \frac{1}{\tau_b}a_b(\tau_b|\gamma)\left(\rho(\tau_b) - E_{\mathrm{s}}a_b(\tau_b|\gamma)\right) \\
&\quad + \frac{1}{\tau_b}\gamma\ln\left(\frac{d_0}{c\tau_b}\right)a_b(\tau_b|\gamma)\left(\frac{1}{2}\rho(\tau_b) - E_{\mathrm{s}}a_b(\tau_b|\gamma)\right) \\
&\quad - \ln\left(\frac{d_0}{c\tau_b}\right)a_b(\tau_b|\gamma)\frac{\partial}{\partial\tau_b}\rho(\tau_b).
\end{aligned} \tag{A.6.19}$$

Then, the result of $\frac{\partial^2}{\partial\gamma\partial\tau_b} f_{\mathrm{ML}}(\tau_b|\gamma)$ for $\tau_b = \tau_{b,0}$ is given by

$$\begin{aligned}\frac{\partial^2}{\partial\gamma\partial\tau_b} f_{\mathrm{ML}}(\tau_b|\gamma)\bigg|_{\tau_b=\tau_{b,0}} &= \frac{1}{\tau_{b,0}}\tilde{a}_{b,0}(\rho(\tau_{b,0}) - E_{\mathrm{s}}\tilde{a}_{b,0}) \\ &\quad - \frac{1}{\tau_{b,0}}\gamma \ln\left(\frac{d_0}{c\tau_{b,0}}\right)\tilde{a}_{b,0}\left(E_{\mathrm{s}}\tilde{a}_{b,0} - \frac{1}{2}\rho(\tau_{b,0})\right) \\ &\quad - \ln\left(\frac{d_0}{c\tau_{b,0}}\right)\tilde{a}_{b,0}\dot{\rho}_{\mathrm{ns},0} \\ &= \frac{1}{\tau_{b,0}}\tilde{a}_{b,0}(a_{b,0}E_{\mathrm{s}} + \rho_{\mathrm{ns},0} - E_{\mathrm{s}}\tilde{a}_{b,0}) \\ &\quad - \frac{1}{\tau_{b,0}}\gamma \ln\left(\frac{d_0}{c\tau_{b,0}}\right)\tilde{a}_{b,0}\left(E_{\mathrm{s}}\tilde{a}_{b,0} - \frac{1}{2}a_{b,0}E_{\mathrm{s}} - \frac{1}{2}\rho_{\mathrm{ns},0}\right) \\ &\quad - \ln\left(\frac{d_0}{c\tau_{b,0}}\right)\tilde{a}_{b,0}\dot{\rho}_{\mathrm{ns},0}.\end{aligned} \tag{A.6.20}$$

A.7 Proof of Proposition 5.2.2

The bias can be written as

$$\begin{aligned}\mathrm{E}_{n_b(t)}\left\{\hat{\tau}_{b,\mathrm{ML}}(\gamma) - \tau_{b,0}\right\} &= -\frac{\mathrm{E}_{n_b(t)}\left\{\frac{\partial^2}{\partial\gamma\partial\tau_b} f_{\mathrm{ML}}(\tau_b|\gamma)\Big|_{\tau_b=\tau_{b,0}}(\gamma-\gamma_0)\right\}}{\mathrm{E}_{n_b(t)}\left\{\frac{\partial^2}{\partial\tau_b\partial\tau_b} f_{\mathrm{ML}}(\tau_b|\gamma)\Big|_{\tau_b=\tau_{b,0}}\right\}} \\ &= -\frac{(\gamma-\gamma_0)\mathrm{E}_{n_b(t)}\left\{\frac{\partial^2}{\partial\gamma\partial\tau_b} f_{\mathrm{ML}}(\tau_b|\gamma)\Big|_{\tau_b=\tau_{b,0}}\right\}}{\mathrm{E}_{n_b(t)}\left\{\frac{\partial^2}{\partial\tau_b\partial\tau_b} f_{\mathrm{ML}}(\tau_b|\gamma)\Big|_{\tau_b=\tau_{b,0}}\right\}}.\end{aligned} \tag{A.7.1}$$

Then, we need the expression of $\mathrm{E}_{n_b(t)}\left\{ \frac{\partial^2}{\partial\gamma\partial\tau_b} f_{\mathrm{ML}}(\tau_b|\gamma)\Big|_{\tau_b=\tau_{b,0}} \right\}$, which can be written as

$$\begin{aligned}\mathrm{E}_{n_b(t)}\left\{ \frac{\partial^2}{\partial\gamma\partial\tau_b} f_{\mathrm{ML}}(\tau_b|\gamma)\Big|_{\tau_b=\tau_{b,0}} \right\} &= \frac{1}{\tau_{b,0}}\tilde{a}_{b,0}(E_{\mathrm{s}}a_{b,0} - E_{\mathrm{s}}\tilde{a}_{b,0}) \\ &\quad - \frac{1}{\tau_{b,0}}\gamma \ln\left(\frac{d_0}{c\tau_{b,0}}\right)\tilde{a}_{b,0}\left(E_{\mathrm{s}}\tilde{a}_{b,0} - \frac{1}{2}E_{\mathrm{s}}a_{b,0}\right) \\ &= \frac{1}{\tau_{b,0}}E_{\mathrm{s}}\tilde{a}_{b,0}(a_{b,0} - \tilde{a}_{b,0}) \\ &\quad - \frac{1}{\tau_{b,0}}\gamma \ln\left(\frac{d_0}{c\tau_{b,0}}\right)E_{\mathrm{s}}\tilde{a}_{b,0}\left(\tilde{a}_{b,0} - \frac{1}{2}a_{b,0}\right).\end{aligned} \tag{A.7.2}$$

Substituting (A.7.2) into (A.7.1), we obtain the final expression of the bias from

$$\begin{aligned}&\mathrm{E}_{n_b(t)}\left\{\hat{\tau}_{b,\mathrm{ML}}(\gamma) - \tau_{b,0}\right\} \\ &= -\frac{\frac{1}{\tau_{b,0}}(\gamma-\gamma_0)E_{\mathrm{s}}\tilde{a}_{b,0}(a_{b,0}-\tilde{a}_{b,0}) - \frac{1}{\tau_{b,0}}\gamma(\gamma-\gamma_0)\ln\left(\frac{d_0}{c\tau_{b,0}}\right)E_{\mathrm{s}}\tilde{a}_{b,0}\left(\tilde{a}_{b,0}-\frac{1}{2}a_{b,0}\right)}{\frac{1}{\tau_{b,0}^2}\gamma(1+\gamma)E_{\mathrm{s}}\tilde{a}_{b,0}^2 - \frac{1}{\tau_{b,0}^2}\gamma\left(1+\frac{1}{2}\gamma\right)E_{\mathrm{s}}\tilde{a}_{b,0}a_{b,0} + 8\pi^2\bar{\beta}^2E_{\mathrm{s}}\tilde{a}_{b,0}a_{b,0}} \\ &= -\frac{\frac{1}{\tau_{b,0}}(\gamma-\gamma_0)E_{\mathrm{s}}(a_{b,0}-\tilde{a}_{b,0}) - \frac{1}{\tau_{b,0}}\gamma(\gamma-\gamma_0)\ln\left(\frac{d_0}{c\tau_{b,0}}\right)E_{\mathrm{s}}\left(\tilde{a}_{b,0}-\frac{1}{2}a_{b,0}\right)}{\frac{1}{\tau_{b,0}^2}\gamma(1+\gamma)E_{\mathrm{s}}\tilde{a}_{b,0} - \frac{1}{\tau_{b,0}^2}\gamma\left(1+\frac{1}{2}\gamma\right)E_{\mathrm{s}}a_{b,0} + 8\pi^2\bar{\beta}^2E_{\mathrm{s}}a_{b,0}} \\ &= -\frac{(\gamma-\gamma_0)(a_{b,0}-\tilde{a}_{b,0}) - \gamma(\gamma-\gamma_0)\ln\left(\frac{d_0}{c\tau_{b,0}}\right)\left(\tilde{a}_{b,0}-\frac{1}{2}a_{b,0}\right)}{\gamma(1+\gamma)\tilde{a}_{b,0} - \gamma\left(1+\frac{1}{2}\gamma\right)a_{b,0} + 8\pi^2\bar{\beta}^2\tau_{b,0}^2a_{b,0}}\tau_{b,0} \\ &= -\frac{(\gamma-\gamma_0)(a_{b,0}-\tilde{a}_{b,0}) - \gamma(\gamma-\gamma_0)\ln\left(\frac{d_0}{c\tau_{b,0}}\right)\left(\tilde{a}_{b,0}-\frac{1}{2}a_{b,0}\right)}{8\pi^2\bar{\beta}^2\tau_{b,0}^2a_{b,0} - \left(\gamma(a_{b,0}-\tilde{a}_{b,0}) + \gamma^2\left(\frac{1}{2}a_{b,0}-\tilde{a}_{b,0}\right)\right)}\tau_{b,0}.\end{aligned} \tag{A.7.3}$$

A.8 Proof of Proposition 5.2.3

The error variance can be written as

$$
\begin{aligned}
&\mathrm{E}_{n_b(t)}\left\{(\hat{\tau}_{b,\mathrm{ML}}(\gamma)-\tau_{b,0})^2\right\}\\
&=\mathrm{E}_{n_b(t)}\Bigg\{\frac{(\gamma-\gamma_0)^2}{\left(\frac{1}{\tau_{b,0}^2}\gamma(1+\gamma)E_{\mathrm{s}}\tilde{a}_{b,0}-\frac{1}{\tau_{b,0}^2}\gamma\left(1+\frac{1}{2}\gamma\right)E_{\mathrm{s}}a_{b,0}+8\pi^2\bar{\beta}^2E_{\mathrm{s}}a_{b,0}\right)^2}\\
&\quad\left(\frac{1}{\tau_{b,0}}(a_{b,0}E_{\mathrm{s}}+\rho_{\mathrm{ns},0}-E_{\mathrm{s}}\tilde{a}_{b,0})\right.\\
&\quad\left.-\frac{1}{\tau_{b,0}}\gamma\ln\left(\frac{d_0}{c\tau_{b,0}}\right)\left(E_{\mathrm{s}}\tilde{a}_{b,0}-\frac{1}{2}a_{b,0}E_{\mathrm{s}}-\frac{1}{2}\rho_{\mathrm{ns},0}\right)-\ln\left(\frac{d_0}{c\tau_{b,0}}\right)\dot{\rho}_{\mathrm{ns},0}\right)^2\Bigg\}\\
&=\frac{(\gamma-\gamma_0)^2}{\left(\frac{1}{\tau_{b,0}^2}\gamma(1+\gamma)E_{\mathrm{s}}\tilde{a}_{b,0}-\frac{1}{\tau_{b,0}^2}\gamma\left(1+\frac{1}{2}\gamma\right)E_{\mathrm{s}}a_{b,0}+8\pi^2\bar{\beta}^2E_{\mathrm{s}}a_{b,0}\right)^2}\\
&\quad\mathrm{E}_{n_b(t)}\Bigg\{\left(\frac{1}{\tau_{b,0}}(a_{b,0}E_{\mathrm{s}}+\rho_{\mathrm{ns},0}-E_{\mathrm{s}}\tilde{a}_{b,0})\right.\\
&\quad\left.-\frac{1}{\tau_{b,0}}\gamma\ln\left(\frac{d_0}{c\tau_{b,0}}\right)\left(E_{\mathrm{s}}\tilde{a}_{b,0}-\frac{1}{2}a_{b,0}E_{\mathrm{s}}-\frac{1}{2}\rho_{\mathrm{ns},0}\right)-\ln\left(\frac{d_0}{c\tau_{b,0}}\right)\dot{\rho}_{\mathrm{ns},0}\right)^2\Bigg\}\\
&=\frac{(\gamma-\gamma_0)^2}{\left(\frac{1}{\tau_{b,0}^2}\gamma(1+\gamma)E_{\mathrm{s}}\tilde{a}_{b,0}-\frac{1}{\tau_{b,0}^2}\gamma\left(1+\frac{1}{2}\gamma\right)E_{\mathrm{s}}a_{b,0}+8\pi^2\bar{\beta}^2E_{\mathrm{s}}a_{b,0}\right)^2}\\
&\quad\mathrm{E}_{n_b(t)}\Bigg\{\left(\frac{1}{\tau_{b,0}}(a_{b,0}E_{\mathrm{s}}-E_{\mathrm{s}}\tilde{a}_{b,0})-\frac{1}{\tau_{b,0}}\gamma\ln\left(\frac{d_0}{c\tau_{b,0}}\right)\left(E_{\mathrm{s}}\tilde{a}_{b,0}-\frac{1}{2}a_{b,0}E_{\mathrm{s}}\right)\right.\\
&\quad\left.+\left(\frac{1}{\tau_{b,0}}+\frac{1}{2\tau_{b,0}}\gamma\ln\left(\frac{d_0}{c\tau_{b,0}}\right)\right)\rho_{\mathrm{ns},0}-\ln\left(\frac{d_0}{c\tau_{b,0}}\right)\dot{\rho}_{\mathrm{ns},0}\right)^2\Bigg\}\\
&=\frac{(\gamma-\gamma_0)^2\mathrm{E}_{n_b(t)}\left\{(k_1+k_2\rho_{\mathrm{ns},0}-k_3\dot{\rho}_{\mathrm{ns},0})^2\right\}}{\left(\frac{1}{\tau_{b,0}^2}\gamma(1+\gamma)E_{\mathrm{s}}\tilde{a}_{b,0}-\frac{1}{\tau_{b,0}^2}\gamma\left(1+\frac{1}{2}\gamma\right)E_{\mathrm{s}}a_{b,0}+8\pi^2\bar{\beta}^2E_{\mathrm{s}}a_{b,0}\right)^2},
\end{aligned}
\tag{A.8.1}
$$

where we have

$$
\begin{aligned}
k_1&=\frac{1}{\tau_{b,0}}(a_{b,0}E_{\mathrm{s}}-E_{\mathrm{s}}\tilde{a}_{b,0})-\frac{1}{\tau_{b,0}}\gamma\ln\left(\frac{d_0}{c\tau_{b,0}}\right)\left(E_{\mathrm{s}}\tilde{a}_{b,0}-\frac{1}{2}a_{b,0}E_{\mathrm{s}}\right)\\
&=\frac{1}{\tau_{b,0}}E_{\mathrm{s}}a_{b,0}\left(1-\frac{\tilde{a}_{b,0}}{a_{b,0}}+\gamma\ln\left(\frac{d_0}{c\tau_{b,0}}\right)\left(\frac{1}{2}-\frac{\tilde{a}_{b,0}}{a_{b,0}}\right)\right),
\end{aligned}
\tag{A.8.2}
$$

$$k_2 = \frac{1}{\tau_{b,0}} + \frac{1}{2\tau_{b,0}}\gamma \ln\left(\frac{d_0}{c\tau_{b,0}}\right), \tag{A.8.3}$$

$$k_3 = \ln\left(\frac{d_0}{c\tau_{b,0}}\right). \tag{A.8.4}$$

The expression $\mathrm{E}_{n_b(t)}\left\{\left(k_1 + k_2\rho_{\mathrm{ns},0} - k_3\dot{\rho}_{\mathrm{ns},0}\right)^2\right\}$ can be solved as

$$\begin{aligned}
&\mathrm{E}_{n_b(t)}\left\{\left(k_1 + k_2\rho_{\mathrm{ns},0} - k_3\dot{\rho}_{\mathrm{ns},0}\right)^2\right\} \\
&= \mathrm{E}_{n_b(t)}\left\{k_1^2 + k_2^2\rho_{\mathrm{ns},0}^2 + k_3^2\dot{\rho}_{\mathrm{ns},0}^2 + 2k_1k_2\rho_{\mathrm{ns},0} - 2k_1k_3\dot{\rho}_{\mathrm{ns},0} - 2k_2k_3\rho_{\mathrm{ns},0}\dot{\rho}_{\mathrm{ns},0}\right\} \\
&= \mathrm{E}_{n_b(t)}\left\{k_1^2 + k_2^2\rho_{\mathrm{ns},0}^2 + k_3^2\dot{\rho}_{\mathrm{ns},0}^2 - 2k_1k_3\dot{\rho}_{\mathrm{ns},0} - 2k_2k_3\rho_{\mathrm{ns},0}\dot{\rho}_{\mathrm{ns},0}\right\}.
\end{aligned} \tag{A.8.5}$$

We have to consider the results

$$\mathrm{E}_{n_b(t)}\left\{\dot{\rho}_{\mathrm{ns},0}\right\} = 0, \tag{A.8.6a}$$

$$\mathrm{E}_{n_b(t)}\left\{\rho_{\mathrm{ns},0}^2\right\} = \frac{1}{2}E_{\mathrm{s}}\sigma_{\mathrm{n}}^2, \tag{A.8.6b}$$

$$\mathrm{E}_{n_b(t)}\left\{\dot{\rho}_{\mathrm{ns},0}^2\right\} = 2\pi^2 E_{\mathrm{s}}\bar{\beta}^2\sigma_{\mathrm{n}}^2, \tag{A.8.6c}$$

$$\mathrm{E}_{n_b(t)}\left\{\rho_{\mathrm{ns},0}\dot{\rho}_{\mathrm{ns},0}\right\} = 0. \tag{A.8.6d}$$

Substituting (A.8.6a), (A.8.6b), (A.8.6c) and (A.8.6d) into (A.8.5), we have

$$\mathrm{E}_{n_b(t)}\left\{\left(k_1 + k_2\rho_{\mathrm{ns},0} - k_3\dot{\rho}_{\mathrm{ns},0}\right)^2\right\} = k_1^2 + \frac{1}{2}E_{\mathrm{s}}\sigma_{\mathrm{n}}^2k_2^2 + 2\pi^2E_{\mathrm{s}}\bar{\beta}^2\sigma_{\mathrm{n}}^2k_3^2. \tag{A.8.7}$$

Therefore, we obtain

$$\begin{aligned}
\mathrm{E}_{n_b(t)}\left\{\left(\hat{\tau}_{b,\mathrm{ML}}(\gamma)-\tau_{b,0}\right)^2\right\} &= \frac{(\gamma-\gamma_0)^2}{\left(\frac{1}{\tau_{b,0}^2}\gamma(1+\gamma)E_{\mathrm{s}}\tilde{a}_{b,0}-\frac{1}{\tau_{b,0}^2}\gamma\left(1+\frac{1}{2}\gamma\right)E_{\mathrm{s}}a_{b,0}+8\pi^2\bar{\beta}^2E_{\mathrm{s}}a_{b,0}\right)^2} \\
&\quad \left(\frac{1}{\tau_{b,0}^2}E_{\mathrm{s}}^2a_{b,0}^2\left(1-\frac{\tilde{a}_{b,0}}{a_{b,0}}+\gamma\ln\left(\frac{d_0}{c\tau_{b,0}}\right)\left(\frac{1}{2}-\frac{\tilde{a}_{b,0}}{a_{b,0}}\right)\right)^2\right. \\
&\quad \left.+\frac{1}{2\tau_{b,0}^2}E_{\mathrm{s}}\sigma_{\mathrm{n}}^2\left(1+\frac{1}{2}\gamma\ln\left(\frac{d_0}{c\tau_{b,0}}\right)\right)^2+2\pi^2E_{\mathrm{s}}\bar{\beta}^2\sigma_{\mathrm{n}}^2\ln^2\left(\frac{d_0}{c\tau_{b,0}}\right)\right) \\
&= \frac{\tau_{b,0}^2(\gamma-\gamma_0)^2}{\left(\frac{\tilde{a}_{b,0}}{a_{b,0}}\gamma(1+\gamma)-\gamma\left(1+\frac{1}{2}\gamma\right)+8\pi^2\bar{\beta}^2\tau_{b,0}^2\right)^2} \\
&\quad \left(\left(1-\frac{\tilde{a}_{b,0}}{a_{b,0}}+\gamma\ln\left(\frac{d_0}{c\tau_{b,0}}\right)\left(\frac{1}{2}-\frac{\tilde{a}_{b,0}}{a_{b,0}}\right)\right)^2\right. \\
&\quad \left.+\frac{1}{2}\frac{1}{a_{b,0}^2}\frac{\sigma_{\mathrm{n}}^2}{E_{\mathrm{s}}}\left(1+\frac{1}{2}\gamma\ln\left(\frac{d_0}{c\tau_{b,0}}\right)\right)^2+\frac{1}{a_{b,0}^2}\frac{\sigma_{\mathrm{n}}^2}{E_{\mathrm{s}}}2\pi^2\bar{\beta}^2\tau_{b,0}^2\ln^2\left(\frac{d_0}{c\tau_{b,0}}\right)\right).
\end{aligned} \tag{A.8.8}$$

A.9 Proof of Proposition 5.3.1

In order to obtain the expression of the error between the estimated and the true values of the ToA for the analysis method derived from the Taylor expansion, we should additionally calculate the first derivative of $f_{\mathrm{ML}}(\tau_b|\gamma)$ for $\tau_b=\tau_{b,0}$, i.e.,

$$\left.\frac{\partial}{\partial\tau_b}f_{\mathrm{ML}}(\tau_b|\gamma)\right|_{\tau_b=\tau_{b,0}} = -\frac{1}{\tau_{b,0}}\gamma\left(E_{\mathrm{s}}\tilde{a}_{b,0}-E_{\mathrm{s}}a_{b,0}-\rho_{\mathrm{ns},0}\right)\tilde{a}_{b,0}-2\tilde{a}_{b,0}\dot{\rho}_{\mathrm{ns},0}. \tag{A.9.1}$$

Substituting (A.9.1), (A.6.17) and (A.7.2) into (5.3.4), we obtain the final value of the error between the estimated and the true values of the ToA from

$$
\begin{aligned}
&\hat{\tau}_{b,\mathrm{ML}}(\gamma) - \tau_{b,0} \\
&= -\left(\frac{1}{\frac{1}{\tau_{b,0}^2}\gamma(1+\gamma)E_{\mathrm{s}}\tilde{a}_{b,0}^2 - \frac{1}{\tau_{b,0}^2}\gamma\left(1+\frac{1}{2}\gamma\right)E_{\mathrm{s}}\tilde{a}_{b,0}a_{b,0} + 8\pi^2\bar{\beta}^2 E_{\mathrm{s}}\tilde{a}_{b,0}a_{b,0}} \right) \\
&\quad \left(-\frac{1}{\tau_{b,0}}\gamma\left(E_{\mathrm{s}}\tilde{a}_{b,0} - E_{\mathrm{s}}a_{b,0} - \rho_{\mathrm{ns},0}\right)\tilde{a}_{b,0} - 2\tilde{a}_{b,0}\dot{\rho}_{\mathrm{ns},0} \right. \\
&\quad \left. + \frac{1}{\tau_{b,0}}(\gamma-\gamma_0)E_{\mathrm{s}}\tilde{a}_{b,0}(a_{b,0}-\tilde{a}_{b,0}) - \frac{1}{\tau_{b,0}}\gamma(\gamma-\gamma_0)\ln\left(\frac{d_0}{c\tau_{b,0}}\right)E_{\mathrm{s}}\tilde{a}_{b,0}\left(\tilde{a}_{b,0} - \frac{1}{2}a_{b,0}\right) \right) \\
&= -\left(\frac{1}{\frac{1}{\tau_{b,0}^2}\gamma(1+\gamma)E_{\mathrm{s}}\tilde{a}_{b,0} - \frac{1}{\tau_{b,0}^2}\gamma\left(1+\frac{1}{2}\gamma\right)E_{\mathrm{s}}a_{b,0} + 8\pi^2\bar{\beta}^2 E_{\mathrm{s}}a_{b,0}} \right) \\
&\quad \left(-\frac{1}{\tau_{b,0}}\gamma\left(E_{\mathrm{s}}\tilde{a}_{b,0} - E_{\mathrm{s}}a_{b,0} - \rho_{\mathrm{ns},0}\right) - 2\dot{\rho}_{\mathrm{ns},0} \right. \\
&\quad \left. + \frac{1}{\tau_{b,0}}(\gamma-\gamma_0)E_{\mathrm{s}}(a_{b,0}-\tilde{a}_{b,0}) - \frac{1}{\tau_{b,0}}\gamma(\gamma-\gamma_0)\ln\left(\frac{d_0}{c\tau_{b,0}}\right)E_{\mathrm{s}}\left(\tilde{a}_{b,0} - \frac{1}{2}a_{b,0}\right) \right).
\end{aligned}
\tag{A.9.2}
$$

A.10 Proof of Proposition 5.3.2

The bias can be written as

$$
\begin{aligned}
&\mathrm{E}_{n_b(t)}\left\{\hat{\tau}_{b,\mathrm{ML}}(\gamma)-\tau_{b,0}\right\}\\
&=-\frac{1}{\frac{1}{\tau_{b,0}^2}\gamma(1+\gamma)E_{\mathrm{s}}\tilde{a}_{b,0}-\frac{1}{\tau_{b,0}^2}\gamma\left(1+\frac{1}{2}\gamma\right)E_{\mathrm{s}}a_{b,0}+8\pi^2\bar{\beta}^2E_{\mathrm{s}}a_{b,0}}\\
&\quad\left(-\frac{1}{\tau_{b,0}}\gamma E_{\mathrm{s}}\left(\tilde{a}_{b,0}-a_{b,0}\right)+\frac{1}{\tau_b}(\gamma-\gamma_0)E_{\mathrm{s}}(a_{b,0}-\tilde{a}_{b,0})\right.\\
&\quad\left.-\frac{1}{\tau_{b,0}}\gamma(\gamma-\gamma_0)\ln\left(\frac{d_0}{c\tau_{b,0}}\right)E_{\mathrm{s}}\left(\tilde{a}_{b,0}-\frac{1}{2}a_{b,0}\right)\right) \qquad \text{(A.10.1)}\\
&=-\frac{\gamma\left(a_{b,0}-\tilde{a}_{b,0}\right)+(\gamma-\gamma_0)\left(a_{b,0}-\tilde{a}_{b,0}+\gamma\ln\left(\frac{d_0}{c\tau_{b,0}}\right)\left(\frac{1}{2}a_{b,0}-\tilde{a}_{b,0}\right)\right)}{\gamma(1+\gamma)\tilde{a}_{b,0}-\gamma\left(1+\frac{1}{2}\gamma\right)a_{b,0}+8\pi^2\bar{\beta}^2\tau_{b,0}^2a_{b,0}}\tau_{b,0}\\
&=-\frac{(2\gamma-\gamma_0)\left(a_{b,0}-\tilde{a}_{b,0}\right)+\gamma(\gamma-\gamma_0)\ln\left(\frac{d_0}{c\tau_{b,0}}\right)\left(\frac{1}{2}a_{b,0}-\tilde{a}_{b,0}\right)}{8\pi^2\bar{\beta}^2\tau_{b,0}^2a_{b,0}-\left(\gamma(a_{b,0}-\tilde{a}_{b,0})+\gamma^2\left(\frac{1}{2}a_{b,0}-\tilde{a}_{b,0}\right)\right)}\tau_{b,0}.
\end{aligned}
$$

A.11 Proof of Proposition 5.3.3

Then, we can obtain the error variance by taking the expectation of the square of (5.3.10) from

$$
\begin{aligned}
&\mathrm{E}_{n_b(t)}\left\{(\hat{\tau}_{b,\mathrm{ML}}(\gamma)-\tau_{b,0})^2\right\} \\
&= \mathrm{E}_{n_b(t)}\Bigg\{ \left(\frac{1}{\tau_{b,0}^2}\gamma(1+\gamma)E_{\mathrm{s}}\tilde{a}_{b,0}-\frac{1}{\tau_{b,0}^2}\gamma\left(1+\frac{1}{2}\gamma\right)E_{\mathrm{s}}a_{b,0}+8\pi^2\bar{\beta}^2E_{\mathrm{s}}a_{b,0}\right)^{-2} \\
&\quad \left(-\frac{1}{\tau_{b,0}}\gamma\left(E_{\mathrm{s}}\tilde{a}_{b,0}-E_{\mathrm{s}}a_{b,0}-\rho_{\mathrm{ns},0}\right)-2\dot{\rho}_{\mathrm{ns},0}+\frac{1}{\tau_{b,0}}(\gamma-\gamma_0)(E_{\mathrm{s}}a_{b,0}+\rho_{\mathrm{ns},0}-E_{\mathrm{s}}\tilde{a}_{b,0})\right. \\
&\quad \left.-\frac{1}{\tau_{b,0}}\gamma(\gamma-\gamma_0)\ln\left(\frac{d_0}{c\tau_{b,0}}\right)\left(E_{\mathrm{s}}\tilde{a}_{b,0}-\frac{1}{2}E_{\mathrm{s}}a_{b,0}-\frac{1}{2}\rho_{\mathrm{ns},0}\right)-(\gamma-\gamma_0)\ln\left(\frac{d_0}{c\tau_{b,0}}\right)\dot{\rho}_{\mathrm{ns},0}\right)^2\Bigg\} \\
&= \mathrm{E}_{n_b(t)}\Bigg\{ \left(\frac{1}{\tau_{b,0}^2}\gamma(1+\gamma)E_{\mathrm{s}}\tilde{a}_{b,0}-\frac{1}{\tau_{b,0}^2}\gamma\left(1+\frac{1}{2}\gamma\right)E_{\mathrm{s}}a_{b,0}+8\pi^2\bar{\beta}^2E_{\mathrm{s}}a_{b,0}\right)^{-2} \\
&\quad \left(\frac{1}{\tau_{b,0}}\gamma E_{\mathrm{s}}\left(a_{b,0}-\tilde{a}_{b,0}\right)+\frac{1}{\tau_{b,0}}(\gamma-\gamma_0)E_{\mathrm{s}}(a_{b,0}-\tilde{a}_{b,0})\right. \\
&\quad +\frac{1}{\tau_{b,0}}\gamma(\gamma-\gamma_0)\ln\left(\frac{d_0}{c\tau_{b,0}}\right)E_{\mathrm{s}}\left(\frac{1}{2}a_{b,0}-\tilde{a}_{b,0}\right) \\
&\quad +\left(\frac{1}{\tau_{b,0}}\gamma+\frac{1}{\tau_{b,0}}(\gamma-\gamma_0)+\frac{1}{2}\frac{1}{\tau_{b,0}}\gamma(\gamma-\gamma_0)\ln\left(\frac{d_0}{c\tau_{b,0}}\right)\right)\rho_{\mathrm{ns},0} \\
&\quad \left.-\left(2+(\gamma-\gamma_0)\ln\left(\frac{d_0}{c\tau_{b,0}}\right)\right)\dot{\rho}_{\mathrm{ns},0}\right)^2\Bigg\} \\
&= \frac{\mathrm{E}_{n_b(t)}\left\{\left(k_4+k_5\rho_{\mathrm{ns},0}-k_6\dot{\rho}_{\mathrm{ns},0}\right)^2\right\}}{\frac{1}{\tau_{b,0}^4}E_{\mathrm{s}}^2a_{b,0}^2\left(\frac{\tilde{a}_{b,0}}{a_{b,0}}\gamma(1+\gamma)-\gamma\left(1+\frac{1}{2}\gamma\right)+8\pi^2\bar{\beta}^2\tau_{b,0}^2\right)^2},
\end{aligned}
\tag{A.11.1}
$$

where k_4, k_5 and k_6 are given by

$$\begin{aligned} k_4 &= \frac{1}{\tau_{b,0}}\gamma E_{\mathrm{s}}\left(a_{b,0}-\tilde{a}_{b,0}\right)+\frac{1}{\tau_{b,0}}(\gamma-\gamma_0)E_{\mathrm{s}}(a_{b,0}-\tilde{a}_{b,0}) \\ &\quad+\frac{1}{\tau_{b,0}}\gamma(\gamma-\gamma_0)\ln\left(\frac{d_0}{c\tau_{b,0}}\right)E_{\mathrm{s}}\left(\frac{1}{2}a_{b,0}-\tilde{a}_{b,0}\right) \\ &= \frac{1}{\tau_{b,0}}E_{\mathrm{s}}a_{b,0}\left((2\gamma-\gamma_0)\left(1-\frac{\tilde{a}_{b,0}}{a_{b,0}}\right)+\gamma(\gamma-\gamma_0)\ln\left(\frac{d_0}{c\tau_{b,0}}\right)\left(\frac{1}{2}-\frac{\tilde{a}_{b,0}}{a_{b,0}}\right)\right), \end{aligned} \tag{A.11.2}$$

$$\begin{aligned} k_5 &= \frac{1}{\tau_{b,0}}\gamma+\frac{1}{\tau_{b,0}}(\gamma-\gamma_0)+\frac{1}{2}\frac{1}{\tau_{b,0}}\gamma(\gamma-\gamma_0)\ln\left(\frac{d_0}{c\tau_{b,0}}\right) \\ &= \frac{1}{\tau_{b,0}}\gamma+\frac{1}{\tau_{b,0}}(\gamma-\gamma_0)\left(1+\frac{1}{2}\gamma\ln\left(\frac{d_0}{c\tau_{b,0}}\right)\right), \end{aligned} \tag{A.11.3}$$

$$k_6 = 2+(\gamma-\gamma_0)\ln\left(\frac{d_0}{c\tau_{b,0}}\right). \tag{A.11.4}$$

As obtained, the solution of $\mathrm{E}_{n_b(t)}\left\{\left(k_4+k_5\rho_{\mathrm{ns},0}-k_6\dot{\rho}_{\mathrm{ns},0}\right)^2\right\}$ is given by

$$\mathrm{E}_{n_b(t)}\left\{\left(k_4+k_5\rho_{\mathrm{ns},0}-k_6\dot{\rho}_{\mathrm{ns},0}\right)^2\right\} = k_4^2+\frac{1}{2}E_{\mathrm{s}}\sigma_{\mathrm{n}}^2k_5^2+2\pi^2E_{\mathrm{s}}\bar{\beta}^2\sigma_{\mathrm{n}}^2k_6^2. \tag{A.11.5}$$

Therefore, the error variance can be written as

$$
\begin{aligned}
&\mathrm{E}_{n_b(t)}\left\{(\hat{\tau}_{b,\mathrm{ML}}(\gamma)-\tau_{b,0})^2\right\}\\
&=\frac{k_4^2+\frac{1}{2}E_\mathrm{s}\sigma_\mathrm{n}^2k_5^2+2\pi^2E_\mathrm{s}\bar{\beta}^2\sigma_\mathrm{n}^2k_6^2}{\frac{1}{\tau_{b,0}^4}E_\mathrm{s}^2a_{b,0}^2\left(\frac{\tilde{a}_{b,0}}{a_{b,0}}\gamma(1+\gamma)-\gamma\left(1+\frac{1}{2}\gamma\right)+8\pi^2\bar{\beta}^2\tau_{b,0}^2\right)^2}\\
&=\left(\frac{1}{\tau_{b,0}^2}E_\mathrm{s}^2a_{b,0}^2\left((2\gamma-\gamma_0)\left(1-\frac{\tilde{a}_{b,0}}{a_{b,0}}\right)+\gamma(\gamma-\gamma_0)\ln\left(\frac{d_0}{c\tau_{b,0}}\right)\left(\frac{1}{2}-\frac{\tilde{a}_{b,0}}{a_{b,0}}\right)\right)^2\right.\\
&\quad+\frac{1}{2\tau_{b,0}^2}E_\mathrm{s}\sigma_\mathrm{n}^2\left(\gamma+(\gamma-\gamma_0)\left(1+\frac{1}{2}\gamma\ln\left(\frac{d_0}{c\tau_{b,0}}\right)\right)\right)^2\\
&\quad\left.+2\pi^2E_\mathrm{s}\bar{\beta}^2\sigma_\mathrm{n}^2\left(2+(\gamma-\gamma_0)\ln\left(\frac{d_0}{c\tau_{b,0}}\right)\right)^2\right)\\
&\quad\tau_{b,0}^4E_\mathrm{s}^{-2}a_{b,0}^{-2}\left(\frac{\tilde{a}_{b,0}}{a_{b,0}}\gamma(1+\gamma)-\gamma\left(1+\frac{1}{2}\gamma\right)+8\pi^2\bar{\beta}^2\tau_{b,0}^2\right)^{-2}\\
&=\left(\left((2\gamma-\gamma_0)\left(1-\frac{\tilde{a}_{b,0}}{a_{b,0}}\right)+\gamma(\gamma-\gamma_0)\ln\left(\frac{d_0}{c\tau_{b,0}}\right)\left(\frac{1}{2}-\frac{\tilde{a}_{b,0}}{a_{b,0}}\right)\right)^2\right.\\
&\quad+\frac{1}{2}\frac{1}{a_{b,0}^2}\frac{\sigma_\mathrm{n}^2}{E_\mathrm{s}}\left(\gamma+(\gamma-\gamma_0)\left(1+\frac{1}{2}\gamma\ln\left(\frac{d_0}{c\tau_{b,0}}\right)\right)\right)^2\\
&\quad\left.+\frac{1}{a_{b,0}^2}\frac{\sigma_\mathrm{n}^2}{E_\mathrm{s}}2\pi^2\bar{\beta}^2\tau_{b,0}^2\left(2+(\gamma-\gamma_0)\ln\left(\frac{d_0}{c\tau_{b,0}}\right)\right)^2\right)\\
&\quad\tau_{b,0}^2\left(\frac{\tilde{a}_{b,0}}{a_{b,0}}\gamma(1+\gamma)-\gamma\left(1+\frac{1}{2}\gamma\right)+8\pi^2\bar{\beta}^2\tau_{b,0}^2\right)^{-2}.
\end{aligned}
\tag{A.11.6}
$$

A.12 Proof of Remark 5.3.4

$$
\begin{aligned}
\mathrm{E}_{n_b(t)}\left\{(\hat{\tau}_{b,\mathrm{ML}}(\gamma)-\tau_{b,0})^2\right\}\big|_{\gamma=\gamma_0} &= \frac{\frac{1}{2}\frac{1}{a_{b,0}^2}\frac{\sigma_{\mathrm{n}}^2}{E_{\mathrm{s}}}\gamma_0^2+\frac{1}{a_{b,0}^2}\frac{\sigma_{\mathrm{n}}^2}{E_{\mathrm{s}}}2\pi^2\bar{\beta}^2\tau_{b,0}^2 4}{\left(\gamma_0(1+\gamma_0)-\gamma_0\left(1+\frac{1}{2}\gamma_0\right)+8\pi^2\bar{\beta}^2\tau_{b,0}^2\right)^2}\tau_{b,0}^2 \\
&= \frac{\frac{1}{a_{b,0}^2\mathrm{SNR}}\left(\frac{1}{2}\gamma_0^2+8\pi^2\bar{\beta}^2\tau_{b,0}^2\right)}{\left(\frac{1}{2}\gamma_0^2+8\pi^2\bar{\beta}^2\tau_{b,0}^2\right)^2}\tau_{b,0}^2 \\
&= \frac{\tau_{b,0}^2}{a_{b,0}^2\mathrm{SNR}\left(\frac{1}{2}\gamma_0^2+8\pi^2\bar{\beta}^2\tau_{b,0}^2\right)} \\
&= \frac{1}{a_{b,0}^2\mathrm{SNR}\left(8\pi^2\bar{\beta}^2+\frac{\gamma_0^2}{2\tau_{b,0}^2}\right)}.
\end{aligned}
\tag{A.12.1}
$$

A.13 Proof of Proposition 5.3.4

The error variance can be written as

$$
\begin{aligned}
&\mathrm{E}_{n_b(t)}\left\{(\hat{\tau}_{b,\mathrm{ML}}(\gamma)-\tau_{b,0})^2\right\}\\
&=\mathrm{E}_{n_b(t)}\Bigg\{\left(\frac{1}{\tau_{b,0}^2}\gamma(1+\gamma)E_{\mathrm{s}}\tilde{a}_{b,0}-\frac{1}{\tau_{b,0}^2}\gamma\left(1+\frac{1}{2}\gamma\right)E_{\mathrm{s}}a_{b,0}+8\pi^2\bar{\beta}^2E_{\mathrm{s}}a_{b,0}\right)^{-2}\\
&\quad\left(-\frac{1}{\tau_{b,0}}\gamma\left(E_{\mathrm{s}}\tilde{a}_{b,0}-E_{\mathrm{s}}a_{b,0}-\rho_{\mathrm{ns},0}\right)-2\dot{\rho}_{\mathrm{ns},0}\right.\\
&\quad\left.+\frac{1}{\tau_{b,0}}(\gamma-\gamma_0)E_{\mathrm{s}}(a_{b,0}-\tilde{a}_{b,0})-\frac{1}{\tau_{b,0}}\gamma(\gamma-\gamma_0)\ln\left(\frac{d_0}{c\tau_{b,0}}\right)E_{\mathrm{s}}\left(\tilde{a}_{b,0}-\frac{1}{2}a_{b,0}\right)\right)^2\Bigg\}\\
&=\mathrm{E}_{n_b(t)}\Bigg\{\left(\frac{1}{\tau_{b,0}^2}\gamma(1+\gamma)E_{\mathrm{s}}\tilde{a}_{b,0}-\frac{1}{\tau_{b,0}^2}\gamma\left(1+\frac{1}{2}\gamma\right)E_{\mathrm{s}}a_{b,0}+8\pi^2\bar{\beta}^2E_{\mathrm{s}}a_{b,0}\right)^{-2}\\
&\quad\left(-\frac{1}{\tau_{b,0}}\gamma\left(E_{\mathrm{s}}\tilde{a}_{b,0}-E_{\mathrm{s}}a_{b,0}\right)+\frac{1}{\tau_{b,0}}(\gamma-\gamma_0)E_{\mathrm{s}}(a_{b,0}-\tilde{a}_{b,0})\right.\\
&\quad\left.-\frac{1}{\tau_{b,0}}\gamma(\gamma-\gamma_0)\ln\left(\frac{d_0}{c\tau_{b,0}}\right)E_{\mathrm{s}}\left(\tilde{a}_{b,0}-\frac{1}{2}a_{b,0}\right)+\frac{1}{\tau_{b,0}}\gamma\rho_{\mathrm{ns},0}-2\dot{\rho}_{\mathrm{ns},0}\right)^2\Bigg\}\\
&=\frac{\mathrm{E}_{n_b(t)}\left\{(k_7+k_8\rho_{\mathrm{ns},0}-k_9\dot{\rho}_{\mathrm{ns},0})^2\right\}}{\frac{1}{\tau_{b,0}^4}E_{\mathrm{s}}^2a_{b,0}^2\left(\frac{\tilde{a}_{b,0}}{a_{b,0}}\gamma(1+\gamma)-\gamma\left(1+\frac{1}{2}\gamma\right)+8\pi^2\bar{\beta}^2\tau_{b,0}^2\right)^2},
\end{aligned}
\tag{A.13.1}
$$

where k_7, k_8 and k_9 are given by

$$
\begin{aligned}
k_7&=-\frac{1}{\tau_{b,0}}\gamma E_{\mathrm{s}}\left(\tilde{a}_{b,0}-a_{b,0}\right)+\frac{1}{\tau_{b,0}}(\gamma-\gamma_0)E_{\mathrm{s}}(a_{b,0}-\tilde{a}_{b,0})\\
&\quad-\frac{1}{\tau_{b,0}}\gamma(\gamma-\gamma_0)E_{\mathrm{s}}\ln\left(\frac{d_0}{c\tau_{b,0}}\right)\left(\tilde{a}_{b,0}-\frac{1}{2}a_{b,0}\right)\\
&=\frac{1}{\tau_{b,0}}E_{\mathrm{s}}a_{b,0}\left(\gamma\left(1-\frac{\tilde{a}_{b,0}}{a_{b,0}}\right)+(\gamma-\gamma_0)\left(1-\frac{\tilde{a}_{b,0}}{a_{b,0}}\right)\right.\\
&\quad\left.+\gamma(\gamma-\gamma_0)\ln\left(\frac{d_0}{c\tau_{b,0}}\right)\left(\frac{1}{2}-\frac{\tilde{a}_{b,0}}{a_{b,0}}\right)\right)\\
&=\frac{1}{\tau_{b,0}}E_{\mathrm{s}}a_{b,0}\left((2\gamma-\gamma_0)\left(1-\frac{\tilde{a}_{b,0}}{a_{b,0}}\right)+\gamma(\gamma-\gamma_0)\ln\left(\frac{d_0}{c\tau_{b,0}}\right)\left(\frac{1}{2}-\frac{\tilde{a}_{b,0}}{a_{b,0}}\right)\right),
\end{aligned}
\tag{A.13.2}
$$

$$k_8 = \frac{1}{\tau_{b,0}}\gamma, \tag{A.13.3}$$

$$k_9 = 2. \tag{A.13.4}$$

As seen in (A.8.6b)-(A.8.7), $\mathrm{E}_{n_b(t)}\left\{\left(k_7 + k_8\rho_{\mathrm{ns},0} - k_9\dot{\rho}_{\mathrm{ns},0}\right)^2\right\}$ is given by

$$\mathrm{E}_{n_b(t)}\left\{\left(k_7 + k_8\rho_{\mathrm{ns},0} - k_9\dot{\rho}_{\mathrm{ns},0}\right)^2\right\} = k_7^2 + \frac{1}{2}E_{\mathrm{s}}\sigma_{\mathrm{n}}^2 k_8^2 + 2\pi^2 E_{\mathrm{s}}\bar{\beta}^2\sigma_{\mathrm{n}}^2 k_9^2. \tag{A.13.5}$$

Therefore, we obtain

$$\begin{aligned}
&\mathrm{E}_{n_b(t)}\left\{\left(\hat{\tau}_{b,\mathrm{ML}}(\gamma) - \tau_{b,0}\right)^2\right\} \\
&= \frac{k_7^2 + \frac{1}{2}E_{\mathrm{s}}\sigma_{\mathrm{n}}^2 k_8^2 + 2\pi^2 E_{\mathrm{s}}\bar{\beta}^2\sigma_{\mathrm{n}}^2 k_9^2}{\frac{1}{\tau_{b,0}^4}E_{\mathrm{s}}^2 a_{b,0}^2\left(\frac{\tilde{a}_{b,0}}{a_{b,0}}\gamma(1+\gamma) - \gamma\left(1+\frac{1}{2}\gamma\right) + 8\pi^2\bar{\beta}^2\tau_{b,0}^2\right)^2} \\
&= \left(\frac{1}{\tau_{b,0}^2}E_{\mathrm{s}}^2 a_{b,0}^2\left((2\gamma-\gamma_0)\left(1-\frac{\tilde{a}_{b,0}}{a_{b,0}}\right) + \gamma(\gamma-\gamma_0)\ln\left(\frac{d_0}{c\tau_{b,0}}\right)\left(\frac{1}{2}-\frac{\tilde{a}_{b,0}}{a_{b,0}}\right)\right)^2\right. \\
&\quad \left. + \frac{1}{2\tau_{b,0}^2}\gamma^2 E_{\mathrm{s}}\sigma_{\mathrm{n}}^2 + 8\pi^2 E_{\mathrm{s}}\bar{\beta}^2\sigma_{\mathrm{n}}^2\right) \\
&\quad \tau_{b,0}^4 E_{\mathrm{s}}^{-2} a_{b,0}^{-2}\left(\frac{\tilde{a}_{b,0}}{a_{b,0}}\gamma(1+\gamma) - \gamma\left(1+\frac{1}{2}\gamma\right) + 8\pi^2\bar{\beta}^2\tau_{b,0}^2\right)^{-2} \\
&= \frac{\left((2\gamma-\gamma_0)\left(1-\frac{\tilde{a}_{b,0}}{a_{b,0}}\right) + \gamma(\gamma-\gamma_0)\ln\left(\frac{d_0}{c\tau_{b,0}}\right)\left(\frac{1}{2}-\frac{\tilde{a}_{b,0}}{a_{b,0}}\right)\right)^2 + \frac{1}{a_{b,0}^2}\frac{\sigma_{\mathrm{n}}^2}{E_{\mathrm{s}}}\left(\frac{1}{2}\gamma^2 + 8\pi^2\bar{\beta}^2\tau_{b,0}^2\right)}{\left(\frac{\tilde{a}_{b,0}}{a_{b,0}}\gamma(1+\gamma) - \gamma\left(1+\frac{1}{2}\gamma\right) + 8\pi^2\bar{\beta}^2\tau_{b,0}^2\right)^2}\tau_{b,0}^2.
\end{aligned} \tag{A.13.6}$$

A.14 Proof of Remark 5.3.8

$$\begin{aligned}\mathrm{E}_{n_b(t)}\left\{(\hat{\tau}_{b,\mathrm{ML}}(\gamma)-\tau_{b,0})^2\right\}\big|_{\gamma=\gamma_0} &= \frac{\frac{1}{a_{b,0}^2}\frac{\sigma_\mathrm{n}^2}{E_\mathrm{s}}\left(\frac{1}{2}\gamma^2+8\pi^2\bar{\beta}^2\tau_{b,0}^2\right)}{\left(\gamma_0(1+\gamma_0)-\gamma_0\left(1+\frac{1}{2}\gamma_0\right)+8\pi^2\bar{\beta}^2\tau_{b,0}^2\right)^2}\tau_{b,0}^2 \\ &= \frac{\tau_{b,0}^2}{\frac{E_\mathrm{s}}{\sigma_\mathrm{n}^2}a_{b,0}^2\left(\frac{1}{2}\gamma_0^2+8\pi^2\bar{\beta}^2\tau_{b,0}^2\right)} \\ &= \frac{1}{\mathrm{SNR}a_{b,0}^2\left(8\pi^2\bar{\beta}^2+\frac{\gamma_0^2}{2\tau_{b,0}^2}\right)}.\end{aligned} \tag{A.14.1}$$

A.15 Proof of Proposition 5.5.1

Then, the AB of the ML estimator can be developed as

$$\begin{aligned}&\mathrm{E}_{n_b(t),\mathbf{v},\mathbf{q}}\{\hat{\tau}_{b,\mathrm{ML}}(\gamma)-\tau_{b,0}\} \\ &= \mathrm{E}_{\mathbf{v},\mathbf{q}}\left\{-\frac{(2\gamma-\gamma_0)\left(a_{b,0}-\tilde{a}_{b,0}\right)+\gamma(\gamma-\gamma_0)\ln\left(\frac{d_0}{c\tau_{b,0}}\right)\left(\frac{1}{2}a_{b,0}-\tilde{a}_{b,0}\right)}{8\pi^2\bar{\beta}^2\tau_{b,0}^2a_{b,0}-\left(\gamma(a_{b,0}-\tilde{a}_{b,0})+\gamma^2\left(\frac{1}{2}a_{b,0}-\tilde{a}_{b,0}\right)\right)}\tau_{b,0}\right\} \\ &= -\tau_{b,0}\left((2\gamma-\gamma_0)\left(a_{b,0}-\tilde{a}_{b,0}\right)+\gamma(\gamma-\gamma_0)\ln\left(\frac{d_0}{c\tau_{b,0}}\right)\left(\frac{1}{2}a_{b,0}-\tilde{a}_{b,0}\right)\right) \\ &\quad \mathrm{E}_{\mathbf{v},\mathbf{q}}\left\{\frac{1}{8\pi^2\bar{\beta}^2\tau_{b,0}^2a_{b,0}-\left(\gamma(a_{b,0}-\tilde{a}_{b,0})+\gamma^2\left(\frac{1}{2}a_{b,0}-\tilde{a}_{b,0}\right)\right)}\right\}.\end{aligned} \tag{A.15.1}$$

The expression $\mathrm{E}_{\mathbf{v},\mathbf{q}}\left\{\frac{1}{8\pi^2\bar{\beta}^2\tau_{b,0}^2 a_{b,0}-\left(\gamma(a_{b,0}-\tilde{a}_{b,0})+\gamma^2\left(\frac{1}{2}a_{b,0}-\tilde{a}_{b,0}\right)\right)}\right\}$ can be solved by including the expression of the effective bandwidth given by (A.3.21). Then, we have

$$
\begin{aligned}
&\mathrm{E}_{\mathbf{v},\mathbf{q}}\left\{\frac{1}{8\pi^2\bar{\beta}^2\tau_{b,0}^2 a_{b,0}-\left(\gamma(a_{b,0}-\tilde{a}_{b,0})+\gamma^2\left(\frac{1}{2}a_{b,0}-\tilde{a}_{b,0}\right)\right)}\right\}\\
&=\sum_{k=1}^{4} p_v(v_n)p_q(q_n)\frac{1}{8\pi^2\tau_{b,0}^2 a_{b,0}\frac{1}{4\pi^2}\frac{\sum_{n=1}^{N-1}(\omega_0-\frac{v_n q_n\pi}{2T})^2}{N-1}-\left(\gamma(a_{b,0}-\tilde{a}_{b,0})+\gamma^2\left(\frac{1}{2}a_{b,0}-\tilde{a}_{b,0}\right)\right)}\\
&=\left(\frac{1}{4}\frac{1}{\frac{2}{N-1}\tau_{b,0}^2 a_{b,0}\sum_{n=1}^{N-1}\left(\omega_0-\frac{(+1)(+1)\pi}{2T}\right)^2-\left(\gamma(a_{b,0}-\tilde{a}_{b,0})+\gamma^2\left(\frac{1}{2}a_{b,0}-\tilde{a}_{b,0}\right)\right)}\right.\\
&\quad+\frac{1}{4}\frac{1}{\frac{2}{N-1}\tau_{b,0}^2 a_{b,0}\sum_{n=1}^{N-1}\left(\omega_0-\frac{(+1)(-1)\pi}{2T}\right)^2-\left(\gamma(a_{b,0}-\tilde{a}_{b,0})+\gamma^2\left(\frac{1}{2}a_{b,0}-\tilde{a}_{b,0}\right)\right)}\\
&\quad+\frac{1}{4}\frac{1}{\frac{2}{N-1}\tau_{b,0}^2 a_{b,0}\sum_{n=1}^{N-1}\left(\omega_0-\frac{(-1)(+1)\pi}{2T}\right)^2-\left(\gamma(a_{b,0}-\tilde{a}_{b,0})+\gamma^2\left(\frac{1}{2}a_{b,0}-\tilde{a}_{b,0}\right)\right)}\\
&\quad\left.+\frac{1}{4}\frac{1}{\frac{2}{N-1}\tau_{b,0}^2 a_{b,0}\sum_{n=1}^{N-1}\left(\omega_0-\frac{(-1)(-1)\pi}{2T}\right)^2-\left(\gamma(a_{b,0}-\tilde{a}_{b,0})+\gamma^2\left(\frac{1}{2}a_{b,0}-\tilde{a}_{b,0}\right)\right)}\right)\\
&=\left(\frac{1}{4}\frac{2}{\frac{2}{N-1}\tau_{b,0}^2 a_{b,0}\sum_{n=1}^{N-1}\left(\omega_0-\frac{\pi}{2T}\right)^2-\left(\gamma(a_{b,0}-\tilde{a}_{b,0})+\gamma^2\left(\frac{1}{2}a_{b,0}-\tilde{a}_{b,0}\right)\right)}\right.\\
&\quad\left.+\frac{1}{4}\frac{2}{\frac{2}{N-1}\tau_{b,0}^2 a_{b,0}\sum_{n=1}^{N-1}\left(\omega_0+\frac{\pi}{2T}\right)^2-\left(\gamma(a_{b,0}-\tilde{a}_{b,0})+\gamma^2\left(\frac{1}{2}a_{b,0}-\tilde{a}_{b,0}\right)\right)}\right).
\end{aligned}
\tag{A.15.2}
$$

By developing the summations, we can rewrite

$$\begin{aligned}
&\mathrm{E}_{\mathbf{v},\mathbf{q}}\left\{\frac{1}{8\pi^2\bar{\beta}^2\tau_{b,0}^2 a_{b,0}-\left(\gamma(a_{b,0}-\tilde{a}_{b,0})+\gamma^2\left(\frac{1}{2}a_{b,0}-\tilde{a}_{b,0}\right)\right)}\right\}\\
&=\frac{1}{2}\left(\frac{1}{\frac{2}{N-1}(N-1)\tau_{b,0}^2 a_{b,0}\left(\omega_0-\frac{\pi}{2T}\right)^2-\left(\gamma(a_{b,0}-\tilde{a}_{b,0})+\gamma^2\left(\frac{1}{2}a_{b,0}-\tilde{a}_{b,0}\right)\right)}\right.\\
&\quad\left.+\frac{1}{\frac{2}{N-1}(N-1)\tau_{b,0}^2 a_{b,0}\left(\omega_0+\frac{\pi}{2T}\right)^2-\left(\gamma(a_{b,0}-\tilde{a}_{b,0})+\gamma^2\left(\frac{1}{2}a_{b,0}-\tilde{a}_{b,0}\right)\right)}\right)\\
&=\frac{1}{2}\left(\frac{1}{2\tau_{b,0}^2 a_{b,0}\left(\omega_0-\frac{\pi}{2T}\right)^2-\left(\gamma(a_{b,0}-\tilde{a}_{b,0})+\gamma^2\left(\frac{1}{2}a_{b,0}-\tilde{a}_{b,0}\right)\right)}\right.\\
&\quad\left.+\frac{1}{2\tau_{b,0}^2 a_{b,0}\left(\omega_0+\frac{\pi}{2T}\right)^2-\left(\gamma(a_{b,0}-\tilde{a}_{b,0})+\gamma^2\left(\frac{1}{2}a_{b,0}-\tilde{a}_{b,0}\right)\right)}\right).
\end{aligned}\tag{A.15.3}$$

By substituting (A.15.3) into (A.15.1), we obtain the final expression of the AB for the outdoor case

$$\begin{aligned}
&\mathrm{E}_{n_b(t),\mathbf{v},\mathbf{q}}\{\hat{\tau}_{b,\mathrm{ML}}(\gamma)-\tau_{b,0}\}\\
&=-\frac{1}{2}\tau_{b,0}\left((2\gamma-\gamma_0)(a_{b,0}-\tilde{a}_{b,0})+\gamma(\gamma-\gamma_0)\ln\left(\frac{d_0}{c\tau_{b,0}}\right)\left(\frac{1}{2}a_{b,0}-\tilde{a}_{b,0}\right)\right)\\
&\quad\left(\frac{1}{2\tau_{b,0}^2 a_{b,0}\left(\omega_0-\frac{\pi}{2T}\right)^2-\left(\gamma(a_{b,0}-\tilde{a}_{b,0})+\gamma^2\left(\frac{1}{2}a_{b,0}-\tilde{a}_{b,0}\right)\right)}\right.\\
&\quad\left.+\frac{1}{2\tau_{b,0}^2 a_{b,0}\left(\omega_0+\frac{\pi}{2T}\right)^2-\left(\gamma(a_{b,0}-\tilde{a}_{b,0})+\gamma^2\left(\frac{1}{2}a_{b,0}-\tilde{a}_{b,0}\right)\right)}\right).
\end{aligned}\tag{A.15.4}$$

Appendix B

MATLAB® Files

B.1 MATLAB® File for the Second-derivative Gaussian Pulse (Fig. 3.1)

```
tau_p = 0.2877e-9;
Tp    = 0.7e-9;
t     = linspace(0,2e-9,10000);
%%%%second-derivative Gaussian pulse
alpha = 2*pi*(t/tau_p).^2;
p     = (1-2*alpha).*exp(-alpha);
plot(t,p, 'k'),title('Second-derivate Gaussian Pulse'),
xlabel('t (s)'),ylabel('p(t)')
```

B.2 MATLAB® File for the Transmitted Signal (Fig. 3.2)

```
%%%%%Transmitted signal
alpha_1 = 2*pi*((t-0.5*Tp)/tau_p).^2;
s       = (1-2*alpha_1).*exp(-alpha_1);
Es      = sum((abs(s)).^2);
figure,plot(t,s,'r-'),title('Transmitted signal'),
xlabel('t (s)'),ylabel('s(t)')
```

B.3 MATLAB® File for the Transmitted Signal Delayed (Fig. 3.3)

```
%%%%%Transmitted signal, which is delayed
tau     = 0.65e-9;
alpha_2 = 2*pi*((t-0.5*Tp-tau)/tau_p).^2;
s_tau   = (1-2*alpha_2).*exp(-alpha_2);
figure,
plot (t,s_tau),
title('Transmitted signal, which is delayed '),
xlabel('t (s)'),ylabel('s(t-\tau)')
```

B.4 MATLAB® File for the Received Signal (Fig. 3.4)

```
%received signal
a_b   = 1;
sigma = 0.05;
noise = (1/sqrt(2)) * sigma* (randn(1,length(t))
        + j*randn(1,length(t)));
r     = a_b*s_tau+noise;
figure,
plot(t,r,'c'),title('Received signal'),
xlabel('t (s)'),ylabel('r(t)')
```

B.5 MATLAB® File for the Signal Waveforms (Fig. 3.5)

```
% Program for the signal waveforms
plot(t, r,'c',t,s_tau,'b-.',t,s,'r--'),
legend('r(t)','s(t-\tau)','s(t)'),title('Signal waveforms'),
xlabel('t (s)'),ylabel('f(t)'), grid on
```

B.6 MATLAB® File for the Signal Waveforms for $d_b = 6$ m. (Fig. 3.7)

```
tau_p   = 0.2877e-9;
```

```
Tp      = 0.7e-9;
t       = linspace(0,2.5e-8,10000);
f0      = 1.9e9;
d0      = 0.05;
db      = 6;
gamma   = 2.5;
c       = 3e8;
tau     = db/c;
k       = c^2/(16*pi^2*d0^2*f0^2)
%transmit signal
alpha_1 = 2*pi*((t-0.5*Tp)/tau_p).^2;
s       = (1-2*alpha_1).*exp(-alpha_1);
Es      = sum((abs(s)).^2);
alpha_2 = 2*pi*((t-0.5*Tp-tau)/tau_p).^2;
%transmit signal, which is delayed
s_tau   = (1-2*alpha_2).*exp(-alpha_2);
a_b     = sqrt(k*(d0/db)^gamma)
SNR     = 40;
sigma   = sqrt(a_b^2*Es/10^(SNR/10))
noise   = (1/sqrt(2)) * sigma* (randn(1,length(t))
          + j*randn(1,length(t)));
%received signal
r       = a_b*s_tau+noise;
plot(t, r,'c',t,a_b*s_tau,'b--'),legend('r(t)','a_bs(t-\tau)'),
title('Signal waveforms for d_b= 6 m'),
xlabel('t (s)'),ylabel('f(t)'), grid on
```

B.7 MATLAB® File for the Effective Bandwidth for the Second-derivative Gaussian Pulse (Fig. 3.8)

```
%%%Indoor beta
tau_p_range     = [0.2:0.01:0.4]*1e-9;
Tp              = 0.7e-9;
tau             = 0.65e-9
d0              = 0.05;  dmax     = 6;
c               = 3e8;
tau_min         = d0/c;  tau_max  = dmax/c;
t0              = 1.005*tau_max;
```

```
d_t             = tau/1e5;
t               = (1e-100:d_t:t0);
n_tau_p         = 0;
for tau_p = tau_p_range
    n_tau_p     = n_tau_p +1;
%%%%%%%Transmit signal
alpha_1         = 2*pi*((t-Tp/2-tau)/tau_p).^2;
s               = (1-2*alpha_1).*exp(-alpha_1);
S               = fft(s);
%%%%%%%Theorical RMSE
beta1(n_tau_p)  = (1/tau_p)*sqrt(5/(2*pi));
%%%%%%%Simlation
alpha           = 2*pi*((t-Tp/2-tau)/tau_p).^2;
alpha_der       = 4*pi*(t-Tp/2-tau)./tau_p^2;
p_derivative2   = (9-12*alpha+4*alpha.^2)
                      .*exp(-2*alpha).*alpha_der.^2;
beta2(n_tau_p)  = 1/(2*pi)*sqrt(sum(p_derivative2)/sum(s.^2));
Es_sim(n_tau_p) = sum(s.*s)*d_t;
Es_theo(n_tau_p)= 3*tau_p/8;
bandwith_theo(n_tau_p)= 15*pi/(4*tau_p);
bandwith_sim(n_tau_p) = sum(p_derivative2)*d_t;
end
plot(tau_p_range,beta1,'x-',tau_p_range,beta2,'ro-.'),
legend('Simulation','Theory'),
title('Effective Bandwidth'),
xlabel('\tau_p (s)'),ylabel('\beta (Hz)')
figure,
plot(tau_p_range,Es_sim,'x-',tau_p_range,Es_theo,'ro-.'),
legend('Simulation','Theory'),
title('Energy of the transmitted signal'),
xlabel('\tau_p (s)'),ylabel('E_s(Joule)')
figure,
plot(tau_p_range,bandwith_theo,'x-',
tau_p_range,bandwith_sim,'ro-.')
legend('Simulation','Theory'),title('Square of the Bandwidth'),
xlabel('\tau_p (s)'),ylabel('W (Hz^2)')
```

B.8 MATLAB® File for the MSK Modulation

```
function msk = MSK_mod(frame,R_B,fc,tau,t, t_sample)
T     = 1/R_B;
N     = ceil(T/t_sample);
delay = round(tau/t_sample);
v     = frame(1:2:length(frame));
q     = frame(2:2:length(frame));
v_aux = v(1)*ones(1,N);
q_aux = [];
for i=2:length(v)
    v_aux = [v_aux v(i)*ones(1,2*N)];
end
for i=1:length(q)-1
    q_aux = [q_aux q(i)*ones(1,2*N)];
end
q_aux = [q_aux q(end)*ones(1,N)];
v_t   = [v_aux zeros(1, length(t)-length(v_aux))];
q_t   = [q_aux zeros(1, length(t)-length(q_aux))];
I_t   = v_t.*cos(pi*t/(2*T)).*cos(2*pi*fc*t);
Q_t   = q_t.*sin(pi*t/(2*T)).*sin(2*pi*fc*t);
msk   = I_t+Q_t;
msk   = [zeros(1,delay) msk(1:(end-delay))];
```

B.9 MATLAB® File for the MSK Signals (Fig. 3.17)

```
frame    =   [1 1 -1 -1 ];
R_B      =   400e3;
fc       =   2*R_B;
f0       =   1.9e9;
d0       =   100;
dmax     =   3e3;
gamma    =   2.5;
c        =   3e8;
k        =   c^2/(16*pi^2*d0^2*f0^2);
tau_max  =   dmax/c;
t0       =   2*tau_max;
tau      =   3000/c;
t_sample =   tau/1e5;
```

```
t         =   (1e-100:t_sample:t0);
%%%%%%%%% transmit signal
s         =   MSK_mod(frame,R_B,fc,0,t, t_sample);
%%%%%%%%% transmit signal delayed
s_tau     =   MSK_mod(frame, R_B, fc, tau, t, t_sample);
Es        =   sum(s.*conj(s));
a_b       =   sqrt(k*(d0/(tau*c))^gamma);
%%%%%%%%% let us fix SNR
SNR       = 60;
SNR_lin   = 10^(SNR/10);
sigma_n   = sqrt(a_b^2*Es/SNR_lin);
%%%%%%%% noise
noise     = (1/sqrt(2)) *sigma_n* (randn(1,length(t))
          + j*randn(1,length(t)));
%%%%%%%%% received signal
r         = a_b*s_tau+noise;

plot(t,s,t,s_tau,'r--'),
legend('s(t)','s(t-\tau_b)'),title('Waveforms for d_b=3km'),
xlabel('t (s)'),ylabel('waveforms'),
figure, plot(t,r,'c'),
legend('r(t)'),title('Received signal for d_b=3km'),
xlabel('t (s)'),ylabel('r(t)')
```

B.10 MATLAB® File for the Square Root of the Expectation of the Effective Bandwidth Square for a MSK Signal (Fig. 3.18)

```
%%%%%%% Outdoor %%%%%%%%
%%%Transmitted signal is a MSK signal
f0           = 2e9; %pag 140 wireless communication systems
R_B_range    = linspace(1e3,20e3,20)
N_R          = 1000;
N_bits       = 2
n_R_B        = 0;
for R_B      = R_B_range
    n_R_B    = n_R_B + 1;
    T        = 1./R_B;
```

```
    Ts      = (N_bits-1) * T;
    T0      = 1.005 * Ts;
    t_sample= Ts/1e6;
    t       = (1e-100:t_sample:T0);
    for n_R = 1:N_R
        frame   = sign(2 * rand(1,N_bits) -  1);
        %transmitted signal
        s       = MSK_mod(frame,R_B,f0,0,t, t_sample);
        %derivative of the transmitted signal
        d_s     = s_derivative(frame,R_B,f0,t, t_sample);
        b2(n_R) = 1/(2*pi)*sqrt(sum(d_s.^2)/sum(s.^2));
    end
   R_B
   %Theorical beta
   beta1(n_R_B) = sqrt(f0^2 + 1/(16*T^2));
   %simulated beta
   beta2(n_R_B) = mean(b2);
end
figure
plot(R_B_range,beta1,'-+',R_B_range,beta2,'r-o'),
legend('Theory','Simulation'),
title('Effective Bandwidth'),
xlabel('R_B (bps)'),ylabel('\beta (Hz)')
```

B.11 MATLAB® File for Theoretical RMSE as a Function of $\mathrm{SNR}_{\mathrm{Rx}}$ (Fig. 3.19)

```
%%%%%%% Outdoor %%%%%%%%
%%%Transmitted signal is a MSK signal
f0          = 0.9e9;
d0          = 100;
dmax        = 3e3;
gamma       = 4;
c           = 3e8;
k           = c^2./(16*pi^2*d0^2*f0.^2);
tau         = 1000/c;
SNR_range   = [-20:5:20];
R_B         = 12.2e3;
```

```
T           = 1/R_B;

%Theorical RMSE
beta2    = f0.^2 + 1/(16*T^2);
MCRB_MC  = 1./sqrt(10.^(SNR_range./10)*8*pi^2*beta2);
MCRB_ML  = 1./sqrt(10.^(SNR_range./10)
              *(8*pi^2*beta2 + gamma^2/(2*tau^2)));

beta3    = (16*f0.^2 + 1/T^2)
           ./(16*f0.^4 + 1/(16*T^4)-2*f0.^2*(1/T^2));
ACRB_MC  = sqrt((1./(10.^(SNR_range./10)*8*pi^2))*beta3);
ACRB_ML  = sqrt((1./(10.^(SNR_range/10)*2))
           * (1./(2*(2*pi*f0-pi/(2*T)).^2
              + gamma^2/(2*tau^2))
              + 1./(2*(2*pi*f0+pi/(2*T)).^2
              + gamma^2/(2*tau^2))));
figure
plot(SNR_range,ACRB_MC*c,'-+',SNR_range,MCRB_MC*c,'-.x',
     SNR_range,ACRB_ML*c,'--o',SNR_range,MCRB_ML*c,':s')
legend('ToA: ACRB','ToA: MCRB','SS-ToA: ACRB','SS-ToA: MCRB'),
title('RMSE as a function of the SNR_{Rx}:Outdoor scenario'),
xlabel('SNR_{Rx} (dB)'),ylabel('RMSE (m)')
```

B.12 MATLAB® File for the Theoretical RMSE as a Function of the Central Frequency (Fig. 3.23)

```
%%%%%%% Outdoor %%%%%%%%
%%%Transmitted signal is a MSK signal
f0 = linspace(100e6,2e9,20);
d0          = 100;
dmax        = 3e3;
gamma       = 4;
c           = 3e8;
k           = c^2./(16*pi^2*d0^2*f0.^2);
tau         = 1000/c;
SNR_range   = 15;
R_B         = 12.2e3;
T           = 1/R_B;
```

```
%Theorical RMSE
beta2   = f0.^2 + 1/(16*T^2);
MCRB_MC = 1./sqrt(10.^(SNR_range./10)*8*pi^2*beta2);
MCRB_ML = 1./sqrt(10.^(SNR_range./10)
            *(8*pi^2*beta2 + gamma^2/(2*tau^2)));

beta3   = (16*f0.^2 + 1/T^2)
          ./(16*f0.^4 + 1/(16*T^4)-2*f0.^2*(1/T^2));
ACRB_MC = sqrt((1./(10.^(SNR_range./10)*8*pi^2))*beta3);
ACRB_ML = sqrt((1./(10.^(SNR_range/10)*2))
          * (1./(2*(2*pi*f0-pi/(2*T)).^2
            + gamma^2/(2*tau^2))
            + 1./(2*(2*pi*f0+pi/(2*T)).^2+ gamma^2/(2*tau^2))));
figure
plot(f0,ACRB_MC*c,'-+',f0,MCRB_MC*c,'-.x',SNRf0,
      ACRB_ML*c,'--o',SNR_f0,MCRB_ML*c,':s')
legend('ToA: ACRB','ToA: MCRB','SS-ToA: ACRB','SS-ToA: MCRB'),
title('RMSE as a function of the f_0: Outdoor scenario'),
xlabel('f_0 (Hz)'),ylabel('RMSE (m)')
```

B.13 MATLAB® File for the RMSE of the Position Estimate as a Function of $\mathrm{SNR}_{\mathrm{Rx}}$: Indoor Scenario (Fig. 4.1)

```
%%%%%%% Indoor %%%%%%%%
%%%Transmit signal is a second derivative Gaussian pulse
tau_p       = 0.2877e-9;
Tp          = 0.7e-9;
f0          = 16/(3*pi*tau_p);
d0          = 0.1;
dmax        = 6;
gamma       = 2;
c           = 3e8;
k           = c^2/(16*pi^2*d0^2*f0^2);
tau         = 3/c;
tau_min     = d0/c;
tau_max     = dmax/c;
```

```
t0          = 1.2*(tau + Tp);
SNR_range   = [-20:2:50];
n_SNR       = 0;
N_R         = 1000;
t_sample    = tau/5e4;
t           = (1e-100:t_sample:t0);
d_t         = t(2)-t(1);
%%%%%%%%%%%%%%% Infinite duration %%%%%%%%%%%%%%%%%
%tansmit signal
alpha_inf = 2*pi*((t-0.5*Tp)/tau_p).^2;
s_inf     = (1-2*alpha_inf).*exp(-alpha_inf);
S_inf     = fft(s_inf);
Es_inf    = sum((abs(s_inf)).^2);
%receive signal
alpha_inf_2 = 2*pi*((t-0.5*Tp-tau)/tau_p).^2;
s_tau_inf   = (1-2*alpha_inf_2).*exp(-alpha_inf_2);
%%%%%%%%%%%%%% Finite duration%%%%%%%%%%%%%%%%%%%%%%
%tansmit signal
t1        = (1e-100:t_sample:Tp);
alpha_fin = 2*pi*((t1-0.5*Tp)/tau_p).^2;
s_fin_p   = (1-2*alpha_fin).*exp(-alpha_fin);
s_fin     = [s_fin_p zeros(1,length(t)-length(s_fin_p))];
S_fin     = fft(s_fin);
Es_fin    = sum((abs(s_fin)).^2);
%receive signal
s_tau_fin = [zeros(1,length(1e-100:t_sample:tau)) s_fin_p];
s_tau_fin = [s_tau_fin zeros(1,length(t)- length(s_tau_fin))];
a_b       = sqrt(k*(d0/(tau*c))^gamma);
ab_range  = sqrt(k*(d0./(t*c)).^gamma);
for SNR = SNR_range
    n_SNR = n_SNR+1;
    for n_R = 1:N_R
        %let us fix SNR
        SNR_lin =   10^(SNR/10);
        noise = (randn(1,length(t)) + j*randn(1,length(t)));
    %%%%%%%%%%%%%%% Infinite duration %%%%%%%%%%%%%%%%%%
        sigma_n_inf      = sqrt(Es_inf*a_b^2/SNR_lin);
        noise_inf        = (1/sqrt(2))*sigma_n_inf*noise;
        r_inf            = a_b * s_tau_inf + noise_inf;
        R_inf            = fft(r_inf);
```

```
        rho              = real(ifft(R_inf.*conj(S_inf)));
        [C I]            = max(rho);
        hat_tau_b_MC_inf = t(I);
        error_MC_inf(n_R)= hat_tau_b_MC_inf-tau;
        corr_inf         = ab_range.^2* Es_inf-2*ab_range.* rho;
        [C I]            = min(corr_inf);
        hat_tau_b_ML_inf = t(I);
        error_ML_inf(n_R)= hat_tau_b_ML_inf-tau;
    %%%%%%%%%%%%%% Finite duration%%%%%%%%%%%%%%%%%%%%%%%%%%%%%
        sigma_n_fin      = sqrt(Es_fin*a_b^2/SNR_lin);
        noise_fin        = (1/sqrt(2))* sigma_n_fin*noise;
        r_fin            = a_b *s_tau_fin + noise_fin;
        R_fin            = fft(r_fin);
        rho_fin          = real(ifft(R_fin.*conj(S_fin)));
        [C I]            = max(rho_fin);
        hat_tau_b_MC_fin = t(I);
        error_MC_fin(n_R)= hat_tau_b_MC_fin-tau;
        corr_fin         = ab_range.^2*Es_fin
                           -2*ab_range.*rho_fin;
        [C I]            = min(corr_fin);
        hat_tau_b_ML_fin = t(I);
        error_ML_fin(n_R)= hat_tau_b_ML_fin-tau;
    end
    SNR
    RMS_ML_inf(n_SNR) = sqrt(mean(error_ML_inf.^2));
    RMS_MC_inf(n_SNR) = sqrt(mean(error_MC_inf.^2));
    RMS_ML_fin(n_SNR) = sqrt(mean(error_ML_fin.^2));
    RMS_MC_fin(n_SNR) = sqrt(mean(error_MC_fin.^2));
end
%%% Theorical RMSE for Infinite duration
beta_inf  =   (1/tau_p)*sqrt(5/(2*pi));
En_MC_inf =   1./sqrt(10.^(SNR_range./10)*8*pi^2*beta_inf^2);
En_ML_inf =   1./sqrt(10.^(SNR_range./10)*
                   (8*pi^2*beta_inf^2 + gamma^2/(2*tau^2)));
%%% Theorical RMSE for Finite duration
beta_fin  =(1/tau_p)*sqrt(1/(2*pi))
             *sqrt((15*erf(Tp/tau_p*sqrt(pi))
            + (-30*(Tp/tau_p*sqrt(pi))
            + 28*(Tp/tau_p*sqrt(pi))^3
            - 8*(Tp/tau_p*sqrt(pi))^5)*exp(-pi*(Tp/tau_p)^2))
```

```
              / (3*erf(Tp/tau_p*sqrt(pi))
            + (2*(Tp/tau_p)
            - 4*pi*(Tp/tau_p)^3)*exp(-pi*(Tp/tau_p)^2)));
En_MC_fin = 1./sqrt(10.^(SNR_range./10)*8*pi^2*beta_fin^2);
En_ML_fin = 1./sqrt(10.^(SNR_range./10)
               *(8*pi^2*beta_fin^2 + gamma^2/(2*tau^2)));
plot(SNR_range,RMS_MC_fin*c,'+',SNR_range,RMS_MC_inf*c,'o',
SNR_range,En_MC_fin*c,':',SNR_range,En_MC_inf*c,'-.',
SNR_range,RMS_ML_fin*c,'x',SNR_range,RMS_ML_inf*c,'s',
SNR_range,En_ML_fin*c,'--', SNR_range,En_ML_inf*c,'-'),
legend('MC: Simulation for Finite Duration Pulse',
'MC: Simulation for Infinite Duration Pulse',
'MC: Theory for Finite Duration Pulse',
'MC: Theory for Infinite Duration Pulse',
'ML: Simulation for Finite Duration Pulse',
'ML: Simulation for Infinite Duration Pulse',
'ML: Theory for Finite Duration Pulse',
'ML: Theory for Infinite Duration Pulse'),
title('RMSE as a function of the received SNR: Indoor scenario'),
xlabel('SNR (dB)'),ylabel('RMSE (m)')
```

B.14 MATLAB® File for the RMSE of the Position Estimate as a Function of γ_b: Indoor Scenario (Fig. 4.3)

```
%%%%%%% Indoor %%%%%%%%
tau_p   = 0.2877e-9;       Tp   = 0.7e-9;
f0      = 16/(3*pi*tau_p); c    = 3e8;
d0      = 0.05;            dmax = 6;
k       = c^2/(16*pi^2*d0^2*f0^2);
SNR     = 100;             tau     = 3/c;
tau_min = d0/c;            tau_max = dmax/c;
t0      = 2*tau_max;
gamma_range = [1.6:0.05:3.5];
n_gamma     = 0;     N_R     = 1000;
t_sample    = tau/5e4;
t           = (1e-100:t_sample:t0);
%tansmit signal
alpha_1 = 2*pi*((t-0.5*Tp)/tau_p).^2;
```

```
s       = (1-2*alpha_1).*exp(-alpha_1);
S       = fft(s);
Es      = sum((abs(s)).^2);
%receive signal
alpha_2 = 2*pi*((t-0.5*Tp-tau)/tau_p).^2;
s_tau   = (1-2*alpha_2).*exp(-alpha_2);
for gamma = gamma_range
    n_gamma = n_gamma+1;
    for n_R = 1:N_R
        a_b     = sqrt(k*(d0/(tau*c))^gamma);
        SNR_lin = 10^(SNR/10);
        sigma_n = sqrt(Es/SNR_lin);
        noise   = (1/sqrt(2))*sigma_n*(randn(1,length(t))
                  + j*randn(1,length(t)));
        r       = a_b*s_tau+noise;
        R       = fft(r);
        rho          = real(ifft(conj(S).*R));
        [C I]        = max(rho);
        hat_tau_b_MC = t(I);
        error_MC(n_R)= hat_tau_b_MC-tau;
        corr         = a_b^2*Es-2*a_b*rho;
        [C I]        = min(corr);
        hat_tau_b_ML = t(I);
        error_ML(n_R)= hat_tau_b_ML-tau;
    end
    RMS_ML(n_gamma) = sqrt(mean(error_ML.^2));
    RMS_MC(n_gamma) = sqrt(mean(error_MC.^2));
end

%Theorical RMSE
beta     = sqrt(5/(2*pi*tau_p^2));
ab_range = sqrt(k*(d0./(tau*c)).^gamma_range);
En_MC    = sqrt(1./(10^(SNR/10)*ab_range.^2*8*pi^2*beta^2));
En_ML    = sqrt(1./(10^(SNR/10)*ab_range.^2
              .*(8*pi^2*beta^2+gamma_range.^2/(2*tau^2))));
plot(gamma_range,RMS_MC*c,'+',gamma_range,En_MC*c,'--',
gamma_range,RMS_ML*c,'^',gamma_range,En_ML*c,':'),
legend('MC: Simulation','MC: Theory',
'ML: Simulation','ML: Theory'),
title('RMSE as a function of \gamma_b: Indoor scenario'),
```

```
xlabel('\gamma_b'),ylabel('RMSE (m)')
```

B.15 MATLAB® File for the RMSE of the Position Estimate as a Function of the Distance between the Transmitter and the Receiver: Indoor Scenario (Fig. 4.4)

```
%%%%%%% Indoor %%%%%%%%
tau_p = 0.2877e-9;       Tp = 0.7e-9;
f0    = 16/(3*pi*tau_p); c  = 3e8;
d0    = 0.05;            dmax = 6;
gamma = 2;               SNR=100;
k     = c^2/(16*pi^2*d0^2*f0^2);
tau_min   = d0/c;   tau_max = dmax/c;
t0        = 2*tau_max;
tau_range = linspace(tau_min,tau_max,30);
n_tau     = 0;       N_R = 1000;
t_sample  = tau_min/5e3;
t         = (1e-100:t_sample:t0);
%tansmit signal
alpha_1 = 2*pi*((t-0.5*Tp)/tau_p).^2;
s       = (1-2*alpha_1).*exp(-alpha_1);
S       = fft(s);
Es      = sum((abs(s)).^2);
ab_range= sqrt(k*(d0./(t*c)).^gamma);
for tau = tau_range
    n_tau = n_tau+1;
    for n_R = 1:N_R
        %receive signal
        alpha_2 = 2*pi*((t-0.5*Tp-tau)/tau_p).^2;
        s_tau   = (1-2*alpha_2).*exp(-alpha_2);
        a_b     = sqrt(k*(d0/(tau*c))^gamma);
        SNR_lin = 10^(SNR/10);
        sigma_n = sqrt(Es/SNR_lin);
        noise   = (1/sqrt(2))*sigma_n * (randn(1,length(t))
                   + j*randn(1,length(t)));
        r       = a_b*s_tau+noise;
        R       = fft(r);
        rho     = real(ifft(conj(S).*R));
```

```
        [C I]   = max(rho);
        hat_tau_b_MC    = t(I);
        error_MC(n_R)   = hat_tau_b_MC-tau;
        corr    = ab_range.^2*Es-2*ab_range.*rho;
        [C I]   = min(corr);
        hat_tau_b_ML    = t(I);
        error_ML(n_R)   = hat_tau_b_ML-tau;
    end
    tau
    RMS_ML(n_tau) = sqrt(mean(error_ML.^2));
    RMS_MC(n_tau) = sqrt(mean(error_MC.^2));
end
%Theorical RMSE
beta    = sqrt(5/(2*pi*tau_p^2));
ab_range= sqrt(k*(d0./(tau_range*c)).^gamma);
En_MC   = sqrt(1./(10^(SNR/10)*ab_range.^2*8*pi^2*beta^2));
En_ML   = sqrt(1./(10^(SNR/10)*ab_range.^2
          .*(8*pi^2*beta^2+gamma.^2./(2*tau_range.^2))));
plot(tau_range*c,RMS_MC*c,'+',tau_range*c,En_MC*c,'--',
     tau_range*c,RMS_ML*c,'^',tau_range*c,En_ML*c,':'),
legend('MC: Simulation','MC: Theorical',
       'ML: Simulaton','ML: Theorical'),
title('Indoor Tau estimation - RMSE as a function of \tau_b'),
      xlabel('\tau_b'),ylabel('RMSE (m)')
```

B.16 MATLAB® File for the RMSE of the Position Estimate as a Function of $\mathrm{SNR}_{\mathrm{Rx}}$: Outdoor Scenario (Fig. 4.5)

```
%%%%% Outdoor %%%%%%%%
f0    = 0.9e9; d0 = 100;  dmax =3e3;
gamma = 4;     c  = 3e8;
k     = c^2/(16*pi^2*d0^2*f0^2);
tau   = 500/c;  SNR_range = (0:2:55);
n_SNR = 0;      N_R_frame = 20;  N_R_noise = 50;
N_bits= 2;      R_B       = 140e3; %wireless communication p.12
T     = 1/R_B;  Ts        = T*(N_bits-1);  t0 = 1.005*(Ts+tau);
t_sample = t0/1e6;         t    = 1e-100:t_sample:t0;
```

```
a_b      = sqrt(k*(d0/(tau*c))^gamma);
ab_range = sqrt(k*(d0./(t*c)).^gamma);
for SNR = SNR_range
   n_SNR = n_SNR+1;
   SNR_lin =   10^(SNR/10);
   for n_R_frame = 1:N_R_frame
       frame = sign(2 * rand(1,N_bits) -  1);
       s     = MSK_mod(frame,R_B,f0,0,t, t_sample);
       S     = fft(s);
       Es    = sum((abs(s)).^2);
       delay = round(tau/t_sample);
       s_tau = [zeros(1,delay) s(1:(end- delay))];
       sigma_n =   sqrt(Es*a_b^2/SNR_lin);
       for n_R_noise = 1:N_R_noise
            n_R_noise
            noise   = (1/sqrt(2))*sigma_n*(randn(1,length(t))
                      + j*randn(1,length(t)));
            %received signal
            r = a_b*s_tau+noise;
            R = fft(r);
            rho  = real(ifft(conj(S).*R));
            [C I] = max(rho);
            hat_tau_b_MC  = t(I);
            error_noise_MC(n_R_noise) = hat_tau_b_MC-tau;
            corr = ab_range.^2*Es - 2*ab_range.*rho;
            [C I] = min(corr);
            hat_tau_b_ML = t(I);
            error_noise_ML(n_R_noise) = hat_tau_b_ML-tau;
        end
        error_MC(n_R_frame)= mean (error_noise_MC.^2);
        error_ML(n_R_frame)= mean (error_noise_ML.^2);
    end
    RMS_ML(n_SNR) = sqrt(mean(error_ML));
    RMS_MC(n_SNR) = sqrt(mean(error_MC));
end
%%%Theorical RMSE
beta2     = f0^2 + 1/(16*T^2);
MCRB_MC   = 1./sqrt(10.^(SNR_range./10)*8*pi^2*beta2);
MCRB_ML   = 1./sqrt(10.^(SNR_range./10)
            *(8*pi^2*beta2 + gamma^2/(2*tau^2)));
```

```
beta3     = (16*f0^2 + 1/T^2)
             /(16*f0^4 + 1/(16*T^4)- 2*f0^2 *(1/T^2));
ACRB_MC   = sqrt((1./(10.^(SNR_range./10)*8*pi^2))*beta3);
ACRB_ML   = sqrt((1./(10.^(SNR_range./10)*2))
            * (1/(2*(2*pi*f0-pi/(2*T))^2+ gamma^2/(2*tau^2))
            + 1/(2*(2*pi*f0+pi/(2*T))^2+ gamma^2/(2*tau^2))));
figure,
plot(SNR_range,RMS_MC*c,'+',SNR_range,ACRB_MC*c,'-',
SNR_range,MCRB_MC*c,'--',SNR_range,RMS_ML*c,'o',
SNR_range,ACRB_ML*c,'-.',SNR_range,MCRB_ML*c,':')
legend('MC: Simulation','MC: ACRB','MC Analysis: MCRB',
'ML Simulation','ML Analysis: ACRB','ML Analysis: MCRB'),
title('RMSE as a function of the SNR_{Rx}: Outdoor scenario'),
xlabel('SNR (dB)'),ylabel('RMSE (m)')
```

B.17 MATLAB® File for the Comparison of the Theoretical Bias of the Position Estimate as a Function of δ_γ for the Friedlander and the Taylor Expansion Methods for Several Values of γ_0 (Fig. 5.1)

```
%%%%%%% Indoor %%%%%%%%
tau_p   = 0.2877e-9;
d0      = 0.05;
c       = 3e8;
tau     = 3/c;
gamma_0_range       = [1.6:0.5:3.5];
delta_gamma         = [-1.5:0.1:1.5];
n_gamma             = 0;
beta    = sqrt(5/(2*pi*tau_p^2));
g       = d0/(c*tau);
for gamma_0 = gamma_0_range
    n_gamma = n_gamma+1;
    temp= g.^(delta_gamma/2);
    num1 = (gamma_0 + 2*delta_gamma).*(1-temp)
           + delta_gamma.*(gamma_0+delta_gamma)
            .*log(g).*(1/2-temp);
    den1 = 8*pi^2*beta^2*tau^2
           -(gamma_0+delta_gamma)
```

```
            .*(1-temp+(gamma_0+delta_gamma).*(1/2-temp));
    T_Bias_ML(n_gamma,:) = -tau*num1./den1;
    numF = delta_gamma.*(1-temp+(gamma_0+delta_gamma)
            .*log(g).*(1/2-temp));
    T_Bias_ML_F(n_gamma,:) = -tau*numF./den1;
end
hold on,
plot(delta_gamma,T_Bias_ML_F(1,:)*c,':+',
delta_gamma,T_Bias_ML_F(2,:)*c,':+',
delta_gamma,T_Bias_ML_F(3,:)*c,':+',
delta_gamma,T_Bias_ML_F(4,:)*c,':+',
delta_gamma,T_Bias_ML(5,:)*c,':+'),
plot(delta_gamma,T_Bias_ML(1,:)*c,'--o',
delta_gamma,T_Bias_ML(2,:)*c,'--o',
delta_gamma,T_Bias_ML(3,:)*c,'--o',
delta_gamma,T_Bias_ML(4,:)*c,'--o',
delta_gamma,T_Bias_ML(5,:)*c,'--o'),
legend('Friedlander(\gamma_0 = 1.6)','\gamma_0 = 2',
'\gamma_0 = 2.5','\gamma_0 = 3','\gamma_0 = 3.5','TE'),
title('Bias as a function of \delta_\gamma : Indoor scenario'),
xlabel('\delta_\gamma'),ylabel('Bias (m)')
```

B.18 MATLAB® File for the Comparison of the Theoretical RMSE of the Position Estimate as a Function of δ_γ for the Friedlander and the Taylor Expansion Methods for Several Values of γ_0 and Large SNR (Fig. 5.3)

```
tau_p   = 0.2877e-9;  f0   = 16/(3*pi*tau_p); d0  = 0.05;
c       = 3e8;        k    = c^2/(16*pi^2*d0^2*f0^2);
tau     = 3/c;        SNR  = 200;      SNR = 10^(SNR/10);
gamma_0_range = [1.6 3.5]; delta_gamma = [-1.5:0.1:1.5];
n_gamma = 0;  beta = sqrt(5/(2*pi*tau_p^2));  g = d0/(c*tau);
for gamma_0 = gamma_0_range
    n_gamma = n_gamma+1; temp = g.^(delta_gamma/2);
    ab_0    = sqrt(k*(d0/(tau*c))^gamma_0);
    den = (temp.*(gamma_0+delta_gamma)
```

```
            .*(1+gamma_0+delta_gamma)
          - (gamma_0+delta_gamma)
            .*(1+gamma_0/2+delta_gamma/2)
          + 8*pi^2*beta^2*tau^2).^2;
    num2 =  ((gamma_0 + 2*delta_gamma).*(1-temp)
          + delta_gamma.*(gamma_0+delta_gamma)
            .*log(g).*(1/2-temp)).^2
          + (1/2)*(1./(ab_0.^2.*SNR))
            .*((gamma_0+delta_gamma)
          + delta_gamma
              .*(1+ (gamma_0+delta_gamma)/2.*log(g))).^2
          + (1./(ab_0.^2*SNR)).*2*pi^2*beta^2*tau^2
              .*(2+ delta_gamma.*log(g)).^2;
    T_RMSE_ML_without(n_gamma,:) = sqrt(tau^2*num2./den);
    num1 = ((gamma_0 + 2*delta_gamma).*(1-temp)
           + delta_gamma.*(gamma_0+delta_gamma)
            .*log(g).*(1/2-temp)).^2
           + (1/(ab_0^2*SNR))*((gamma_0+delta_gamma).^2/2
           + 8*pi^2*beta^2*tau^2);
    T_RMSE_ML_with(n_gamma,:) = sqrt(tau^2*num1./den);
    num_F_without = (1-temp+(gamma_0+delta_gamma)
                     .*log(g).*(1/2-temp)).^2
                    + (1/2)* (1./(ab_0^2.*SNR))
                     .*(1+1/2*(gamma_0+delta_gamma).*log(g)).^2
                    + (1./(ab_0^2.*SNR))
                     .* 2*pi^2*beta^2*tau^2*(log(g))^2;
    T_RMSE_ML_F_without(n_gamma,:) = delta_gamma.*tau
                                     .*sqrt(*num_F_without./den);
    num_F_with = (1-temp+(gamma_0+delta_gamma)
                  .*log(g).*(1/2-temp)).^2 ;
    T_RMSE_ML_F_with(n_gamma,:) = delta_gamma.*tau.*
                                  sqrt(num_F_with./den);
end
hold on,
plot(delta_gamma,T_RMSE_ML_F_without(1,:)*c,'-.s',
delta_gamma,T_RMSE_ML_F_without(2,:)*c,'-.s'),
plot(delta_gamma,T_RMSE_ML_F_with(1,:)*c,'-.x',
delta_gamma,T_RMSE_ML_F_without(2,:)*c,'-.x'),
plot(delta_gamma,T_RMSE_ML_without(1,:)*c,'--o',
delta_gamma,T_RMSE_ML_without(2,:)*c,'--o')
```

```
plot(delta_gamma,T_RMSE_ML_with(1,:)*c,':+',
delta_gamma,T_RMSE_ML_with(2,:)*c,':+'),
legend('F without ECD(\gamma_0 = 1.6)','(\gamma_0 = 3.5)',
'F with ECD(\gamma_0 = 1.6)','(\gamma_0 = 3.5)',
'TE without ECD (\gamma_0 = 1.6)','(\gamma_0 = 3.5)',
'TE with ECD'),
title('RMSE as a function of \delta_\gamma : Indoor scenario'),
xlabel('\delta_\gamma'),ylabel('RMSE (m)')
```

B.19 MATLAB® File for the Comparison of the Theoretical RMSE of the Position Estimate as a Function of δ_γ for the Friedlander and the Taylor Expansion Methods for Several Values of γ_0 (Fig. 5.4)

```
tau_p   = 0.2877e-9;
d0      = 0.05;    c  = 3e8;
tau     = 3/c;
SNR     = 20;      SNR = 10^(SNR/10);
gamma_0_range     = [1.6 3.5];
delta_gamma       = [-1.5:0.1:1.5]; n_gamma = 0;
beta    = sqrt(5/(2*pi*tau_p^2));   g  = d0/(c*tau);
for gamma_0 = gamma_0_range
    n_gamma = n_gamma+1;
    temp = g.^(delta_gamma/2);
    den  = (temp.*(gamma_0+delta_gamma).*(1+gamma_0+delta_gamma)
          - (gamma_0+delta_gamma).*(1+gamma_0/2+delta_gamma/2)
          + 8*pi^2*beta^2*tau^2).^2;
    num2 = ((gamma_0 + 2*delta_gamma).*(1-temp)
          + delta_gamma.*(gamma_0+delta_gamma)
           .*log(g).*(1/2-temp)).^2
          + (1/2)*(1./SNR).*((gamma_0+delta_gamma)
          + delta_gamma.*(1+ (gamma_0+delta_gamma)/2
            .*log(g))).^2
          + (1./SNR).*2*pi^2*beta^2*tau^2
           .*(2+ delta_gamma.*log(g)).^2;
    T_RMSE_ML_without(n_gamma,:) = sqrt(tau^2*num2./den);
    num1 = ((gamma_0 + 2*delta_gamma).*(1-temp)
           + delta_gamma.*(gamma_0+delta_gamma)
```

```
            .*log(g).*(1/2-temp)).^2
          + (1/SNR)*((gamma_0+delta_gamma).^2/2
          + 8*pi^2*beta^2*tau^2);
    T_RMSE_ML_with(n_gamma,:) = sqrt(tau^2*num1./den);
    num_F_without = (1-temp+(gamma_0+delta_gamma)
                     .*log(g).*(1/2-temp)).^2
                    + (1/2)* (1./SNR)
                     .*(1+1/2*(gamma_0+delta_gamma).*log(g)).^2
                    + (1./SNR)
                     .* 2*pi^2*beta^2*tau^2*(log(g))^2;
    T_RMSE_ML_F_without(n_gamma,:) = delta_gamma.*tau
                                     .*sqrt(num_F_without./den);
    num_F_with = (1-temp+(gamma_0+delta_gamma).*log(g)
                  .*(1/2-temp)).^2 ;
    T_RMSE_ML_F_with(n_gamma,:) = delta_gamma.*tau
                                  .*sqrt(num_F_with./den);

end
figure,
hold on,
plot(delta_gamma,T_RMSE_ML_F_without(1,:)*c,'b-s',
delta_gamma,T_RMSE_ML_F_without(2,:)*c,'b-*'),
plot(delta_gamma,T_RMSE_ML_F_with(1,:)*c,'m:^',
delta_gamma,T_RMSE_ML_F_with(2,:)*c,'m:p'),
plot(delta_gamma,T_RMSE_ML_without(1,:)*c,'g-x',
delta_gamma,T_RMSE_ML_without(2,:)*c,'g-o'),
plot(delta_gamma,T_RMSE_ML_with(1,:)*c,'r:+',
delta_gamma,T_RMSE_ML_with(2,:)*c,'r:d'),
legend('F without ECD (\gamma_0 = 1.6)',
'F without ECD (\gamma_0 = 3.5)',
'F with ECD (\gamma_0 = 1.6)',
'F with ECD (\gamma_0 = 3.5)',
'TE without ECD (\gamma_0 = 1.6)',
'TE without ECD (\gamma_0 = 3.5)',
'TE with ECD (\gamma_0 = 1.6)',
'TE with ECD (\gamma_0 = 3.5)'),
title('RMSE as a function of \delta_\gamma : Indoor scenario'),
xlabel('\delta_\gamma'),ylabel('RMSE (m)')
```

B.20 MATLAB® File for the Comparison of the Theoretical RMSE of the Position Estimate as a Function of δ_γ for the Friedlander and the Taylor Expansion Methods for Several Values of $\mathrm{SNR}_{\mathrm{Rx}}$ (Fig. 5.5)

```
%%%%% Indoor %%%%%%%%
tau_p    = 0.2877e-9;
d0       = 0.05;
c        = 3e8;
tau      = 3/c;
SNR_range= [20 100];  SNR_range   = 10.^(SNR_range/10);
gamma_0  = 2.5;       delta_gamma = [-1.5:0.1:1.5];
n_SNR    = 0;
beta     = sqrt(5/(2*pi*tau_p^2)); g = d0/(c*tau);
for SNR = SNR_range
    n_SNR= n_SNR+1;
    temp = g.^(delta_gamma/2);
    den  = (temp.*(gamma_0+delta_gamma).*(1+gamma_0+delta_gamma)
          - (gamma_0+delta_gamma).*(1+gamma_0/2+delta_gamma/2)
          + 8*pi^2*beta^2*tau^2).^2;
    num = ((gamma_0 + 2*delta_gamma).*(1-temp)
          + delta_gamma.*(gamma_0+delta_gamma)
           .*log(g).*(1/2-temp)).^2
          + (1/2)*(1./SNR).*((gamma_0+delta_gamma)
          + delta_gamma.*(1+ (gamma_0+delta_gamma)/2
            .*log(g))).^2
          + (1./SNR).*2*pi^2*beta^2*tau^2
           .*(2+ delta_gamma.*log(g)).^2;
    T_RMSE_ML_without(n_SNR,:) = sqrt(tau^2*num./den);
    num1 = ((gamma_0 + 2*delta_gamma).*(1-temp)
           + delta_gamma.*(gamma_0+delta_gamma)
            .*log(g).*(1/2-temp)).^2
           + (1/SNR)*((gamma_0+delta_gamma).^2/2
           + 8*pi^2*beta^2*tau^2);
    T_RMSE_ML_with(n_SNR,:) = sqrt(tau^2*num1./den);
    num_F_without = (1-temp+(gamma_0+delta_gamma)
                     .*log(g).*(1/2-temp)).^2
                    + (1/2)* (1./SNR)
                     .*(1+1/2*(gamma_0+delta_gamma).*log(g)).^2
```

```
                    + (1./SNR)
                     .* 2*pi^2*beta^2*tau^2*(log(g))^2;
    T_RMSE_ML_F_without(n_SNR,:) = delta_gamma.*tau
                                    .*sqrt(num_F_without./den);
    num_F_with = (1-temp+(gamma_0+delta_gamma)
                  .*log(g).*(1/2-temp)).^2 ;
    T_RMSE_ML_F_with(n_SNR,:) = delta_gamma.*tau
                                  .*sqrt(num_F_with./den);
end
figure,
hold on,
plot(SNR_range,T_RMSE_ML_F_without(1,:)*c,'b-s',
SNR_range,T_RMSE_ML_F_without(2,:)*c,'b-*'),
plot(SNR_range,T_RMSE_ML_F_with(1,:)*c,'m:^',
SNR_range,T_RMSE_ML_F_with(2,:)*c,'m:p'),
plot(SNR_range,T_RMSE_ML_without(1,:)*c,'g-x',
SNR_range,T_RMSE_ML_without(2,:)*c,'g-o'),
plot(SNR_range,T_RMSE_ML_with(1,:)*c,'r:+',
SNR_range,T_RMSE_ML_with(2,:)*c,'r:d'),
legend('F without ECD (SNR_{Rx}=20)',
'F without ECD (SNR_{Rx}=100)',
'F with ECD (SNR_{Rx}=20)',
'F with ECD (SNR_{Rx}=100)',
'TE without ECD (SNR_{Rx}=20)',
'TE without ECD (SNR_{Rx}=100)',
'TE with ECD (SNR_{Rx}=20)',
'TE with ECD (SNR_{Rx}=100)'),
title('RMSE as a function of \delta_\gamma : Indoor scenario'),
xlabel('\delta_\gamma'),ylabel('RMSE (m)')
```

B.21 MATLAB® File for the Taylor Expansion Method With the Expectation of the Cross-derivative for the RMSE of the Position Estimate as a Function of δ_γ for the Indoor Scenario and Several Values of γ_0 (Fig. 5.6)

```
%%%%%%% Indoor %%%%%%%%
```

```
tau_p   = 0.2877e-9;
d0      = 0.05;
c       = 3e8;
tau     = 3/c;
SNR     = 0;
SNR     = 10^(SNR/10);
gamma_0_range     = [1.5:0.5:3.5];
gamma_0_range(1)  = 1.6;
delta_gamma       = [-1.5:0.1:1.5];
n_gamma = 0;
beta    = sqrt(5/(2*pi*tau_p^2));
g       = d0/(c*tau);

for gamma_0 = gamma_0_range
    n_gamma = n_gamma+1;
    temp    = g.^(delta_gamma/2);
    num1    = ((gamma_0 + 2*delta_gamma).*(1-temp)
              + delta_gamma.*(gamma_0+delta_gamma)
                 .*log(g).*(1/2-temp)).^2
              + (1/SNR)*((gamma_0+delta_gamma).^2/2
                                  + 8*pi^2*beta^2*tau^2);
    den1     = (temp.*(gamma_0+delta_gamma)
                .*(1+gamma_0+delta_gamma)
              - (gamma_0+delta_gamma)
                .*(1+gamma_0/2+delta_gamma/2)
              + 8*pi^2*beta^2*tau^2).^2;
    T_RMSE_ML1(n_gamma,:) = sqrt(tau^2*num1./den1);
end
hold on,
plot(delta_gamma,T_RMSE_ML1(1,:)*c,'b--o',
delta_gamma,T_RMSE_ML1(2,:)*c,'b--s',
delta_gamma,T_RMSE_ML1(3,:)*c,'b--^',
delta_gamma,T_RMSE_ML1(4,:)*c,'b--p',
delta_gamma,T_RMSE_ML1(5,:)*c,'b--+')
legend('\gamma_0 = 1.6','\gamma_0 = 2',
     '\gamma_0 = 2.5','\gamma_0 = 3','\gamma_0 = 3.5'),
title('RMSE as a function of \delta_\gamma : Indoor scenario'),
xlabel('\delta_\gamma'),ylabel('RMSE (m)')
```

B.22 MATLAB® File for the Taylor Expansion Method With the Expectation of the Cross-derivative for the RMSE of the Position Estimate as a Function of δ_γ for the Indoor Scenario and Several Values of $\mathrm{SNR}_{\mathrm{Rx}}$ (Fig. 5.7)

```
%%%%%%% Indoor %%%%%%%%
tau_p    = 0.2877e-9;
d0       = 0.05;
c        = 3e8;
tau      = 3/c;
SNR_range   = [10:20:90];
SNR_range   = 10.^(SNR_range/10);
gamma_0     = 2.5;
delta_gamma = [-1.5:0.1:1.5];
n_SNR       = 0;
beta        = sqrt(5/(2*pi*tau_p^2));
g           = d0/(c*tau);

for SNR = SNR_range
    n_SNR= n_SNR+1;
    temp = g.^(delta_gamma/2);
    num1 = ((gamma_0 + 2*delta_gamma).*(1-temp)
           + delta_gamma.*(gamma_0+delta_gamma)
             .*log(g).*(1/2-temp)).^2
           + (1/SNR)*((gamma_0+delta_gamma).^2/2
           + 8*pi^2*beta^2*tau^2);
    den1     = (temp.*(gamma_0+delta_gamma)
                .*(1+gamma_0+delta_gamma)
              - (gamma_0+delta_gamma)
                .*(1+gamma_0/2+delta_gamma/2)
              + 8*pi^2*beta^2*tau^2).^2;
    T_RMSE_ML1(n_SNR,:) = sqrt(tau^2*num1./den1);
end
hold on,
plot(delta_gamma,T_RMSE_ML1(1,:)*c,'b--o',
delta_gamma,T_RMSE_ML1(2,:)*c,'b--s',
delta_gamma,T_RMSE_ML1(3,:)*c,'b--^',
```

```
delta_gamma,T_RMSE_ML1(4,:)*c,'b--p',
delta_gamma,T_RMSE_ML1(5,:)*c,'b--+')
legend('SNR_{Rx} = 10','SNR_{Rx} = 30','SNR_{Rx} = 50',
'SNR_{Rx} = 70','SNR_{Rx} = 90' ),
title('RMSE as a function of \delta_\gamma : Indoor scenario'),
xlabel('\delta_\gamma'),ylabel('RMSE (m)')
```

B.23 MATLAB® File for the Simulation of the Bias and the RMSEs as a Function of $\mathrm{SNR_{RX}}$ for the Indoor Scenario (Fig. 5.10-5.13)

```
%%%%%%% Indoor %%%%%%%%
%%%%Imperfect PLE %%%%%
tau_p = 0.2877e-9;
Tp    = 0.7e-9;
f0    = 16/(3*pi*tau_p);
d0    = 0.05;
dmax  = 6;
c     = 3e8;
k     = c^2/(16*pi^2*d0^2*f0^2);
SNR_range = [-10:5:50];
tau       = 3/c;
tau_min   = d0/c;
tau_max   = dmax/c;
t0        = 1.5*tau_max;
gamma_0   = 2;
imp_gamma = 2.5;
n_snr     = 0;
N_R       = 1000;
imp_gamma = 2.5;
t_sample  = tau/1e6;
t         = (1e-100:t_sample:t0);
tau_range = t;
%tansmit signal
alpha_1 = 2*pi*((t-0.5*Tp)/tau_p).^2;
s       = (1-2*alpha_1).*exp(-alpha_1);
S       = fft(s);
Es      = sum((abs(s)).^2);
```

```
%receive signal
alpha_2    = 2*pi*((t-0.5*Tp-tau)/tau_p).^2;
s_tau      = (1-2*alpha_2).*exp(-alpha_2);
ab_0       = sqrt(k*(d0/(tau*c))^gamma_0);
ab_perfect = sqrt(k*(d0./(tau_range*c)).^gamma_0);
a_b        = sqrt(k*(d0./(tau*c)).^imp_gamma);
a_b_range  = sqrt(k*(d0./(tau_range*c)).^imp_gamma);
beta       = sqrt(5/(2*pi*tau_p^2));
for SNR = SNR_range
    n_snr   = n_snr+1;
    SNR_lin = 10^(SNR/10);
    sigma_n = sqrt(Es*ab_0^2/SNR_lin);
    for n_R = 1:N_R
        noise = (1/sqrt(2)) * sigma_n
                *(randn(1,length(t))+j*randn(1,length(t)));
        r   =   ab_0*s_tau+noise;
        R   =   fft(r);
        rho             =   real(ifft(conj(S).*R));
        [C I]           =   max(rho);
        hat_tau_b_MC    =   t(I);
        error_MC(n_R)   =   hat_tau_b_MC- tau;
        corr1     =   a_b_range.^2*Es-2*a_b_range.*rho;
        [C1 I1]   =   min(corr1);
        hat_tau_b_ML1        =   t(I1);
        error_ML_IPLE(n_R)   =   hat_tau_b_ML1- tau;
        corr2     =   ab_perfect.^2*Es-2*ab_perfect.*rho;
        [C2 I2]   =   min(corr2);
        hat_tau_b_ML2       =   t(I2);
        error_ML_PLE(n_R)   =   hat_tau_b_ML2- tau;
    end
    S_Bias_ML_IPLE(n_snr) = mean(error_ML_IPLE);
    S_Bias_ML_PLE(n_snr)  = mean(error_ML_PLE);
    S_Bias_MC(n_snr)      = mean(error_MC);
    num = (2*imp_gamma-gamma_0)*(ab_0-a_b)
          + imp_gamma*(imp_gamma-gamma_0)
           *log(d0/(c*tau))*(ab_0/2-a_b);
    den =  8*pi^2*beta^2*tau^2*ab_0
           -(imp_gamma*(ab_0-a_b)+imp_gamma^2*(ab_0/2-a_b));
    T_Bias_ML(n_snr)      = -tau*num/den;
    numF= (imp_gamma-gamma_0)*(ab_0-a_b)
```

```
        - imp_gamma*(imp_gamma-gamma_0)
          *log(d0/(c*tau))*(a_b - ab_0/2);
    T_Bias_ML_F(n_snr)    = -tau*numF./den;
    S_RMSE_ML_IPLE(n_snr) = sqrt(mean(error_ML_IPLE.^2));
    S_RMSE_ML_PLE(n_snr)  = sqrt(mean(error_ML_PLE.^2));
    S_RMSE_MC(n_snr)      = sqrt(mean(error_MC.^2));
    num1 = ((2*imp_gamma-gamma_0)*(1-a_b/ab_0)
           + imp_gamma*(imp_gamma-gamma_0)
            *log(d0/(c*tau))*(1/2-a_b/ab_0) )^2
           + (sigma_n^2/(Es*ab_0^2))
            *(imp_gamma^2/2+8*pi^2*beta^2*tau^2);
    den1 = ((a_b/ab_0)*imp_gamma*(1+imp_gamma)
           -imp_gamma*(1+imp_gamma/2)
           + 8 *pi^2*beta^2*tau^2)^2;
    T_RMSE_ML_with(n_snr) = sqrt(tau^2*num1/den1);
    num2 = ((2*imp_gamma-gamma_0)*(1-a_b/ab_0)
           + imp_gamma*(imp_gamma-gamma_0)
             *log(d0/(c*tau))*(1/2-a_b/ab_0) )^2
           + (1/2)*(sigma_n^2/(Es*ab_0^2))
             *(imp_gamma+ (imp_gamma-gamma_0)
             *(1+imp_gamma/2*log(d0/(c*tau))))^2
           + sigma_n^2/(Es*ab_0^2)*2*pi^2*beta^2*tau^2
             *(2+ (imp_gamma-gamma_0)*log(d0/(c*tau)))^2;
    T_RMSE_ML_without(n_snr)   = sqrt(tau^2*num2/den1);
    num3 = (1-a_b/ab_0+imp_gamma*log(d0/(c*tau))
            *(1/2-a_b/ab_0))^2
           +(1/2)*(sigma_n^2/(Es*ab_0^2))
             *(1+imp_gamma/2*log(d0/(c*tau)))^2
           + (sigma_n^2/(Es*ab_0^2))*2*pi^2*beta^2*tau^2
             *(log(d0/(c*tau)))^2;
    T_RMSE_ML_F_without(n_snr) = tau.*sqrt((imp_gamma
                                 -gamma_0).^2.*num3/den1);
    num4 = (1-a_b/ab_0+imp_gamma*log(d0/(c*tau))
            *(1/2-a_b/ab_0))^2;
    T_RMSE_ML_F_with(n_snr)    = tau.*sqrt((imp_gamma
                                 -gamma_0).^2.*num4/den1);
    T_MC_PLE(n_snr) =  1/sqrt(SNR_lin*8*pi^2*beta^2);
    T_ML_PLE(n_snr) =  1/sqrt(SNR_lin*(8*pi^2*beta^2
                              + gamma_0^2/(2*tau^2)));
end
```

```
figure,plot(SNR_range,S_Bias_MC*c,'p',
SNR_range,S_Bias_ML_PLE*c,'s',
SNR_range,S_Bias_ML_IPLE*c,'*',
SNR_range,T_Bias_ML_F*c,'-+',
SNR_range,T_Bias_ML*c,'-o'),
legend('MC Simulation','ML: Perfect PLE',
'ML: Imperfect PLE','ML: Friedlander',
'ML: Taylor Expansion'),
title('Bias as a function of SNR_{Rx}: Indoor scenario'),
xlabel('SNR_{Rx} (dB)'),ylabel('Bias (m)')
figure,plot(SNR_range,S_RMSE_MC*c,'+',
SNR_range,T_MC_PLE*c,'--',
SNR_range,S_RMSE_ML_PLE*c,'o',SNR_range,T_MC_PLE*c,'-.',
SNR_range,S_RMSE_ML_IPLE*c,'s',
SNR_range,T_RMSE_ML_F_without*c,':v',
SNR_range,T_RMSE_ML_F_with*c,':x',
SNR_range,T_RMSE_ML_without*c,':p',
SNR_range,T_RMSE_ML_with*c,'-'),
legend('MC Simulation','MC Analysis',
'ML Simulation: Perfect PLE','ML Analysis: Perfect PLE',
'ML Simulation: Imperfect PLE','ML Analysis: F without ECD',
'ML Analysis: F with ECD','ML Analysis: TE without ECD',
'ML Analysis: TE with ECD'),
title('RMSE as a function of SNR_{Rx}: Indoor scenario'),
xlabel('SNR_{Rx} (dB)'),ylabel('RMSE (m)')
```

B.24 MATLAB® File for the Simulation of the Bias and the RMSEs as a Function of δ_γ for the Indoor Scenario (Fig. 5.14-5.17)

```
%%%%%%% Indoor %%%%%%%%
%%%%Imperfect PLE %%%%%
tau_p = 0.2877e-9;
Tp    = 0.7e-9;
f0    = 16/(3*pi*tau_p);
d0    = 0.05;
dmax  = 6;
c     = 3e8;
```

```
k     = c^2/(16*pi^2*d0^2*f0^2);
SNR   = 20;
tau   = 3/c;
tau_min = d0/c;
tau_max = dmax/c;
t0      = 1.5*tau_max;
gamma_0  = 2;
n_gamma  = 0;
N_R      = 5000;
t_sample = tau/1e6;
tau_range=t;
imperfect_gamma_range = [1.6:0.1:3.5];
t                     = (1e-100:t_sample:t0);
%tansmit signal
alpha_1 = 2*pi*((t-0.5*Tp)/tau_p).^2;
s       = (1-2*alpha_1).*exp(-alpha_1);
S       = fft(s);
Es      = sum((abs(s)).^2);
%receive signal
alpha_2 = 2*pi*((t-0.5*Tp-tau)/tau_p).^2;
s_tau   = (1-2*alpha_2).*exp(-alpha_2);
ab_0    = sqrt(k*(d0/(tau*c))^gamma_0);
ab_perfect = sqrt(k*(d0./(tau_range*c)).^gamma_0);
beta    = sqrt(5/(2*pi*tau_p^2));
SNR_lin = 10^(SNR/10);
sigma_n = sqrt(Es*ab_0^2/SNR_lin);
for imp_gamma = imperfect_gamma_range
    n_gamma = n_gamma+1;
    %let us fix SNR
    a_b       = sqrt(k*(d0./(tau*c)).^imp_gamma);
    a_b_range = sqrt(k*(d0./(tau_range*c)).^imp_gamma);
    for n_R = 1:N_R
        noise = (1/sqrt(2)) * sigma_n
                *(randn(1,length(t))+j*randn(1,length(t)));
        r     =   ab_0*s_tau+noise;
        R     =   fft(r);
        rho              =   real(ifft(conj(S).*R));
        [C I]            =   max(rho);
        hat_tau_b_MC     =   t(I);
        error_MC(n_R)    =   hat_tau_b_MC- tau;
```

```
    corr1     =   a_b_range.^2*Es-2*a_b_range.*rho;
    [C1 I1]   =   min(corr1);
    hat_tau_b_ML1        =   t(I1);
    error_ML_IPLE(n_R)   =   hat_tau_b_ML1- tau;
    corr2     =   ab_perfect.^2*Es-2*ab_perfect.*rho;
    [C2 I2]   =   min(corr2);
    hat_tau_b_ML2        =   t(I2);
    error_ML_PLE(n_R)    =   hat_tau_b_ML2- tau;
end
S_Bias_ML_IPLE(n_gamma) = mean(error_ML_IPLE);
S_Bias_ML_PLE(n_gamma)  = mean(error_ML_PLE);
S_Bias_MC(n_gamma)      = mean(error_MC);
num = (2*imp_gamma-gamma_0)*(ab_0-a_b)
      + imp_gamma*(imp_gamma-gamma_0)
       *log(d0/(c*tau))*(ab_0/2-a_b);
den = 8*pi^2*beta^2*tau^2*ab_0)-(imp_gamma*(ab_0-a_b)
      +imp_gamma^2*(ab_0/2-a_b));
T_Bias_ML(n_gamma) = -tau*num/den;
numF= (imp_gamma-gamma_0)*(ab_0-a_b)-imp_gamma
       *(imp_gamma-gamma_0)*log(d0/(c*tau))*(a_b - ab_0/2);
T_Bias_ML_F(n_gamma) = -tau*numF./den;
S_RMSE_ML_IPLE(n_gamma) = sqrt(mean(error_ML_IPLE.^2));
S_RMSE_ML_PLE(n_gamma)  = sqrt(mean(error_ML_PLE.^2));
S_RMSE_MC(n_gamma)      = sqrt(mean(error_MC.^2));
num1 = ((2*imp_gamma-gamma_0)*(1-a_b/ab_0)
       + imp_gamma*(imp_gamma-gamma_0)
         *log(d0/(c*tau))*(1/2-a_b/ab_0) )^2
       +(sigma_n^2/(Es*ab_0^2))
         *(imp_gamma^2/2+8*pi^2*beta^2*tau^2);
den1 = ((a_b/ab_0)*imp_gamma*(1+imp_gamma)
       - imp_gamma*(1+imp_gamma/2) + 8 *pi^2*beta^2*tau^2)^2;
T_RMSE_ML_with(n_gamma) = sqrt(tau^2*num1/den1);
num2 = ((2*imp_gamma-gamma_0)*(1-a_b/ab_0)
       + imp_gamma*(imp_gamma-gamma_0)
         *log(d0/(c*tau))*(1/2-a_b/ab_0) )^2
       + (1/2)*(sigma_n^2/(Es*ab_0^2))
        *(imp_gamma+ (imp_gamma-gamma_0)
        *(1+imp_gamma/2*log(d0/(c*tau))))^2
       + sigma_n^2/(Es*ab_0^2)*2*pi^2*beta^2*tau^2
        *(2+ (imp_gamma-gamma_0)*log(d0/(c*tau)))^2;
```

```
    T_RMSE_ML_without(n_gamma) = sqrt(tau^2*num2/den1);
    num3 = (1-a_b/ab_0+imp_gamma*log(d0/(c*tau))
             *(1/2-a_b/ab_0))^2
           +(1/2)*(sigma_n^2/(Es*ab_0^2))
             *(1+imp_gamma/2*log(d0/(c*tau)))^2
           +(sigma_n^2/(Es*ab_0^2))*2*pi^2*beta^2*tau^2
             *(log(d0/(c*tau)))^2;
    T_RMSE_ML_F_without(n_gamma) = tau.*sqrt((imp_gamma
                                    -gamma_0).^2.*num3/den1);
    num4 = (1-a_b/ab_0+imp_gamma*log(d0/(c*tau))
            *(1/2-a_b/ab_0))^2;
    T_RMSE_ML_F_with(n_gamma) = tau.*sqrt((imp_gamma
                                  -gamma_0).^2.*num4/den1);
end
T_MC_PLE   =  1/sqrt(SNR_lin*8*pi^2*beta^2)
              *ones(1,length(imperfect_gamma_range));
T_ML_PLE   =  1/sqrt(SNR_lin*(8*pi^2*beta^2
              + gamma_0^2/(2*tau^2)))
                *ones(1,length(imperfect_gamma_range));
x= imperfect_gamma_range
   - gamma_0*ones(1,length(imperfect_gamma_range));
figure,plot(x,S_Bias_MC*c,'p',x,S_Bias_ML_PLE*c,'s',
x,S_Bias_ML_IPLE*c,'*',x,T_Bias_ML_F*c,'-+',
x,T_Bias_ML*c,'-o'),
legend('MC Simulation','ML: Perfect PLE',
'ML: Imperfect PLE','ML: Friedlander',
'ML: Taylor epansion'),
title('Bias as a function of (\gamma-\gamma_0): Indoor scenario'),
xlabel('( \gamma - \gamma_0 )'),ylabel('Bias (m)')
figure,plot(x,S_RMSE_MC*c,'+',x,T_MC_PLE*c,'--',
x,S_RMSE_ML_PLE*c,'o',x,T_MC_PLE*c,'-.',
x,S_RMSE_ML_IPLE*c,'s',x,T_RMSE_ML_F_without*c,':v',
x,T_RMSE_ML_F_with*c,':x',x,T_RMSE_ML_without*c,':p',
x,T_RMSE_ML_with*c,'-'),
legend('MC Simulation','MC Analysis',
'ML Simulation: Perfect PLE','ML Analysis: Perfect PLE',
'ML Simulation: Imperfect PLE','ML Analysis: F without ECD',
'ML Analysis: F with ECD','ML Analysis: TE without ECD',
'ML Analysis: TE with ECD'),
title('RMSE as a function of (\gamma-\gamma_0): Indoor scenario'),
```

```
xlabel('(\gamma -\gamma_0)'),ylabel('RMSE (m)')
```

B.25 MATLAB® File for the Simulation of the RMSE and the Bias as a Function of $\mathrm{SNR_{RX}}$ for the Outdoor Scenario (Fig. 5.18-5.22)

```
%%%%%%% Outdoor %%%%%%%%
%%%Imperfect PLE%%%%%%%%
f0    = 0.9e9;
w0    = 2*pi*f0;
d0    = 100;
dmax  = 3e3;
c     = 3e8;
k     = c^2/(16*pi^2*d0^2*f0^2);
tau   = 500/c;
gamma_0   = 5;
imp_gamma = 6;
N_R_frame = 20;
N_R_noise = 50;
N_bits    = 2;
R_B       = 15e6;%unrealistic bit rate
T         = 1/R_B;
Ts        = T*(N_bits-1);
t0        = 1.005*(Ts+tau);
t_sample  = t0/1e6;
t         = 1e-100:t_sample:t0;
tau_range = t;
ab_0              = sqrt(k*(d0./(tau*c)).^gamma_0);
ab_range_perfect = sqrt(k*(d0./(tau_range*c)).^gamma_0);
a_b               = sqrt(k*(d0./(tau*c)).^imp_gamma);
ab_range          = sqrt(k*(d0./(tau_range*c)).^imp_gamma);
SNR_range = [-10:5:45];
n_snr     = 0;
for SNR = SNR_range
    n_snr   = n_snr+1;
    SNR_lin = 10^(SNR/10);
   for n_R_frame = 1:N_R_frame
       frame   = sign(2 * rand(1,N_bits) -  1);
```

```
s       = MSK_mod(frame,R_B,f0,0,t, t_sample);
S       = fft(s);
Es      = sum((abs(s)).^2);
delay   = round(tau/t_sample);
s_tau   =[zeros(1,delay) s(1:(end- delay))];
sigma_n = sqrt(Es*ab_0^2/SNR_lin);
for n_R_noise = 1:N_R_noise
     noise = (1/sqrt(2))* sigma_n
             *(randn(1,length(t))+j*randn(1,length(t)));
     %received signal
     r   = ab_0*s_tau+noise;

     R   = fft(r);
     rho = real(ifft(conj(S).*R));

     [C_MC I_MC]                = max(rho);
     hat_tau_b_MC               = t(I_MC);
     error_noise_MC(n_R_noise) = hat_tau_b_MC-tau;

     corr_ML_PLE
      = ab_range_perfect.^2*Es - 2*ab_range_perfect.*rho;
     [C_ML_PLE I_ML_PLE]           = min(corr_ML_PLE);
     hat_tau_b_ML_PLE              = t(I_ML_PLE);
     error_noise_ML_PLE(n_R_noise)
      = hat_tau_b_ML_PLE-tau;

     corr_ML_IPLE
      = ab_range.^2*Es - 2*ab_range.*rho;
     [C_ML_IPLE I_ML_IPLE]          = min(corr_ML_IPLE);
     hat_tau_b_ML_IPLE              = t(I_ML_IPLE);
     error_noise_ML_IPLE(n_R_noise)
      = hat_tau_b_ML_IPLE-tau;

end
error_MC(n_R_frame)      = mean(error_noise_MC);
error_ML_PLE(n_R_frame)  = mean(error_noise_ML_PLE);
error_ML_IPLE(n_R_frame) = mean(error_noise_ML_IPLE);

MSE_MC(n_R_frame)      = mean((error_noise_MC).^2);
MSE_ML_PLE(n_R_frame)  = mean((error_noise_ML_PLE).^2);
```

```
      MSE_ML_IPLE(n_R_frame) = mean((error_noise_ML_IPLE).^2);
      w=[];
      for i= 1:2:length(frame)
             w = [w w0-frame(i)*frame(i+1)/(2*T)];
      end
      beta2 = (1/(4*pi^2))*sum(w.^2)/(N_bits-1);

      num1  = ((2*imp_gamma-gamma_0)*(1-a_b/ab_0)
              + imp_gamma*(imp_gamma-gamma_0)
               *log(d0/(c*tau))*(1/2-a_b/ab_0) )^2
              + (sigma_n^2/(Es*ab_0^2))
               *(imp_gamma^2/2+8*pi^2*beta2*tau^2);
      den1  = ((a_b/ab_0)*imp_gamma*(1+imp_gamma)
              - imp_gamma*(1+imp_gamma/2)
                + 8 *pi^2*beta2*tau^2)^2;
      T_MSE_ML_with(n_R_frame) = tau^2*num1/den1;
      n_R_frame

end
Bias_MC(n_snr)      = mean(error_MC);
Bias_ML_PLE(n_snr)  = mean(error_ML_PLE);
Bias_ML_IPLE(n_snr) = mean(error_ML_IPLE);

S_RMSE_MC(n_snr)      = sqrt(mean(MSE_MC));
S_RMSE_ML_PLE(n_snr)  = sqrt(mean(MSE_ML_PLE));
S_RMSE_ML_IPLE(n_snr) = sqrt(mean(MSE_ML_IPLE));

Average_T_RMSE_ML_with(n_snr) = sqrt(mean(T_MSE_ML_with));

num1      = (2*imp_gamma-gamma_0)*(ab_0-a_b)
            +imp_gamma*(imp_gamma-gamma_0)
             *log(d0/(c*tau))*(ab_0/2-a_b);
num2      = 1/(2*tau^2*ab_0*(w0-pi/(2*T))^2
            -(imp_gamma*(ab_0-a_b)
           +imp_gamma^2*(ab_0/2-a_b)))
           + 1/(2*tau^2*ab_0*(w0+pi/(2*T))^2
           -(imp_gamma*(ab_0-a_b)
           +imp_gamma^2*(ab_0/2-a_b)));
AB(n_snr)       =    -(1/2)*tau*num1*num2;
```

```
    den3      = 8*pi^2*tau^2*ab_0*(f0^2+1/(16*T^2))
                -(imp_gamma*(ab_0-a_b)
                +imp_gamma^2*(ab_0/2-a_b));
    LBB(n_snr)      =    -tau*num1/den3;

    ACRB_MC(n_snr)   =  sqrt(((16*f0^2 + 1/T^2)
                       /(10.^(SNR./10)*8*pi^2
                         *(16*f0^4 + 1/(16*T^4)
                       - (1/T^2)*2*f0^2))));
    ACRB_ML(n_snr)   = sqrt((1./(2*10.^(SNR./10)))
                       *(1/(2*(2*pi*f0-pi/(2*T))^2
                       + gamma_0^2/(2*tau^2))
                       + 1/(2*(2*pi*f0+pi/(2*T))^2
                       + gamma_0^2/(2*tau^2))));
end
figure,plot(SNR_range,Bias_MC*c,'+',
SNR_range,Bias_ML_PLE*c,'o',
SNR_range,Bias_ML_IPLE*c,'s',
SNR_range,AB*c,'--',SNR_range,LBB*c,'-.'),
legend('MC Simulation',
'ML Simulation: Perfect PLE',
'ML Simulation: Imperfect PLE',
'ML Theory: Taylor with ECD',
'ML Theory: Lower/Upper Bound'),
title('Bias as a function of SNR_{Rx}: Outdoor scenario'),
xlabel('SNR_{Rx} (dB)'),ylabel('Bias (m)')
figure,plot(SNR_range,S_RMSE_MC*c,'+',
SNR_range,ACRB_MC*c,'--',
SNR_range,S_RMSE_ML_PLE*c,'o',
SNR_range,ACRB_ML*c,'-.',
SNR_range,S_RMSE_ML_IPLE*c,'s',
SNR_range,Average_T_RMSE_ML_with*c,':'),
legend('MC Simulation',
'ToA: ACRB',
'ML Simulation: Perfect PLE',
'SS-ToA: ACRB',
'ML Simulation: Imperfect PLE',
'ML Theory: Averaged TE with ECD'),
title('RMSE as a function of SNR_{Rx}: Outdoor scenario'),
xlabel('SNR_{Rx} (dB)'),ylabel('RMSE (m)')
```

B.26 MATLAB® File for the Simulation of the RMSE and the Bias as a Function of δ_γ for the Outdoor Scenario (Figures 5.23 and 5.24)

```
%%%%%%% Outdoor %%%%%%%%
%%%Transmitted signal is a MSK signal

f0      = 0.9e9;
w0      = 2*pi*f0;
d0      = 100;
dmax    = 3e3;
c       = 3e8;
k       = c^2/(16*pi^2*d0^2*f0^2);
tau     = 500/c;
gamma_0 = 5;
imperfect_gamma_range = [3.7:0.2:6.5];
n_gamma     = 0;
N_R_frame   = 20;
N_R_noise   = 50;
N_bits      = 2;
R_B         = 15e6;
T           = 1/R_B;
Ts          = T*(N_bits-1);
t0          = 1.005*(Ts+tau);
t_sample    = t0/5e6;
t           = 1e-100:t_sample:t0;
tau_range   = t;
SNR         = 32;
SNR_lin     = 10^(SNR/10);
ab_0              = sqrt(k*(d0./(tau*c)).^gamma_0);
ab_range_perfect = sqrt(k*(d0./(tau_range*c)).^gamma_0);
for imp_gamma = imperfect_gamma_range
    n_gamma = n_gamma+1;
    a_b      = sqrt(k*(d0./(tau*c)).^imp_gamma);
    ab_range = sqrt(k*(d0./(tau_range*c)).^imp_gamma);
   for n_R_frame = 1:N_R_frame
       frame    = sign(2 * rand(1,N_bits) -  1);
       s        = MSK_mod(frame,R_B,f0,0,t, t_sample);
       S        = fft(s);
```

```
Es       = sum((abs(s)).^2);
delay    = round(tau/t_sample);
s_tau    = [zeros(1,delay) s(1:(end- delay))];
sigma_n  = sqrt(Es*ab_0^2/SNR_lin);

for n_R_noise = 1:N_R_noise
     noise   = (1/sqrt(2))* sigma_n
            *(randn(1,length(t)) + j*randn(1,length(t)));
     %received signal
     r   = ab_0*s_tau+noise;

     R   = fft(r);
     rho = real(ifft(conj(S).*R));
     [C_MC I_MC]                = max(rho);
     hat_tau_b_MC               = t(I_MC);
     error_noise_MC(n_R_noise) = hat_tau_b_MC-tau;
     corr_ML_PLE                = ab_range_perfect.^2*Es
                                  -2*ab_range_perfect.*rho;
     [C_ML_PLE I_ML_PLE]        = min(corr_ML_PLE);
     hat_tau_b_ML_PLE           = t(I_ML_PLE);
     error_noise_ML_PLE(n_R_noise)
                                = hat_tau_b_ML_PLE-tau;
     corr_ML_IPLE               = ab_range.^2*Es
                                  -2*ab_range.*rho;
     [C_ML_IPLE I_ML_IPLE]      = min(corr_ML_IPLE);
     hat_tau_b_ML_IPLE          = t(I_ML_IPLE);
     error_noise_ML_IPLE(n_R_noise)
                                = hat_tau_b_ML_IPLE-tau;

 end
 error_MC(n_R_frame)       = mean(error_noise_MC);
 error_ML_PLE(n_R_frame)   = mean(error_noise_ML_PLE);
 error_ML_IPLE(n_R_frame)  = mean(error_noise_ML_IPLE);
 MSE_MC(n_R_frame)       = mean((error_noise_MC).^2);
 MSE_ML_PLE(n_R_frame)   = mean((error_noise_ML_PLE).^2);
 MSE_ML_IPLE(n_R_frame)  = mean((error_noise_ML_IPLE).^2);
 w=[];
 for i= 1:2:length(frame)
        w = [w 2*pi*f0-frame(i)*frame(i+1)/(2*T)];
 end
```

```
        beta2 = (1/(4*pi^2))*sum(w.^2)/(N_bits-1);
        num1  = ((2*imp_gamma-gamma_0)*(1-a_b/ab_0)
                + imp_gamma*(imp_gamma-gamma_0)
                 *log(d0/(c*tau))*(1/2-a_b/ab_0) )^2
                + (sigma_n^2/(Es*ab_0^2))
                 *(imp_gamma^2/2+8*pi^2*beta2*tau^2);
        den1  = ((a_b/ab_0)*imp_gamma*(1+imp_gamma)
                - imp_gamma*(1+imp_gamma/2)
                + 8 *pi^2*beta2*tau^2)^2;
        T_MSE_ML_with(n_R_frame) = tau^2*num1/den1;
    end
    Bias_MC(n_gamma)      = mean(error_MC);
    Bias_ML_PLE(n_gamma)  = mean(error_ML_PLE);
    Bias_ML_IPLE(n_gamma) = mean(error_ML_IPLE);

    S_RMSE_MC(n_gamma)      = sqrt(mean(MSE_MC));
    S_RMSE_ML_PLE(n_gamma)  = sqrt(mean(MSE_ML_PLE));
    S_RMSE_ML_IPLE(n_gamma) = sqrt(mean(MSE_ML_IPLE));
    Average_T_RMSE_ML_with(n_gamma) = sqrt(mean(T_MSE_ML_with));
    num1      = (2*imp_gamma-gamma_0)*(ab_0-a_b)
                +imp_gamma*(imp_gamma-gamma_0)
                 *log(d0/(c*tau))*(ab_0/2-a_b);
    num2      = 1/(2*tau^2*ab_0*(w0-pi/(2*T))^2
                -(imp_gamma*(ab_0-a_b)
                +imp_gamma^2*(ab_0/2-a_b)))
                + 1/(2*tau^2*ab_0*(w0+pi/(2*T))^2
                -(imp_gamma*(ab_0-a_b)
                +imp_gamma^2*(ab_0/2-a_b)));
    AB(n_gamma)        =    -(1/2)*tau*num1*num2;
    den3      = 8*pi^2*tau^2*ab_0*(f0^2+1/(16*T^2))
                -(imp_gamma*(ab_0-a_b)
                +imp_gamma^2*(ab_0/2-a_b));
    LBB(n_gamma)      =    -tau*num1/den3;
end
ACRB_MC   =  sqrt(((16*f0^2 + 1/T^2)
            /(10.^(SNR./10)*8*pi^2
            *(16*f0^4 + 1/(16*T^4)
            - (1/T^2)*2*f0^2)))
            *ones(1,length(imperfect_gamma_range)));
ACRB_ML   =  sqrt((1./(2*10.^(SNR./10)))
```

```
              *(1/(2*(2*pi*f0-pi/(2*T))^2
              + gamma_0^2/(2*tau^2))
              + 1/(2*(2*pi*f0+pi/(2*T))^2
              + gamma_0^2/(2*tau^2))))
               *ones(1,length(imperfect_gamma_range));
x= imperfect_gamma_range
   - gamma_0*ones(1,length(imperfect_gamma_range));
figure,plot(x,Bias_MC*c,'+',
x,Bias_ML_PLE*c,'o',
x,Bias_ML_IPLE*c,'s',
x,AB*c,'--',x,LBB*c,'-.'),
legend('MC Simulation',
'ML Simulation: Perfect PLE',
'ML Simulation: Imperfect PLE',
'ML Theory: Taylor with ECD',
'ML Theory: Lower/Upper Bound'),
title('Bias as a function of \delta_{\gamma)}: Outdoor scenario'),
xlabel('\delta_{\gamma)'),ylabel('Bias (m)')
figure,plot(x,S_RMSE_MC*c,'+',
x,ACRB_MC*c,'--',
x,S_RMSE_ML_PLE*c,'o',
x,ACRB_ML*c,'-.',
x,S_RMSE_ML_IPLE*c,'s',
x,Average_T_RMSE_ML_with*c,':'),
legend('MC Simulation',
'ToA: ACRB',
'ML Simulation: Perfect PLE',
'SS-ToA: ACRB',
'ML Simulation: Imperfect PLE',
'ML Theory: Averaged TE with ECD'),
title('RMSE as a function of \delta_{\gamma)}: Outdoor scenario'),
xlabel('\delta_{\gamma)} '),ylabel('RMSE (m)')
```

Bibliography

[1] A. Goldsmith, *Wireless Communications*. London, UK: Cambridge University Press, 2005.

[2] T. S. Rappaport, J. H. Reed, and B. D. Woerner, "Position location using wireless communications on highways of the future," *IEEE Commun. Mag.*, vol. 34, no. 10, pp. 33–41, Oct. 1996.

[3] J. H. Reed, K. J. Krizman, B. D. Woerner, and T. S. Rappaport, "An overview of the challenges and progress in meeting the E-911 requirement for location service," *IEEE Commun. Mag.*, pp. 30–37, Apr. 1998.

[4] J. J. Caffery and G. L. Stuber, "Overview of radiolocation in CDMA cellular systems," *IEEE Commun. Mag.*, pp. 38–45, Apr. 1998.

[5] K. Pahlavan, P. Krishnamurthy, and J. Beneat, "Wideband radio propagation modeling for indoor geolocation applications," *IEEE Commun. Mag.*, vol. 36, no. 4, pp. 60–65, Apr. 1998.

[6] J. Werb and C. Lanzl, "Designing a positioning system for finding things and people indoors," *IEEE Spectr.*, vol. 35, no. 9, pp. 71–78, Sep. 1998.

[7] K. Pahlavan, X. Li, and J.-P. Makela, "Indoor geolocation science and technology," *IEEE Commun. Mag.*, pp. 112–118, Feb. 2002.

[8] R. Subrata and A. Y. Zormaya, "Evolving cellular automata for location management in mobile computing networks," *IEEE Trans. Parallel Distrib. Syst.*, vol. 14, no. 1, pp. 13–26, Jan. 2003.

[9] S. S. Soliman and C. E. Wheatley, "Geolocation technologies and applications for third generation wireless," *Wireless Commun. Comput.*, vol. 2, no. 3, pp. 229–251, May 2002.

[10] D. Slepian, "Estimation of signal parameters in the presences of noise," *IRE Trans. Inform. Theory*, vol. 3, pp. 68–89, Mar. 1954.

[11] P. Swerling, "Parameter estimation for waveforms in additive Gaussian noise," *J. Soc. Indust. Appl. Math.*, vol. 7, no. 2, pp. 152–166, Jun. 1959.

[12] G. C. Carter, *Coherence and Time Delay Estimation*. New York, NY: IEEE Press, 1993.

[13] B. T. Sieskul, F. Zheng, and T. Kaiser, "Time-of-arrival estimation in path attenuation," in *Proc. 10th IEEE International Workshop on Signal Processing Advances in Wireless Communications 2009 (SPAWC 2009)*, Perugia, Italy, Jun. 2009, pp. 573–577.

[14] B. Friedlander, "Sensitivity analysis of the maximum likelihood direction-finding algorithm," *IEEE Trans. Aerosp. Electron. Syst.*, vol. 26, no. 6, pp. 953–968, Nov. 1990.

[15] M. Viberg and A. L. Swindlehurst, "Analysis of the combined effects of finite sample and model errors on array processing performance," *IEEE Trans. Signal Process.*, vol. 42, no. 11, p. 30733083, Nov. 1994.

[16] C. D. Richmond, "On the threshold region mean-squared error performance of maximum-likelihood direction-of arrival estimation in the presence of signal model mismatch," in *Proc. Fourth IEEE Workshop on Sensor Array and Multichannel Processing 2006 (SAM 2006)*, Waltham, MA, Jul. 2006, pp. 268– 272.

[17] A. Ferrol, P. Larzabal, and M. Viberg, "Performance prediction of maximum-likelihood direction-of-arrival estimation in the presence of modeling errors," *IEEE Trans. Signal Process.*, vol. 56, no. 10, pp. 4785–4793, Oct. 2008.

[18] S. Srinivasa and M. Haenggi, "Path loss exponent estimation in large wireless networks," in *Proc. IEEE Information Theory and Applications Workshop (ITA'09)*, San Diego, CA, Feb. 2009, pp. 124–129.

[19] X. Zhao, L. Razoumov, and L. J. Greenstein, "Path loss estimation algorithms and results for RF sensor networks," in *Proc. IEEE Veh. Tech. Conf.*, vol. 7, Los Angeles, LA, Sep. 2004, pp. 4593– 4596.

[20] J. Zhang, R. A. Kennedy, and T. D. Abhayapala, "Cramér-Rao lower bounds for the synchronization of UWB signals," *EURASIP Journal on Applied Signal Processing*, vol. 2005, no. 3, pp. 426–438, 2005.

[21] B. Sklar, *Digital Communications: Fundamentals and Applications*, 2nd ed. Upper Saddle River, New Jersey: Prentice Hall, 2001.

[22] B. T. Sieskul, F. Zheng, and T. Kaiser, "A hybrid SS-ToA wireless NLoS geolocation based on path attenuation: Mobile position estimation," in *Proc. IEEE Wireless Commun. Network. Conf. (WCNC 2009)*, Budapest, Hungary, Apr. 2009, pp. 1–6.

[23] D. C. Rife and R. R. Boorstyn, "Single-tone parameter estimation from discrete-time observations," *IEEE Trans. Inf. Theory*, vol. 20, no. 5, pp. 591–598, Sep. 1974.

[24] Y. Qi, H. Kobayashi, and H. Suda, "Analysis of wireless geolocation in a non-line-of-sight environment," *IEEE Trans. Wireless Commun.*, vol. 5, no. 3, pp. 672–681, Mar. 2006.

[25] ——, "On time-of-arrival positioning in a multipath environment," *IEEE Trans. Veh. Technol.*, vol. 55, no. 5, pp. 1516–1526, Sep. 2006.

[26] M. I. Skolnik, *Introduction to Radar Systems*, 2nd ed. New York, NY: McGraw-Hill, 1980.

[27] H. Urkowitz, *Signal Theory and Random Process*. Norwell, MA: Artech House, 1983.

[28] H. V. Poor, *An Introduction to Signal Detection and Estimation*, 2nd ed. New York, NY: Springer-Verlag Inc., 1994.

[29] C. W. Helstrom, *Elements of Signal Detection and Estimation*. Englewood Cliffs, NJ: Prentice Hall, 1995.

[30] R. N. McDonough and A. D. Whalen, *Detection of Signals in Noise*, 2nd ed. New York, NY: Academic Press, 1995.

[31] H. L. Van Trees, *Detection, Estimation, and Modulation Theory, Part I: Detection, Estimation, and Linear Modulation Theory*. New York, NY: John Wiley & Sons, Inc., 2001.

[32] R. D. Hippenstiel, *Detection theory: Applications and Digital Signal Processing*. Boca Raton, Florida: CRC Press, 2002.

[33] B. C. Levy, *Principles of Signal Detection and Parameter Estimation*. New York, NY: Springer, 2008.

[34] V. Erceg, L. J. Greenstein, S. Y. Tjandra, S. R. Parkoff, A. Gupta, B. Kulic, A. A. Julius, and R. Bianchi, "An empirically based path loss model for wireless channels in suburban environments," *IEEE J. Sel. Areas Commun.*, vol. 17, no. 7, pp. 1516–1526, Jul. 1999.

[35] R. A. Wooding, "The multivariate distribution of complex normal variables," *Biometrika*, vol. 43, no. 1/2, pp. 212–215, Jun. 1956.

[36] N. R. Goodman, "Statistical analysis based on a certain multivariate complex gaussian distribution (an introduction)," *Ann. Math. Stat.*, vol. 34, no. 1, pp. 152–177, Mar. 1963.

[37] K. S. Miller, "Complex Gaussian processes," *SIAM Review*, vol. 11, no. 4, pp. 544–567, Oct. 1969.

[38] ——, *Complex Stochastic Processes: An Introduction to Theory and Application*. Reading, MA: Addison-Wesley, 1974.

[39] B. T. Sieskul and T. Kaiser, "Cramér-Rao bound for TOA estimations in UWB positioning systems," in *IEEE International Conference on Ultra-Wideband (ICU 2005)*, Zurich, Switzerland, Sep. 2005, pp. 408–413.

[40] S. M. Kay, *Fundamentals of Statistical Signal Processing: Estimation Theory*. Englewood Cliffs, NJ: Prentice-Hall, 1993.

[41] C. L. Bennett and G. F. Ross, "Time-domain electromagnetics and its applications," *Proc. IEEE*, vol. 66, no. 3, pp. 299–318, Mar. 1978.

[42] R. A. Scholtz, "Multiple access with time-hopping impulse modulation," in *Proc. Military Communications Conference (MILCOM'93)*, vol. 2, Boston, MA, Oct. 1993, pp. 447–450.

[43] M. Z. Win and R. A. Scholtz, "Ultra-wide bandwidth time-hopping spread-spectrum impulse radio for wireless multiple access communications," *IEEE Trans. Commun.*, vol. 48, no. 4, pp. 679–691, Apr. 2000.

[44] W. C. van Etten, *Introduction to Random Signals and Noise*. West Sussex, England: John Wiley & Sons, 2005.

[45] D. Dardari, C.-C. Chong, and M. Z. Win, "Improved lower bounds on time-of-arrival estimation error in realistic UWB channels," in *IEEE International Conference on Ultra-Wideband 2006*, Waltham, MA, Sep. 2006, pp. 531–537.

[46] J. Minkoff, *Signal Processing Fundamental and Applications for Communications and Sensing Systems*. Nordwood, MA: Artech House, 2002.

[47] M. F. Zanuy, *Sistemas de Comunicaciones*. Barcelona, Spain: Marcombo-Boixareu, 2001.

[48] M. Schwartz, *Mobile Wireless Communications*. London, UK: Cambridge University Press, 2005.

[49] J. G. Proakis, *Digital Communications*, 4th ed. New York, NY: McGraw Hill, 2001.

[50] M. Moeneclaey, "On the true and the modified Cramer-Rao bounds for the estimation of a scalar parameter in the presence of nuisance parameters," *IEEE Trans. Commun.*, vol. 46, no. 11, pp. 1536–1544, Nov. 1998.

[51] A. Vretblad, *Fourier Analysis and Its Applications*. New York, NY: Springer, 2003.

[52] B. T. Sieskul, F. Zheng, and T. Kaiser, "On designs of Gaussian monocycle for UWB ranging using time delay estimation," 2009, in preparation.

[53] F.-T. Chau and Y.-Z. Liang, *Chemometrics: From Basics to Wavelet Transform*. China: Wiley-IEEE, 2004.

[54] J. Shirahama and T. Ohtsuki, "RSS-based localization in environments with different path loss exponent for each link," in *Proc. IEEE Veh. Tech. Conf.*, Marina Bay, Singapore, May 2008, pp. 1509–1512.

[55] B. T. Sieskul, F. Zheng, and T. Kaiser, "NLoS geolocation based on path attenuation: Unknown path loss exponents," 2009, in preparation.

[56] G. Mao, B. D. Anderson, and B. Fidan, "Path loss exponent estimation for wireless sensor network localization," *Computer Networks*, vol. 51, no. 10, pp. 2467–2483, Jul. 2007.

[57] N. Benvenuto and F. Santucci, "A least squares path-loss estimation approach to handover algorithms," *IEEE Trans. Veh. Technol.*, vol. 48, no. 2, pp. 437–447, Mar. 1999.

[58] K. Sharman, T. Durrani, M. Wax, and T. Kailath, "Asymptotic performance of eigenstructure spectral analysis methods," in *Proc. IEEE Conf. Acoustics, Speech, and Signal Processing (ICASSP'84)*, San Diego, CA, Mar. 1984, pp. 440–443.

[59] P. Stoica and A. Nehorai, "MUSIC, maximum likelihood and Cramér-Rao bound," *IEEE Trans. Acoust., Speech, Signal Process.*, vol. 37, no. 5, pp. 720–741, May 1989.

[60] M. Viberg and B. Ottersten, "Sensor array processing based on subspace fitting," *IEEE Trans. Signal Process.*, vol. 39, no. 5, pp. 1110–1121, May 1991.

[61] B. T. Sieskul, F. Zheng, and T. Kaiser, "Time-of-arrival estimation in fading channels," 2009, in preparation.

[62] S. W. Smith, *The Scientist and Engineer's Guide to Digital Signal Processing*, 2nd ed. San Diego, CA: California Technical Publishing, 1999.

[63] A. Torger and A. Farina, "Real-time partitioned convolution for ambiophonics surround sound," in *Proc. 2001 IEEE Workshop on Applications of Signal Processing to Audio and Acoustics (WASPAA'01)*, New Paltz, NY, Oct. 2001, pp. 195–198.

[64] E. Armelloni, C. Giottoli, and A. Farina, "Implementation of real-time partitioned convolution on a DSP board," in *Proc. 2003 IEEE Workshop on Applications of Signal Processing to Audio and Acoustics (WASPAA'03)*, New Paltz, NY, Oct. 2003, pp. 71–74.

[65] B. T. Sieskul, C. Kupferschmidt, and T. Kaiser, "Spatial fading correlation for semicircle scattering: Angular spread and spatial frequency approximations," 2009, in preparation.

[66] J. K. Patel and C. B. Read, *Handbook of the Normal Distribution*, 2nd ed. New York, NY: CRC Press, 1996.

[67] A. P. Prudnikov, Y. A. Brychkov, and O. I. Marichev, *Integrals and Series: Direct Laplace Transforms*. London, UK: Gordon and Beach Science, 1992.

[68] D. D. Fitts, *Principles Of Quantum Mechanics: As Applied To Chemistry And Chemical Physics*. London, UK: Cambridge University Press, 1999.